The integrative role of uPAR in outside-in signalling in human oesophageal squamous cell carcinoma cells

Yael-Leah Dahan

A thesis submitted to the Faculty of Science, University of the Witwatersrand, Johannesburg, in fulfilment of the requirements for the degree of Doctor of Philosophy.

Johannesburg, 2011

Declaration

I declare that this thesis is my own, unaided work. It is being submitted for the Degree of Doctor of Philosophy at the University of the Witwatersrand, Johannesburg. It has not been submitted before for any degree or examination at any other University.

(Y.L. Dahan)

14 Day of December 2011 in Johannesburg.

Abstract

Early investigations of the urokinase type plasminogen activator (uPA) receptor (uPAR) and its ligand, uPA, were limited to their role in degradation of the extracellular matrix (ECM) and invasion. Emerging evidence revealed that uPAR and its relationship with uPA and/or transmembrane proteins, such as the integrins, affects cell-ECM adhesion events and proliferation. These events are tightly coordinated and essential for epithelial tissue development. However, unregulated expression of molecules involved in cell adhesion and proliferation plays a significant role in tumour development and metastasis. The overexpression of uPAR is linked to several cancer types, including human oesophageal squamous cell carcinoma (HOSCC). This study examines the contribution of uPAR, and its communication with extracellular components, to cell-ECM adhesion and/or proliferation of HOSCC cells. The confirmation of the uPAR and β1-integrin expression as well as uPA secretion in the HOSCC cells lines, established these lines as excellent models for further investigation. In all the HOSCC cell lines, uPAR associated with integrin-linked kinase, a scaffolding protein in cell-ECM adhesion events. Data presented in this investigation confirmed that the interaction of uPAR with uPA or β1-integrin contributed to adhesion of the HOSCC cell lines on collagen type I and vitronectin. It was clearly established that uPAR also played a part in the proliferation of all the HOSCC cell lines. The uPAR role in proliferation is influenced by: **a)** The absence or presence of collagen type I or vitronectin substrates; **b)** The activation of uPAR by endogenous uPA; **c)** The uPAR/β1-integrin interaction; **d)** the presence of transforming growth factor β and epidermal growth factor. In the current study, it was successfully demonstrated that uPAR, and its relationship with the ECM and growth factors, contributes to adhesion and proliferation during the progression of HOSCC. This gives uPAR a considerable value as a therapeutic target for HOSCC.

Dedication

This thesis is dedicated to my uncle Saleh Ezer

Acknowledgement

First and foremost, I am very grateful to my supervisor and mentor Prof. R.B. Veale for all his guidance and support during the years.

I would like to thank Mrs. E. Scott for always having cells ready and for making all the tissue culture solutions. I also want to thank her for always being amazing and caring.

Thank-you to Mrs.C. Lalkahn for all her help with the confocal microscope.

Many thanks to all my lab colleagues who encouraged and supported me during my PhD, it has been a pleasure working with you.

To my family, dad, mom, Nurit, Justin, Coby and extended family, Victor and Sylvia, thanks so much for being supportive. Special thanks to my sister Nurit, who without fail always manages to put a smile on my face. Thanks to all my wonderful friends for believing in me and for their consistent encouragement.

Research output

SASBMB XXth Conference, 3-6 July 2006, University of Kwazulu-Natal.
Publication: **Dahan**, Y.L., Metcalfe, C. and Veale, R.B. (2006). Urokinase receptor and matrix metalloprotease-7 expression in human oesophageal squamous carcinoma cells – the role of nuclear β-catenin? Proc. XXth SASBMB Conference, Pietermaritzburg, South Africa. p145.

Bio-08 Conference, 21-25 January 2008, Rhodes University.
Publication: **Dahan**, Y.L. and Veale, R.B. (2008). Complex formation between the urokinase receptor, integrin linked kinase and caveolin in human oesophageal squamous cell carcinoma cell lines. Proc. Bio-08 Conference, Grahamstown, South Africa. p167.

LEICA confocal workshop, August 2009.
Talk: **Dahan** Y.L. (2009). Adhesion based signaling in oesophageal carcinoma. uPAR and β1-integrin colocalization

Table of Contents

Declaration i
Abstract ii
Dedication iii
Acknowledgement iv
Research output v
List of Figures xi
List of tables xiv
List of Abbreviations xx
List of symbols xxiii
Chapter 1: Literature review 1
1.1 Cell-adhesion events 2
1.1.1 Cell-Cell adhesion 2
1.1.2 Cell-ECM adhesion 3
1.1.2.a The ECM 3
1.1.2.b The Integrins 4
1.1.2.c Integrin activation 5
1.1.2.d Cell-ECM adhesion-based signalling via the integrins (outside-in signalling) 6
1.2 Proliferation and the role of growth factors 9
1.3. The plasminogen activation pathway 10
1.3.1 The uPA and uPAR are involved in ECM degradation and associate with the integrins 10
1.3.2 uPAR and its ligand uPA 11
1.3.3 uPAR role in cell-ECM adhesion and proliferation 13
1.3.4 Role of uPA and uPAR in pathology 13
1.4 Human oesophageal squamous cell carcinoma 14
1.5 Cell-ECM adhesion and uPAR in HOSCC 15
Aims 16
Chapter 2: uPAR and the ligands uPA and β1-integrin are expressed in five moderately differentiated HOSCC cell lines 18
2.1. Introduction 18
2.2 Materials and methods 21
2.2.1 Cell lines and tissue culture 21
2.2.2 RNA extraction 21
2.2.3 cDNA synthesis 22
2.2.4 Primers 23
2.2.5 Reverse transcriptase-polymerase chain reaction (RT-PCR) 23
2.2.6 Antibodies 23
2.2.7 Treatment of the cells with β1P1 24

2.2.8 Whole cell extraction 25
2.2.9 Collection and concentration of conditioned medium 25
2.2.10 Protein estimation of the whole cell samples 26
2.2.11 Immunoprecipitation of uPAR 27
2.2.12 Immunoprecipitation of β1-integrin 27
2.2.13 Sample preparation for Sodium dodecyl sulphate-polyacrylamide gel electrophoresis (SDS-PAGE) 28
2.2.14 SDS-PAGE 28
2.2.15 Western blot procedure (detection of uPAR) 29
2.2.16 Western blot procedure (detection of actin) 29
2.2.17 Western blot procedure (detection of uPA) 30
2.2.18 Western blot procedure (detection of β1-integrin) 30
2.2.19 Image analysis 31
2.2.20 Indirect immunofluorescence and confocal microscopy 31
2.2.21 Double immunofluorescence and confocal microscopy 31
2.3 Results 33
2.3.1 The expression of uPAR in the HOSCC cells 33
2.3.2 The distribution of uPAR in the HOSCC cells 33
2.3.3 The HOSCC cells secrete uPA 37
2.3.4 β1-integrin expression in the HOSCC cells 38
2.3.5 uPAR localises to the same region as β1-integrin in the HOSCC cells 39
2.3.6 The uPAR/β1-integrin interaction in the HOSCC cells 39
2.3.7 Stability of the uPAR/β1-integrin interaction 41
2.4 Discussion 43
Chapter 3: The uPAR forms a unique cell-ECM adhesion complex with ILK and caveolin in the HOSCC cell lines 46
3.1 Introduction 46
3.2. Materials and methods 48
3.2.1 Cell Lines and tissue culture 48
3.2.2 Antibodies 48
3.2.3 Treatment of the cells with β1P1 48
3.2.4 Whole cell extraction 48
3.2.5 Protein estimation 49
3.2.6 Immunoprecipitation 49
3.2.7 Preparation of samples for an SDS-PAGE 49
3.2.8 Western blot procedure (detection of actin) 49
3.2.9 Western blot procedure (detection of ILK) 49
3.2.10 Western blot (detection of caveolin) 50

3.2.11 Western blot (detection of uPAR) 50
3.2.12 Western blot (β1-integrin) 50
3.2.13 Image analysis 51
3.3 Results 52
3.3.1 The interaction of uPAR with ILK in the HOSCC cell lines 52
3.3.2. The role of β1-integrin in the uPAR-ILK interaction 52
3.3.3 The role of caveolin in the uPAR/ILK interaction 54
3.4 Discussion 57
Chapter 4: The role of uPAR in the adhesion of HOSCC cells 59
4.1. Introduction 59
4.2 Materials and methods 61
4.2.1 Cell Lines and tissue culture 61
4.2.2 Coating of tissue culture dishes with BSA, collagen type I or vitronectin 61
4.2.3 Preparation of the collagen type I-coated and vitronectin-coated dishes for adhesion assay 61
4.2.4 Adhesion assay 61
4.2.5 Analysis of data (Statistical analysis) 62
4.3 Results 63
4.3.1 Adhesion of the HOSCC cells onto collagen type I substrate 63
4.3.2 The uPAR impact on adhesion of the HOSCC cell lines on collagen type I substrate 63
4.3.3 Adhesion of the HOSCC cells on vitronectin substrate 65
4.3.4 The uPAR impact on adhesion of the HOSCC cell lines on vitronectin 68
4.4 Discussion 72
Chapter 5: The role of uPAR mechanisms in cell-ECM adhesion based proliferation of the HOSCC cell lines 74
5.1 Introduction 74
5.2 Materials and methods 76
5.2.1 Cell Lines and tissue culture 76
5.2.2 Coating of tissue culture dishes with collagen type I or vitronectin 76
5.2.3 Antibodies 76
5.2.4 Cell Proliferation assay (MTT) 76
5.2.5 Statistical analysis 78
5.3. Results 79
5.3.1. Influence of uPAR on proliferation of the HOSCC cells in the absence of ECM . 79
5.3.2. Influence of uPAR on proliferation of HOSCC cells in the presence of collagen type I substrate 81
5.3.3. Influence of uPAR on proliferation of the HOSCC cells on a vitronectin substrate 81

5.3.4. The interaction of cellular uPAR with vitronectin and its influence on proliferation of the HOSCC cells on vitronectin substrate 85
5.3.5. The influence of the uPAR/ vitronectin interaction on proliferation of the HOSCC cells provided with collagen type I and vitronectin 85
5.4 Discussion 88
Chapter 6: The influence of growth factors, extracellular matrix and uPAR on the proliferation of the HOSCC cells 91
6.1 Introduction 91
6.2 Materials and methods 93
6.2.1 Cell Lines and tissue culture 93
6.2.2 Coating of tissue culture dishes with collagen type I or vitronectin 93
6.2.3. Antibodies 93
6.2.4 Cell Proliferation assay 93
6.2.5 Statistical analysis 94
6.3 Results 95
6.3.1 EGFR activation affects on proliferation of the HOSCC cells in the absence of ECM and the role of uPAR 95
6.3.2. EGFR activation affects on proliferation of the HOSCC cells in the presence of collagen type I and the role of uPAR 97
6.3.3 EGFR activation affects on proliferation of the HOSCC cells in the presence of vitronectin substrate and the role of uPAR 99
6.3.4 EGFR activation affects on proliferation of the HOSCC cells in the presence of collagen type I and vitronectin combination substrate and the role of uPAR 100
6.4 Discussion 103
Chapter 7: General discussion 106
7.1 The relationship between the major players in ECM degradation, adhesion-based signalling and proliferation 106
7.2 What is the nature of the uPAR and cell-ECM adhesion relationship? 107
7.3. How does the uPAR relationship with uPA, β1-integrin and cell-ECM adhesion feed into proliferation? 109
7.4 Does uPAR have a role during the progression of HOSCC? 112
7.5 A way forward 113
Chapter 8: References 115
Chapter 9: Appendix A 131
9.1 List of Reagents 131
Appendix B 132
9.2.1 Trypsin/EDTA solution 132
9.2.2 DMEM/Hams 12 (3:1) medium 132
9.2.3 Phosphate buffer saline (1x) 133
9.2.4 Phenol 133
9.2.5 Agarose gel (1 %) 133

9.2.6 Tris-Acetate-EDTA (TAE) 20X 134
9.2.7 Loading buffer 134
9.2.8 PBS/PMSF/Trasylol solution 134
9.2.9 RIPA buffer 134
9.2.10 Laemmli single lysis buffer 135
9.2.11 Coomassie Blue solution (0.25%) 135
9.2.12 Destaining solution 135
9.2.13 Elution solution 135
9.2.14 Example of standard curve (protein estimation) 136
9.2.15 Laemmli double lysis buffer 136
9.2.16 Immunoprecipitation buffer 136
9.2.17 Separating gel 137
9.2.18 Stacking gel 137
9.2.19 Electrophoresis buffer 137
9.2.20 Destain solution 137
9.2.21 Towbin electrophoresis transfer buffer (Towbin *et al*., 1979) 138
9.2.22 Tris Buffer Saline 138
9.2.23 Developer solution 138
9.2.24 Fixer solution 138
9.2.25 BLOTTO 139
9.2.26 Paraformaldehyde (4%) 139
Appendix C 140
9.3.1 The uPAR sequencing results from the HOSCC cell lines 141
9.3.2 Adhesion assays statistical data on collagen type I 145
9.3.3 Adhesion assays statistical data on vitronectin 148
9.3.4. Proliferation assays statistical data (in the absence of ECM) 151
9.3.5. Proliferation assays statistical data (in the presence of collagen type I) 153
9.3.6. Proliferation assays statistical data (in the presence of vitronectin) 154
9.3.7. Proliferation assays statistical data (in the presence of collagen type I and vitronectin) 156
9.3.8. Proliferation assays statistical data of EGF treatments (in the absence of ECM) 156
9.3.9. Proliferation assays statistical data of EGF treatments (in the presence of collagen type I) 158
9.3.10. Proliferation assays statistical data of EGF treatments (in the presence of vitronectin) 160
9.3.11. Proliferation assays statistical data after EGF treatments (in the presence of collagen type I and vitronectin) 160

List of Figures

		Page
Figure 1.1:	The different integrin heterodimers and their interaction with components of the ECM.	**5**
Figure 1.2:	Inactive "bent" conformation of integrin heterodimer versus active integrin conformation.	**6**
Figure 1.3:	"Outside-in" signalling mediated by ECM-Integrin interaction.	**8**
Figure 1.4:	Role of uPA, uPAR and PAI-1 in ECM proteolysis.	**12**
Figure 2.1:	The uPAR mRNA is transcribed in all the HOSCC cells.	**34**
Figure 2.2:	Western blot and semi-quantitative analysis of uPAR protein expression in the HOSCC cell lines.	**35**
Figure 2.3:	The localisation of uPAR in the HOSCC cells.	**36**
Figure 2.4:	Western blot and semi-quantitative analysis of uPA secreted into the conditioned medium of the HOSCC cell lines.	**37**
Figure 2.5:	Western blot and semi-quantitative analysis of β1-integrin protein expressed by the HOSCC cell lines.	**38**
Figure 2.6:	β1-integrin and uPAR localise in the same regions of the HOSCC cells	**40**
Figure 2.7:	The interaction between uPAR and β1-integrin in the HOSCC cells.	**41**
Figure 2.8:	Western blot and semi-quantitative analysis of uPAR interaction with β1-integrin in WHCO6 cells exposed to β1P1 blocking peptide or $\beta1P1^{Sc}$ control peptide.	**42**
Figure 3.1:	ILK expression and the interaction between uPAR and ILK in the HOSCC cell lines.	**53**
Figure 3.2:	Analysis of the ILK interaction with uPAR in WHCO6 cells line exposed to β1P1 or $\beta1P1^{Sc}$ control.	**54**
Figure 3.3:	Caveolin expression and the interaction between uPAR and caveolin in HOSCC cell lines.	**55**
Figure 3.4:	The interaction of ILK or caveolin with uPAR was detected in the WHCO6 cells but not the MCF-7 cell line.	**56**

Figure 4.1: Adhesion of the HOSCC cell lines on collagen type I ECM substrate. **64**

Figure 4.2: Adhesion of the HOSCC cells on collagen type I upon addition of exogenous uPA. **66**

Figure 4.3: Adhesion of the HOSCC cell lines on collagen type I substrate upon disruption of the uPAR/β1-integrin interaction. **67**

Figure 4.4: Adhesion of the HOSCC cell lines on vitronectin substrate. **68**

Figure 4.5: Adhesion of the HOSCC cells on vitronectin substrate upon addition of exogenous uPA. **69**

Figure 4.6: Adhesion of the HOSCC cell lines on vitronectin substrate upon disruption of the uPAR/β1-integrin interaction. **71**

Figure 5.1: Investigation of the role of uPAR on proliferation of the HOSCC cells in the absence of ECM. **80**

Figure 5.2: Investigation of the role of uPAR on proliferation of the HOSCC cells in the presence of collagen type I substrate. **82**

Figure 5.3: Investigation of the role of uPAR on proliferation of the HOSCC cells in the presence of vitronectin substrate. **84**

Figure 5.4: Investigation of the role of cellular uPAR/vitronectin interaction on proliferation of the HOSCC cell, using TGFβ. **86**

Figure 5.5: The proliferation of the WHCO5 and WHCO6 cells in the presence of collagen type I and vitronectin combination substrate. **87**

Figure 6.1: The proliferation of the different HOSCC cell lines upon exposure to EGF. **96**

Figure 6.2: Investigation of the role of uPAR in EGF stimulation of proliferation of HOSCC cells **96**

Figure 6.3: The proliferation of the different HOSCC cell lines on collagen type I substrate upon exposure to EGF. **98**

Figure 6.4: Investigation of the role of uPAR in EGF stimulated proliferation of HOSCC cells on collagen type I substrate. **98**

Figure 6.5: The proliferation of the different HOSCC cell lines on vitronectin substrate upon exposure to EGF. **99**

Figure 6.6: The proliferation of the different HOSCC cell lines on collagen type I and vitronectin combination substrate upon exposure to EGF. **101**

Figure 6.7: Investigation of the role of uPAR in EGF stimulated proliferation of HOSCC cells on collagen type I and vitronectin combination substrate. **102**

Figure 7.1: The complex containing uPAR, caveolin and ILK provides structural stability during cell-ECM adhesion based events. **107**

Figure 7.2: uPAR influenced cell-ECM adhesion based proliferation in the HOSCC cells. **111**

Figure A.1: Example of a protein estimation standard curve. **136**

Figure C.1: The pRc/CMV-uPAR vector. **140**

Figure C.2: Chromatogram of the uPAR sequence from the pRc/CMV-uPAR plasmid (using T7 primer). **141**

Figure C.3: Chromatogram of the uPAR sequence from the SNO cell line (using the reverse primer). **142**

Figure C.4: Chromatogram of the uPAR sequence from the WHCO1 cell line (using the reverse primer). **142**

Figure C.5: Chromatogram of the uPAR sequence from the WHCO3 cell line (using the reverse primer). **143**

Figure C.6: Chromatogram of the uPAR sequence from the WHCO5 cell line (using the reverse primer). **143**

Figure C.7: Chromatogram of the uPAR sequence from the WHCO6 cell line (using the reverse primer). **144**

List of tables

		Page
Table 1.1.	One way ANOVA of the numbers of adherent HOSCC cells on collagen type I	**145**
Table 1.2.	P-values calculated by Tukey's multiple comparison post-ANOVA test (comparison between adhesion of the HOSCC cell lines on collagen type I)	**145**
Table 1.3.a.	The mean and standard deviation of the number of adherent HOSCC cells on collagen type I versus BSA	**145**
Table 1.3.b.	P-values calculated by an unpaired Student's t-test (comparison between the number of adherent HOSCC cells on collagen type I versus BSA)	**145**
Table 1.4.	One way ANOVA of the numbers of adherent HOSCC cells on collagen type I, in the absence or presence of 0.5 nM and 1 nM uPA	**146**
Table 1.5.	P-values calculated by Dunnett's multiple comparison post-ANOVA test (comparison between adhesion of the SNO cells on collagen type I, in the absence or presence of 0.5 nM and 1 nM uPA)	**146**
Table 1.6.a.	The mean and standard deviation of the number of adherent HOSCC cells on collagen type I versus BSA, in the presence of 0.5 nM uPA	**146**
Table 1.6.b.	P-values calculated by an unpaired Student's t-test (comparison between the number of adherent HOSCC cells on collagen type I versus BSA, in the presence of 0.5 nM uPA)	**146**
Table 1.7.a.	The mean and standard deviation of the number of adherent HOSCC cells on collagen type I versus BSA, in the presence of 1 nM uPA	**146**
Table 1.7.b.	P-values calculated by an unpaired Student's t-test (comparison between the number of adherent HOSCC cells on collagen type I versus BSA, in the presence of 1 nM uPA)	**147**
Table 1.8.a.	The mean and standard deviation of the number of adherent HOSCC cells on collagen type I in the presence of $\beta1P1^{Sc}$ versus $\beta1P1$ peptides	**147**
Table 1.8.b.	P-values calculated by an unpaired Student's t-test (comparison between the number of adherent HOSCC cells on collagen type I in the presence of $\beta1P1^{Sc}$ versus $\beta1P1$ peptides)	**147**
Table 1.9.a.	The mean and standard deviation of the number of adherent HOSCC cells on collagen type I versus BSA, in the presence of $\beta1P1^{Sc}$ peptide	**147**

Table 1.9.b.	P-values calculated by an unpaired Student's t-test (comparison between the number of adherent HOSCC cells on collagen type I versus BSA, in the presence of β1P1^{Sc} peptide)	**147**
Table 1.10.a.	The mean and standard deviation of the number of adherent HOSCC cells on collagen type I versus BSA, in the presence of β1P1 peptide.	**147**
Table 1.10.b.	P-values calculated by an unpaired Student's t-test (comparison between the number of adherent HOSCC cells on collagen type I versus BSA, in the presence of β1P1 peptide)	**148**
Table 2.1.	One way ANOVA of the numbers of adherent HOSCC cells on vitronectin	**148**
Table 2.2.	P-values calculated by Tukey's multiple comparison post-ANOVA test (comparison between adhesion of the HOSCC cells on vitronectin)	**148**
Table 2.3.a.	The mean and standard deviation of the number of adherent HOSCC cells on vitronectin versus BSA	**148**
Table 2.3.b.	P-values calculated by an unpaired Student's t-test (comparison between the number of adherent HOSCC cells on vitronectin versus BSA	**149**
Table 2.4.	One way ANOVA of the numbers of adherent HOSCC cells on vitronectin, in the absence or presence of 0.5 nM and 1 nM uPA	**149**
Table 2.5.	P-values calculated by Dunnett's multiple comparison post-ANOVA test (comparison between adhesion of the WHCO3 cells on vitronectin, in the absence or presence of 0.5 nM and 1 nM uPA)	**149**
Table 2.6.a.	The mean and standard deviation of the number of adherent HOSCC cells on vitronectin versus BSA, in the presence of 0.5 nM uPA	**149**
Table 2.6.b	P-values calculated by an unpaired Student's t-test (comparison between the number of adherent HOSCC cells on vitronectin versus BSA, in the presence of 0.5 nM uPA)	**149**
Table 2.7.a.	The mean and standard deviation of the number of adherent HOSCC cells on vitronectin versus BSA, in the presence of 1 nM uPA	**150**
Table 2.7.b.	P-values calculated by an unpaired Student's t-test (comparison between the number of adherent HOSCC cells on vitronectin versus BSA, in the presence of 1 nM uPA).	**150**
Table 2.8.a.	The mean and standard deviation of the number of adherent HOSCC cells on vitronectin in the presence of β1P1^{Sc} versus β1P1 peptides	**150**
Table 2.8.b.	P-values calculated by an unpaired Student's t-test (comparison between the number of adherent HOSCC cells on vitronectin in the presence of β1P1^{Sc} versus β1P1 peptides)	**150**

Table 2.9.a.	The mean and standard deviation of the number of adherent HOSCC cells on vitronectin versus BSA, in the presence of β1P1^{Sc} peptide	**150**
Table 2.9.b.	P-values calculated by an unpaired Student's t-test (comparison between the number of adherent HOSCC cells on vitronectin versus BSA, in the presence of β1P1^{Sc} peptide)	**150**
Table 2.10.a.	The mean and standard deviation of the number of adherent HOSCC cells on vitronectin versus BSA, in the presence of β1P1 peptide	**151**
Table 2.10.b	P-values calculated by an unpaired Student's t-test (comparison between the number of adherent HOSCC cells on vitronectin versus BSA, in the presence of β1P1 peptide)	**151**
Table 3.1.a	The mean and standard deviation of the number of viable HOSCC cells in the absence and presence of suPAR	**151**
Table 3.1.b	P-values calculated by an unpaired Student's t-test (comparison between the number of viable HOSCC cells in the absence or presence of suPAR)	**151**
Table 3.2.	One way ANOVA of the numbers of viable HOSCC cells in the absence or presence of 0.5 nM, 1 nM and 5 nM uPA	**152**
Table 3.3.a	The mean and standard deviation of the number of viable HOSCC cells in the presence of β1P1^{Sc} versus β1P1 peptides	**152**
Table 3.3.b	P-values calculated by an unpaired Student's t-test (comparison between the number of viable HOSCC cells in the presence of β1P1^{Sc} versus β1P1 peptides)	**152**
Table 3.4.a.	The mean and standard deviation of the number of viable HOSCC cells in the absence or presence of TGFβ	**152**
Table 3.4.b.	P-values calculated by an unpaired Student's t-test (comparison between the number of viable HOSCC cells in the absence or presence TGFβ)	**152**
Table 4.1.a	The mean and standard deviation of the number of viable HOSCC cells on collagen type I in the absence or presence of suPAR	**153**
Table 4.1.b	P-values calculated by an unpaired Student's t-test (comparison between the number of viable HOSCC cells on collagen type I in the absence or presence suPAR)	**153**
Table 4.2.	One way ANOVA of the numbers of viable HOSCC cells on collagen type I, in the absence or presence of 0.5 nM, 1 nM and 5 nM uPA	**153**
Table 4.3.a.	The mean and standard deviation of the number of viable HOSCC cells on collagen type I, in the presence of β1P1^{Sc} versus β1P1 peptides	**153**
Table 4.3.b.	P-values calculated by an unpaired Student's t-test (comparison between the number of viable HOSCC cells on collagen type I in the presence of β1P1^{Sc} versus β1P1 peptides)	**153**

Table 5.1.a.	The mean and standard deviation of the number of viable HOSCC cells on vitronectin in the absence or presence of suPAR	**154**
Table 5.1.b.	P-values calculated by an unpaired Student's t-test (comparison between the number of viable HOSCC cells on vitronectin in the absence or presence of suPAR)	**154**
Table 5.2.a.	The mean and standard deviation of the number of viable HOSCC cells on vitronectin in the presence of IgG control or anti-uPA antibody	**154**
Table 5.2.b.	P-values calculated by an unpaired Student's t-test (comparison between the number of viable HOSCC cells in the presence of IgG control or anti-uPA antibody)	**154**
Table 5.3.	One way ANOVA of the numbers of viable HOSCC cells on vitronectin in the absence or presence of 0.5 nM, 1 nM and 5 nM uPA	**154**
Table 5.4,	P-values calculated by Dunnett's multiple comparison post-ANOVA test (comparison between the number of viable HOSCC cells of the WHCO5 cells on vitronectin, in the absence or presence of 0.5 nM and 1 nM uPA)	**155**
Table 5.5.a.	The mean and standard deviation of the number of viable HOSCC cells on vitronectin in the presence of $\beta1P1^{Sc}$ versus β1P1 peptides	**155**
Table 5.5.b.	P-values calculated by an unpaired Student's t-test (comparison between the number of viable HOSCC cells on vitronectin in the presence of $\beta1P1^{Sc}$ versus β1P1 peptides)	**155**
Table 5.6.a.	The mean and standard deviation of the number of viable HOSCC cells on vitronectin in the absence or presence of TGFβ	**155**
Table 5.6.b.	P-values calculated by an unpaired Student's t-test (comparison between the number of viable HOSCC cells on vitronectin in the absence or presence of TGFβ)	**155**
Table 6.1.a.	The mean and standard deviation of the number of viable HOSCC cells, on collagen type I and vitronectin, in the absence or presence of suPAR	**156**
Table 6.1.b.	P-values calculated by an unpaired Student's t-test (comparison between the number of viable HOSCC cells, on collagen type I and vitronectin, in the absence or presence of suPAR)	**156**
Table 6.2.a.	The mean and standard deviation of the number of viable HOSCC cells, on collagen type I and vitronectin, in the absence or presence of TGFβ	**156**
Table 6.2.b.	P-values calculated by an unpaired Student's t-test (comparison between the number of viable HOSCC cells, on collagen type I and vitronectin, in the absence or presence of TGFβ)	**156**
Table 7.1.a.	The mean and standard deviation of the number of viable HOSCC cells in the absence or presence of EGF	**156**

Table 7.1.b.	P-values calculated by an unpaired Student's t-test (comparison between the number of viable HOSCC cells, in the absence or presence of EGF	**157**
Table 7.2.a.	The mean and standard deviation of the number of viable HOSCC cells treated with or without EGF, in the presence of anti-uPAR antibody	**157**
Table 7.2.b.	P-values calculated by an unpaired Student's t-test (comparison between the number of viable HOSCC cells treated with or without EGF, in the presence of anti-uPAR antibody)	**157**
Table 7.2.c.	The mean and standard deviation of the number of viable WHCO6 cells treated with or without EGF, in the presence of IgG control	**157**
Table 7.2.d.	P-values calculated by an unpaired Student's t-test (comparison between the number of viable WHCO6 cells treated with or without EGF, in the presence of IgG control)	**157**
Table 7.3.a.	The mean and standard deviation of the number of viable HOSCC cells treated with or without EGF, in the presence of β1P1	**157**
Table 7.3.b.	P-values calculated by an unpaired Student's t-test (comparison between the number of viable WHCO6 cells treated with or without EGF, in the presence of β1P1)	**158**
Table 8.1.a.	The mean and standard deviation of the number of viable HOSCC cells, on collagen type I in the absence or presence of EGF	**158**
Table 8.1.b.	P-values calculated by an unpaired Student's t-test (comparison between the number of viable HOSCC cells on collagen type I in the absence or presence of EGF)	**158**
Table 8.2.a.	The mean and standard deviation of the number of viable HOSCC cells, on collagen type I, treated with or without EGF, in the presence of anti-uPAR antibody	**158**
Table 8.2.b.	P-values calculated by an unpaired Student's t-test (comparison between the number of viable HOSCC cells on collagen type I treated with or without EGF, in the presence of anti-uPAR antibody	**158**
Table 8.2.c.	The mean and standard deviation of the number of viable HOSCC cells on collagen type I, treated with or without EGF, in the presence of IgG control	**159**
Table 8.2.d.	P-values calculated by an unpaired Student's t-test (comparison between the number of viable WHCO3 cells on collagen type I treated with or without EGF, in the presence of IgG control	**159**
Table 8.3.a.	The mean and standard deviation of the number of viable HOSCC cells, on collagen type I, treated with or without EGF, in the presence of β1P1	**159**
Table 8.3.b.	P-values calculated by an unpaired Student's t-test (comparison between the number of viable HOSCC cells on collagen type I treated with or without EGF, in the presence of β1P1)	**159**

Table 8.3.c.	The mean and standard deviation of the number of viable WHCO6 cells on collagen type I treated with or without EGF, in the presence of $\beta1P1^{Sc}$	**159**
Table 8.3.d.	P-values calculated by an unpaired Student's t-test (comparison between the number of viable WHCO6 cells on collagen type I treated with or without EGF, in the presence of $\beta1P1^{Sc}$)	**159**
Table 9.1.a.	The mean and standard deviation of the number of viable HOSCC cells on vitronectin in the absence or presence of EGF	**160**
Table 9.1.b.	The mean and standard deviation of the number of viable HOSCC cells on vitronectin in the absence or presence of EGF	**160**
Table 10.1.a.	The mean and standard deviation of the number of viable HOSCC cells, on collagen type I and vitronectin, in the absence or presence of EGF	**160**
Table 10.1.b.	P-values calculated by an unpaired Student's t-test (comparison between the number of viable HOSCC cells, on collagen type I and vitronectin, in the absence and presence of EGF)	**160**
Table 10.2.a.	The mean and standard deviation of the number of viable HOSCC cells, on collagen type I and vitronectin, treated with or without EGF, in the presence of anti-uPAR antibody	**160**
Table 10.2.b.	P-values calculated by an unpaired Student's t-test (comparison between the number of viable HOSCC cells, on collagen type I and vitronectin, treated with or without EGF, in the presence of anti-uPAR antibody)	**161**
Table 10.2.c.	The mean and standard deviation of the number of viable WHCO6 cells, on collagen type I and vitronectin, treated with or without EGF, in the presence of IgG control	**161**
Table 10.2.d.	P-values calculated by an unpaired Student's t-test (comparison between the number of viable WHCO6 cells, on collagen type I and vitronectin, treated with or without EGF, in the presence of IgG control)	**161**
Table 10.3.a.	The mean and standard deviation of the number of viable HOSCC cells, on collagen type I and vitronectin, treated with or without EGF, in the presence of $\beta1P1$	**161**
Table 10.3.b.	P-values calculated by an unpaired Student's t-test (comparison between the number of viable HOSCC cells, on collagen type I and vitronectin, treated with or without EGF, in the presence of $\beta1P1$)	**161**
Table 10.3.c.	The mean and standard deviation of the number of viable WHCO6 cells, on collagen type I and vitronectin, treated with or without EGF, in the presence of $\beta1P1^{Sc}$	**161**
Table 10.3.d.	P-values calculated by an unpaired Student's t-test (comparison between the number of viable WHCO6 cells, on collagen type I and vitronectin, treated with or without EGF, in the presence of $\beta1P1^{Sc}$)	**162**

List of Abbreviations

Abs	Absorbance
AP-1	activator protein-1
ADP	Adenosine diphosphate
ANOVA	Analysis of variance
ATF	amino terminal fragment
ATP	Adenosine triphosphate
BLAST	Basic Local Alignment Search Tool
bp	base pairs
BSA	Bovine serum albumin
Ca^{2+}	Calcium
CD	cluster of differentiation
Cdc42	Cell division cycle 42
CK	Casein Kinase
cm	centimetre
C-terminal	Carboxyl-terminal
cytoD	Cytochalasin D
dH_2O	distilled water
DMEM	Dulbecco's Modified Eagle's Medium
DMSO	Dimethyl sulphoxide
dNTP	nucleotides
E-cadherins	Epithelial-cadherins
ECM	Extracellular matrix
EDTA	Ethylenediaminetetra-acetic acid
EGF	Epidermal growth factor
EGF-R	EGF-receptor
ERK	Extracellular signal-related kinase
F-actin	Filamentous actin
FAK	Focal adhesion kinase
FITC	Fluorescein isothiocyanate
G-actin	Globular actin
GDP	Guanosine 5′-diphosphate

GFD	Growth factor domain
GPI	Glycosyl-phosphatidylinositol
GSK-3β	Glycogen synthase kinase-3β
GTP	Guanosine 5′-triphosphate
HCl	Hydrochloric acid
HMW	High molecular weight
HOSCC	Human oesophageal squamous cell carcinoma
HRP	Horse radish peroxidase
IgG	Immunoglobulin
ILK	Integrin linked kinase
IP samples	Immunoprecipitated samples
JNK	c-jun N-terminal protein kinase
kb	Kilo-base-pairs
kDa	kilo-Daltons
L	Litre
LEF/TCF	Lymphoid enhancer factor/T-cell factor
LMW	Low molecular weight
LRP	Low density lipoprotein receptor related protein
mA	Milli-Amps
MAPK	Mitogen activated protein kinase
min	Minutes
mM	Milli-molar
mm	Millimetre
MMP	Matrix metalloproteases
MTT	3-(4,5-Dimethylthiazol-2-yl)-2,5-Diphenyltetrazolium Bromide
N-cadherins	Neuronal-cadherins
NF-κB	Nuclear factor-kappa B,
ng	Nanograms
NLS	Nuclear localisation signal
nm	Nanometers
N-terminal	Amino-terminal
p53	Tumour protein 53
PAI-1	Plasminogen activator inhibitor-1
PBS	Phosphate Buffer Saline

P-cadherin	Placental-cadherins
PCR	Polymerase chain reaction
PDK	Phosphoinositidyl dependent kinase
PH domain	Pleckstrin homology domain
PI3-K	Phosphoinositide-3-kinase
PINCH	Particularly interesting new cysteine-histidine rich protein
PKC	Protein kinase C
pmols	pico-mols
PMSF	Phenylmethylsulfonyl fluoride
Rac1	Ras-related c3 botulinum toxin substrate 1;
RGD	Arginine-glycine-aspartic acid
rpm	Revolutions per minute
RT-PCR	Reverse transcriptase-polymerase chain reaction
SCC	Squamous cell carcinoma
SDS-PAGE	Sodium dodecyl sulphate-polyacrylamide gel electrophoresis
sec	Second
STAT	Signal transducer and activator of transcription
suPAR	Soluble uPAR
TAE	Tris-Acetate-EDTA
Taq	*Thermus aquaticus*
TBS	Tris buffered saline
TCA	Trichloroactic acid
TEMED	N,N,N’N’-tetramethylenediamine
TGFβ	Transforming growth factor β
TRAIL	TNF-related apoptosis-inducing ligand
TRITC	Tetramethylrhodamine isothiocyanate
uPA	Urokinase type plasminogen activator
uPAR	Urokinase-type plasminogen activator receptor
wnt	Wingless-type
x *g*	times gravity
μg	Micro-gram
μl	Micro-litres
μM	Micro-molar

List of symbols

α alpha

β beta

γ gamma

Chapter 1: Literature review

The body's amazing ability to perform a range of operations in a coordinated manner resides in its specific organs. The general organ plan consists of several layers of cells interacting with each other and/or with the surrounding extracellular matrix (ECM) (Wodarz, 2002; Nelson, 2003; Lopez *et al*., 2008). Aside from the fact that these cell-cell and cell-ECM adhesion events establish functional units, these events trigger a cascade of signalling pathways critical for cell differentiation and proliferation (ffrench-Constant and Colognato, 2004; Gooding *et al*., 2004, Charalabopoulos *et al*., 2005; Lopez *et al*., 2008).

The ECM is a complex environment consisting of polysaccharides, hyaluronic acid, structural components, such as the collagens, laminins, fibronectin or vitronectin (Orgel *et al*., 2006; Petreaca and Martins-Green, 2007; Daley *et al*., 2008). Although the ECM was originally, thought to only have a structural function, it is in fact so important in providing signals to the cells leading to events such as migration and proliferation (Larsen *et al.*, 2006; Daley *et al*., 2008; Streuli and Akhtar, 2009). The communication from the ECM to the cells requires cell-ECM adhesion molecules such as the integrins (Srichai and Zent, 2010; Lamar and DiPresio, 2011). In fact, integrin have a significant role in cell signalling events such as proliferation in addition to their structural one (Srichai and Zent, 2010).

There has been an interesting research development over the years with the discovery of the relationship between "anti-adhesion" and adhesion molecules with respect to their influence on cell-ECM adhesion events (Blasi and Sidenius, 2010). The role of anti-adhesion proteolytic molecules such as uPAR and its ligand, uPA, was previously limited to ECM degradation, invasion and tissue destruction (Colombi *et al*., 1984). It has since been established that these key members of the plasminogen activation pathway also participate and direct cellular signalling events such as cell-ECM adhesion and proliferation (Czekay *et al*., 2003; Guerrero *et al*., 2004; Piccolella *et al*., 2008).

These "anti-adhesion" and ECM proteolysis molecules work together with cell adhesion molecules to influence proliferation, which is central to normal physiological roles such as tissue development and wound repair (Plesner *et al*., 1997; Friedl and Brocker, 2000; Piccolella *et al*., 2008; D'Alessio *et al*., 2008). In pathological conditions, adhesion and anti-adhesion events are crucial to tumour development and subsequent metastasis since both

adhesion and proliferation are necessary components of the transformed state (Hirohashi and Kanai, 2003; Janes and Watt, 2006; Hanahan and Weinberg, 2011).

The focus of this study is on the urokinase-type plasminogen activator receptor (uPAR) and its roles in cell-ECM adhesion based events such as proliferation. This was further extended to understanding these events in the context of human oesophageal squamous cell carcinoma. Since this study entails several details of seemingly diverse topics, it is necessary to introduce issues such as: 1) cell-ECM adhesion mediated by the integrins; 2) cell-ECM adhesion based proliferation of epithelial cells; 3) uPAR and uPA and their role in cell-ECM adhesion events; 4) human oesophageal squamous cell carcinoma (HOSCC) and 5) the relationship between cell-ECM adhesion events, unregulated uPAR expression and HOSCC progression.

1.1 Cell-adhesion events

The study of cell adhesion in its broad sense includes several molecules such as the cadherins, integrins, selectins and immunoglobulins (Brakebusch and Fässler, 2003; Charalabopoulos *et al*., 2005). The cadherins and integrins are the main cell adhesion molecules necessary to mediate cell-cell, and cell-ECM adhesion (Nair *et al*., 2005; Charalabopoulos *et al*., 2005).

1.1.1 Cell-Cell adhesion

Cadherins such as epithelial (E), placental (P)- and neuronal (N)-cadherins are transmembrane glycoproteins, which mediate calcium dependent, homotypic adhesion between cells (Chitaev and Troyanovsky, 1998; Gooding *et al*., 2004; Koch *et al*., 2004). E-cadherin is composed of an amino terminal extracellular domain, a transmembrane domain and a carboxyl terminal cytoplasmic tail domain (Gooding *et al*., 2004). The extracellular domain is involved in the homotypic interaction between cadherins on neighbouring cells, meaning that E-cadherin only associates with E-cadherin (Gooding *et al*., 2004; Koch *et al*., 2004). The cadherins bind to β- or γ-catenin and these catenins in turn interact with α-catenin, which associates with the actin cytoskeleton (Gooding *et al*., 2004). Therefore, the catenins provide the link between the cadherins and the actin cytoskeleton (Adams *et al*., 1996; Obama and Ozawa, 1997; Chitaev and Troyanovsky, 1998).

1.1.2 Cell-ECM adhesion

1.1.2.a The ECM

Attachment of cells to the ECM is essential for providing structural support and maintaining tissue integrity, cell migration, cell cycle progression and regulating tissue growth and morphogenesis (Brakebusch *et al*., 2002; Daley *et al*., 2008; Petreaca and Martins-Green, 2007).

The ECM is composed of an intricate network consisting of several glycosylated and non-glycosylated proteins such as fibronectin, vitronectin, collagen and laminin at varying concentrations depending on the tissue type it surrounds (Ivaska and Heino, 2000; DeClerck *et al*., 2004; Kolácná *et al*., 2007, Daley *et al*., 2008). In this project, the ECM components collagen type I and vitronectin are used in *in vitro* analysis of cell adhesion and proliferation (chapter 4, 5 and 6) and therefore warrant a more detailed analysis.

Collagen type I belongs to the collagen superfamily, of which there are at least 29 known types (Orgel *et al*., 2006; Carter and Raggio, 2009). Collagen type I is part of the fibrous collagens and consists of two α1 (I) and one α2 (I) helix chains, which twist together to form a triple helix (Ricard-blum and Ruggiero, 2005; Kolácná *et al*., 2007). Subsequently, this triple helix and its association with other triple helixes result in the formation of the microfibril and the bases of the collagen fibril network, which forms the structural bases of mammalian connective tissue (Orgel *et al*., 2006).

Vitronectin (75 kDa molecule) exists as a soluble plasma form or as part of ECM (Schvartz *et al*., 1999). In the plasma it is found as a folded monomer either in the form of a single chain (75 kDa) or a two chain form (65 and 10 kDa) held together by disulphide bonds (Schvartz *et al*., 1999). In the ECM, the vitronectin occurs as a multimeric form and binds to the ECM by interacting with collagen or heparin present in the ECM (Schvartz *et al*., 1999; Hollier *et al*., 2005). Vitronectin is present in loose connective tissue, as well as the basement membrane of blood vessels (Hayman *et al*., 1983; Madsen and Sidenius, 2008).

Collagen type I and vitronectin mediate adhesion of cells via adhesion related molecules such as the integrin as well as non-integrin receptors such as the urokinase type plasminogen activator receptor (uPAR) (Schoppet *et al*., 2002; Czekay *et al*., 2003; Wei *et al*., 2005; Daley *et al*., 2008).

1.1.2.b The Integrins

Integrins are heterodimeric transmembrane proteins composed of an α and a β subunit from a possible combination of 18 and 8 molecules, respectively (ffrench-Constant and Colognato, 2004; Nair *et al*., 2005; Petreaca and Martins-Green, 2007). The different α and β subunits form 24 known integrins and thus determine with which component of the ECM it interacts (Figure 1.1) (Ivaska and Heino, 2000; Hynes, 2002). For example, the αvβ3 or αvβ5 integrins bind to vitronectin, while the α1β1 or α2β1 integrins bind to collagen (Figure 1.1) (Ivaska and Heino, 2000; Nair *et al*., 2005). Integrin communication with the ECM is bidirectional, where signalling from inside the cells, "inside-out" signalling, affects the binding affinity between integrins with ECM (Gonzalez *et al*., 2010; Lamar and DiPersio, 2011). Signalling transmitted from the ECM to the cell via the integrins to induce activation of signalling pathways is termed "outside-in" (Gonzalez *et al*., 2010; Lamar and DiPersio, 2011).

Integrins have an extracellular domain, which is able to recognise and bind a sequence such as the classical arginine-glycine-aspartic acid (RGD) sequence within the ECM molecule (for example, vitronectin) (ffrench-Constant and Colognato, 2004; Humphries *et al*., 2006). Integrins also have a transmembrane domain and a short cytoplasmic tail, which interacts with cytoskeleton associated proteins as well as signalling proteins (Brakebusch *et al*., 2002; Srichai and Zent, 2010). The β-integrin subunit (with the exception of β4) binds to the actin cytoskeleton via adaptor proteins such as talin, paxillin and vinculin (Srichai and Zent, 2010). The exception, the β4 integrin subunit cytoplasmic tail has a direct interaction with the keratin intermediate filaments (Jonkman *et al*., 2002).

The anchorage of the integrins to the cytoskeleton is necessary to maintain cell-ECM adhesion (Brakebusch and Fässler, 2003). This was clearly demonstrated by disruption of the actin cytoskeleton polymerisation process with cytochalasin D (Haier *et al*., 1999). The presence of cytochalasin D abrogated the ability of colon carcinoma cells (HT-29) to adhere on collagen type IV, collagen type I, laminin, fibronectin and vitronectin (Haier *et al*., 1999).

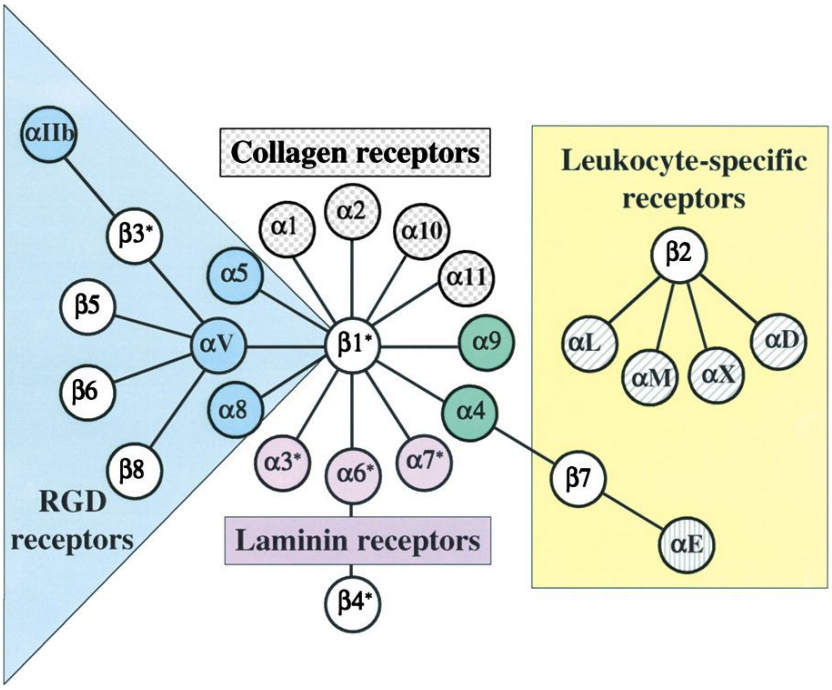

Figure 1.1: The different integrin heterodimers and their interaction with components of the ECM. The diagram is from Hynes (2002).

1.1.2.c Integrin activation

The αβ integrin heterodimer, in its inactive state, exists in a bent conformation (Figure 1.2) (Zolkiewska, 2005; Gonzalez *et al*., 2010). In the bent conformation, the cytoplasmic tails of the α and β subunits associate with each other. The main molecules involved in integrin activation are talin and kindelin (Qin *et al*., 2004; Srichai and Zent, 2010). These molecules bind at different regions to the cytoplasmic tail of the β integrin subunit. Talin binds to the region of the cytoplasmic tail that is proximal to the membrane (Qin *et al*., 2004; Srichai and Zent, 2010). This alters the association between the cytoplamic tails of β and α integrin cytoplasmic subunits (Qin *et al*., 2004; Srichai and Zent, 2010). This leads to the extension of the extracellular region of the α and β integrin subunits, which increases the affinity of integrins to their ligand (Figure 1.2). Kindlin is thought to facilitate the talin induced integrin activation (Srichai and Zent, 2010).

At the extended conformation, the integrins bind to the specific ECM component (Zolkiewska, 2005; Gonzalez *et al*., 2010). This integrin-ECM interaction enables the integrins to transmit signals from the ECM to the cells, which influences cellular proliferation, differentiation, migration or survival, which are critical events to a mammalian cell (ffrench-

Constant and Colognato, 2004; Petreaca and Martins-Green, 2007). These "outside-in" signalling events involve the different interactions of the cytoplasmic tail of the β integrin subunit with various signalling proteins such as focal adhesion kinase (FAK), integrin linked kinase (ILK) and caveolin (discussed below).

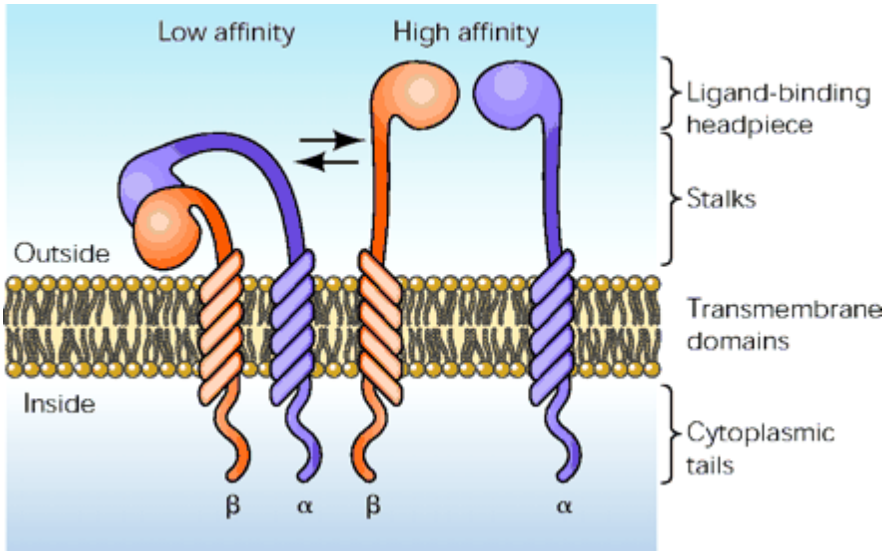

Figure 1.2: inactive "bent" conformation of integrin heterodimer versus active integrin conformation. This image is from Zolkiewska (2005).

1.1.2.d Cell-ECM adhesion-based signalling via the integrins (outside-in signalling)

Focal adhesion kinase is a non-receptor tyrosine kinase, which is present in its inactive form in the cytoplasm (Parsons, 2003). Upon integrin-ECM interaction, FAK is phosphorylated at tyrosine residue 397, by autophosphorylation (Zhao and Guan, 2009). This leads to the recruitment of FAK to focal adhesion sites (cell-ECM contact site) where it associates with the integrin's β-tail (Figure 1.3) (Parsons, 2003; Grashoff *et al*., 2004; Westhoff *et al*., 2004). Subsequently, src tyrosine kinase is recruited to the focal adhesion sites, binds to- and phosphorylates FAK at four additional tyrosine residues thereby increasing its kinase activity (Westhoff *et al*., 2004). The src-induced FAK phosphorylation also creates a binding site on FAK for adapter protein Grb2-son of sevenless (SOS)-Ras complex, which results in the activation of the mitogen activated protein kinase (MAPK)/extracellular signal-related kinase (ERK) signalling pathway (Figure 1.3) (Mukhopadhyay *et al*., 2005). This subsequently leads to the nuclear translocation of ERK and the subsequent activation of several transcription factors that regulate expression of genes involved in proliferation such as *cyclin D1* (Zhao and Guan, 2009).

In addition, activated FAK leads to the phosphorylation of the phosphoinositide-3-kinase (PI3-K) regulatory subunit, p85 (Zhao and Guan, 2009). PI3-K is composed of p85 and a catalytic subunit, p110 (Cantrell, 2001; Zhao and Guan, 2009). PI3-K activity leads to the downstream production of phosphotidylinositol-3,4,5-Trisphosphate as well as phosphotidylinositol-3,4-diphosphate (Rameh and Cantley, 1999; Cantrell, 2001). Phosphoinositidyl dependent kinase (PDK) and ILK recognise and bind to phosphotidylinositol-3,4,5-Trisphosphate, and phosphorylate and activate Akt at Threonine (Thr) 308 and Serine (Ser) 473 respectively (Figure 1.3) (Rameh and Cantley, 1999; Peyrollier *et al*., 2000; Cantrell, 2001; Tran *et al*., 2002; Troussard *et al*., 2003; Janes and Watt, 2004).

ILK is a cytoplasmic protein, which consists of a c-terminal kinase domain, pleckstrin homology (PH)-like domain and an N-terminal domain consisting of five ankyrin repeats (Wickström *et al*, 2010). ILK, which interacts with β1- and β3-integrin subunits, is recruited to the membrane upon cell-ECM adhesion mediated by the integrin (Nho *et al*., 2005). ILK is a scaffolding molecule, which interact with actin associated proteins (parvin and paxillin) and therefore provides the link between the integrins with the actin cytoskeleton (Ho and Bendeck 2009, Fielding and Dedhar, 2009) (discussed in more detail in chapter 3). On the other hand, ILK is a serine threonine kinase and besides having a role in activating Akt (mentioned above), which promotes cell survival, ILK enhances the phosphorylation and therefore reduces activity of glycogen synthase kinase-3β (GSK-3β) (Figure 1.3) (Troussard *et al*., 2003). GSK-3β is involved in the downregulation of cytoplasmic β-catenin and ILK induced GSK-3β phosphorylation leads to an increase of β-catenin in the nucleus (Figure 1.3) (Delcommenne *et al*., 1998; Monick *et al*., 2001; Oloumi *et al*., 2004). In the nucleus, β−catenin forms a transcription factor complex with lymphoid enhancer factor (LEF)/T-cell factor (TCF) to enhance expression of genes involved in proliferation such as *cyclin D1* and *c-myc* (Li *et al*., 2005).

Another interesting molecule involved in the integrin signalling is caveolin. Caveolin is a transmembrane protein and individual monomers assemble to form the structure of the caveolae, which are microinvaginations within the plasma membrane (Agelaki *et al*., 2009; Burgermeister *et al*., 2008). Caveolin can also exist outside of the caveolar structure and it was demonstrated by two separate experiments that the "noncaveolar" caveolin formed a signalling complex with β1-integrin (Wary *et al*., 1998; Kawabe *et al*., 2004). Wary *et al*. (1998) demonstrated that in WI-38 fibroblasts, the interaction between caveolin and α1β1-

integrin and α5β1 led to Fyn activation. This subsequently resulted in the phosphorylation of Shc and the recruitment of Grb2, which led to activation of the Ras-ERK pathway and anchorage dependence growth. Furthermore this Fyn/Shc/Grb2/Ras/ERK pathway was activated in vascular smooth muscle cells upon the interaction of caveolin with β1-integrin (Kawabe *et al*., 2004).

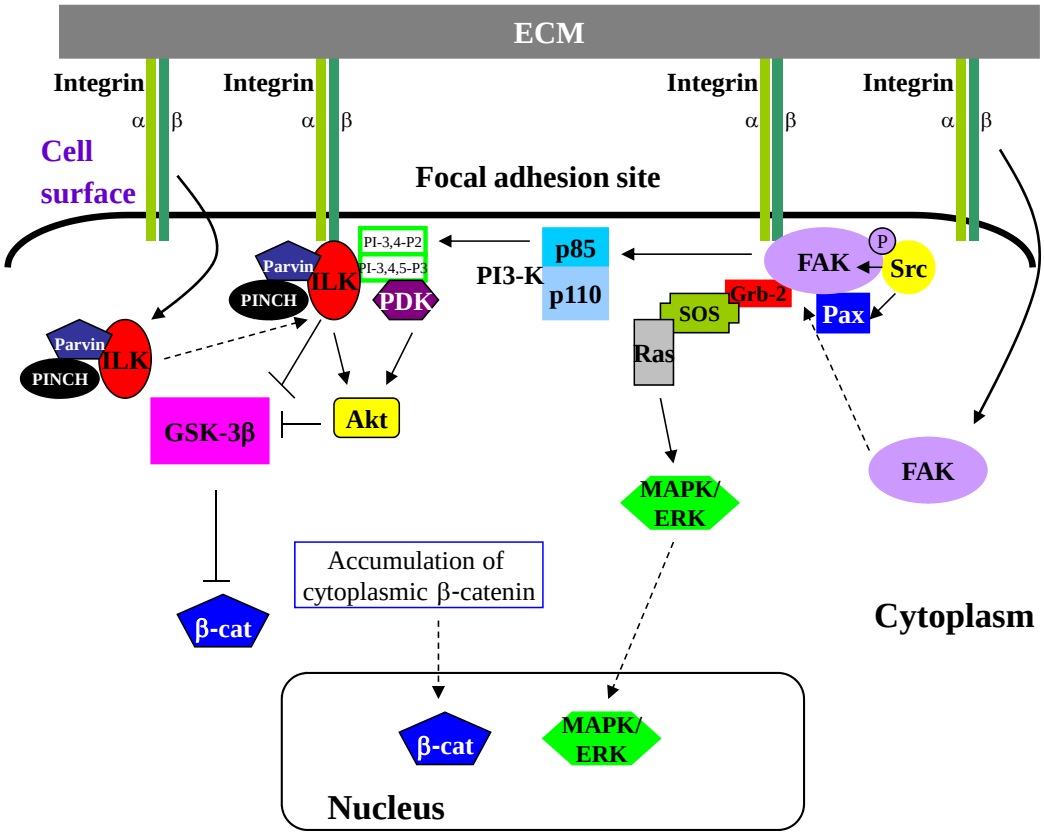

Figure 1.3: "Outside-in" signalling mediated by ECM-Integrin interaction. FAK is phosphorylated by autophosphorylation at a single tyrosine residue upon ECM-integrin interaction and is subsequently translocated to focal adhesion sites, where it binds to integrin β-subunit (Parsons, 2003; Grashoff *et al*., 2004; Westhoff *et al*., 2004). Src is recruited to phosphorylated FAK and phosphorylate, and therefore enhance FAK kinase activity, at 4 additional tyrosine residues (Mukhopadhyay *et al*., 2005). Src also phosphorylates paxillin which leads to activation of MAPK/ERK pathway. Src induced FAK activation also leads to the recruitment of the Grb2-SOS-Ras complex which leads to activation of MAPK/ERK pathway (Mukhopadhyay *et al*., 2005). ERK potentially translocate to the nucleus. FAK also leads to activation of PI3-K's p85 regulatory subunit. This leads to the production of phosphotidylinositol-3,4,5-triphosphate and phosphotidylinositol-3,4-diphosphate(Zhao and Guan, 2009) . ILK and PDK recognise and bind to phosphotidylinositol-3,4,5-triphosphate and subsequently phosphorylate and activate Akt. ILK and Akt can both phosphorylate and decrease GSK-3β activity (Rameh and Cantley, 1999; Peyrollier *et al*., 2000; Cantrell, 2001; Tran *et al*., 2002; Troussard *et al*., 2003; Janes and Watt, 2004). GSK-3β is a regulator of β-catenin in the cytoplasm. An excess of cytoplasmic β-catenin leads to its nuclear translocation (Delcommenne *et al*., 1998; Monick *et al*., 2001; Oloumi *et al*., 2004). **Note:** PI-3,4-P2 = phosphotidylinositol-3,4-diphosphate; Pi-3,4,5,-P3 = phosphotidylinositol-3,4,5-triphosphate; β-cat = β-catenin.

1.2 Proliferation and the role of growth factors

There are several consequences of the cell-ECM interaction such as migration and differentiation, but the one of focus in this study is the cell-ECM induced proliferation (Chapters 5 and 6). In epithelial cells, anchorage dependent growth is necessary for the cells to enter from the G1 to S-phase and commit with cell cycle progression (Petreaca and Martins-Green, 2007). The loss of anchorage can lead to anoikis, which is a form of apoptosis induced by cell detachment (Chiarugi, 2008).

For optimal cell proliferation (at a specific time and on a particular ECM surface) there is a cross-talk between the cell-ECM interaction mediated by the integrins as well as proliferative signalling mediated by the growth factors (Chiarugi, 2008; Streuli and Akhtar, 2009). The growth factors employed in this project in understanding proliferative events relating to the ECM and uPAR in HOSCC are epidermal growth factor (EGF) and transforming growth factor (TGF)β (Chapter 5 and 6). The mode of action that EGF and TGFβ influence proliferation, involves their specific interaction with their respective receptors and is detailed in the text below.

EGF and its receptor (EGFR) are essential for several signalling events leading to cell survival, proliferation as well as maintaining tissue homeostasis (Schneider and Wolf, 2009). However, these molecules are also involved in pathological phenomena such as tumour development and in fact EGFR is overexpressed in several carcinomas such as HOSCC (Veale and Thornley, 1989; Mitsudomi and Yatabe, 2010). EGF activation of EGFR (discussed in chapter 6) leads to the expression of genes involved in cell proliferation such as *cyclin D1* (Schneider and Wolf, 2009; Mitsudomi and Yatabe, 2010). The mechanism in which EGF/EGFR influences cell-ECM induced proliferation is discussed in detail in chapter 6.

TGFβ is secreted by the cells in a latent complex, comprising of the N-terminal polypeptide latency associated protein (LAP) and latent TGFβ binding protein (Kaminska *et al*., 2005; Margadant and Sonnenberg, 2010). Upon release of TGFβ from the complex, the free TGFβ in its active form binds to TGF type II receptor, which is a constitutively active serine/threonine kinase receptor (Kaminska *et al*., 2005; Margadant and Sonnenberg, 2010). This leads to the formation of a heterodimers between TGFβ type I receptor with TGFβ type II receptor and the subsequent phosphorylation of smad 2 and smad 3 (Kaminska *et al*., 2005; Margadant and Sonnenberg, 2010). Consequently, smad 2 and smad 3 bind to smad 4 and are

translocated together to the nucleus. In the nucleus they interact with transcription factors and DNA binding proteins to enhance or inhibit the transcription of genes with smad binding elements in their promoter region (Kaminska *et al*., 2005; Margadant and Sonnenberg, 2010).

The TGFβ relationship with the ECM molecule vitronectin provides an interesting angle in which the growth factor can influence cell-ECM adhesion events. TGFβ binds to vitronectin and interferes with the αV integrin mediated cell-vitronectin adhesion of MG63 osteosarcoma cells (Schoppet *et al*., 2002). Furthermore, TGFβ also interferes with cell-vitronectin adhesion mediated via uPAR as was observed in BAF-3 (mouse B cells) transfected with uPAR (Schoppet *et al*., 2002). This is explored in more detail in chapter 5.

1.3. The plasminogen activation pathway

1.3.1 The uPA and uPAR are involved in ECM degradation and associate with the integrins

uPA and uPAR are most commonly known for their classical role in the degradation of ECM components (Plesner *et al*., 1997). However, it is now well established that urokinase type plasminogen activator receptor (uPAR) also plays a role in cell-ECM adhesion-based signalling, as was mentioned briefly in the text above (Aguirre-Ghiso *et al*., 1999; Wei *et al*., 2005; Tang *et al*., 2008). uPAR interacts with fourth blade repeat β-propeller of the α subunit of the αMβ2 and α3β1 integrins (Wei *et al*., 2001; Pluskota *et al*., 2003; Blasi and Sidenius, 2010). Furthermore a region within the β1-integrin (residues 224-232) is important for the uPAR interaction with β1-integrin (Wei *et al*., 2005).

In the degradation process, uPA in its inactive form (pro-uPA) released by the cells binds to uPAR and trace amounts of plasmin present on the plasma membrane convert pro-uPA to active uPA by cleaving the bond between residues lysine 158 and isoleucine 159 (Figure 1.4.a) (Andreasen *et al*., 2000; Dass *et al*., 2008). This uPA in turn converts cell bound inactive plasminogen into active plasmin leading to a feedback mechanism, known as the reciprocal zymogen activation in which more pro-uPA and plasminogen are converted to their active forms (Plesner *et al*., 1997, Ulisse *et al*., 2009).

Plasmin has broad substrate specificity and is involved in the degradation of several ECM components as well as conversion of certain matrix metalloproteases (MMPs), e.g. MMP -1,

-2, -3 and MMP-9, to their active forms (Baramova *et al*., 1997; Legrand *et al*., 2001; Santala *et al*., 2000; Ulisse *et al*., 2009). This leads to further degradation of the ECM components (Figure 1.4.a) (Ulisse *et al*., 2009). The degradation of ECM is localised to a cell's surface and inhibitors such as αM-antiplasmin inactivate plasmin that diffuses away from this area (Plesner *et al*., 1997; Ulisse *et al*., 2009).

The uPA-uPAR degradation system is controlled by the plasminogen activator inhibitor-1 (PAI-1) of the serine proteinase inhibitor family, which binds to uPA catalytic domain (Plesner *et al*., 1997; Ulisse *et al*., 2009). This inhibitor interacts with active uPA at a 1:1 molar ratio, halting uPA activity (Ulisse *et al*., 2009). Additionally, PAI binds to uPA-uPAR to form a PAI-uPA-uPAR complex (Figure 1.4.b) (Czekay *et al*., 2001). The uPA:PAI-1 interaction induces the binding of uPAR D3 domain (see below) to low density lipoprotein receptor related protein (LRP) (Czekay *et al*., 2001). This leads to a PAI-1:uPA/uPAR:LRP complex which is then endocytosed by the cell (Figure 1.4.b) (Czekay *et al*., 2001). Subsequently, PAI-1-uPA is degraded by the lysosome while uPAR and LRP are recycled to the plasma membrane (Figure 1.4.b) (Czekay *et al*., 2001).

Although uPAR, and its ligand uPA, involvement with ECM proteolysis has been widely studied, it is also now known that uPAR, usually bound to uPA, interacts with the integrins and results in several downstream events such as cell proliferation, migration and enhancement of the integrin-ECM interaction (Aguirre-Ghiso *et al*., 2003; Guerrero *et al*., 2004; Wei *et al*., 2005). It is currently established that uPAR binds directly to β1, β2, β3 and β5, αv and αm integrin subunits, and several complexes such as α3β1 and αvβ3 (Wei *et al*., 2001; Tarui *et al*., 2003; Blasi and Sidenius, 2010).

1.3.2 uPAR and its ligand uPA

Prior to discussing the uPAR structure, it is necessary to mention uPA, as most of the uPAR dependent pathways require uPA binding. Pro-uPA, also known as single chain uPA is a 55 kilodalton (kDa) serine protease (Ploug *et al*., 2001). Pro-uPA consists of 3 domains; the growth factor domain (GFD), a kringle domain and a serine protease domain (Andreasen *et al*., 2000; Stepanova and Tkachuk, 2002). The cleavage of pro-uPA by plasmin, discussed above, generates a two chain uPA with two domains: the amino terminal fragment (ATF), which consists of the GFD and kringle domains, and the low molecular weight (LMW)-uPA,

which contains the serine protease catalytic domain (Higazi, *et al*., 1996; Stepanova and Tkachuk, 2002; Dass *et al*., 2008).

Pro-uPA or uPA both bind to uPAR with high affinity (dissociation constant, K_d: 10^{-10} to 10^{-9} M) via the GFD domain (Higazi, *et al*., 1996; Simon *et al*., 1996). The residues in this domain, which bind to uPAR are present in an omega loop shape (Ploug *et al*., 2001). uPAR, also known as "cluster of differentiation" (CD) 87, is a heavily glycosylated molecule present on the cell surface (Roldan *et al*., 1990). uPAR consists of three homologous domains (D1,D2 and D3) with D1 and D3 being at the amino- and carboxyl-terminals respectively (Ossowski and Aguirre-Ghiso, 2000). The D3 domain at the carboxyl terminal is anchored to the plasma membrane via glycosyl-phosphatidylinositol (GPI) (Andreasen *et al*., 2000). D1 residues (arginine 53, leucine 55, tyrosine 57 and leucine 66) and D3 residues (histidine 251) form the binding site for uPA (Andreasen *et al*., 2000; Ploug *et al*., 2001).

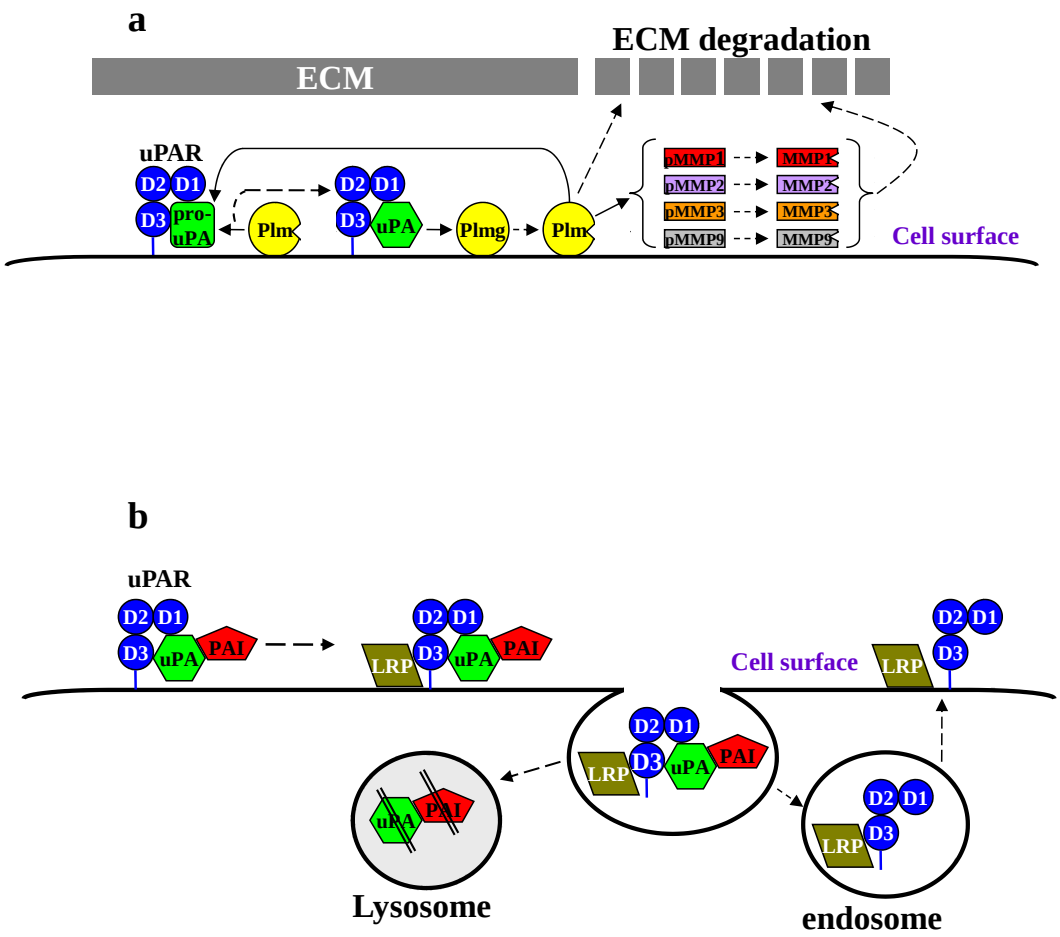

Figure 1.4: Note: Legend for this figure continues on the following page.

Figure 1.4: Role of uPA, uPAR and PAI-1 in ECM proteolysis. (a) Pro-uPA or uPA bind to uPAR domain 1 and 3. Trace amounts of plasmin convert pro-uPA to its active form (uPA). uPA in turn converts inactive plasminogen into active plasmin. Plasmin results in degradation of ECM components. Plasmin also converts pro-MMPs to active MMPs, which are also involved in degrading ECM components. **(b)** PAI binds to uPA and the PAI:uPA interaction leads to the association of uPAR domain 3 with LRP. Subsequently, the complex formation of PAI:uPA/uPAR:LRP is endocytosed by

the cell. uPA:PAI undergo lysosomal degradation, while uPAR and LRP are recycled to the plasma membrane. **Note:** D1 = domain 1; D2 =domain 2; D3 = domain 3; Plm = plasmin; Plmg = plasminogen; pMMP = pro-MMP. My synthesis of the composite picture was generated using information from several references.

uPAR in its non-glycosylated native form is 35 kilo-Daltons (kDa), while the glycosylated form is 55 kDa (Tarui *et al*, 2003). At the membrane, the uPAR isoform that consists of all three domains is necessary for its interaction with uPA, β1-integrin and vitronectin (Ossowski and Aguirre-Ghiso, 2000; Ploug *et al*., 2001; Chaurasia *et al*., 2006; Sato *et al*., 2011). The fact that uPAR does not possess a cytoplasmic tail, but is still able to initiate events leading to cell adhesion and migration was explained by the exciting discovery that uPAR is able to interact with transmembrane proteins such as the integrins and induce adhesion based signalling pathways (Wei *et al*., 1999; Yebra *et al*., 1999).

1.3.3 uPAR role in cell-ECM adhesion and proliferation

The interaction of uPAR with its ligands such as the integrins, vitronectin and uPA influences the cell signalling events such as adhesion and proliferation (Liu *et al*., 2002; Tang *et al*., 2008). The PAI-1 molecule mentioned above competes with uPAR for vitronectin binding, therefore decreasing the uPAR mediated cell-vitronectin adhesion (Deng *et al*., 2001). However, Czeskay *et al.* (2003) argued that PAI-1 decreases the uPA-uPAR-vitronectin adhesion by binding to uPA and causing endocytosis of uPAR and integrins in an LRP dependent manner (described above). It is also suggested by the same researchers that PAI-1 can also decrease the adhesion between uPAR and fibronectin or type-1 collagen via the same mechanism (Czekay *et al*., 2003). The role of uPAR in cell-ECM adhesion and proliferation is discussed in more detail in the following chapters.

1.3.4 Role of uPA and uPAR in pathology

Tumour invasion and metastasis involve the migration of cells from the primary tumour to secondary sites, which is the lethal part of cancer (Fidler, 2002). uPAR is involved with the essential steps of ECM proteolysis and tumour invasion (Plesner *et al*., 1997, Wei *et al*., 2001; Ulisse *et al*., 2009). However, seeing that uPAR is also involved in cell signalling events, uPAR may also contribute to tumour growth and invasion by increasing cell adhesion, proliferation and migration (Wei *et al*., 2005; Liu *et al*., 2002).

Interestingly, Aguirre-Ghiso *et al*. (2003) demonstrated that uPAR also enhances metastasis by inducing the transition of the cancer from dormant to proliferative stage in HEp3 head and neck squamous cell carcinoma cells. In HEp3 cells, the ERK/p38 ratio determines the state of dormancy: a high ERK/p38 ratio leads to a proliferative state, while a high p38/ERK ratio leads to a dormant state (Aguirre-Ghiso *et al.*, 2003). High uPA and uPAR expression, led to a high ERK/p38 ratio, and the proliferation of Hep-3 cultured *in vivo* (Aguirre-Ghiso *et al*., 2003).

With that being said the increased uPAR or uPA expression is generally associated with progression of tumour invasion and metastasis and with poor survival rates (Hong *et al*., 1996; Shiomi *et al*., 2000; Bacchiocchi *et al*., 2008). Examples of such cancers are adenocarcinomas such as endometrial and gastric adenocarcinomas, melanoma, glioblastoma and squamous cell carcinomas such as oral carcinomas and importantly for the current study oesophageal squamous cell carcinomas (Bhattacharya *et al*., 2001; Hong *et al*., 1996; Memarzadeh *et al*., 2002; Nozaki *et al*., 1998; Rofstad *et al*., 2004; Shiomi *et al*., 2000; Bacchiocchi *et al*., 2008).

1.4 Human oesophageal squamous cell carcinoma

HOSCC is a tumour of the epithelium in the oesophagus that invariably progresses to metastatic disease (Stoner *et al.*, 2007). HOSCC occurs with high incidents reported in countries such as China, Japan, Iran, France, Italy, Uruguay and South Africa (Gore *et al.*, 1997; Lu, 2000; Stoner and Gupta, 2001; Stoner *et al*., 2007). In South Africa, oesophageal cancer is common among ethnic groups such as the Xhosa and Thembu in areas such as Transkei, Kimberly, Port Elizabeth, East London and the Western Cape (McGlashan, 1988; McGlashan *et al*., 2003; Pacella-Norman *et al*., 2002; Melhado *et al*., 2010). In South Africa, the ratio of male to female with HOSCC is significantly high, and the risk of acquiring HOSCC increases with age (McGlashan, 1988; Pacella-Norman *et al*., 2002).

The occurrence of HOSCC is due to a combination between environmental and genetic factors (Lu, 2000; Stoner and Gupta, 2001; Stoner *et al*., 2007). Environmental factors characterized as high risk in HOSCC are: 1) a diet lacking in riboflavins, proteins, vitamins such as Vitamin A, C, E and minerals such as magnesium and zinc; 2) use of alcohol, opium and tobacco; 3) consumption of high salt food that may be contaminated with microbial toxins, nitrosamines and hot beverages (Gore *et al*., 1997; Lu, 2000; Stoner and

Gupta, 2001; Kuwano *et al*., 2003; Koshy *et al*., 2004; Kollarova, *et al*., 2007; Stoner *et al*., 2007). Examples of genetic factors that contribute to HOSCC include increased cyclin D1 expression, mutation in p53, reduced Retinoblastoma gene expression, overexpression of EGF-R, increased telomerase expression, elevated expression of cyclooxygenase-2 and nitric oxide synthase (Gore *et al*., 1997; Lu, 2000; Mandard *et al*., 2000; Stoner *et al*., 2007).

HOSCC histopathologies changes in epithelium are associated with esophagitis, atrophy, mild to severe dysplasia, carcinoma *in situ* and finally invasive carcinoma (Mandard *et al*., 2000; Kuwano *et al*., 2003). Invasion, angiogenesis, cell migration and importantly to this study, high proliferative state, of the primary tumour are hallmarks steps that contribute to metastasis of HOSCC (Smeds *et al*., 2002; Hanahan and Weinberg, 2011). Indeed, progression of HOSCC is often associated with lymph node metastasis, which further spreads to the cervical nodes (Kuwano *et al*., 2003). There is also the formation of intramural metastases from the HOSCC to the stomach (Kuwano *et al*., 2003).

HOSCC is an escalating health problem in South Africa with a high mortality rate and statistics worldwide show that unfortunately only 1 in 5 HOSCC patients survive more than 3 years after diagnosis (Stoner *et al*., 2007). Therefore, it is crucial to understand the underlying molecular events that are involved in the development of HOSCC (McGlashan, 1988; Pacella-Norman *et al*., 2002).

1.5 Cell-ECM adhesion and uPAR in HOSCC

Cell-ECM adhesion is necessary for events such as migration, proliferation and invasion, which are necessary events in carcinoma development (Lamar and DiPersio, 2011). Two recent studies demonstrated that detachment of the EC9706 and KYSE 170 HOSCC cell lines from the ECM led to anoikis via TRAIL-induced apoptosis and caspase-3 activation respectively (Liu *et al*., 2009; Ortiz *et al*., 2010). Furthermore, the overexpression of molecules involved in cell-ECM adhesion based events in HOSCC, fascin and β1-integrin, is linked with poor prognosis of HOSCC and Docetaxel resistance (Mori *et al*., 2008; Ortiz *et al*., 2010). Docetaxel is an anti-mitotic chemotherapy drug (Mori *et al*., 2008). This illustrates the significance of adhesion-based events in HOSCC.

Studies on uPA/uPAR established that there is a link of uPA/uPAR expression and HOSCC (Shiomi *et al*., 2000; Veale *et al*., 1990). Patients with immunodetection of uPA in their

HOSCC tumours, had a survival of 0% over a 5 year period versus patients which had a 60% survival over the same period and uPA was not immunodetected in their HOSCC tumours (Shiomi *et al*., 2000). Furthermore, *in situ* hybridyzation and immunohistochemistry confirmed that the uPAR mRNA and protein were only detected in HOSCC tissue and not in untransformed epithelium (Shiomi *et al*., 2000).

The uPAR protein is involved in cell-ECM adhesion events in carcinoma cells such as colon, breast, head and neck squamous cell carcinoma and oral squamous cell carcinoma (Liu *et al*., 2002; Ahmed *et al*., 2003; Jo *et al*., 2003; Liang *et al*., 2008). Additionally, uPAR contributes to the proliferation of cancers such as breast and prostate carcinoma (Gandhari *et al*., 2006; Piccolella *et al*., 2008). In spite of this, the role of uPAR in cell adhesion and proliferation in squamous cell carcinoma of the oesophagus is a glaring omission from the literature.

Cell-ECM adhesion and proliferation are important events in the development of HOSCC and the increased expression of uPA and uPAR is linked with HOSCC as well as decreased survival rate (Shiomi *et al*., 2000; Mori *et al*., 2008; Liu *et al*., 2009; Ortiz *et al*., 2010). It is therefore essential to understand whether uPAR plays a role in cell adhesion and proliferation of HOSCC. This would provide an understanding to the possible mechanisms in which uPAR may potentiate the HOSCC condition. Furthermore, this would also offer insight to the manner in which communication between cells and their environmental factors influence important events during HOSCC development such as adhesion and proliferation.

Aims

The main question of this study is: is uPAR involved in cell-ECM adhesion based events such as adhesion and proliferation in HOSCC? To answer this, HOSCC cell lines derived from moderately differentiated tumours of South-African patients with metastatic disease are used as an *in vitro* model. The aims of this study are:

1. Determine whether the HOSCC cell lines in this study express uPAR and secrete uPA. Additionally, determine whether uPAR interacts with β1-integrin in the HOSCC cell lines.

2. Determine whether uPAR associates with a molecule that has a relationship with the cytoskeleton and provides uPAR with a link to the cytoskeleton, which is essential during cell-ECM adhesion events.

3. Determine whether uPAR and its interaction with uPA or β1-integrin affect the adhesion of the HOSCC cell lines on collagen type I or vitronectin.

4. Determine whether uPAR and its interaction with β1-integrin or uPA are involved in proliferation of the HOSCC cell lines in the absence of ECM or the presence of collagen type I and vitronectin.

5. Determine whether EGF induces proliferation of the HOSCC cell lines via uPAR mechanisms in the absence of ECM or the presence of collagen type I and vitronectin.

Chapter 2: uPAR and the ligands uPA and β1-integrin are expressed in five moderately differentiated HOSCC cell lines

2.1. Introduction

The specific communication of epithelial cells with their surrounding extracellular matrix (ECM) environment is crucial for the development and structural integrity of epithelial tissue (Petreaca and Martins-Green, 2007; Lopez *et al*., 2008). The expanding research with regards to this topic has produced the fascinating discovery that uPAR, a key protein in the plasminogen activation pathway, also plays a role in cell-ECM adhesion events (Ossowski and Aguirre-Ghiso, 2000; Tang *et al*., 2008). Since the uPAR's role in cell-ECM adhesion events is the focus of this project, it is necessary to provide background on uPAR and the different factors that affect its role in cell-ECM adhesion. This necessarily includes the expression of uPAR and its ligands.

The uPAR gene is located on chromosome 19q13.2 and the full uPAR transcript consists of 7 exons (Thunø *et al*., 2009). The combination of exons (2 + 3) (4 + 5) and (6 + 7) code for the 3 respective domains (D1, D2 and D3) of the uPAR protein (de Bock and Wang, 2004; Thunø *et al*., 2009). The uPAR protein has 5 potential N-linked glycosylation sites and the addition of the glycosylphosphotidyl inositol tail (GPI) onto the domain 3 (D3) at Gly283 of uPAR allows for uPAR to attach to the plasma membrane (Ploug *et al*., 1998; Yuan and Huang, 2007). The uPAR linked to the plasma membrane can exist in the D2D3 and D1D2D3 isoforms (Mazzieri *et al*., 2006; Piccolella *et al*., 2008). The D2D3 uPAR isoform forms due to the cleavage of the linker region between D1 and D2 (Stewart and Sayer, 2009). This cleavage is mediated by serine proteases such as chymotrypsin as well as its own ligand uPA (Montuori *et al*., 2002; Stewart and Sayer, 2009). Importantly, the full uPAR isoform (D1D2D3) is necessary to interact with its ligands such as uPA, integrins and vitronectin to carry out the cell-ECM adhesion based events (Behrendt *et al*., 1996; Li *et al*., 2003; Mazzieri *et al*., 2006; Chaurasia *et al*., 2006; Blasi and Sidenius, 2010).

The major ligand of uPAR is uPA, which is secreted as a high molecular weight single chain pro-uPA isoform and binds to uPAR with high affinity (K_d 10^{-10} to 10^{-9} M) (Simon *et al*., 1996). This leads to activation of the plasminogen activation pathway (see chapter 1 for more detail). Furthermore, the activation of uPAR with high molecular weight uPA also affects

cell-ECM adhesion and proliferation in cells such as breast carcinoma, prostate and head and neck squamous cell carcinoma (Liu *et al*., 2002; Czekay *et al*., 2003; Piccolella *et al*., 2008).

Other ligands of uPAR include the integrins, which are the major cell surface receptors involved in cell-ECM adhesion (Ossowski and Aguirre-Ghiso, 2000; Blasi and Sidenius, 2010). The uPAR protein has the ability to interact with several integrin types such as αvβ3, α3β1, α3β1 and α5β1 (Ulisse *et al*., 2009; Blasi and Sidenius, 2010). Pertinent to this study is the interaction of uPAR with β1-integrin at the cell surface, which affects cell-ECM adhesion based events in several cell types such as breast carcinoma, colon carcinoma as well as head and neck squamous cell carcinoma (Liu *et al*., 2002; Ahmed *et al*., 2003; Jo *et al*., 2007). This interaction relies on the full glycosylation of β1-integrin, since this produces the mature β1-integrin isoform (130 kDa) that is present at the plasma membrane (She *et al*., 2010).

The research regarding the role of the uPAR/β1-integrin interaction in cell-ECM adhesion events, has greatly benefitted from the use of short synthetic peptides such as P25, M25, α325 and β1P1, which specifically interfere and reduce the β1-integrin/uPAR interaction (Jo *et al*., 2007; Wei *et al*., 2005; Blasi and Sidenius, 2010). Wei *et al*. (2005) discovered that the serine residue at region 227 of β1-integrin is particularly important for the uPAR/β1-integrin interaction. This led to the subsequent development of a 9 aa peptide surrounding that region (β1P1) which is mapped to aa 224-232 of β1-integrin. This peptide disrupts the uPAR interaction with cell surface β1-integrin and functionally reduces cell-ECM adhesion events as was observed, for example, in mouse kidney epithelial cells (Wei *et al*., 2005).

Although cell-ECM adhesion is essential for normal physiological functioning of epithelial cells, it can also play an important role in pathological phenomena such as in carcinoma development (Charalabopoulos *et al*., 2005). In HOSCC, the cell-ECM adhesion and proliferation contribute to tumour development and therefore it is of vital importance to study the cell-ECM adhesion events in HOSCC (Smeds *et al*., 2002; Mori *et al*., 2008; Liu *et al*., 2009; Ortiz *et al*., 2010). The increased uPAR expression was observed in HOSCC *in vivo* compared to normal oesophageal squamous cells and uPAR role in cell-ECM adhesion was observed in several carcinomas (see above; Kan *et al*., 2001; Kashyap *et al*., 2009). However, the role of uPAR in cell-ECM adhesion events in HOSCC has been overlooked.

This part of the study examines the uPAR expression, uPA secretion and β1-integrin expression and in five HOSCC cell lines derived from moderately differentiated tumours from patients with metastatic disease (Veale and Thornley, 1989). Furthermore, this investigation

analyses whether there is a relationship between uPAR and β1-integrin in the HOSCC cell lines. The results from this section enable us to proceed with the next part of this study. This entails analysing the uPAR role in cell-ECM adhesion events in HOSCC.

2.2 Materials and methods

Note: All experiments were performed at room temperature, unless indicated otherwise.

A complete record of the reagents and their origin is listed in Appendix A (Chapter 9).

2.2.1 Cell lines and tissue culture

The HOSCC cell lines used in the current study are of South-African origin and derived from moderately differentiated tumours from patients with metastatic disease (Veale and Thornley, 1989). The cell lines: SNO (Bey *et al*., 1976) and Wits Human Carcinoma of the Oesophagus 1(WHCO1), WHCO3, WHCO5 and WHCO6 (Veale and Thornley, 1989) are from the Cell Biology Laboratory, School of Molecular and Cell Biology, University of the Witwatersrand.

The cells were passaged at 60 to 80 % confluency with trypsin/ethylenediaminetetra-acetic acid (EDTA) solution (Appendix 9.2.1). The cell lines were maintained in a Corning®10 cm tissue culture dishes supplemented with Dulbecco's Modified Eagle's Medium (DMEM)/Hams F12 (3:1) medium (Appendix 9.2.2) and 10% foetal calf serum (FCS). The cell lines were incubated at 37^{o}C in 5% carbon dioxide (CO_2) atmosphere in a humidified incubator.

Note for the following text:
DMEM/Hams F12 (3:1) medium is referred to as tissue culture medium in the following text.

2.2.2 RNA extraction

The RNA extraction was the first necessary step for the reverse transcriptase-polymerase chain reaction (RT-PCR) procedure. RNA was extracted from the HOSCC cell lines using TRIzol, which maintains RNA integrity while breaking down cell and cell components.

Cell at 60 to 80% confluency were rinsed four times with sterile phosphate buffered saline (PBS, Appendix 9.2.3). On the last rinse, a thin layer of PBS was left on top of the cells. Cells were scraped into that layer of PBS using a rubber policeman and transferred to an Eppendorf

tube. The cell suspension was centrifuged at 1145 x *g* for 3 min and excess PBS was removed. The cells were lyzed with 1 ml of TRIzol and the lysate was incubated for 5 min at room temperature. Chloroform (200 µl) was added to the lysate, mixed for 15 sec by shaking and incubated for 2 min at room temperature. Samples were centrifuged at 12000 x *g* for 15 min at 4^{o}C. The aqueous phase was placed into a new Eppendorf tube and 450 µl of isopropanol was added to precipitate the RNA. The samples were incubated for 10 min at room temperature and centrifuged at 12000 x *g* for 10 min at 4^{o}C. The supernatant was removed and the pellet was washed with 1 ml of 75% ethanol and centrifuged at 7500 x *g* for 5 min. The RNA pellet was resuspended in 50 µl of sterile Sigma nuclease free distilled water (dH_2O) and incubated for 10 min at 60^{o}C. The samples were stored at -70^{o}C.

2.2.3 cDNA synthesis

The reverse transcription of cDNA from newly extracted RNA (section 2.2.2) of the HOSCC cell lines was the next necessary step for RT-PCR.

Extracted RNA (2 µl) and 2 µl of random hexamer primers were added to an Eppendorf tube and incubated at 60^{o}C for 10 min. The mixture was placed on ice for 5 min and centrifuged at 1145 x *g* for 5 min. 5 µl of Moloney Murine Leukemia Virus-Reverse Transcriptase buffer (5x), 0.6 µl RNAsin, 2 µl dNTP mix, 1 µl Moloney Murine Leukemia Virus-Reverse Transcriptase and 12.4 µl dH_2O were added to the Eppendorf tube. The reaction mixture was incubated for 90 min at 37^{o}C. Subsequently, the mixture was incubated for 10 min at 90^{o}C to terminate the reaction. The sample was placed on ice for 5 min. 50 µl of phenol (Appendix 9.2.4):chloroform (25:24) and 25 µl of dH_2O was added to the mixture and vortexed for 10 sec. The mixture was centrifuged at 12 000 x *g* for 5 min and formed 2 phases. The aqueous phase was placed into a new Eppendorf tube and 70 µl of chloroform was added. The mixture was centrifuged at 12 000 x *g* for 5 min. The aqueous phase was placed in a new Eppendorf tube and 3 volumes of 100% ethanol as well as 10% 3 M sodium acetate (pH 5.2) were added. The mixture was incubated overnight at -20^{o}C. Subsequently the precipitated cDNA was centrifuged at 12000 x *g* for 20 min at 4^{o}C. The pellet was resuspended in 10 µl of sterile dH_2O. Samples were stored at -70^{o}C.

2.2.4 Primers

The following primers were used to amplify a 400 bp region of uPAR from newly synthesized cDNA. These primers were published in a paper by Wang *et al*. (2006).

The uPAR forward primer, 5' CTGGAGCTGGTGGAGAAAAG 3'
and uPAR reverse primer, 5' TGTTGCAGCATTTCAGGAAG 3'
Both primers were synthesized by Inqaba Biotec.

2.2.5 Reverse transcriptase-polymerase chain reaction (RT-PCR)

The cDNA of the different HOSCC cell lines was used to perform PCR reaction. The pRc/CMV-uPAR plasmid containing full length uPAR cDNA was used as a positive control (Appendix C; Kjøller and Hall, 2001). The cDNA (1 μl), 39 μl of PCR Master mix, 33 pmol of uPAR forward primer, 33 pmol of uPAR reverse primer and 5μl of *Taq* polymerase were added to a PCR tube. The mixture was centrifuged at 1145 x *g* for 10 sec and the PCR tube was placed in the thermal cycler (Hybaid, OmniGene). The PCR reaction consisted of 35 cycles. In the first cycle, the denaturing temperature of 94^{o}C was 5 min. Each cycle included a denaturing temperature of 94^{o}C (40 sec, with exception to the first cycle), an annealing temperature of 52^{o}C (40 sec), elongation temperature of 72^{o}C (1 min, with exception to the last cycle). In the last cycle, the duration of the elongation temperature was 10 min.

A 1% agarose gel (Appendix 9.2.5) was placed in Sigma Aldrich Electrophoresis Unit filled with Tris-acetate-EDTA (TAE) buffer (Appendix 9.2.6). 8 μl of ethidium bromide (1%) was added to the TAE buffer. The PCR products (5 μl) and GeneRuler 100 bp Plus DNA ladder were mixed with 5 μl of loading buffer (Appendix 9.2.7) and electrophoresed on the 1% agarose gel at a constant voltage of 72V.

2.2.6 Antibodies

Primary antibodies

-Rabbit anti-uPAR (FL-290) antibody (Santa Cruz Biotechnology, Inc) designated as anti-uPAR antibody.

-Rabbit anti-uPAR (399R) antibody (American Diagnostica) designated as anti-uPAR (399R) antibody.
-Rabbit anti-uPA (H-140) antibody (Santa Cruz Biotechnology, Inc) designated as anti-uPA antibody.
-Goat anti-β1-integrin (N-20) antibody (Santa Cruz Biotechnology, Inc) designated as anti-β1-integrin antibody.
-Rabbit anti-β-actin antibody (Sigma) designated as anti-actin antibody.

Secondary antibodies

-Horseradish peroxidase (HRP)-conjugated goat anti-rabbit antibody (Sigma) designated as HRP-anti-rabbit antibody.

-HRP-conjugated rabbit anti-goat antibody (Bio Yeda) designated as HRP-anti-goat antibody.
- Exactacruz ^{TM} F HRP-conjugated anti-rabbit antibody (Santa Cruz Biotechnology, Inc) designated as Exactacruz^{TM} HRP-anti-rabbit antibody.
-Fluoroscine isothiocyanate conjugated goat anti-rabbit antibody (Cappel) designated as FITC-anti-rabbit antibody.
-Tetramethylrhodamine isothiocyanate conjugated rabbit anti-goat antibody (Sigma) designated as TRITC-anti-goat antibody.

2.2.7 Treatment of the cells with β1P1

The β1P1 peptide (NLDSPEGGF) binds to uPAR and interferes with the uPAR/β1-integrin interaction in lung fibroblast and lung carcinoma cells (Wei *et al.*, 2005; Tang *et al.*, 2008). This peptide was used to analyse the interaction between uPAR and β1-integrin in the current study. The β1P1^{Sc} peptide (EDGLFNPSG) which contains a scrambled sequence of the β1P1 peptide, served as control peptide.

Prior to the experiment, the cells were passaged and cultured into 2 tissue culture dishes. Cells at 60% confluency were rinsed with 2 ml of PBS and tissue culture medium (4 ml) was added to the cells. After 4 hours, the cells were rinsed with 4 ml of tissue culture medium and 8 ml of tissue culture medium supplemented with either 0.02 mM β1P1^{Sc} control peptide or 0.02 mM β1P1 peptide was added to the cells. This is the concentration of peptide used to treat cells *in vitro* over a 24 hour period (Wei *et al.*, 2005). The cells were incubated at 37^{o}C in 5%

CO_2 atmosphere in a humidified incubator for 24 hours. The following day a whole cell extraction was performed (described in section 2.2.8 below).

2.2.8 Whole cell extraction

Whole cell extractions were performed on the HOSCC cell lines and cells treated with β1P1 or $\beta1P1^{Sc}$.

Cells at 60 to 80% confluency were rinsed four times with PBS/phenyl-methyl-sulphonyl-fluoride (PMSF)/trasylol (Appendix 9.2.8). On the last rinse, a thin layer of PBS was left on top of the cells. Cells were scraped into the layer of PBS and transferred to an Eppendorf tube. The cell suspension was centrifuged at 1145 x *g* for 5 min. Excess PBS was removed and a volume of radio-immunoprecipitation assay (RIPA) buffer (Appendix 9.2.9) between 350 µl to 750 µl was added in relation to the size of the pellet. The mixture was vortexed briefly and incubated on ice for 30 min. The samples were centrifuged at 12 000 x *g* for 10 min at 4^{o}C. The supernatant was subsequently placed in a new Eppendorf tube and stored at -70^{o}C.

2.2.9 Collection and concentration of conditioned medium

The conditioned medium collected from the HOSCC cell lines was used to analyse the concentration of uPA secreted by the HOSCC cell lines. **Day 1:** The HOSCC cell lines were harvested at 60% to 80% confluency and placed into Nunc^{TM} 6 cm tissue culture dish and maintained in tissue culture medium supplemented with10% FCS. The cells were incubated at 37^{o}C in 5% CO_2 atmosphere in a humidified incubator for 24 hours. **Day 2:** The cells were rinsed twice with 1 ml of PBS and 2.5 ml of tissue culture medium was added to the cells. After 4 hours, the cells were rinsed twice with 2 ml of tissue culture medium. Subsequently, 4 ml of tissue culture medium was added to the dish. **Day 3:** After 24 hours, the conditioned medium of the cells was collected and placed into Eppendorf tubes. Trasylol and PMSF (at a final concentration of 10 µl/ml and 1 mM, respectively) were added to the conditioned medium and samples were stored at -70^{o}C overnight. The cells remaining in the dish were harvested and counted with a haemocytometer. This established the number of cells that conditioned the medium.

Day 4: The conditioned medium was freeze dried and the chloroform/methanol method was used to concentrate the conditioned medium based on the protocol by Wessel and Flügge (1984). dH_2O (200 µl) was added to the freeze dried samples. Methanol (480 µl) and 120 µl of chloroform were added to the samples which were mixed by vortexing. dH_2O (640 µl) was added to the mixture, which was vortexed and centrifuged at 12 000 x *g* for 5 min at 4^{o}C. This formed two distinct phases and the upper layer was removed. Methanol (300 µl) was added, which was then vortexed and centrifuged at 12 000 x *g* for 30 min at 4^{o}C. The supernatant was removed and the pellet was air-dried under the laminar flow. The pellet was resuspended in Laemmli single lysis buffer (Appendix 9.2.10). The tubes containing the concentrated conditioned medium were immersed in boiling water for 5 min.

2.2.10 Protein estimation of the whole cell samples

Protein estimation was performed according to the protocol proposed by Bramhall *et al.* (1969) to determine the protein concentration. This method was specifically developed for protein extracts with a high concentration of detergent and reducing agents.

Filter paper (Whatman) were rinsed in distilled water (dH_2O) (20 min), 95% ethanol (5 min), 99.99% ethanol (5 min), acetone (5 min) and dried in a fume hood. Bovine serum albumin (BSA) was solubilised in RIPA buffer, to create a range of protein standards with a final concentration of 1 micro-gram (µg), 3 µg, 6 µg, 12 µg, 16 µg and 20 µg. These protein standards were spotted onto the prepared filter paper to create a standard curve. 5 µl of the whole cell samples of the HOSCC cells (from section 2.2.8) were also spotted onto the filter paper, which was subsequently dried in fume hood.

The filter paper was fixed in 7.5% trichloroactic acid (TCA) for 40 min and stained with 0.25% Coomassie Blue solution (Appendix 9.2.11) for 5 min to rinse off excess TCA. This was followed by staining of the filter paper with 0.25% Coomassie Blue solution for 40 min and destaining in destaining solution (Appendix 9.2.12) for 2 to 4 hours in the dark. The filter paper was dried briefly and the circles containing the protein (stained blue) were placed in 5 ml of elution solution (Appendix 9.2.13), overnight in the dark. The following day, the absorbance (Abs) of the various samples was read at 596 nanometers (nm) (Beckman Du®64 Spectrophotometer), with elution solution used as a "blank" (Abs set at 0). The Abs at 596 nm

of the protein standards was used to create the standard curve (Appendix 9.2.14). The protein concentration (in μg) of the whole cell samples was calculated from the standard curve.

2.2.11 Immunoprecipitation of uPAR

This procedure was used to isolate uPAR and associated proteins from the HOSCC cell lines and cells treated with β1P1 or β1P1^{Sc}. Immunoprecipitation was performed using the Exactacruz^{TM} F kit and the experimental procedure was performed according to the manufacture manual. This kit specifically eliminates the detection of heavy and light chain IgG during the Western blot procedure that follows immunoprecipitation.

Day 1: For each immunoprecipitation reaction, 3 μl of anti-uPAR (399R) antibody, 40 μl of Exactacruz^{TM} beads and 500 μl of PBS were added to an Eppendorf tube. The mixture was incubated overnight at 4^{o}C. **Day 2:** the mixture was centrifuged at 12 000 x *g* for 30 sec. The supernatant was removed and 500 μl of PBS was added to the tube which was centrifuged at 12 000 x *g* for 30 sec. This step was repeated twice. The supernatant was removed and 600 μg of whole cell sample of an HOSCC cell line (prepared in section 2.2.8) was added to the pellet containing beads and conjugated antibody. RIPA buffer was added to make a final volume of 750 μl in each reaction tube. As a negative control, 750 μl of RIPA buffer (without whole cell sample) was added to a tube containing beads and conjugated antibody. The reaction mix was incubated overnight at 4^{o}C. **Day 3:** The reaction mix was centrifuged at 12 000 x *g* for 30 sec. The supernatant was removed and 500 μl of PBS was added to each tube, which was centrifuged at 12 000 x *g* for 30 seconds. This step was repeated twice. The supernatant was removed and the pellet was resuspended in 40 μl of Laemmli double lysis buffer (Appendix 9.2.15). The tubes containing the anti-uPAR immunoprecipitated samples (uPAR IP samples) were immersed in boiling water for 5 min. IP samples were stored at -20^{o}C. The immunoprecipitation reaction was followed by a Western blotting procedure to detect uPAR and β1-integrin in the uPAR IP samples (described in section 2.2.15 and 2.2.18 respectively).

2.2.12 Immunoprecipitation of β1-integrin

This procedure was done to purify β1-integrin and associated proteins from the HOSCC cell lines. **Day 1:** anti-β1-integrin antibody (3 μl), 500 μg of RIPA whole cell sample was added

to an Eppendorf tube. As a control, 3 µl of anti-β1-integrin was mixed with 400 µl of RIPA buffer in an Eppendorf tube. The samples were incubated overnight at 4^{o}C. **Day 2:** Protein-G beads (30 µl) were added to each sample and immunoprecipitation buffer (IP buffer) (Appendix 9.2.16) was added to make a final volume of 600 µl. The reaction mix was incubated overnight at 4^{o}C. **Day 3:** The reaction mix was centrifuged at 12 000 x *g* for 30 sec. The supernatant was removed and 500 µl of IP-buffer was added to the pellet, which was centrifuged at 12 000 x *g* for 30 seconds. This step was repeated. The supernatant was removed and 500 µl of 0.1% of the IP-buffer was added to the pellet. The supernatant was removed and the pellet was resuspended in 40 µl of Laemmli single lysis buffer. The tubes containing the anti-β1-integrin immunoprecipitated samples (β1-integrin IP samples) were immersed in boiling water for 5 min. Samples were stored at -20^{o}C. The immunoprecipitation reaction was followed by a Western blot to detect uPAR (described in section 2.2.15).

2.2.13 Sample preparation for Sodium dodecyl sulphate-polyacrylamide gel electrophoresis (SDS-PAGE)

The whole cell samples from section 2.2.8 were prepared for an SDS-PAGE gel. The samples were diluted with an equal volume of Laemmli double lysis buffer. The tubes containing the samples were immersed in boiling water for 5 min. The samples were centrifuged briefly at 1145 x *g*.

2.2.14 SDS-PAGE

A 10% SDS-PAGE was prepared according to the protocol by Laemmli (1970). The gel was prepared by pouring a separating gel (Appendix 9.2.17) in-between a sealed silicone and glass plate using the Mighty Small^{TM} dual gel caster. Once the separating gel had polymerised, a stacking gel (Appendix 9.2.18) was poured and a comb was placed in the stacking gel to create wells. The polymerised gel was placed in the Mighty Small ^{TM} Unit filled with electrophoresis buffer (Appendix 9.2.19). Whole cell samples (15 µg, section 2.2.13), concentrated conditioned medium samples according to 5 x 10^{6} cells (section 2.2.9) and 20 µl of uPAR and β1-integrin IP samples of each of the HOSCC cell line were loaded into the different wells. In a separate lane, 2.5 µl of PageRuler^{TM} prestained protein ladder was loaded. The protein ladder contains standard proteins with molecular weights of 10, 15, 25, 40, 55, 70,

100, 130 and 170 kilodaltons (kDa). The whole cell lysate samples and the pre-stained ladder were electrophoresed on the gel at a constant current of 25 milli-Amps (mA) until the 10 kDa band was a cm from the bottom of the gel. To view the resolved samples on the gel, the gel was stained with 0.25% Coomassie Blue solution (1 hour) and destained for 2 hours with destaining solution (Appendix 9.2.20).

2.2.15 Western blot procedure (detection of uPAR)

Western blotting was performed according to the protocol proposed by Towbin *et al*. (1979). The whole cell samples of the HOSCC cell lines (15 μg, section 2.2.13) and IP samples (20 μl, section 2.2.11 and 2.2.12) were electrophoresed on a 10% SDS-PAGE gel (section 2.2.14). **Part 1**: The resolved proteins were electro-transferred onto Sartorius nitrocellulose using the Biorad mini trans-blot system filled with Towbin electrophoresis transfer buffer (Appendix 9.2.21, Towbin *et al*., 1979) at 400 mA for 2 hours. **Part 2:** The nitrocellulose was rinsed 3 times in Tris buffer saline (TBS, Appendix 9.2.22). The nitrocellulose was incubated in 5% BSA in TBS containing 0.1% Tween 20 (TBS-T) for 1 hour. Nitrocellulose was rinsed thrice with TBS-T and incubated with anti-uPAR antibody (1:5000) in TBS-T for 18 hours at 4^{o}C. The nitrocellulose was rinsed 5 times (at 5 min intervals) with TBS-T and rinsed once (for 5 min) with 5% skim milk in TBS-T. The nitrocellulose was subsequently incubated in HRP-anti-rabbit antibody (1:10000) in TBS for an hour, in the dark. In the case of detecting uPAR in the uPAR IP samples and β1-integrin IP samples, the nitrocellulose was incubated with Exactacruz^{TM} HRP-anti-rabbit antibody (1:10000), in the dark. All subsequent steps in this procedure were performed in a dark environment. The nitrocellulose was rinsed 6 times (at 5 min intervals) with TBS-T. **Part 3:** The nitrocellulose was placed in a luminol:peroxide (1:1) solution from the SuperSignal West Pico Chemiluminescent Substrate kit for 5 min. The nitrocellulose was sealed with nylon and exposed onto hyperfilm (Separations) for 10 min. The hyperfilm was developed for 5 min in developer solution (Appendix 9.2.23), rinsed with water, fixed for 5 min in fixer solution (Appendix 9.2.24), and rinsed with water.

2.2.16 Western blot procedure (detection of actin)

The detection of actin in the Western blot was used as a loading control. The whole cell samples of the HOSCC cell lines (15 μg section 2.2.13) were electrophoresed on a 10% SDS-PAGE gel (section 2.2.14). **Part 1:** performed according to the “Part 1” procedure described

in materials and methods, section 2.2.15. **Part 2:** The nitrocellulose was rinsed 3 times in TBS and incubated in casein based BLOTTO solution (Appendix 9.2.25), for an hour. Nitrocellulose was rinsed thrice with PBS and incubated with anti-actin antibody (1:5000) in PBS for an hour. The nitrocellulose was rinsed 6 times with PBS at 5 min intervals. The nitrocellulose was incubated with HRP-anti-rabbit antibody (1:10000) in PBS for an hour, in the dark. All subsequent steps in this procedure were performed in a dark environment. The nitrocellulose was rinsed 6 times with PBS at 5 min intervals. **Part 3:** performed according to the "Part 3" procedure described in materials and methods, section 2.2.15.

2.2.17 Western blot procedure (detection of uPA)

The Western blot was performed according to the procedure described in materials and methods, section 2.2.15, with the following exception:

Concentrated conditioned medium samples according to 5 x 10^6 cells (prepared in section 2.2.9) were electrophoresed on a 10% SDS-PAGE.
Part 2: the primary antibody used in the procedure was anti-uPA antibody (1:1000) in TBS-T.

2.2.18 Western blot procedure (detection of β1-integrin)

The whole cell samples of the HOSCC cell lines (15 μg, section 2.2.13) and uPAR IP samples (20 μl, section 2.2.11) were electrophoresed on a 10% SDS-PAGE gel (section 2.2.14). **Part 1:** performed according to the "Part 1" procedure described in materials and methods, section 2.2.15. **Part 2:** The nitrocellulose was rinsed 3 times in TBS and incubated in BLOTTO solution, for an hour. Nitrocellulose was rinsed thrice with PBS and incubated with anti-β1-integrin antibody (1:750) in PBS for 2 hours. The nitrocellulose was rinsed 6 times with PBS at 5 min intervals. The nitrocellulose was incubated with HRP-anti-goat antibody (1:30000) in PBS for an hour, in the dark. All subsequent steps in this procedure were performed in a dark environment. The nitrocellulose was rinsed 6 times with PBS at 5 min intervals. **Part 3:** performed according to the "Part 3" procedure described in materials and methods, section 2.2.15.

2.2.19 Image analysis

Labworks ™ Image Acquisition and Analysis software (Labworks version 4.5) was used for densitometric analysis to quantitatively determine the concentration level of uPAR, uPA, actin and β1-integrin in the respective Western blots.

2.2.20 Indirect immunofluorescence and confocal microscopy

Indirect immunofluorescence was performed to detect the localization of uPAR in each of the HOSCC cell lines. Cells at 60% confluency were rinsed 3 times with PBS and fixed with 4% paraformaldehyde (Appendix 9.2.26) for 30 min. The cells were subsequently rinsed with PBS and the 10 cm dish was cut into a shape of a slide. The slide was rinsed 5 times with PBS and cells were permeabilized with 0.25% Triton-X-100 for 10 min. The slide was rinsed 3 times with PBS, followed by a rinse with dH_2O and then air-dried. A DAKO pen was used to draw circles to create wells on the slide. The wells were designated as the experimental and negative-control. The cells in the wells were rehydrated with 1% BSA in PBS for 30 min. The cells in the experimental and negative-control wells were incubated with anti-uPAR antibody (1:1000) in PBS or just PBS respectively, for 16 hours at 4^oC. Subsequently, the cells were rinsed 6 times with PBS at 1 min intervals. The cells in the experimental and control wells were incubated with FITC-anti-rabbit antibody (1:500) in PBS for 1 hour, in the dark. All subsequent steps in this procedure were performed in a dark environment. The cells were rinsed 6 times with PBS at 1 min intervals and 10 µl of VECTASHIELD® HardSet™ Mounting Medium was added to each well. The cells were viewed with Zeiss LSM 410 confocal microscope at a magnification of 400 x (FITC excitation wavelength = 488 nm; Pinhole: 20).

2.2.21 Double immunofluorescence and confocal microscopy

Double immunofluorescence was performed to detect the localization of uPAR and β1-integrin in the HOSCC cell lines. This was done according to the procedure described in materials and methods, section 2.2.20, with the following exception:

Primary antibodies: The cells in the experimental wells were incubated with anti-uPAR antibody (1:500) and anti-β1-integrin antibody (1:500) in PBS at a 1:1 ratio. The final concentration of both antibodies was therefore 1:1000.

Secondary antibodies: the cells in the experimental and negative control wells were incubated with FITC-anti rabbit antibody (1:250) and TRITC-anti goat antibody (1:250). The final concentration of both antibodies was therefore 1:500.

Excitation wavelength: The cells were viewed with Zeiss LSM (410) confocal microscope at a magnification of 400 x (FTIC excitation wavelength = 488 nm; TRITC excitation wavelength = 568 nm; Pinhole: 20).

2.3 Results

2.3.1 The expression of uPAR in the HOSCC cells

The PCR product of 400 bp, which correspond to the targeted uPAR transcript region, was successfully amplified from the cDNA of the HOSCC cells or the pRc/CMV-uPAR vector (Figure 2.1.a). This vector contains full length uPAR cDNA and served as a positive control (Appendix C). Sequencing analysis confirmed that the PCR products match the uPAR transcript region spanning exons 3 to 5 (Figure 2.1.b). This means that the uPAR transcript is expressed in all the HOSCC cell lines.

The uPAR protein (60 kDa) is present in the cell extracts of all the HOSCC cell lines as established by Western blotting analysis (Figure 2.2.a). uPAR was not detected in cell extracts of HEK293 cells, which do not express uPAR (figure not shown; Chaurasia *et al*., 2006). There is also a detection of the unglycosylated or cleaved uPAR (35 kDa) protein in the cell extract of the WHCO5 cell line (Figure 2.2.a). Importantly, the results confirm that the full uPAR isoform (60 kDa), which is involved in cell-ECM adhesion events, is expressed in the HOSCC cell lines.

The expression of actin (42 kDa) in the whole cell extracts of the HOSCC cell lines verified the equal loading concentration of the whole cell extract used for the uPAR Western blot. Densitometric analysis of the uPAR Western blot established that expression level of the uPAR protein varied within the HOSCC cell lines. The highest concentration of total uPAR was in the WHCO6 cell line, while the lowest was in the SNO cell lines. The difference in expression of uPAR between the two cell lines being a substantial 14.22 fold (Figure 2.2.b).

2.3.2 The distribution of uPAR in the HOSCC cells

The localization of uPAR within the HOSCC cells was at the cytoplasmic and membrane regions (white arrow), perinuclear region (blue arrow) and excluded from the nucleus (purple arrow) (Figure 2.3). Since uPAR is a membrane protein, membrane staining of uPAR was expected but proved to be indistinct. The apparent low level nuclear signal observed in the WHCO1 cells, is interpreted as a product of the relatively higher background (Figure 2.3). The negative control (only FITC-conjugated antibody) did not produce a fluorescence signal illustrating the specificity of this reaction.

a.

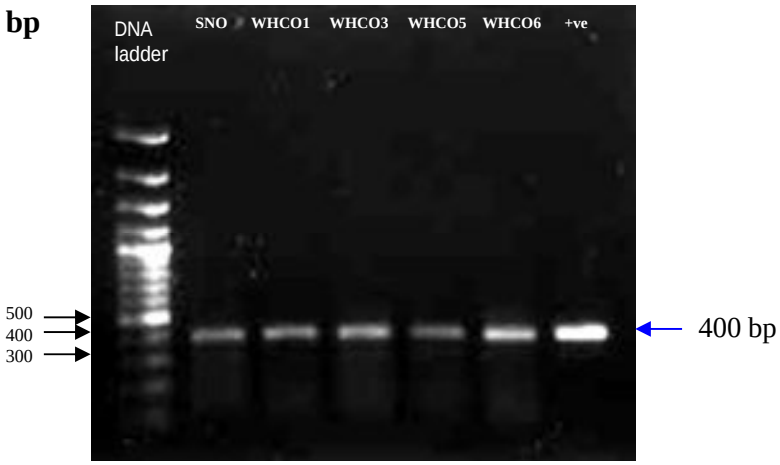

b.i.

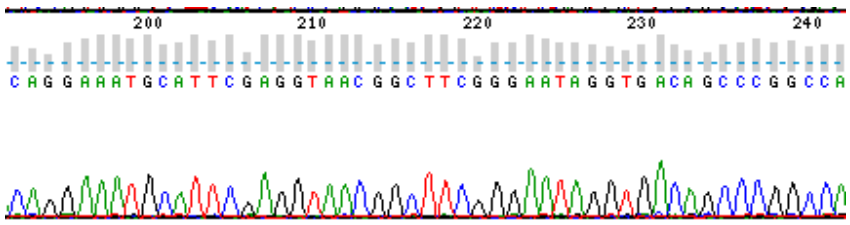

b.ii GENE ID: 5329 PLAUR | plasminogen activator, urokinase receptor [Homo sapiens]

Query 195	GAAATGCATTCGAGGTAACGGCTTCGGGAATAGGTGACAGCCCGGC	240
Sbjct 582	GAAATGCATTCGAGGTAACGGCTTCGGGAATAGGTGACAGCCCGGC	537

Figure 2.1: The uPAR mRNA is transcribed in all the HOSCC cells. **(a)** The PCR products of all the HOSCC cell lines and the positive control were present at 400 bp (blue arrow). Agarose gel = 1%. **(b.i)** A section of the sequencing result of WHCO5 PCR product. The WHCO5 PCR product was used as an example to represent the other HOSCC cell lines, which all showed similar results. **(b.ii)** Part of the BLAST result of the sequence analysis. **Note:** for full sequencing result of all the HOSCC cell lines refer to Appendix C; + ve = positive control (pRc/CMV-uPAR vector; Appendix C).

a.

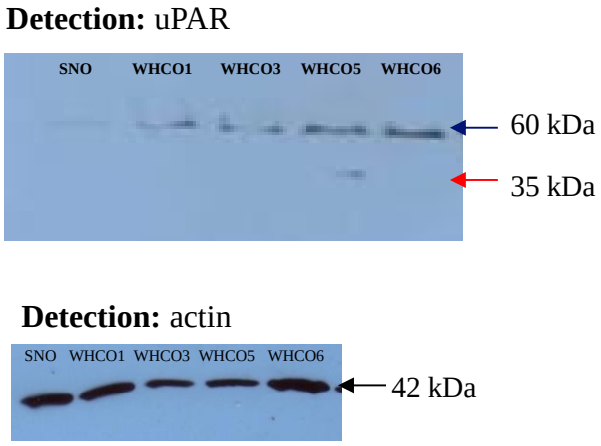

b.

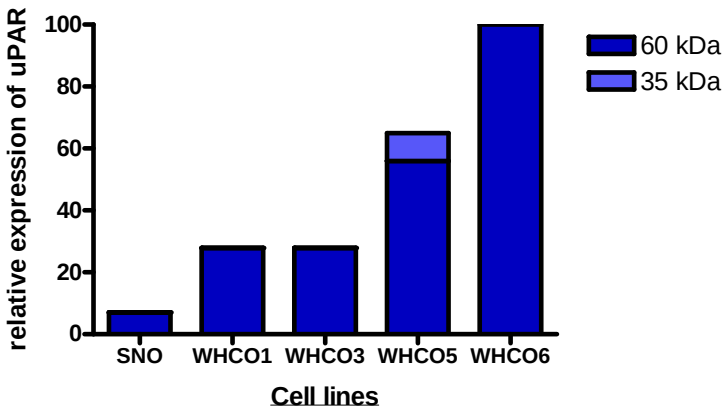

Figure 2.2: Western blot and semi-quantitative analysis of uPAR protein expression in the HOSCC cell lines. **(a)** The uPAR protein is expressed in all the HOSCC cell lines. Blue arrow = uPAR (60 kDa) and red arrow = unglycosylated or cleaved uPAR (35 kDa). The actin Western blot was used as a loading control. **(b)** Histogram of the associated uPAR Western blot represents the relative expression levels of uPAR across the HOSCC cell lines. The maximum expression level of uPAR was set at 100%.

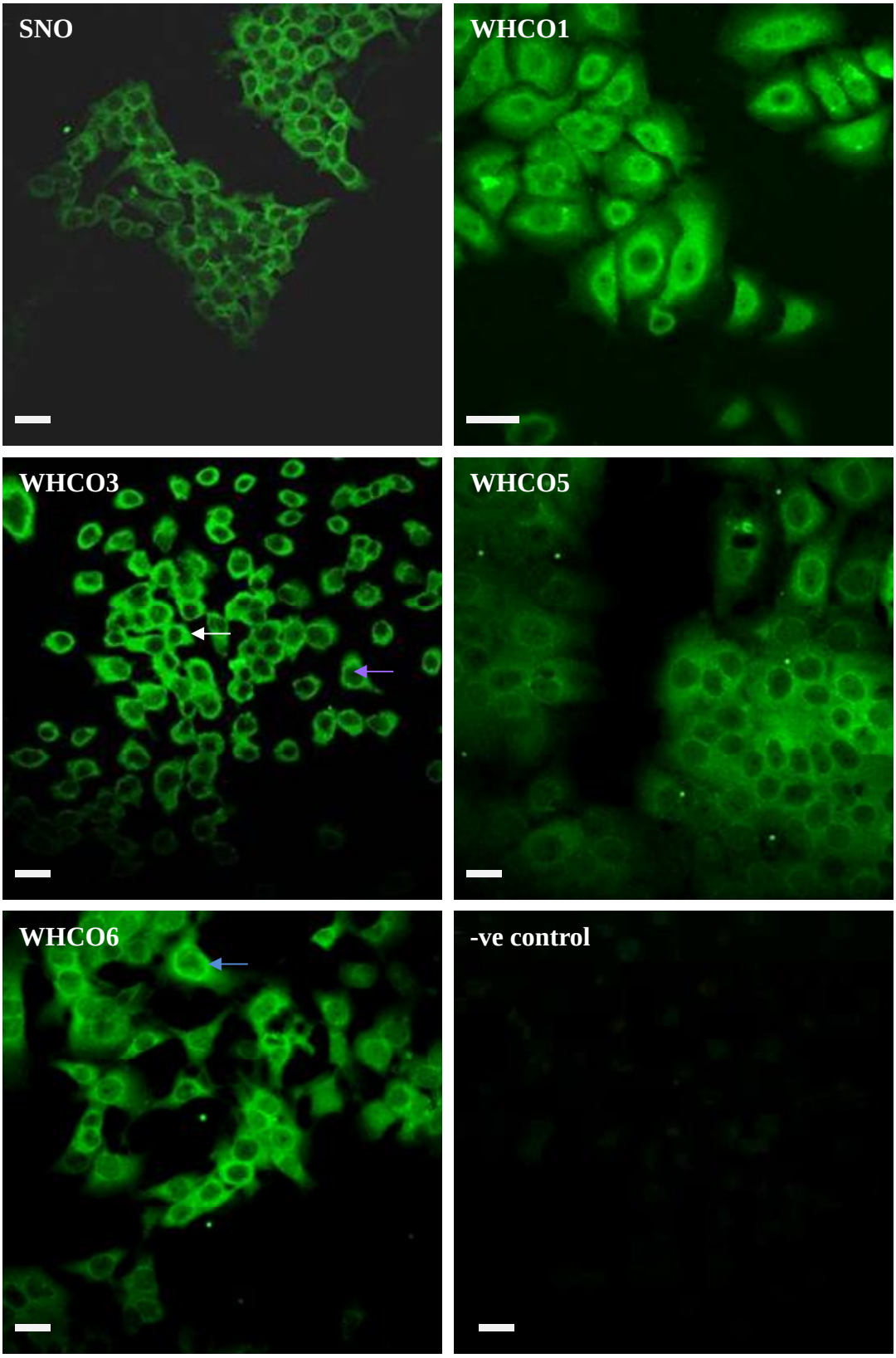

Figure 2.3: The localisation of uPAR in the HOSCC cells. The presence of uPAR appears as a green fluorescence in the HOSCC cells. uPAR localized in the cytoplasm and membrane region (white arrow), perinuclear region (blue arrow) and not in the nucleus (purple arrow). **Note:** – ve control = negative control; Fluorescence excitation wavelength = 488 nm; Bar = 25 μm

2.3.3 The HOSCC cells secrete uPA

The HOSCC cells conditioned serum-free medium for 24 hours. The full isoform uPA (55 kDa) was present in the medium conditioned by the HOSCC cell lines as established by Western blotting (Figure 2.4.a). Furthermore, a 40 kDa fragment, which corresponds to the cleaved uPA product under reducing conditions, was present in the conditioned medium of the WHCO1 and the WHCO5 cells (Figure 2.4.a). These results confirm that all the HOSCC cell lines secrete uPA. Densitometric analysis quantitatively determined that the WHCO5 cell line secreted the highest amount of total uPA per cell line, followed by WHCO1, SNO, WHCO6 and WHCO3 (Figure 2.4.b).

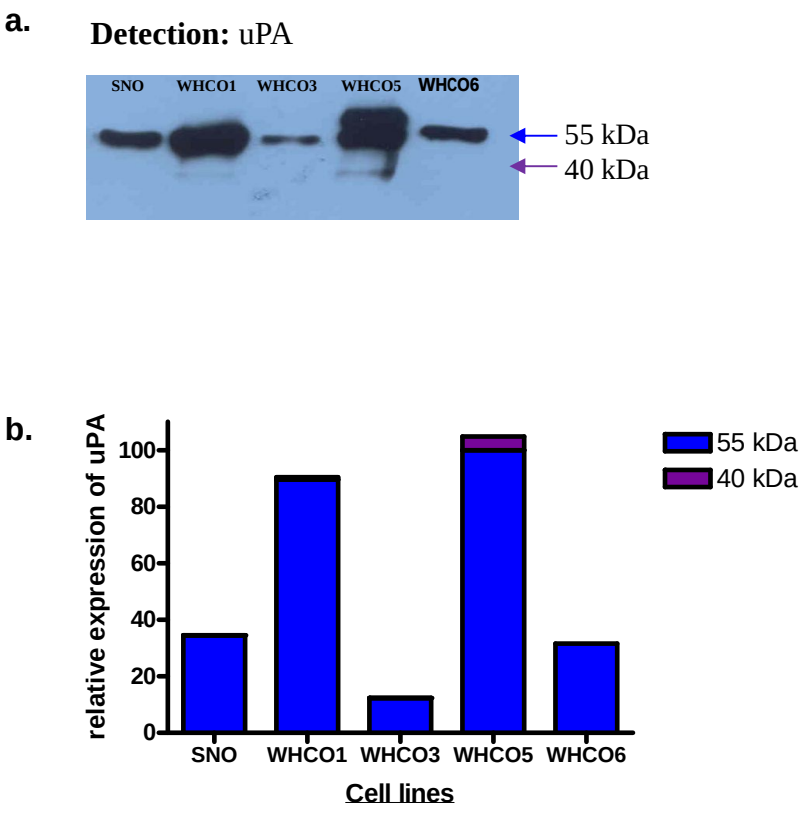

Figure 2.4: Western blot and semi-quantitative analysis of uPA secreted into the conditioned medium of the HOSCC cell lines. (a) Western blot confirmed the presence of full chain uPA (55 kDa, blue arrow) or cleaved uPA (40 kDa, purple arrow) in the conditioned medium of the different HOSCC cell lines. **(b)** Histogram represents semi-quantitative concentration level of uPA of the associated Western blot. The expression of uPA is represented in the histogram as a relative percentage, with the maximum expression of uPA set as 100%.

2.3.4 β1-integrin expression in the HOSCC cells

The expression of partially glycosylated β1-integrin (110 kDa) and the cell-surface associated β1-integrin (130 kDa) isoforms was confirmed in the all the HOSCC cell lines by Western blotting (Figure 2.5). The 130 kDa β1-integrin isoform is the isoform specifically involved in cell-ECM adhesion events. The Western blot for actin was used as a loading control. Densitometric analysis demonstrated that the 110 kDa β1-integrin and the 130 kDa cell surface associated β1-integrin isoform expression was highest in the WHCO1 cells. Furthermore, the concentration of the 130 kDa β1-integrin was higher than the 110 kDa β1-integrin in all the HOSCC cell lines (Figure 2.5).

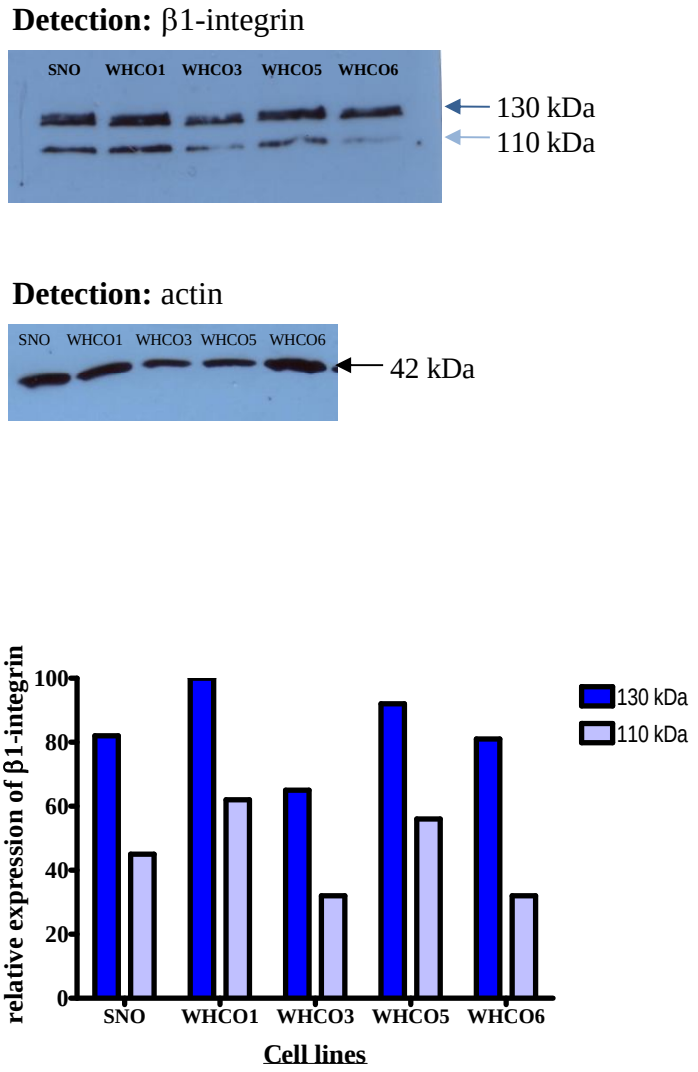

Figure 2.5: Western blot and semi-quantitative analysis of β1-integrin protein expressed by the HOSCC cell lines. The β1-integrin was expressed in all the HOSCC cell lines. Dark blue arrow = 130 kDa cell surface associated β1-integrin and light blue arrow = 110 kDa partially glycosylated β1-integrin. The actin Western blot was used as a loading control. The Histogram of the associated β1-integrin Western blot represents the relative expression levels of β1-integrin across the HOSCC cell lines.

2.3.5 uPAR localises to the same region as β1-integrin in the HOSCC cells

The distribution of uPAR and β1-integrin in the HOSCC cell line were analyzed by double immunofluorescence assay, using specific antibodies directed against uPAR or β1-integrin. In the HOSCC cells, uPAR (green fluorescence) and β1-integrin (red fluorescence) localised to the perinuclear region (white arrow) as well as cellular protrusions (purple arrow) of the HOSCC cell lines (Figure 2.6). The region of similar localisation between uPAR and β1-integrin is seen as yellow fluorescence in the merged image. In the WHCO1, WHCO5 and WHCO6 cell lines, there was also a distinct localisation of uPAR and β1-integrin at the membrane region of certain cells (light blue arrow) (Figure 2.6).

2.3.6 The uPAR/β1-integrin interaction in the HOSCC cells

The uPAR protein and associated proteins were immunoprecipitated from whole cell lysate of the HOSCC cell lines with anti-uPAR antibody. The pre-glycosylated β1-integrin (110 kDa) was present in the anti-uPAR immunoprecipitates of the HOSCC cell lines with the exception of the WHCO5 cell line (Figure 2.7.a). This confirmed the association between uPAR and 110 kDa β1-integrin. It should be noted that SNO expressed the lowest level of uPAR (Figure 2.2.a) yet the concentration of β1-integrin (110 kDa) that immunoprecipitated with uPAR was higher in this cell line compared with the other HOSCC cell lines. The explanation for this is that the ratio of uPAR interacting with β1-integrin (110 kDa) is higher in the SNO cell line than in the other cell lines. The cell-surface associated β1-integrin (130 kDa) was also present in the anti-uPAR immunoprecipitates of the WHCO3 and WHCO6 cell lines (Figure 2.7.a). This established the interaction between uPAR and cell-surface associated β1-integrin, which is of significant importance to this study since this interaction plays a role in cell-ECM adhesion based events.

To confirm whether there is an interaction between uPAR and β1-integrin in the WHCO5 cells, the β1-integrin was immunoprecipitated from the whole cell-lysate of the WHCO5 cell line. A 60 kDa band corresponding to the size of uPAR was present in the anti-β1-integrin immunoprecipitate of the WHCO5 cell line, but not in the negative control (immunoprecipitation beads and anti-β1-integrin antibody only; Figure 2.7.b).

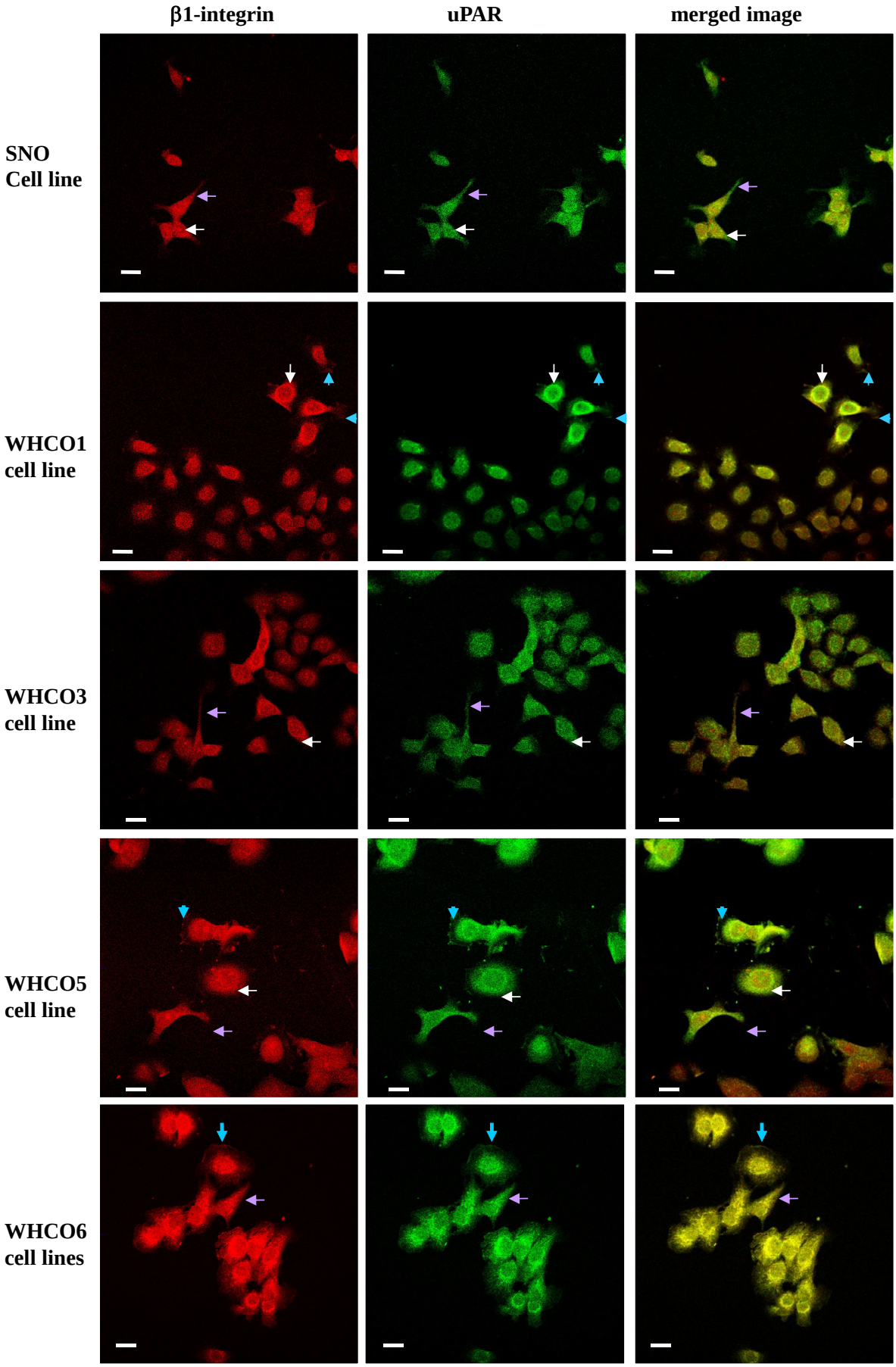

Figure 2.6: β1-integrin and uPAR localise in the same regions of the HOSCC cells. β1-integrin (red) and uPAR (green) were present at the membrane region (light blue arrow), perinuclear region (white arrow) as well as cellular protrusion (purple arrow) of the HOSCC cells. The region with similar localization between uPAR and β1-integrin is in yellow. **Note:** FITC excitation wavelength = 488 nm; TRITC excitation wavelength = 568 nm; Bar = 25 μm.

The light chain IgG band (25 kDa) was present in the anti-β1-integrin immunoprecipitate as well as the negative control (Figure 2.7.b). Thus, there is a positive interaction between uPAR and β1-integrin in the WHCO5 cells.

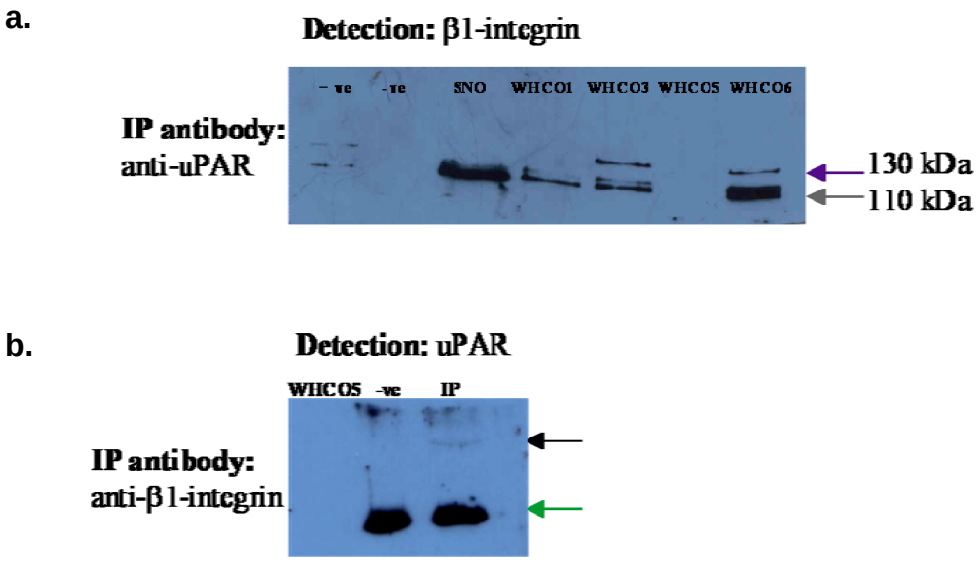

Figure 2.7: The interaction between uPAR and β1-integrin in the HOSCC cells. (a) β1-integrin (110 kDa, grey arrow) was detected in the anti-uPAR immunoprecipitates from the SNO, WHCO1, WHCO3 and WHCO6 cells. Cell-surface associated β1-integrin (130 kDa) was detected in the anti-uPAR immunoprecipitates of WHCO3 and WHCO6 cells (purple arrow). **(b)** uPAR (black arrow) was present in the anti-β1-integrin immunoprecipitate from the WHCO5 cells. The green arrow indicates IgG bands at 25 kDa. **Note:** +ve = positive control (15 μg of WHCO6 whole cell sample); -ve = negative control (beads and IP antibody only); IP= immunoprecipitated samples.

2.3.7 Stability of the uPAR/β1-integrin interaction

The β1P1 peptide generated by Wei *et al*. (2005), which blocks the uPAR interaction with β1-integrin, is used in this study to analyse the role of uPAR/β1-integrin interaction on cell-ECM adhesion based events. A peptide of the same length, containing the same amino acids but in a random sequence ($\beta1P1^{Sc}$ peptide) was used as a control (Wei *et al*., 2005).

It was necessary to confirm that the β1P1 blocking peptide used in this study successfully disrupts the uPAR interaction with β1-integrin in the HOSCC cells. The WHCO6 cell line which has a detectable uPAR interaction with cell-surface associated β1-integrin was chosen for this analysis.

The pre-glycosylated β1-integrin (110 kDa) and cell-surface associated β1-integrin (130 kDa) were detected in the anti-uPAR immunoprecipitates of WHCO6 cells exposed to either the

β1P1^{Sc} control peptide or β1P1 (Figure 2.8.a). Densitometric analysis revealed that the expression of 110 kDa β1-integrin was similar in the anti-uPAR immunoprecipitates of WHCO6 cells treated with either β1P1 blocking peptide or β1P1^{Sc} control peptide (Figure 2.8.b.i). Pertinent to this study, the expression of cell surface associated β1-integrin (130 kDa) was 4.6 fold lower in the anti-uPAR immunoprecipitates of WHCO6 cells treated with β1P1 versus β1P1^{Sc} (Figure 2.8.b.ii). This means that exposure of cells to the β1P1 blocking peptide caused a specific reduction between the interaction of uPAR and cell-surface β1-integrin. The β1P1 peptide thus can serve as a valuable tool in this investigation.

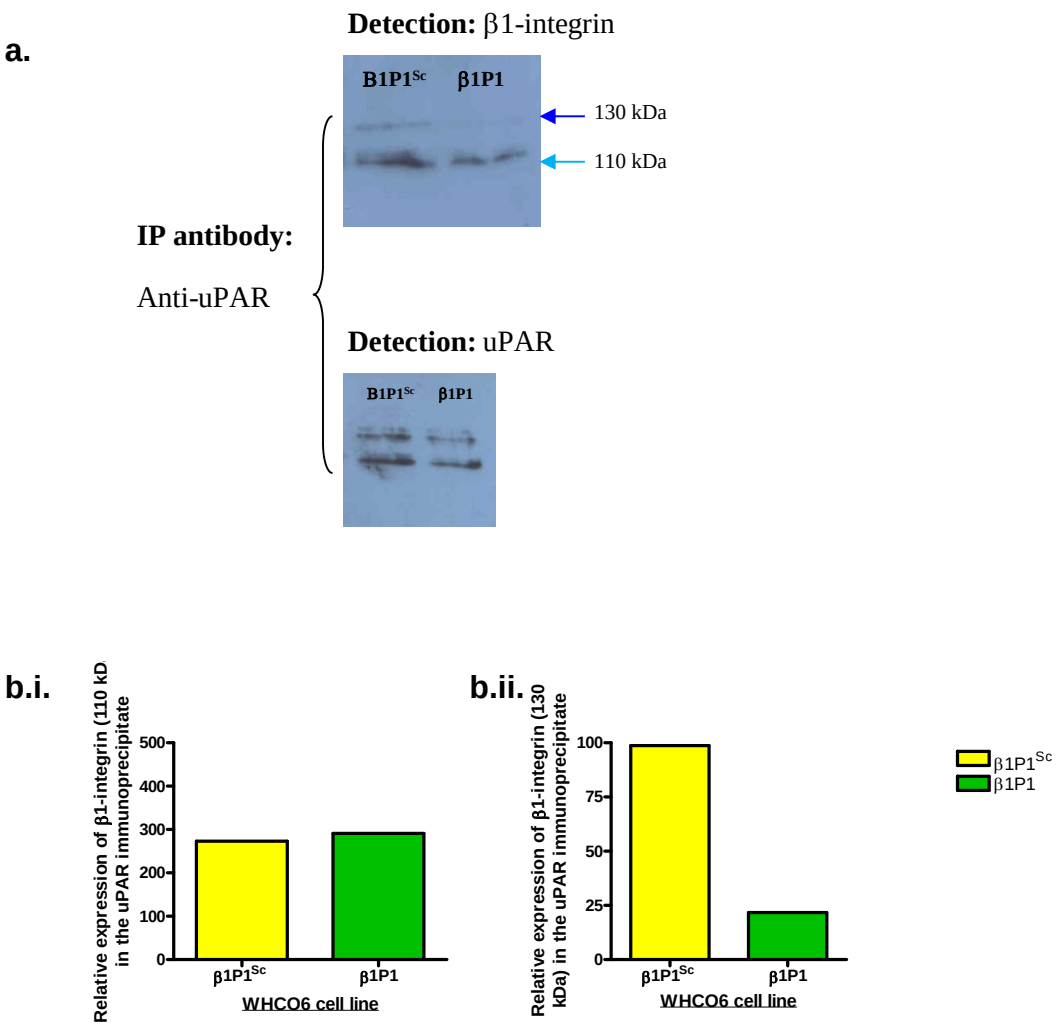

Figure 2.8: Western blot and semi-quantitative analysis of uPAR interaction with β1-integrin in WHCO6 cells exposed to β1P1 blocking peptide or β1P1^{Sc} control peptide. **(a)** The expression of β1-integrin or uPAR in the anti-uPAR immunoprecipitates from WHCO6 cells treated with β1P1 and β1P1^{Sc} control. Light blue arrow = 110 kDa β1-integrin and dark blue arrow = 110 kDa β1-integrin. (**b**) The Histogram represents the relative expression of **(i)** 110 kDa or **(ii)** 130 kDa β1-integrin in the anti-uPAR immunoprecipitated samples of the WHCO6 cells upon exposure to β1P1^{Sc} peptide (yellow bar) or β1P1 peptide (green bar). The relative expression of β1-integrin in the different anti-uPAR immunoprecipitated samples of the WHCO6 cells was standardized according to the amount of uPAR present in these samples. **Note:** IP= immunoprecipitated samples.

2.4 Discussion

The particular function of uPAR in cell-ECM adhesion and proliferation in HOSCC is the focus of this study. This chapter forms the foundation of this study in that it provides the expression of uPAR and two of its ligands, uPA and β1-integrin in five HOSCC cell lines derived from moderately differentiated tumours.

All the HOSCC cell lines expressed the uPAR mRNA transcript with exons 3 to 5 being present in the transcript (Figure 2.1). At a translational level, the predominant uPAR isoform detected in the HOSCC cell lines is the D1D2D3 (60 kDa) isoform (Figure 2.2). Importantly, this is the isoform necessary for interaction with uPA, β1-integrin and vitronectin to carry out cell adhesion events (Behrendt *et al.*, 1996; Li *et al.*, 2003; Sato *et al.*, 2011). Interestingly thyroid cells express the D1D2D3 and the D2D3 uPAR isoforms, but the D2D3 uPAR expression is higher in normal thyroid cells than in papillary and follicular thyroid carcinoma, while anaplastic thyroid carcinoma cells do not express the D2D3 isoform (Ragno *et al.*, 1998). A possible reason for this is that in normal cells, uPAR activity is regulated by proteolytic cleavage of the D1 domain, which limits the effect of uPAR in adhesion-based events (Ragno *et al.*, 1998). This further highlights the significance of the full uPAR isoform in carrying out its events, which may contribute to cancer development and maintains the carcinoma condition.

The uPAR protein was distributed in the perinuclear, cytoplasm and membrane regions of the cells (Figure 2.3) The perinuclear distribution of uPAR is most likely due to the presence of uPAR in the endoplasmic reticulum (which is continuous with the nuclear membrane) where it undergoes glycosylation and addition of the GPI tail (Ploug *et al.*, 1998). The cytoplasmic staining of uPAR can be due to several reasons such as the presence of uPAR in the Golgi (in vesicles en route to the membrane), or also due to internalization of uPAR (Czekay *et al.*, 2001). The presence of uPAR at the cell membrane is of particular importance in this study as membrane bound uPAR is necessary to regulate cell-ECM adhesion events.

The major ligand of uPAR is uPA and previous experiments using radial casinolysis assays by Veale *et al.* (1990) established that the HOSCC cell lines used in this study all have a positive urokinase-like activity. This current study confirmed that uPA is indeed secreted by all the HOSCC cells lines (Figure 2.4). Importantly, uPA contributed to cell adhesion and proliferation in several carcinomas such as breast carcinoma and head and neck squamous cell carcinoma (Czekay *et al.*, 2003; Liu *et al.*, 2002; Gandhari *et al.*, 2006). Therefore the uPA secreted by the HOSCC cell lines may contribute to their adhesion and proliferation.

The β1-integrin is expressed in all the HOSCC cell lines. Additionally, the β1-integrin and uPAR co-distributed to the same region of the HOSCC cell lines (Figure 2.6). Although, the uPAR and β1-integrin localised in similar regions within the HOSCC cells, the resolution of the fluorescence microscope is less than the actual size of these proteins. Therefore, this procedure could not confirm whether uPAR and β1-integrin are in a sufficiently close proximity to identify a direct interaction.

Immunoprecipitation analysis confirmed that uPAR and β1-integrin associate in all five of the HOSCC cell lines (Figure 2.7). In the SNO, WHCO1, WHCO3 and WHCO6 lines, there was a detectable interaction between uPAR and the partially glycosylated β1-integrin (110 kDa) isoform. This β1-integrin isoform is not present at the plasma membrane (She *et al*., 2010). Therefore, the interaction between uPAR and β1-integrin (110 kDa) is not at the cell surface. This interaction possibly occurs in the endoplasmic reticulum as these proteins undergo glycosylation, or in the Golgi vesicles since both proteins are en route to the membrane (Ploug *et al*., 1998; She *et al*., 2010).

There is an interaction between cell surface associated β1-integrin (130 kDa) with uPAR in two of the HOSCC cell lines (WHCO3 and WHCO6). This interaction contributes to adhesion-based events in several transformed cancer cell types such as breast carcinoma, lung carcinoma and head and neck squamous cell carcinoma (Liu *et al*., 2002; Jo *et al*., 2007; Tang *et al*., 2008). This brings about the question, why is the uPAR and cell-surface associated β1-integrin interaction only detectable in these two HOSCC cell lines? At the cell surface, uPAR can also associate with several other receptors such as G protein coupled receptor FPRL1, epidermal growth factor receptor, β3 and αv integrin subunits (Mazzieri *et al*., 2006; Blasi and Sidenius, 2010). The ratio of the uPAR interaction with other cell surface associated molecules, including β1-integrin, is such that the uPAR interaction with β1-integrin may only be detectable in the WHCO3 and WHCO6 cells.

In the presence of β1P1 blocking peptide, there was a reduced interaction between uPAR and cell-surface associated β1-integrin in the WHCO6 cells. This makes the β1P1 peptide an extremely useful tool when analysing the specific role of the interaction in the context of cell adhesion and proliferation. Interestingly, it was only the interaction between uPAR and the cell-surface β1-integin (130 kDa) that was affected upon exposure of the cells to the β1P1 peptide (Figure 2.8). This reiterates the point made earlier, that the interaction between uPAR and 110 kDa β1-integrin does not occur at the cell surface.

In conclusion: The HOSCC cell lines used in this study all express the particular uPAR isoform that can play a part in adhesion-based events. Furthermore, the same HOSCC cell lines all secrete uPA, the major ligand of uPAR, and uPAR interacts with cell-surface associated β1-integrin in two of the HOSCC cell lines (WHCO3 and WHCO6). This data allows us to continue the investigation and establish whether uPAR plays a role in the cell-ECM adhesion based events of the HOSCC cell lines.

Chapter 3: The uPAR forms a unique cell-ECM adhesion complex with ILK and caveolin in the HOSCC cell lines

3.1 Introduction

The connection between cell adhesion molecules and the cytoskeleton provides the structural stability that is crucial for these molecules to establish functional cell adhesion events (Brakebusch and Fässler, 2003; Dagnino, 2011). The uPAR protein plays a role in adhesion based events of several cell types such as endothelial cells, adenoid cystic carcinoma and colon carcinoma onto the extracellular matrix (ECM) (Ahmed *et al*., 2003; Abu-Ali *et al*., 2005; Balsara *et al*., 2011). For uPAR to be actively involved in these cell-ECM adhesion events, it must have a relationship with the cytoskeleton (Chandrasekar *et al*., 2003; Bernstein *et al*., 2004). This was clearly demonstrated in adenoid cystic carcinoma cells, where uPAR assembled with actin adaptor protein, vinculin, at focal adhesions when the cells were plated on collagen type I (Abu-Ali *et al*., 2005).

The cell-surface uPAR is anchored to the cell membrane via a glycosyl phosphotidyl inositol (GPI) tail and does not have a cytoplasmic component (Blasi and Sidenius, 2010). Thus, during uPAR initiated cell-ECM adhesion events, the uPAR relationship with the cytoskeleton requires its interaction with proteins that associate with the cytoskeleton. Integrin linked kinase (ILK) is an important scaffolding protein that connects adhesion molecules such as the integrin β1-subunit, with the actin cytoskeleton (Wickström *et al*., 2010; Dagnino, 2011). Gheyara *et al*. (2007) highlighted this in their research: deletion of ILK in skeletal muscle in mice caused muscular dystrophy. This was most severe in the myofacial junction which had displacement of α7β1 from focal adhesion sites and abnormality in the actin cytoskeleton (Gheyara *et al*., 2007).

ILK interacts with the actin cytoskeleton associated molecule, parvin, and together with PINCH (particularly interesting new cysteine-histidine rich protein) form a tri-peptide complex (Fielding and Dedhar, 2009). This important tri-peptide complex is recruited to the focal adhesion sites upon integrin-ECM interaction, where ILK binds to β1- and β3-integrin subunits (McDonald *et al*., 2008). Additionally, ILK interacts with paxillin Mig2 and Wech, which are also associated with the actin cytoskeleton (McDonald *et al*., 2008; Fielding and Dedhar, 2009; Ho and Bendeck 2009; Wickström *et al*, 2010). Therefore, ILK provides the

necessary bond between the integrins with the actin cytoskeleton during cell-ECM adhesion (Grashoff *et al*., 2004; Oloumi *et al*., 2004, Ho and Bendeck, 2009).

Driver (2007) demonstrated that there is an interaction between ILK and caveolin in the HOSCC cell lines used in this study. In COS-1 kidney cells, this connection between ILK and caveolin led to the retention of ILK at the cell membrane (Chun *et al*., 2005). Interestingly, caveolin also associates with uPAR in endothelial cells and lung carcinoma cells (Cao *et al*., 2004; Tang *et al*., 2008). Pertinent to this study is the fact that both uPAR and ILK can interact with transmembrane β1-integrin and caveolin (chapter 2, Wei *et al*., 2001; Tang *et al*., 2008).

It is established that: 1) the relationship between cell adhesion molecules such as uPAR and the cytoskeleton is essential for cell-ECM adhesion events (Brakebusch and Fässler, 2003); 2) ILK provides a connection for β1-integrin and the actin cytoskeleton (Ho and Bendeck, 2009); 3) Both uPAR and ILK interact with β1-integrin and caveolin (McDonald *et al*., 2008; Wei *et al*., 2005; Drive, 2007; Tang *et al*., 2008). This led us to determine whether uPAR and ILK form a stable complex in HOSCC cells, which would explain a potential link between uPAR and the actin cytoskeleton.

3.2. Materials and methods

3.2.1 Cell Lines and tissue culture

The HOSCC cell lines previously described in section 2.2.1 were used. Human breast cancer (MCF-7) cell line was from the American Type Culture Collection. This cell line does not express caveolin (Agelaki *et al*., 2009). The cell lines were maintained as described in section 2.2.1.

3.2.2 Antibodies

Primary antibodies

-Anti-uPAR (399R) antibody (section 2.2.6).
-Anti-actin antibody (section 2.2.6).
-Anti-β1-integrin antibody (section 2.2.6).
-Rabbit anti-ILK antibody (Sigma) designated as anti-ILK antibody.
-Rabbit anti-caveolin antibody (Sigma) designated as anti-caveolin antibody.

Secondary Antibodies

-HRP-anti-rabbit antibody (section 2.2.6).
-HRP-anti-goat antibody (section 2.2.6).
- Exactacruz^{TM} HRP-anti-rabbit antibody (section 2.2.6).

3.2.3 Treatment of the cells with β1P1

The cells were treated with β1P1^{Sc} control peptide or β1P1 peptide according to the procedure described in section 2.2.7.

3.2.4 Whole cell extraction

Whole cell extraction was performed on all the HOSCC cell lines, cells treated with β1P1 or β1P1^{Sc} and MCF-7 cell line. This was done according to the procedure described in section 2.2.8.

3.2.5 Protein estimation

Protein estimation was performed using the whole cell extracts prepared in section 3.2.4. This was done according to the procedure described in section 2.2.10.

3.2.6 Immunoprecipitation

The uPAR and associated proteins were immunoprecipitated from whole cell extracts prepared in section 3.2.4 according to the procedure described in section 2.2.11. The immunoprecipitation reaction was followed by a Western blotting procedure to detect uPAR, β1-integrin, ILK and caveolin in the uPAR IP samples (described in the following sections).

3.2.7 Preparation of samples for an SDS-PAGE

The whole cell extracts (section 3.2.4) were prepared for an SDS-PAGE. This was done according to the procedure described in section 2.2.13.

3.2.8 Western blot procedure (detection of actin)

The whole cell samples of the HOSCC cell lines (15 μg section 3.2.7) were electrophoresed on a 10% SDS-PAGE gel (section 2.2.14). Western blotting was performed according to the procedure described in materials and methods, section 2.2.16.

3.2.9 Western blot procedure (detection of ILK)

The whole cell samples of the HOSCC cell lines and MCF-7 cell line (15 μg, section 3.2.7) and uPAR IP samples (20 μl, section 3.2.6) were electrophoresed on a 10% SDS-PAGE gel (section 2.2.14). **Part 1:** performed according to the "Part 1" procedure described in materials and methods, section 2.2.15. **Part 2:** The nitrocellulose was rinsed 3 times in TBS and incubated in BLOTTO solution, for an hour. Nitrocellulose was rinsed thrice with PBS and incubated with anti-ILK antibody (1:1500) in PBS for two hours. The nitrocellulose was rinsed 6 times with PBS at 5 min intervals. The nitrocellulose was incubated with HRP-anti-rabbit antibody (1:10000) in PBS for an hour, in the dark. In the case of detecting ILK in the

uPAR IP samples, the nitrocellulose was incubated with Exactacruz^{TM} HRP-anti-rabbit antibody (1:10000), in the dark. All subsequent steps in this procedure were performed in a dark environment. The nitrocellulose was rinsed 6 times with PBS at 5 min intervals. **Part 3:** performed according to the "Part 3" procedure described in materials and methods, section 2.2.15.

3.2.10 Western blot (detection of caveolin)

The whole cell samples of the HOSCC cell lines and MCF-7 cell line (15 μg, section 3.2.7) and uPAR IP samples (20 μl, section 3.2.6) were electrophoresed on a 10% SDS-PAGE gel (section 2.2.14).

Part 1: performed according to the "Part 1" procedure described in materials and methods, section 2.2.15. **Part 2:** The nitrocellulose was rinsed 3 times in TBS and incubated in BLOTTO solution, for an hour. Nitrocellulose was rinsed thrice with PBS and incubated with anti-caveolin antibody (1:5000) in PBS for an hour. The nitrocellulose was rinsed 6 times with PBS at 5 min intervals. The nitrocellulose was incubated with HRP-anti-rabbit antibody (1:10000) in PBS for an hour, in the dark. In the case of detecting caveolin in the uPAR IP samples, the nitrocellulose was incubated with Exactacruz^{TM} HRP-anti-rabbit antibody (1:10000), in the dark. The nitrocellulose was rinsed 6 times with PBS at 5 min intervals. **Part 3:** performed according to the "Part 3" procedure described in materials and methods, section 2.2.15.

3.2.11 Western blot (detection of uPAR)

The uPAR IP samples (20 μl, section 3.2.6) were electrophoresed on a 10% SDS-PAGE gel (section 2.2.14). Western blotting was performed according to the procedure described in materials and methods, section 2.2.15.

3.2.12 Western blot (β1-integrin)

The uPAR IP samples (20 μl, section 3.2.6) were electrophoresed on a 10% SDS-PAGE gel (section 2.2.14). Western blot was performed according to the procedure described in materials and methods, section 2.2.18.

3.2.13 Image analysis

Labworks ^{TM} Image Acquisition and Analysis software (Labworks version 4.5) was used for densitometric analysis to quantitatively determine the concentration ILK, caveolin, actin, uPAR and β1-integrin in the respective Western blots.

3.3 Results

3.3.1 The interaction of uPAR with ILK in the HOSCC cell lines

The ILK protein (50 kDa) is present in all the HOSCC cell lines as verified by Western blotting analysis (Figure 3.1.a). Additionally, densitometric analysis confirmed that the concentration of ILK in the HOSCC cell lines is variable. The expression difference between the cell lines that express the most and the least ILK is 2.1 fold (WHCO1 and WHCO5 cell lines respectively; Figure 3.1.a).

Once the ILK expression in the HOSCC cell lines was established, the next step entailed examining its interaction with uPAR in the HOSCC cell lines. The anti-uPAR antibody was used to immunoprecipitate uPAR protein and associated molecules from the cell lysate of the HOSCC cell lines. The anti-ILK antibody detected the presence of a protein at 50 kDa, the size of ILK, in the anti-uPAR immunoprecipitates of the HOSCC cell lines (Figure 3.1.b). The size of ILK is similar to that of heavy chain IgG that is also present in the anti-uPAR immunoprecipitates. However, the anti-ILK antibody did not produce a reaction band in the lane consisting of the –ve control (beads and anti-uPAR antibody only). Therefore, these results confirm that it is ILK in the anti-uPAR immunoprecipitates and thus demonstrate a specific interaction between ILK and uPAR in all the HOSCC cell lines.

3.3.2. The role of β1-integrin in the uPAR-ILK interaction

All the HOSCC cell lines showed a positive uPAR/ILK interaction and the WHCO6 cell line has a detectable interaction between uPAR and membrane β1-integrin. Therefore, this cell line was chosen as a representative for analysing the relationship between uPAR, ILK and β1-integrin. The β1P1 peptide disrupts the interaction between uPAR and β1-integrin and serves as a valuable tool in this investigation (chapter 2; Wei *et al*., 2005).

The ILK protein was detected in the anti-uPAR immunoprecipitates of the WHCO6 cell lines that were exposed to either β1P1 or $\beta1P1^{Sc}$ control peptide (Figure 3.2). Densitometric analysis confirmed that the concentration of ILK was 1.1 fold higher in the anti-uPAR immunoprecipitate of the WHCO6 cell lines treated with β1P1 peptide versus $\beta1P1^{Sc}$ control peptide (Figure 3.2). This means that the ILK interaction with uPAR is not via β1-integrin,

since the disruption of the uPAR and β1-integrin association, did not influence the uPAR interaction with ILK.

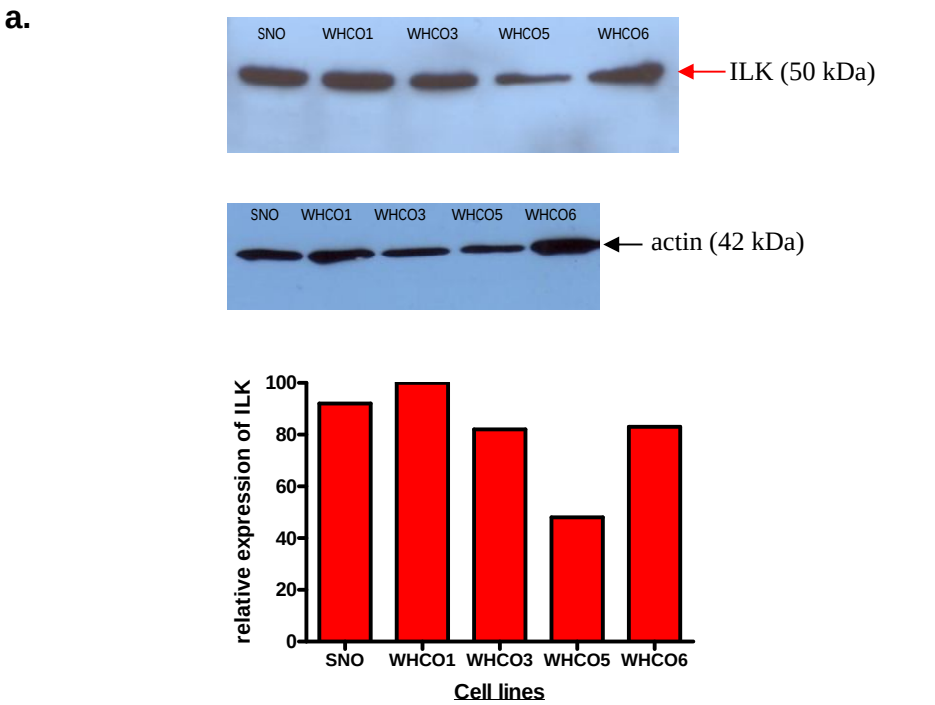

Figure 3.1: ILK expression and the interaction between uPAR and ILK in the HOSCC cell lines.
(a) The ILK expression (50 kDa; red arrow) in all the HOSCC cell lines. The Western blot of actin was used as a loading control. The Histogram of the associated ILK Western blot represents the relative expression levels of ILK across the HOSCC cell lines. **(b)** ILK (red arrow) was detected in the anti-uPAR immunoprecipitates of the HOSCC cell lines. **Note:** +ve = positive control (15 μg of SNO whole cell sample); -ve = negative control (beads and IP antibody only); IP= immunoprecipitated samples.

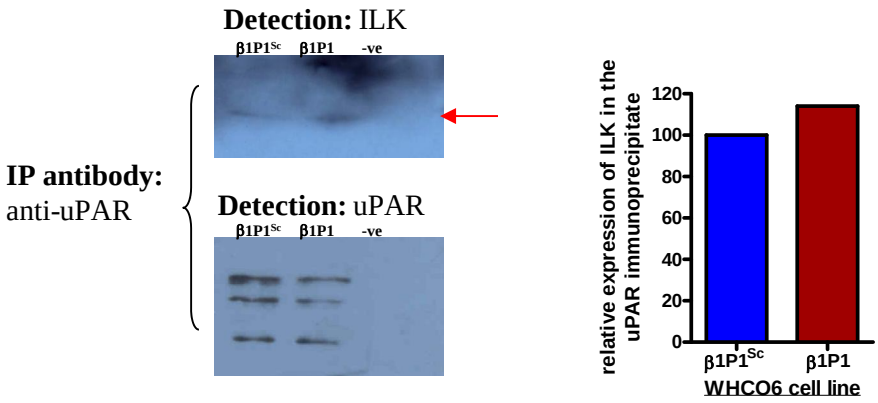

Figure 3.2: Analysis of the ILK interaction with uPAR in WHCO6 cells line exposed to β1P1 or β1P1^{Sc} control. ILK expression (red arrow) in the anti-uPAR immunoprecipitated samples from the WHCO6 cells that were exposed to β1P1^{Sc} control or β1P1. The Histogram represents the relative expression of ILK in the anti-uPAR immunoprecipitated sample of the WHCO6 cells exposed to β1P1^{Sc} peptide (blue bar) or β1P1 peptide (red bar). The relative expression of ILK in the different immunoprecipitated samples of the WHCO6 cells was standardized according to the amount of uPAR present in these samples. **Note:** IP= immunoprecipitated samples.

3.3.3 The role of caveolin in the uPAR/ILK interaction

To explore the association of uPAR and ILK with caveolin, the primary step in this investigation confirmed the presence of caveolin (24 kDa) in all the HOSCC cell lines (Figure 3.3.a). Subsequently, densitometric analysis established that the highest expression of caveolin was in the WHCO6 cell line and the least in the SNO cell line (Figure 3.3.a).

The uPAR protein was immunoprecipitated from the whole cell lysate of the HOSCC cell lines with anti-uPAR antibody. Anti-caveolin antibody produced a reaction band at 24 kDa, the size of caveolin, in the anti-uPAR immunoprecipitated samples of all the HOSCC cell lines (Figure 3.3.b). The anti-caveolin antibody did not identify the presence of the light chain IgG, which is approximately 25 kDa, in the –ve control, which consists of the anti-uPAR antibody and beads (Figure 3.3.b). Therefore, this analysis established that the particular interaction between uPAR and caveolin occurs in all the HOSCC cell lines.

The next step was to investigate the uPAR and ILK interaction in relation to caveolin. The WHCO6 cell line was used as a representative of the HOSCC cell lines while the breast cancer cell line (MCF-7), which does not express caveolin, was used as a negative control cell line (Agelaki *et al*., 2009). Accordingly, the presence of caveolin was established in the

WHCO6 cell line but not in the MCF-7 cell line, by Western blotting analysis (Figure 3.4.a). The ILK expression was confirmed in the WHCO6 and MCF-7 cell lines (Figure 3.4.a).

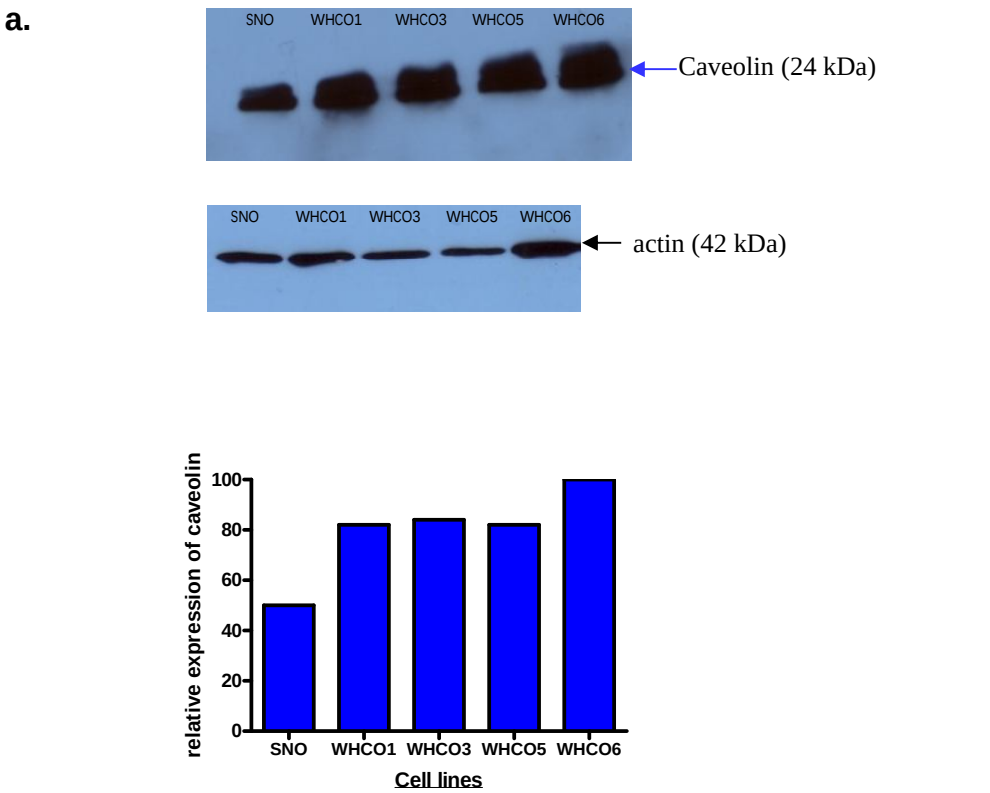

Figure 3.3: Caveolin expression and the interaction between uPAR and caveolin in HOSCC cell lines. (a) Caveolin expression (24 kDa; blue arrow) in all the HOSCC cell lines. The Western blot of actin was used as a loading control. The Histogram of the associated caveolin Western blot represents the relative expression levels of caveolin across the HOSCC cell lines. **(b)** Caveolin at 24 kDa (blue arrow) was detected in the uPAR immunoprecipitate of the HOSCC cell lines. **Note:** +ve = positive control (15 μg of SNO whole cell sample); -ve = negative control (beads and IP antibody only); IP= immunoprecipitated samples.

ILK and caveolin were detected in the anti-uPAR immunoprecipitates of the whole cell lysate of the WHCO6 cells line and not in the anti-uPAR immunoprecipitates of whole cell lysate of the MCF-7 cell line (Figure 3.4.a). Therefore, caveolin is a necessary component in the uPAR interaction with ILK since this interaction occurs in a "caveolin expressing" WHCO6 cell line and not in a "non-caveolin expressing" MCF-7 cell lines.

Validation of this result was the fact that the β1-integrin (110 kDa) was present in the uPAR immunoprecipitates of both the WHCO6 and MCF-7 cell lines (Figure 3.4.b). Therefore, the uPAR immunoprecipitation procedure from whole cell lysate of MCF-7 was successful in immunoprecipitating molecules that associate with uPAR. Further, this confirms that the absence of ILK in the anti-uPAR immunoprecipitate of MCF-7 is due to the biophysiological reduced caveolin expression.

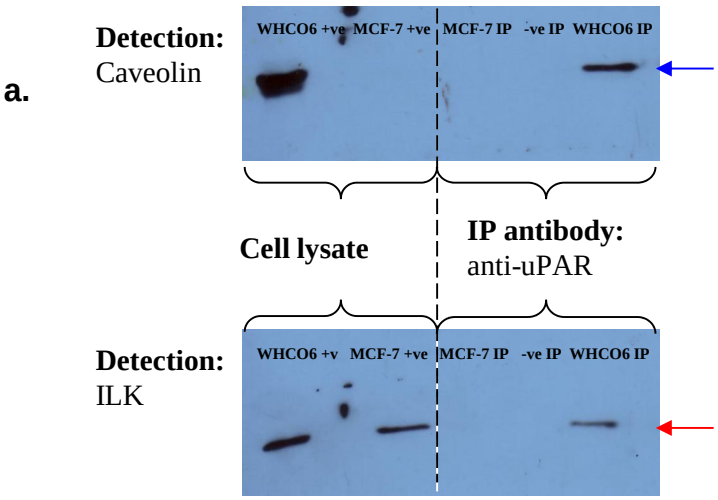

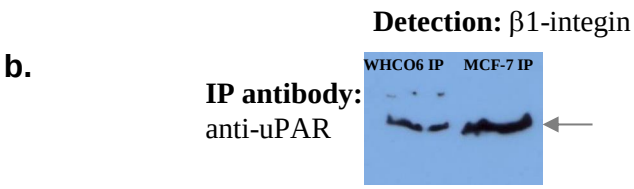

Figure 3.4: The interaction of ILK or caveolin with uPAR was detected in the WHCO6 cells but not the MCF-7 cell line. a) Caveolin (blue arrow) expression occurs in the WHCO6 cell line and not in the MCF-7 cell line, while ILK (red arrow) expression is detected in the WHCO6 and the MCF-7 cell lines. Furthermore, caveolin (blue arrow) and ILK (red arrow) are present in anti-uPAR immunoprecipitate of the WHCO6 cells, but not in the anti-uPAR immunoprecipitate of the MCF-7 cells. **b)** β1-integrin (130 kDa and 110 kDa, grey arrow) were present in the anti- uPAR immunoprecipitate of WHCO6 cells, while the 110 kDa β1-integrin was present in the anti-uPAR immunoprecipitate of MCF-7 cells. **Note:** +ve = positive control (15 μg of WHCO6 or MCF-7 whole cell sample); -ve = negative control (beads and IP antibody only); IP= immunoprecipitated samples

3.4 Discussion

The connection of cell adhesion molecules to the cytoskeleton is crucial for the stability of the cell adhesion complex and adhesion events (Brakebusch and Fässler, 2003; Wickström *et al*., 2010; Dagnino, 2011). This investigation demonstrates the unique interaction between uPAR and ILK in five HOSCC cell lines (Figure 3.1).

The novel interaction between uPAR and ILK in the HOSCC cell lines highlights that the uPAR has a connection to the actin cytoskeleton in these cell lines. This is particularly important for cell-ECM adhesion events that are mediated by uPAR (Bernstein *et al*., 2004; Abu-Ali *et al*., 2005). For instance, the uPAR mediated adhesion of adenoid cystic carcinoma cell lines on collagen type I induced the co-localization of uPAR with actin associated molecules such as vinculin and paxillin (Abu-Ali *et al*., 2005). Therefore the relationship between uPAR and the actin cytoskeleton in HOSCC would be important should these cells utilize uPAR in cell-ECM adhesion events. Interestingly, endogenous uPA was necessary for the association of uPAR with the actin cytoskeleton in corneal fibroblasts (Bernstein *et al*., 2004). Since all the HOSCC cell lines endogenously secrete uPA it is highly likely that uPA, uPAR and ILK form the association with the actin cytoskeleton (chapter 2).

Since uPAR is GPI anchored, and does not have a cytoplasmic tail, the interaction between uPAR and cytoplasmic ILK has to be via other molecules (Blasi and Sidenius, 2010). One of the major transmembrane proteins that interact with ILK is the β1-integrin subunit (McDonald *et al*., 2008). Furthermore, Driver (2007) established that in all the HOSCC cell lines, ILK phosphorylated the myelin basic protein, which has a short sequence corresponding to the cytoplasmic region of β1-integrin. This indicates that there is a relationship between ILK and the cytoplasmic tail of β1-integrin in the HOSCC cell lines (Driver, 2007).

Given the above, it was originally hypothesized that uPAR would interact with ILK via the β1-integrin in the HOSCC cell lines. However, the uPAR interaction with ILK was observed in all the HOSCC cell lines, including the cell lines that did not have a detectable membrane uPAR/β1-integrin interaction (SNO, WHCO1 and WHCO5) (chapter 2). This suggests that the uPAR interaction with ILK is not solely via β1-integrin. Importantly, exposure of the WHCO6 cells to β1P1 peptide, which specifically disrupts the interaction between uPAR and β1-integrin, did not result in the alteration of the uPAR/ILK interaction (Figure 3.2). This served to confirm that the interaction of uPAR with ILK is not via β1-integrin.

This investigation further established the interaction between uPAR and caveolin in all the HOSCC cell lines (Figure 3.3). Since both uPAR and caveolin specifically interact with ILK in all the HOSCC cell lines, caveolin was also hypothesized to be the linking protein between ILK and uPAR (Driver, 2007). In the MCF-7 breast carcinoma cell line, which does not express caveolin, the uPAR interaction with ILK was not detectable (Figure 3.4). Therefore, the positive interaction between ILK and uPAR specifically occurs in cells, such as the HOSCC, which express caveolin. This supports our notion that the ILK and uPAR interaction use caveolin as an intermediate to provide the association between uPAR and ILK and ultimately the actin cytoskeleton.

The HOSCC cell lines used in this investigation are all moderately differentiated (Veale and Thornley, 1989). In spite of this, uPAR associated with ILK or caveolin in all the HOSCC cell lines, which suggests that these interactions serve a central role in these HOSCC cells. This purpose would be to provide uPAR with the structural stability should uPAR mediate cell adhesion events in HOSCC. This latter question is addressed and discussed in the following chapters.

In conclusion: This analysis confirmed that ILK interacts with uPAR in the HOSCC cell lines via caveolin and not via β1-integrin. This unique complex containing uPAR/caveolin/ILK provides the relationship between uPAR and the actin cytoskeleton, which is necessary for uPAR to establish functional cell-ECM adhesion based events.

Chapter 4: The role of uPAR in the adhesion of HOSCC cells

4.1. Introduction

The extracellular matrix (ECM), and its interaction with epithelial cells, plays a key role for epithelial tissue structure and integrity (Daley *et al*., 2008). However, it is also evident that the communication between cells and ECM components, such as collagen, fibronectin, laminin and vitronectin, influences carcinoma development (Ziober *et al*., 2006; Daley *et al*., 2008).

The ECM components of particular relevance to this study are collagen type I and vitronectin, which are linked with the ECM environment of HOSCC. Collagen type I is the major component of the lamina propria underlying the basement membrane of oesophageal squamous cells (Timmer *et al*., 1994; Katsuhiko *et al*., 1997; Matsumoto *et al*., 1997). In HOSCC, the genes of the two collagen type I chains (α1 and α2) are upregulated compared with normal oesophageal squamous cells (Kan *et al*., 2001; Kashyap *et al*., 2009). Additionally, the serum level of the vitronectin ECM molecule is significantly higher in patients with HOSCC compared to healthy control patients (Shao *et al*., 2009).

Integrins are the major cell surface proteins responsible for cell-ECM adhesion and communication (Humphries *et al*., 2006). Pertinent to this study is the fact that uPAR can also influence the adhesion of cells on ECM components such as collagen type I and vitronectin (van der Pluijm *et al*., 2001; Czekay *et al*., 2003). Internalization of uPAR by LRP related mechanism (see general introduction), reduced adhesion of fibrosarcoma cells (HT1080), breast cancer cells (MCF-7) and cervix carcinoma cells (HeLa) on collagen type I and vitronectin (Czekay *et al*., 2003). Sato *et al*. (2011) transfected breast cancer (MDA-MB-231, MDA-MB-435, CAMA and MCF-7) and ovarian cancer cells (Ov-MZ-6) with a uPAR isoform variant, which has reduced ability to interact with uPA. This reduced the adhesion of these cells on collagen type I and vitronectin (Sato *et al*., 2011).

Cell-ECM adhesion based events such as migration, invasion and proliferation play a major role in the development of carcinoma cells (Ziober *et al*., 2006). To understand the possible events that happened during the progression of HOSCC, it is necessary to analyse the underlying mechanisms that regulate cell-ECM adhesion events. This study addresses the question of whether uPAR has an influence on cell-ECM adhesion in five HOSCC cell lines.

This provides insight into whether the uPAR role in cell-ECM adhesion is a feature that occurs in carcinomas or is limited to specific cancer types. Additionally, this investigation would provide an understanding of the possible role of uPAR in cell-ECM adhesion during the progression of HOSCC.

4.2 Materials and methods

4.2.1 Cell Lines and tissue culture

The HOSCC cell lines previously described in section 2.2.1 were used. Cells were maintained as described in section 2.2.1.

4.2.2 Coating of tissue culture dishes with BSA, collagen type I or vitronectin

Adhesion assays were carried out in Nunclon flat bottom 96-well plates. Filter sterilized BSA (0.1%) or 1 μg/ml vitronectin was added to each well and incubated for 3 hours at 37^{o}C. The BSA or vitronectin solution was removed and each well was rinsed with 50 μl of PBS. PBS (50 μl) was added to the BSA-coated and vitronectin-coated wells.

Collagen type I extracted from rat tail collagen (100 μg/ml) was added to each well and incubated for 3 hours at room temperature. The collagen solution was removed and each well was rinsed twice with 50 μl of PBS. This was followed by the addition of 50 μl of PBS into each well and the 96-well plate was sterilized under UV light in the laminar flow for 20 min.

4.2.3 Preparation of the collagen type I-coated and vitronectin-coated dishes for adhesion assay

The PBS from the collagen type I-coated and vitronectin-coated wells was removed. Filter sterilized BSA (0.1%) was added to each well and the 96-well plate was incubated for 30 min at 37^{o}C. BSA is the standard non-ECM coating used *in vitro* (Liang *et al*., 2008; Balsara *et al*., 2011; Sato *et al*., 2011). Each well was rinsed with 50 μl of PBS and the 96-well plate was set for the adhesion assays.

4.2.4 Adhesion assay

Adhesion assays were performed using all the HOSCC cell lines. The cells were passaged at 60 to 80 % confluency with trypsin/EDTA solution. The cell suspension was mixed with 8 ml of tissue culture medium and counted with a haemocytometer. The cell suspension was

centrifuged briefly and the supernatant containing trypsin solution was removed. 2 x 10^5 cells/well were resuspended in 50 µl of tissue culture medium and seeded on the wells coated with BSA, collagen type I or vitronectin. The cells were exposed to the following treatments:

High molecular weight uPA: The cells were supplemented with or without 0.5 nM, 1 nM uPA or without uPA. These concentrations were chosen as ≤1 nM uPA is the physiological concentration of uPA (Nassar *et al*., 2011).

β1P1 and β1P1^{Sc} peptides: The cells were supplemented with 0.1 mM β1P1 peptide or 0.1 mM β1P1^{Sc} control peptide. This is the minimum concentration used by Wei *et al*. (2005) that caused a significant decrease in adhesion of mouse kidney epithelial cells expressing wild type α3 integrin (Wt α3/U cells).

The cells were incubated at 37^{o}C in 5% CO_2 atmosphere in a humidified incubator for 2 hours. This time frame for adhesion assays of these particular HOSCC cell lines was established by Miller (2001). Subsequently, the medium was removed and the attached cells were washed twice with 37^{o}C PBS to remove non-adherent cells.

The number of adherent viable cells on the different surfaces were counted using MTT based on the method used by Xie *et al*. (2009) to count the number of adherent HOSCC cells during the adhesion assay. 100 µl of 0.5 mg/ml MTT in filter sterilized PBS was added to the adherent cells and the cells were incubated at 37^{o}C for 3 hours. The MTT solution was removed and 100 µl of dimethyl sulphoxide (DMSO) was added to dissolve the formazan crystals. In untreated wells of the 96-well plate, 100 µl of DMSO was added, which were set as the "blank wells". After an hour the absorbance reading was determined using a microtiter plate reader at 490 nm. The absorbance reading of the blank wells was subtracted from the absorbance reading of the treated samples. The adhesion assays were performed in triplicates.

4.2.5 Analysis of data (Statistical analysis)

All statistical analysis (one way ANOVA and Student's t-test) were performed using GraphPad Prism version 4.00 statistical program.

4.3 Results

The fibrillar and soluble ECM components, collagen type I and vitronectin, were used to analyse the relationship of uPAR and ECM in terms of HOSCC cell adhesion. The BSA protein, which commonly serves as a non-ECM control during *in vitro* adhesion assays, was utilized for this purpose (Kanse *et al*., 2004; Wei *et al*., 2005). **Statistics tables are presented in Appendix C.**

4.3.1 Adhesion of the HOSCC cells onto collagen type I substrate

Adhesion of the HOSCC cells on the fibrillar ECM component, collagen type I, varied significantly across the HOSCC cell lines ($P<0.05$) (Figure 4.1). The WHCO1 and WHCO5 cells adhered the most on collagen type I and displayed a similar level of adhesion. Adhesion of SNO, WHCO3 and WHCO6 cells on collagen type I was not significantly different from each other (Figure 4.1). However, these cells adhered significantly less on collagen type I than the WHCO1 and WHCO5 cells (Figure 4.1).

In all the HOSCC cell lines, there was a significant increase in adhesion on collagen type I substrate when compared to non-ECM control, BSA ($P<0.05$) (Figure 4.1). This means that the HOSCC cells adhere more on ECM component collagen type I rather then a non-ECM component.

4.3.2 The uPAR impact on adhesion of the HOSCC cell lines on collagen type I substrate

The results above (section 4.3.1) clearly demonstrate that the HOSCC cells adhere on collagen type I. The consequent step in this investigation was to establish whether uPAR plays a role in the adhesion of the HOSCC cells on collagen type I.

Activation of uPAR with different concentrations of uPA did not affect the adhesion of the majority (4 out of 5) of the HOSCC cell lines on collagen type I substrate. There was little variation in adhesion of the particular WHCO1, WHCO3, WHCO5 and WHCO6 cells on collagen type I in the presence of the different uPA concentrations (Figure 4.2.a). Interestingly, there was a significant variation in adhesion of the SNO cells on collagen type I upon exposure to the different concentrations of uPA ($P<0.05$) (Figure 4.2.a). The activation

of uPAR with uPA contributes to the adhesion of specifically the SNO cells on collagen type I substrate. All the HOSCC cells adhered significantly more on collagen type I substrate than on BSA upon activation of uPAR with 0.5 nM and 1 nM uPA (Figure 4.2.b). This demonstrates that the increase in adhesion of the HOSCC cell lines on collagen type I versus BSA is maintained when uPAR is activated by uPA.

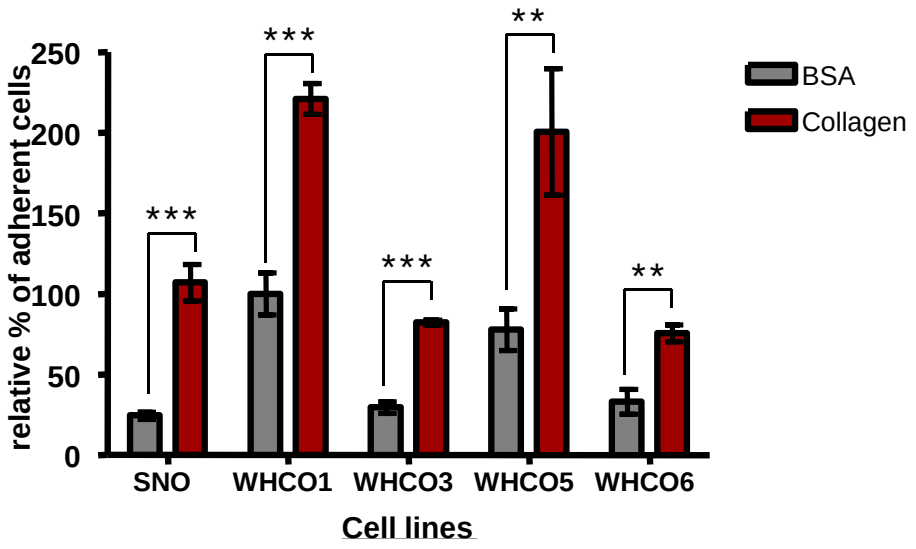

Figure 4.1: Adhesion of the HOSCC cell lines on collagen type I ECM substrate. The histogram represents the adhesion of the cells on collagen type I substrate (red bar) versus non-ECM BSA control (grey bar). A one way ANOVA followed by a Tukey's multiple comparison test was conducted to compare the adhesion of the HOSCC cell lines on collagen type I (statistical results are presented in Appendix C). **Note:** The mean number of adherent WHCO1 cells on BSA, was set at 100%. The adhesion of the WHCO1 cells on BSA was set as a reference point for all the other cell lines. An unpaired Student's t-test was used to compare the adhesion of individual HOSCC cell lines on BSA versus collagen type I. ***P values (for Student's t-test) are indicated by *; * = P<0.05; ** = P<0.01; *** = P<0.001; standard error bars = standard deviation; n=3***

The peptide (β1P1) disrupts the uPAR interaction with β1-integrin, as it competes with β1-integrin for binding to uPAR (chapter 2; Wei *et al*., 2005). This peptide serves as a tool to analyse the uPAR/β1-integrin interaction in terms of adhesion of the HOSCC cells. The $\beta1P1^{Sc}$ peptide served as a control peptide (chapter 2; Wei *et al*., 2005).

The attachment of the SNO, WHCO3 and WHCO5 cells on collagen type I was not substantially changed upon disruption of the uPAR/β1-integrin interaction with β1P1 blocking peptide (Figure 4.3.a). On the other hand, adhesion of the WHCO1 cells on collagen type I was notably[*1] reduced in the presence of β1P1 blocking peptide compared to the

[*1] A notable difference was significant at the 10% level (P<0.1)

presence of β1P1^{Sc} control peptide (Figure 4.3.a). Additionally, there was a significant decrease in adhesion of the WHCO6 cells on collagen type I upon addition of β1P1 blocking peptide versus the addition of β1P1^{Sc} control peptide ($P<0.05$) (Figure 4.3.a). This demonstrated that the interaction between uPAR and β1-integrin contributes to the adhesion of the WHCO1 and WHCO6 cells on collagen type I substrate.

The five HOSCC cell lines adhered significantly more on collagen type I substrate than on BSA in the presence of control peptide, β1P1^{Sc} (Figure 4.3.b). Despite the disruption of their uPAR/β1-integrin interaction with β1P1, the SNO, WHCO1, WHCO3 and WHCO5 cells adhered significantly more on collagen type I substrate then on BSA (Figure 4.3.b). On the contrary, when the uPAR/β1-integrin interaction was reduced in the WHCO6 cells, their adhesion on collagen type I versus BSA was not significantly different (Figure 4.3.b). This result demonstrates that the uPAR interaction with β1-integrin is necessary for the increased adhesion of the WHCO6 cell line on collagen type I versus BSA.

4.3.3 Adhesion of the HOSCC cells on vitronectin substrate

Adhesion of the HOSCC cell lines on vitronectin, which represents one of the soluble components of the ECM, varied significantly within the HOSCC cell lines ($P<0.05$) (Figure 4.4). The WHCO5 cells adhered the most, while the SNO cells adhered the least, on vitronectin substrate (Figure 4.4).

The adhesion of the SNO, WHCO1 and WHCO6 cells was not significantly different on vitronectin versus non-ECM BSA (Figure 4.4). In contrast the WHCO3 and WHCO5 cells adhered significantly more on vitronectin compared with BSA substrate ($P<0.05$) (Figure 4.4). This means that only specific HOSCC cells attach more on vitronectin than on a non-ECM component.

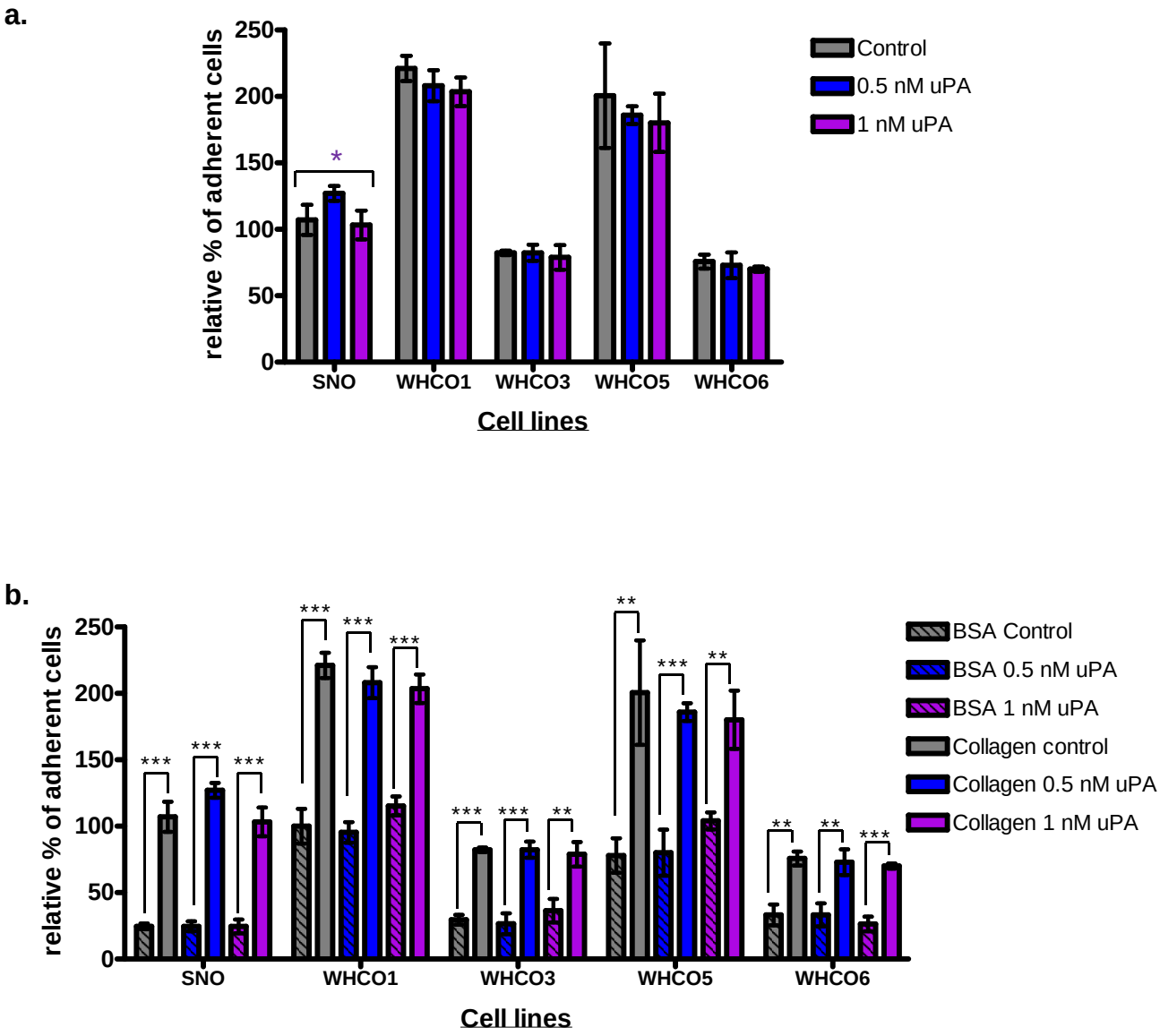

Figure 4.2: Adhesion of the HOSCC cells on collagen type I upon addition of exogenous uPA.
(a) The histogram represents the adhesion of the HOSCC cell lines on collagen type I in the presence of different concentration of uPA (untreated control = striped grey bar; 0.5 nM uPA = striped blue bar; 1 nM uPA = striped purple bar). A one way ANOVA was used to compare the effect of the different uPA treatments on adhesion of the HOSCC cell lines on collagen. **(b)** The histogram represents the adhesion of the cells on collagen type I (solid bar) versus BSA (striped bar) upon treatment with different concentration of uPA versus untreated control. The mean number of adherent WHCO1 cells on BSA, was set at 100%. An unpaired Student's t-test was used to compare the adhesion of the HOSCC cell lines on collagen versus BSA in the absence (control) or presence of uPA (at 0.5 and 1 nM concentrations). ***P values (for the one way ANOVA (purple *) and Student's t-test (black *)) are indicated by *; * = P<0.05; ** = P<0.01; *** = P<0.001; standard error bars = standard deviation; n=3***

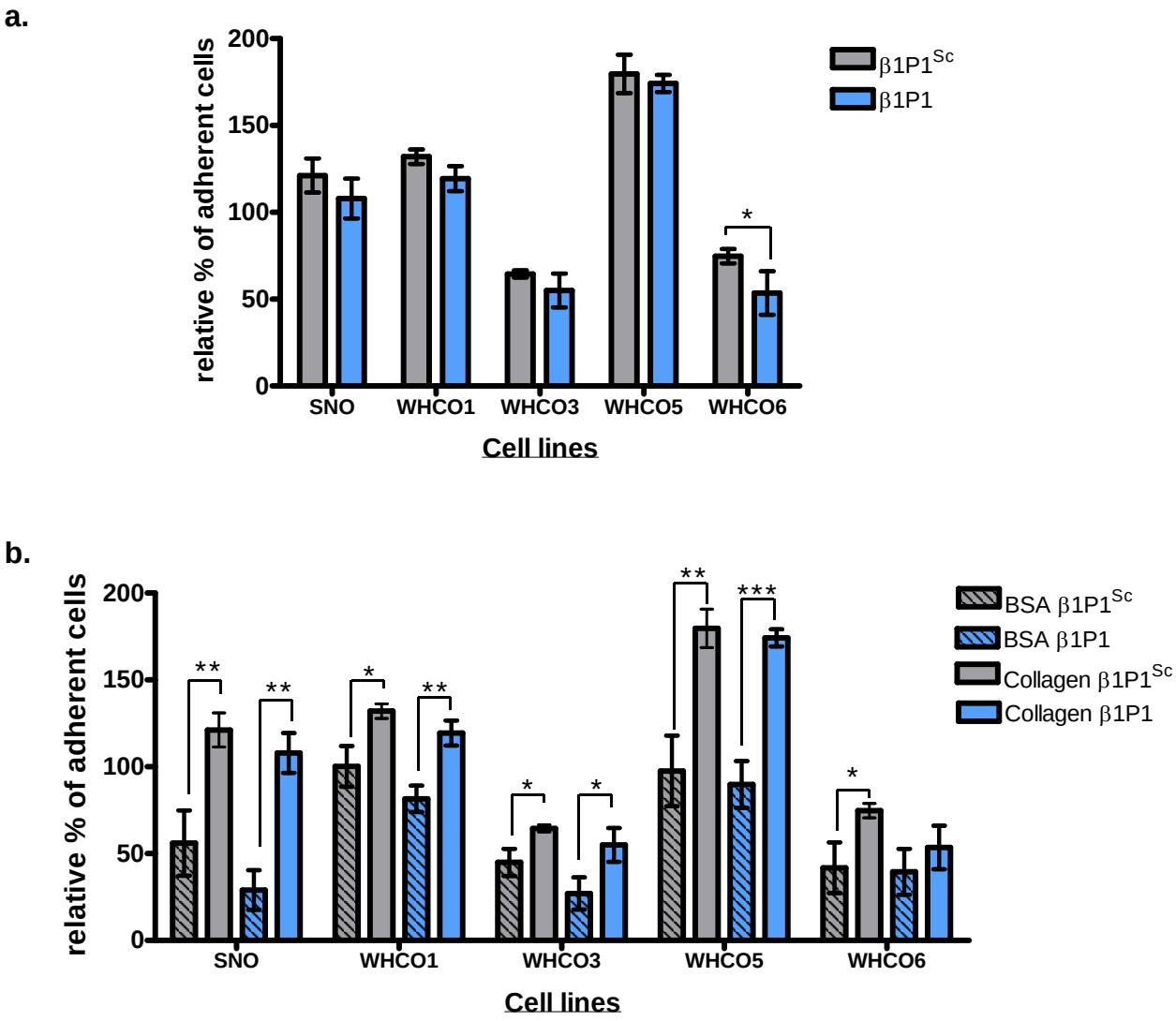

Figure 4.3: Adhesion of the HOSCC cell lines on collagen type I substrate upon disruption of the uPAR/β1-integrin interaction. **(a)** The histogram represents adhesion of the cells on collagen type I in the presence of β1P1 (blue bar) versus $\beta1P1^{Sc}$ control (grey bar). An unpaired Student's t-test was used to compare the adhesion of individual HOSCC cell lines unto collagen type I upon exposure to β1P1 versus $\beta1P1^{Sc}$ control. **(b)** The histogram representing the adhesion of the cells on BSA (striped bar) and collagen upon exposure to β1P1 (blue bar) versus $\beta1P1^{Sc}$ control (grey bar) peptides. An unpaired Student's t-test was used to compare the adhesion of individual HOSCC cell lines unto BSA and collagen type I in the presence of β1P1 or $\beta1P1^{Sc}$. The mean number of adherent WHCO1 cells on BSA, which were exposed to $\beta1P1^{Sc}$, was set at 100%. ***P values (for Student's t-test) are indicated by *; * = P<0.05; ** = P<0.01; *** = P<0.001; standard error bars = standard deviation; n=3***

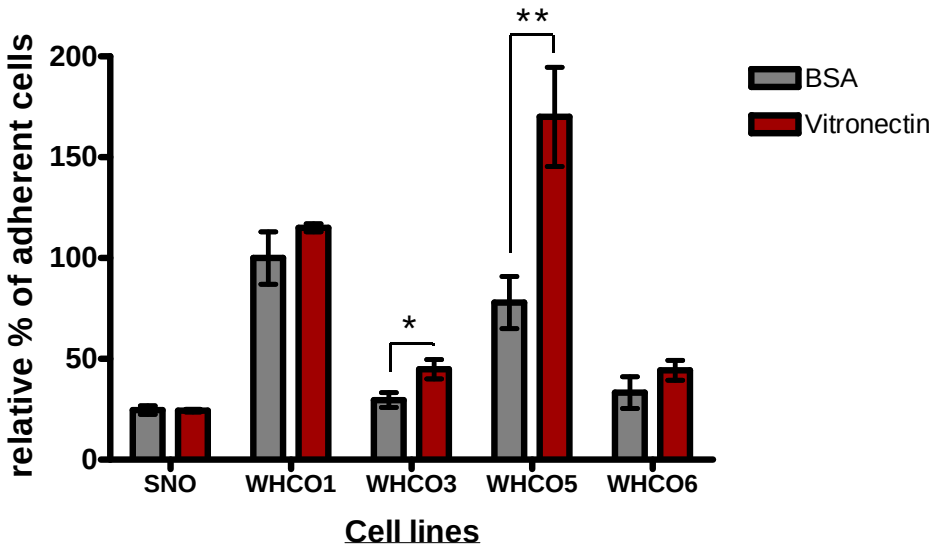

Figure 4.4: Adhesion of the HOSCC cell lines on vitronectin substrate. The histogram represents the adhesion of the cells on vitronectin (red bar) versus BSA (grey bar). A one way ANOVA followed by a Tukey's multiple comparison test was conducted to compare the adhesion of the HOSCC cell lines on vitronectin. **Note:** The mean number of adherent WHCO1 cells on BSA, was set at 100%. An unpaired Student's t-test was used to compare the adhesion of individual HOSCC cell lines on BSA and vitronectin. ***P values (for Student's t-test) are indicated by *; * = P<0.05; ** = P<0.01; *** = P<0.001; standard error bars = standard deviation; n=3***

4.3.4 The uPAR impact on adhesion of the HOSCC cell lines on vitronectin

Vitronectin is one of the ligands of uPAR and therefore the relationship between the two molecules was examined from the adhesion perspective. Activation of uPAR with varying concentrations of uPA did not cause a significant change in adhesion of the SNO, WHCO1, WHCO5 and WHCO6 cell on vitronectin (Figure 4.5.a). On the contrary, there is a significant variation in adhesion of the WHCO3 cells on vitronectin upon activation or uPAR with different uPA concentrations (Figure 4.5.a). Furthermore, when uPAR was activated with 1 nM uPA, the WHCO3 cells adhered significantly more on vitronectin when compared with control (Figure 4.5.a). Therefore, the activation of uPAR by a specific uPA concentration contributes to the adhesion of particularly the WHCO3 cells on vitronectin substrate.

Activation of uPAR with 0.5 nM or 1 nM uPA in the SNO and WHCO1 cells caused little variation in adhesion of these cells on vitronectin versus BSA (Figure 4.5.b). In contrast the

WHCO3, WHCO5 and WHCO6 cells adhered significantly more on vitronectin than on BSA when their uPAR was activated with 0.5 nM or 1 nM uPA (Figure 4.5.b). This demonstrated that the increase in adhesion of the WHCO3 and WHCO5 cell lines on vitronectin versus BSA is maintained upon the uPAR activation with uPA. Importantly, these results further illustrate that the WHCO6 cell line requires uPA activation of uPAR in order to increase adhesion on ECM vitronectin substrate versus non-ECM BSA.

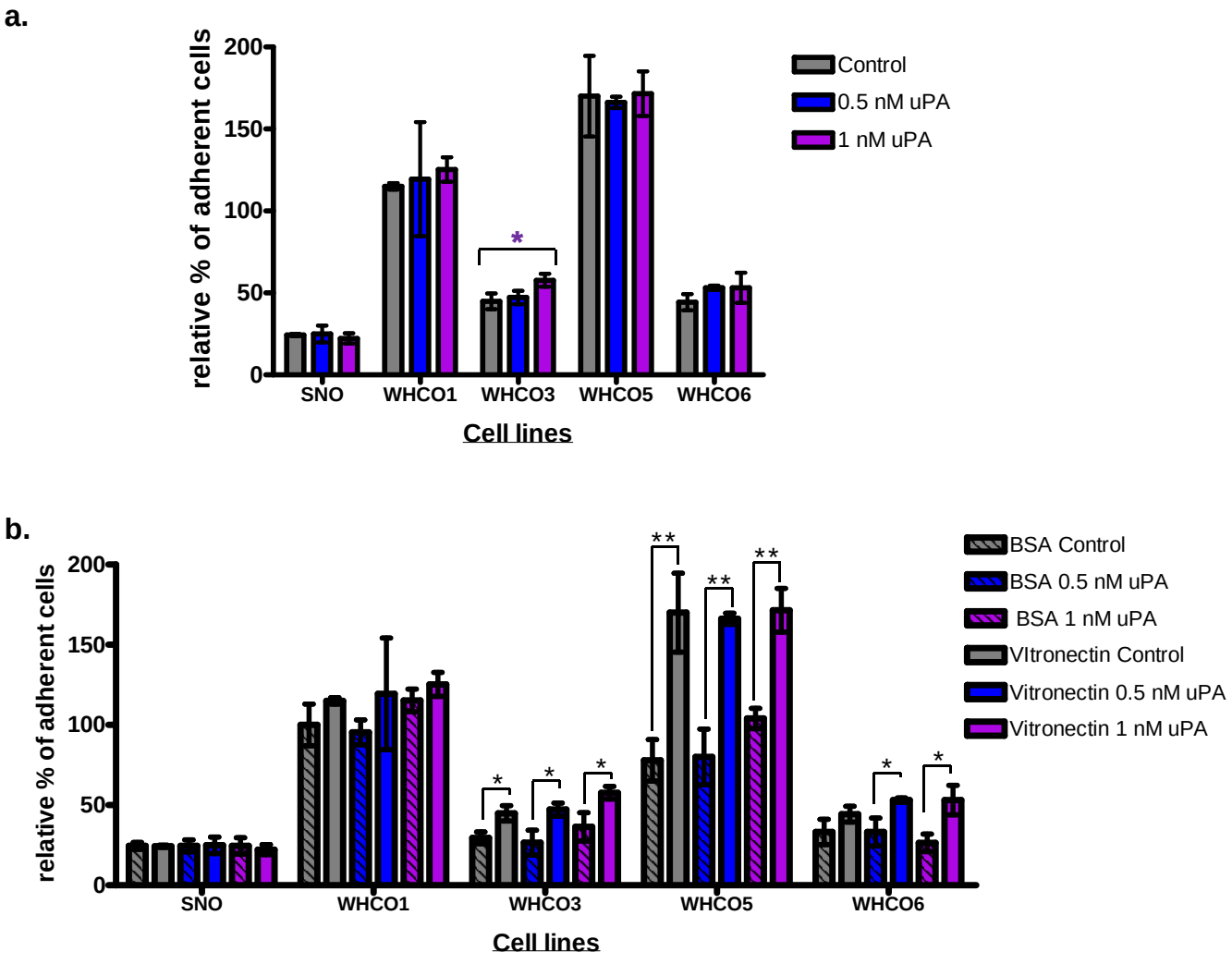

Figure 4.5: Adhesion of the HOSCC cells on vitronectin substrate upon addition of exogenous uPA. (a) The histogram represents the adhesion of the HOSCC cell lines on vitronectin in the presence of different concentration of uPA (untreated control = striped grey bar; 0.5 nM uPA = striped blue bar; 1 nM uPA = striped purple bar). A one way ANOVA was used to compare the effect of the different uPA treatments on adhesion of the HOSCC cell lines on vitronectin. **(b)** The histogram represents the adhesion of the cells on vitronectin and BSA upon treatment with different concentration of uPA versus untreated control. An unpaired Student's t-test was used to compare the adhesion of the HOSCC cell lines on vitronectin versus BSA in the absence (control) or presence of uPA (at 0.5 and 1 nM concentrations). The mean number of adherent WHCO1 cells on BSA, was set at 100%. ***P values (for the one way ANOVA (purple *) and Student's t-test (black *)) are indicated by *; * = P<0.05; ** = P<0.01; *** = P<0.001; standard error bars = standard deviation; n=3***

Blocking the uPAR/β1-integrin interaction with β1P1 blocking peptide did not cause a considerable change in vitronectin adhesion of the SNO, WHCO1, WHCO3 and WHCO5 cells (Figure 4.6.a). The WHCO6 cell line served as an interesting exception since its adhesion on a vitronectin substrate was notably reduced upon the disruption of the uPAR/β1-integrin interaction (Figure 4.6.a). Therefore the interaction between β1-integrin and uPAR contributes to the adhesion of specifically the WHCO6 cell lines on vitronectin.

Under control conditions, in the presence of the $\beta1P1^{Sc}$ control peptide, the adhesion of the majority of the HOSCC cell lines was similar on vitronectin substrate versus BSA (Figure 4.6.b). On the other hand, the WHCO5 HOSCC cells adhered significantly more on vitronectin substrate versus BSA in the presence of $\beta1P1^{Sc}$ ($P<0.05$) (Figure 4.6.b). The disruption of the uPAR/β1-integrin interaction with β1P1 blocking peptide caused little variation in adhesion of the SNO, WHCO3 and WHCO6 cells on vitronectin versus BSA (Figure 4.6.b). However, the WHCO5 cells adhered significantly more on vitronectin versus BSA when their uPAR/β1-integrin interaction was disrupted ($P<0.05$) (Figure 4.6.b). This demonstrates that the increase in adhesion of the WHCO5 cells on vitronectin versus BSA is maintained when the β1-integrin/uPAR interaction is disrupted. In contrast, the WHCO1 cells adhered significantly less on vitronectin than on BSA when the uPAR/β1-integrin interaction was blocked ($P<0.05$) (Figure 4.6.b). This means that the absence of the uPAR interaction with β1-integrin alters the ability of the WHCO1 cells to adhere on vitronectin.

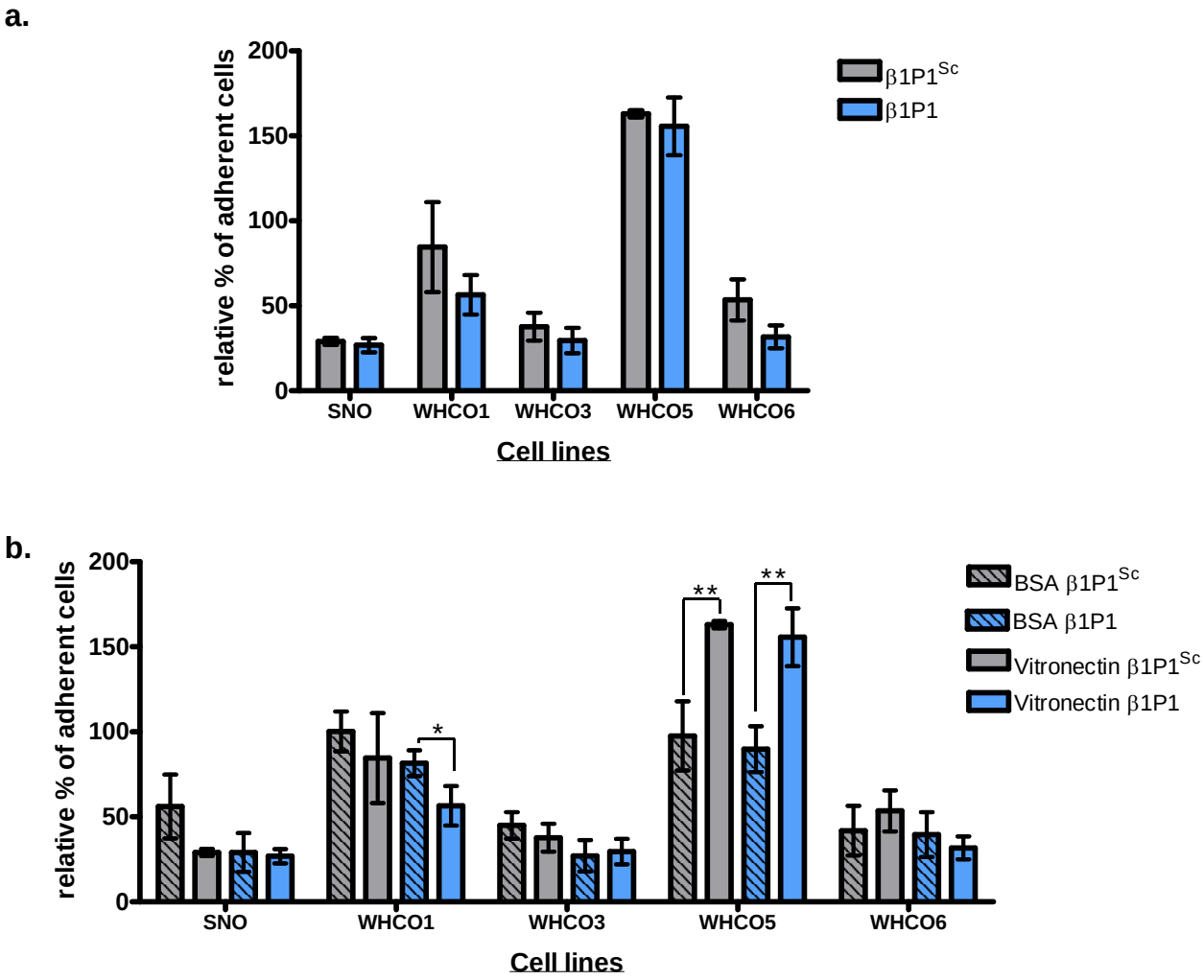

Figure 4.6: Adhesion of the HOSCC cell lines on vitronectin substrate upon disruption of the uPAR/β1-integrin interaction. **(a)** The histogram represents adhesion of the cells on vitronectin upon exposure to β1P1 (blue bar) versus β1P1^{Sc} control (grey bar). An unpaired Student's t-test was used to compare the adhesion of individual HOSCC cell lines unto vitronectin upon exposure to β1P1 versus β1P1^{Sc} control. **(b)** The histogram representing the adhesion of the cells on BSA (striped bar) and vitronectin upon treatment with β1P1 (blue bar) versus β1P1^{Sc} control (grey bar) peptides. An unpaired Student's t-test was used to compare the adhesion of individual HOSCC cell lines unto BSA and vitronectin in the presence of the β1P1 or β1P1^{Sc}. The mean number of adherent WHCO1 cells on BSA, was set at 100%. ***P values (for Student's t-test) are indicated by *; * = P<0.05; ** = P<0.01; *** = P<0.001; standard error bars = standard deviation; n=3***

4.4 Discussion

The current investigation established that the HOSCC cell lines have different adhesive properties on collagen type I or vitronectin with respect to non-ECM BSA control. Additionally, this investigation verified that uPAR plays a role in cell-ECM adhesion in HOSCC.

It is clear that there is a variability between the adhesion of the HOSCC cell lines on ECM components, collagen type I or vitronectin, versus non-ECM BSA. For example, all the HOSCC cell lines adhered significantly more on collagen type I than on BSA. Additionally, the adhesion of the WHCO3 and WHCO5 cells increased on vitronectin versus BSA. These findings mean that the HOSCC cell lines express different ratios of adhesion related molecules to influence their adhesion on a particular substrate. Adhesion molecules involved in cell-ECM interactions are the integrins and non-integrin receptors such the one pertinent to our study, uPAR (Madsen *et al*., 2007). This investigation established that the majority (4 of the 5) of the HOSCC cell lines utilize uPAR during their adhesion on either collagen type I or vitronectin. Therefore, uPAR contributes to cell adhesion of several carcinoma types such as breast, thyroid, oral as well as HOSCC (Ragno *et al*., 1998; van der Pluijm *et al*., 2001; Liang *et al*., 2008).

The interaction of uPAR with uPA or β1-integrin influences adhesion of the HOSCC cell lines. Activation of uPAR by exogenous uPA has a significant impact on adhesion of the SNO cells on collagen type I and the WHCO3 and WHCO6 cells on vitronectin. Tarui *et al*. (2003) discovered that uPA increased the uPAR interaction with α5β1 integrin in solution. It is possible that the uPA/uPAR complex increases the interaction between uPAR and β1-integrin to promote adhesion of the HOSCC cells on these ECM substrates.

The uPAR interaction with β1-integrin plays a part in adhesion of the WHCO1 and WHCO6 cells on collagen type I and the WHCO6 cells on vitronectin. The WHCO6 cells have a detectable uPAR interaction with β1-integrin (chapter 2). These cells therefore utilize this interaction to adhere on collagen type I and vitronectin. Further, this β1-integrin/uPAR interaction was necessary to maintain the increased adhesion of the WHCO6 cells on collagen type I versus non-ECM control. This clearly illustrates the importance of the uPAR/β1-integrin interaction and its role in adhesion of the WHCO6 cells on collagen type I.

Interestingly, in the WHCO1 cell line, the interaction between uPAR and membrane bound β1-integrin was not detectable (chapter 2). Yet, this interaction contributed to the adhesion of these cells on collagen type I. Ghosh *et al*. (2000) demonstrated that the uPAR/β1-integrin interaction in pp126 oral squamous cells increases on collagen type I. It is possible that the same scenario occurred in the WHCO1 cells, which contributed to the adhesion of these cells.

The uPAR/β1-integrin interaction and its contribution to adhesion of the WHCO1 on collagen type I was significant at $P < 0.1$. This suggests that the uPAR interaction with β1-integrin does play a contributing role in the overall adhesion of these cells. The collagen receptors, such as α1β1, α2β1 and α3β1 integrins also play a part in cell adhesion on collagen type I (Humphries *et al*., 2006). It is likely that these collagen receptors, in conjunction with the uPAR/β1-integrin interaction, influence adhesion of the WHCO1 cells on collagen type I.

General comment regarding HOSCC: The HOSCC cell lines used in this study are all the same type of tumour pathologically, but derived from different individuals (Veale and Thornley, 1989). The majority (4 of the 5) of the HOSCC cells utilized their uPAR during adhesion onto collagen type I or vitronectin. The WHCO5 cell line served as an exception (analyzed in general discussion). It is therefore feasible that uPAR played a role in cell-ECM adhesion and subsequent cell-ECM adhesion events during the progression of HOSCC cells to their transformed state.

In conclusion: These findings established that uPAR interaction with uPA or β1-integrin contributes to the adhesion of the majority of the HOSCC cell lines on collagen type I and/or vitronectin.

Chapter 5: The role of uPAR mechanisms in cell-ECM adhesion based proliferation of the HOSCC cell lines

5.1 Introduction

The adhesion of epithelial cells to their extracellular matrix is crucial for their proliferation as it is necessary for their progression into the S-phase of the cell cycle (Cao *et al*., 2000; Petreaca and Martins-Green, 2007). Pertinent to this study is the fact that cell-ECM induced proliferation also plays an important role in the development and maintenance of the transformed state (Ziober *et al*., 2006; Daley *et al*., 2008; Lopez *et al*., 2008).

Cell-ECM-based proliferation is influenced by the ECM as well as adaptor molecules such as the integrins which mediate the interaction between the cells and ECM (Cretu and Brooks, 2007). For example, the β1-integrin, αvβ3 and αvβ5 integrin are necessary for the proliferation of colorectal carcinoma cell line (HT-29) and hepatic colorectal adenocarcinoma metastases (derived from KM12SM cell line) on collagen type I (Conti *et al*., 2008). Additionally, Reinmuth *et al*. (2003) demonstrated that an antagonist of αvβ3 and αvβ5 integrin (S247) reduced the proliferation of murine colon carcinoma cell line (CT26), human endothelial cell line (HUVEC) and human vascular smooth muscle cell line (hVSMC) on vitronectin.

The uPAR protein, which has a role in cell adhesion (chapter 4), also contributes to cell proliferation and this is affected by its interaction with its ligands such as uPA, β1-integrin and vitronectin (Aguirre-Ghiso *et al*., 2003; Jo *et al*., 2007; Piccolella *et al*., 2008; Balsara *et al*., 2011). Endogenous uPA is important for proliferation of cells with a potent autocrine uPA/uPAR signalling system such as breast carcinoma cell line (MDA-MB-231), ovarian carcinoma cell line (OV-MZ-6) and prostate carcinoma cell line (DU145) (Gandhari *et al*., 2006; Piccolella *et al*., 2008). This was established by the addition of recombinant full isoform of uPAR without a GPI tail termed soluble uPAR (suPAR) which decreased proliferation of these cells by sequestering uPA (Wilhelm *et al*., 1994; Gandhari *et al*., 2006; Piccolella *et al*., 2008; Thunø *et al*., 2009).

Exogenous high molecular weight (HMW) uPA and its interaction with uPAR stimulated the proliferation of osteoblastic cell line (Sa-OS-2) and bladder carcinoma endothelial-like cells (ECV304 cells) (Juretic *et al*., 2001; Maupas-Schwalm *et al*., 2009). Additionally, the

interaction of uPAR with β1-integrin plays a part in the proliferation of head and neck squamous cell carcinoma (Aguirre-Ghiso *et al*., 2003; Chaurasia *et al*., 2009). Furthermore, uPAR and its interaction with vitronectin influenced the proliferation of an osteoblastic cell line and human endothelial cells (Juretic *et al*., 2001; Balsara *et al*., 2011).

Uncontrolled proliferation is a crucial step in the transformation of HOSCC and therefore it is crucial to understand the different contributions made to proliferation of HOSCC (Smeds *et al*., 2002; Liu *et al*., 2009; Bird-Lieberman and Fitzgerald, 2009). Based on the demonstration that: 1) cell-ECM communication is important during HOSCC development (Liu *et al*., 2009; Ortiz *et al*., 2010); 2) uPAR contributes to the interaction of the HOSCC cell lines on collagen type I and vitronectin (see chapter 4); and 3) uPAR mechanisms are involved in proliferation of several carcinoma types (Aguirre-Ghiso *et al*., 2003; Gandhari *et al*., 2006); this provides the model to test whether uPAR mechanisms influence the proliferation of the HOSCC cell lines in the absence of ECM or presence of collagen type I and vitronectin. This would provide an understanding of whether there is cross-talk between uPAR and the ECM environment in terms of proliferation of carcinomas.

5.2 Materials and methods

5.2.1 Cell Lines and tissue culture

The HOSCC cell lines previously described in section 2.2.1 were used. Cells were maintained as described in section 2.2.1.

5.2.2 Coating of tissue culture dishes with collagen type I or vitronectin

Proliferation assays were carried out in Nunclon flat bottom 96-well plates. Non coated wells served as control to analyze proliferation in the absence of ECM. The 96-well plates were coated with collagen type I and vitronectin according to the procedure described in section 4.2.2.

The 96-well plates were also coated with a combination of collagen type I and vitronectin. In this procedure, 1 μg/ml vitronectin was added to collagen type I-coated 96-well plates. The plate was incubated for 3 hours at 37^{o}C. Excess vitronectin was removed and each well was rinsed with 50 μl of PBS. PBS (50 μl) was added to the collagen type I and vitronectin-coated wells.

5.2.3 Antibodies

-Anti-uPA antibody (section 2.2.6).

-Rabbit anti-goat IgG designated as IgG control (Sigma).

5.2.4 Cell Proliferation assay (MTT)

Cell proliferation assay was performed using all the HOSCC cell lines using the MTT based method. This gives a measure to the number of viable cells. **Day 1:** The cells were passaged at 60 to 80 % confluency with trypsin/EDTA solution. The cell suspension was mixed in tissue culture medium supplemented with either 10% serum or 1% BSA. The cells were counted using a haemocytometer. The cell suspension was centrifuged briefly and the supernatant containing trypsin solution was removed. 10000 cells/well were resuspended in 200 μl of

tissue culture medium supplemented with 10% FCS and were seeded on non-coated wells or collagen type I-coated wells. Additionally, 1 x 10^5 cells/well were resuspended in 200 µl of tissue culture medium supplemented with 0.1 % BSA on vitronectin or collagen type I and vitronectin coated wells. Serum is rich in vitronectin which is the reason it was not supplemented (Hayman *et al*., 1983). The cells were incubated at 37^{o}C in 5% CO_2 atmosphere in a humidified incubator for 18 hours.

Day 2: The cells were rinsed with 100 µl of PBS and tissue culture medium (100 µl) was added to the cells. The cells were incubated at 37^{o}C in 5% CO_2 atmosphere in a humidified incubator for 4 hours. The cells were rinsed with tissue culture medium and 100 µl of DMEM was added to the cells. The cells growing in the absence of ECM (non-coated wells) or presence of ECM (collagen type I, vitronectin, collagen type I/vitronectin mix), were exposed to the following different treatments:

suPAR: The cells were supplemented with or without 10 nM soluble uPAR (suPAR) for 24 hours. This is the suPAR concentration used by Piccolella *et al*. (2008) to sequester endogenous uPA or reduce the concentration of uPA available to uPAR.

Exogenous uPA: The cells were supplemented with or without 0.5 nM, 1 nM or 5 nM of exogenous uPA for 24 hours.

β1P1: The cells were supplemented with either 0.02 mM β1P1^{Sc} control peptide or 0.02 mM β1P1 peptide for 24 hours. This is the concentration used to treat cells *in vitro* over a 24 hours period (Wei *et al*., 2005).

Anti-uPA antibody: The cells were supplemented with 0.005 mg/ml rabbit IgG control or 0.005 mg/ml anti-uPA antibody for 24 hours.

TGFβ: The cells were supplemented with or without 1 ng/ml TGFβ for 24 hours.

The cells with the different treatments were incubated at 37^{o}C in 5% CO_2 atmosphere in a humidified incubator for 24 hours. **Day 3:** The number of viable cells were counted by MTT method. This method is widely used as a measure of proliferation. 100 µl of 0.5 mg/ml MTT in filter sterilized PBS was added to the adherent cells and the cells were incubated for 3 hours at 37^{o}C. The MTT solution was removed and 100 µl of DMSO was added to dissolve

the formazan crystals. After an hour the absorbance reading was determined using a microtiter plate reader at 490 nm. The proliferation assays were performed in triplicates, under the same tissue culture conditions and in the same time frame. The number of proliferating cells was measured at the end point of an experiment. Clearly detachment may affect the proliferation responses, however in this instance data were generated for comparative purposes rather than an absolute measure

5.2.5 Statistical analysis

All statistical analysis (one way ANOVA and Student's t-test) were performed using GraphPad Prism version 4.00 statistical program.

5.3. Results

5.3.1. Influence of uPAR on proliferation of the HOSCC cells in the absence of ECM

All the HOSCC cell lines under investigation secrete uPA (Chapter 2). To determine the effect of endogenous uPA and its activation of uPAR on proliferation of the HOSCC cell lines, soluble uPAR (suPAR) was used. This is because suPAR binds to and sequesters endogenous uPA that is available to uPAR (Gandhari *et al*., 2006; Piccolella *et al*., 2008). Upon sequestering uPA with suPAR, there was little variation in the proliferation of the HOSCC cell lines in the absence of ECM (Figure 5.1.a). This means that the uPAR activation by endogenous uPA, does not contribute to the proliferation of the HOSCC cell lines in the absence of ECM.

Exogenous uPA was used to establish whether increasing the amount of uPA available to uPAR influences the proliferation of the HOSCC cell lines. There was no noteworthy change in proliferation of the HOSCC cell lines upon exposure to different exogenous uPA concentrations (Figure 5.1.b). Therefore when the amount of uPA that is accessible to uPAR, is above that of endogenous uPA, the proliferation of the HOSCC cell lines is not affected. This event occurs when the HOSCC cell lines proliferate in the absence of ECM.

The β1P1 blocking peptide was used to analyse the uPAR/β1-integrin interaction on cell proliferation since this peptide successfully reduces the association between β1-integrin and uPAR (Chapter 2, Wei *et al*., 2005). The $\beta1P1^{Sc}$ peptide does not have an established interaction with other peptides and served as a control peptide.

Blocking the uPAR interaction with β1-integrin with β1P1 led to little variation in proliferation of the SNO, WHCO1 and WHCO5 cells in the absence of ECM (Figure 5.1.c). On the other hand, the proliferation of the WHCO3 cells was notably[2] reduced upon exposure to β1P1 blocking peptide compared with the exposure to $\beta1P1^{Sc}$ control peptide (Figure 5.1.c). Furthermore, in the presence of β1P1 blocking peptide the proliferation of the WHCO6 cells was significantly decreased when compared to the presence of control peptide ($P<0.05$) (Figure 5.1.c). This confirms that the interaction between uPAR and β1-integrin contributed to the proliferation of specifically the WHCO3 and WHCO6 cells in the absence of ECM.

[2] A notable difference was significant at the 10% level ($P<0.1$)

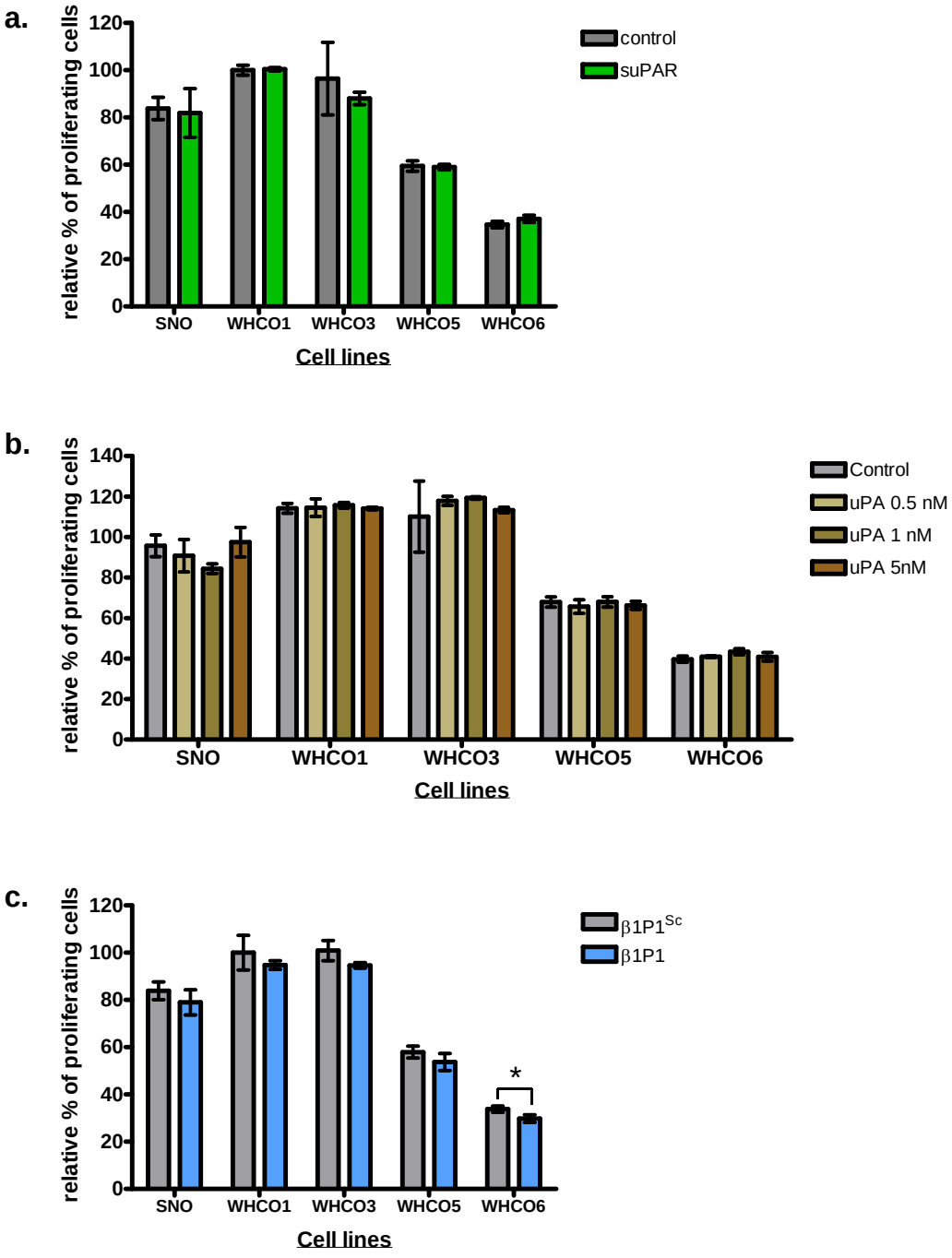

Figure 5.1: Investigation of the role of uPAR on proliferation of the HOSCC cells in the absence of ECM. **(a)** The proliferation of the HOSCC cells in the absence (control, grey bar) or presence of suPAR (green bar). suPAR was used to examine the role of endogenous uPA on proliferation of the HOSCC cells. The mean number of proliferating WHCO1 cells, which were not exposed to suPAR, was set at 100%. **(b)** The proliferation of the HOSCC cells in the absence (control, grey bar) or presence of exogenous uPA (at concentrations of 0.5 nM, 1 nM and 5 nM). The mean number of proliferating WHCO1 cells, which were not exposed to uPA, was set at 100%. **(c)** The proliferation of the HOSCC cells that were exposed to β1P1^{Sc} control peptide (grey bar) or β1P1 (blue bar) in order to examine to role of uPAR/β1-integrin interaction on proliferation. The mean number of proliferating WHCO1 cells, which were exposed to β1P1^{Sc}, was set at 100%. **Note:** An unpaired Student's t-test was used to compare: 1) the proliferation of the HOSCC cells in the absence versus the presence of suPAR and 2) the proliferation of the HOSCC cells exposed to β1P1 blocking peptide versus β1P1^{Sc} control peptide. A one way ANOVA was used to compare the proliferation of the HOSCC cells affected by the different uPA concentrations and untreated control. ***P values are indicated by *; * = P<0.05; ** = P<0.01; *** = P<0.001; Standard error bars = Standard deviation; n= 3***.

5.3.2. Influence of uPAR on proliferation of HOSCC cells in the presence of collagen type I substrate

This section of the study examines the influence of uPAR mechanisms on proliferation of the HOSCC cell lines in the presence of collagen type I substrate.

When endogenous uPA was sequestered by suPAR, there was a minimal change in the proliferation of the WHCO1 and WHCO6 cells compared with untreated control (Figure 5.2.a). On the contrary, the proliferation of the SNO cells was notably reduced when the cells were exposed to suPAR. Furthermore, the proliferation of the WHCO3 and WHCO5 cells decreased significantly in the presence of suPAR ($P<0.05$) (Figure 5.2.a). Therefore, the activation of uPAR by endogenous uPA contributes to the proliferation of the SNO, WHCO3 and WHCO5 cells on collagen type I.

Saturation of uPAR with exogenous uPA did not cause a significant variation in proliferation of the HOSCC cells (Figure 5.2.b). Thus, increasing the concentration of uPA available to uPAR does not change the proliferation of the HOSCC cell lines grown in the presence of collagen type I.

Disruption of the uPAR/β1-integrin interaction with β1P1 peptide in the HOSCC cells, did not result in a noticeable change in the proliferation of the HOSCC cells on collagen type I (Figure 5.2.c). Therefore, the interaction between uPAR and β1-integrin does not influence the proliferation of the HOSCC cell lines in the presence of collagen type I.

5.3.3. Influence of uPAR on proliferation of the HOSCC cells on a vitronectin substrate

Decreasing the concentration of endogenous uPA available to uPAR, with suPAR, had a variable effect on the proliferation of the HOSCC cells on vitronectin. In the presence of suPAR, there were minor changes in the proliferation of the SNO, WHCO1 and WHCO3 cells on vitronectin, compared with untreated control (Figure 5.3.a). By contrast, the proliferation of the WHCO5 and WHCO6 cells decreased significantly upon exposure to suPAR ($P<0.05$) (Figure 5.3.a).

a.

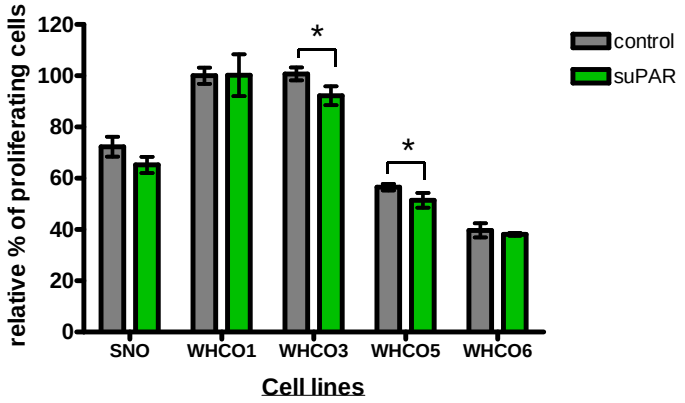

b.

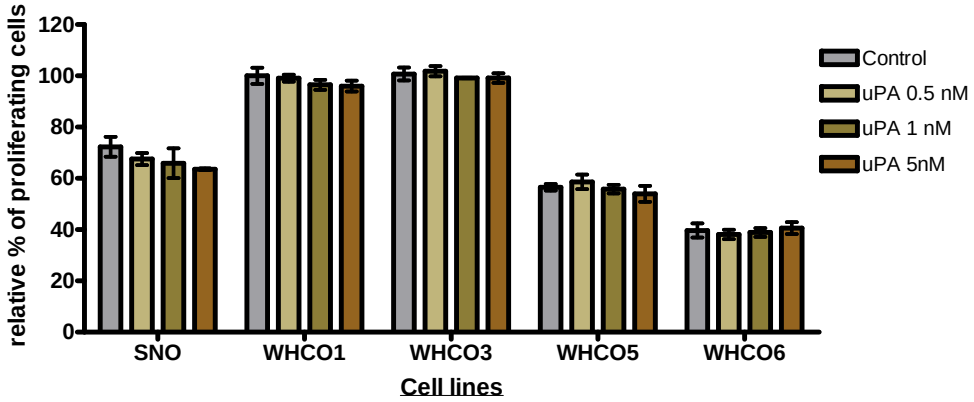

c.

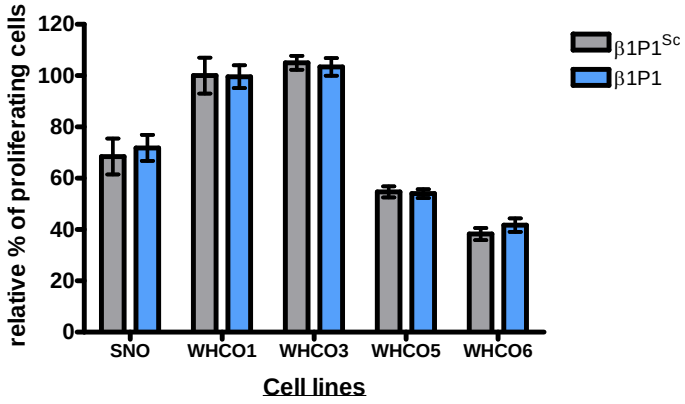

Figure 5.2: Investigation of the role of uPAR on proliferation of the HOSCC cells in the presence of collagen type I substrate. **(a)** The proliferation of the HOSCC cells in the absence (control, grey bar) or presence of suPAR (green bar). The mean number of proliferating WHCO1 cells, which were not exposed to suPAR, was set at 100%. **(b)** The proliferation of the HOSCC cells in the absence (control, grey bar) or presence of exogenous uPA (at concentrations of 0.5 nM, 1 nM and 5 nM). The mean number of proliferating WHCO1 cells, which were not exposed to uPA, was set at 100%. **(c)** The proliferation of the HOSCC cells that were exposed to $\beta1P1^{Sc}$ control peptide (grey bar) or β1P1 (blue bar). The mean number of proliferating WHCO1 cells, which were exposed to $\beta1P1^{Sc}$, was set at 100%. **Note:** An unpaired Student's t-test was used to compare: 1) the proliferation of the HOSCC cells in the absence versus the presence of suPAR and 2) the proliferation of the HOSCC cells exposed to β1P1 blocking peptide versus $\beta1P1^{Sc}$ control peptide. A one way ANOVA was used to compare the proliferation of the HOSCC cells affected by the different uPA concentrations and untreated control. ***P values are indicated by *; * = P<0.05; ** = P<0.01; *** = P<0.001; Standard error bars = Standard deviation; n= 3***.

Soluble uPAR (suPAR) and cellular uPAR bind to the somatomedin B domain of vitronectin (Lash *et al*., 2001; Sidenius *et al*., 2002). Therefore the suPAR effect on proliferation of the WHCO5 and WHCO6 cells on vitronectin substrate is not limited to the role of suPAR in reducing the endogenous uPA/uPAR signalling complex. Consequently, the endogenous uPA activation of uPAR and its influence on proliferation of these specific cells was tested by other means. The anti-uPA antibody was used to sequester endogenous uPA. Since the anti-uPA antibody is directed against an antigen, the control needed to be an antibody directed against an antigen that is not around human cells. The rabbit anti-goat IgG was used as a control, which is referred to as IgG control in the following text.

The presence of the anti-uPA antibody and its function on cell proliferation was measured against the presence of an IgG control. In the presence of the antibody there was no significant change in proliferation of the WHCO6 cells on a vitronectin substrate (Figure 5.3.a.ii). However, the proliferation of the WHCO5 cells on vitronectin, significantly decreased in the presence of anti-uPA antibody ($P<0.05$) (Figure 5.3.a.ii). Therefore the activation of uPAR by endogenous uPA contributes to the proliferation of specifically the WHCO5 cells in the presence of vitronectin.

The activation of uPAR with increasing concentration of exogenous uPA caused little variation in proliferation of the SNO, WHCO1, WHCO3 and WHCO6 cells on vitronectin (Figure 5.3.b). On the contrary, there was a significant variation in the proliferation of the WHCO5 cells in the presence of vitronectin upon exposure to different exogenous uPA concentration ($P<0.05$). Additionally, there was a significant decrease in proliferation of the WHCO5 cells upon activation of uPAR with 1 nM uPA versus untreated control ($P<0.05$). This confirms that increasing the amounts of uPA accessible to uPAR does not increase the proliferation of the HOSCC cells on vitronectin. The proliferation of the WHCO5 cells on vitronectin decreases upon activation of uPAR with exogenous uPA (1 nM).

When the uPAR interaction with β1-integrin was disrupted with β1P1, there was little variation in the proliferation of the majority of the HOSCC cells on vitronectin substrate (Figure 5.3.c). However, the proliferation of the WHCO1 cells was notably reduced in the presence of the β1P1 blocking peptide when compared to the presence of $\beta1P1^{Sc}$ control peptide (Figure 5.3.c). Therefore uPAR/β1-integrin interaction contributes to the proliferation of the WHCO1 cells on vitronectin.

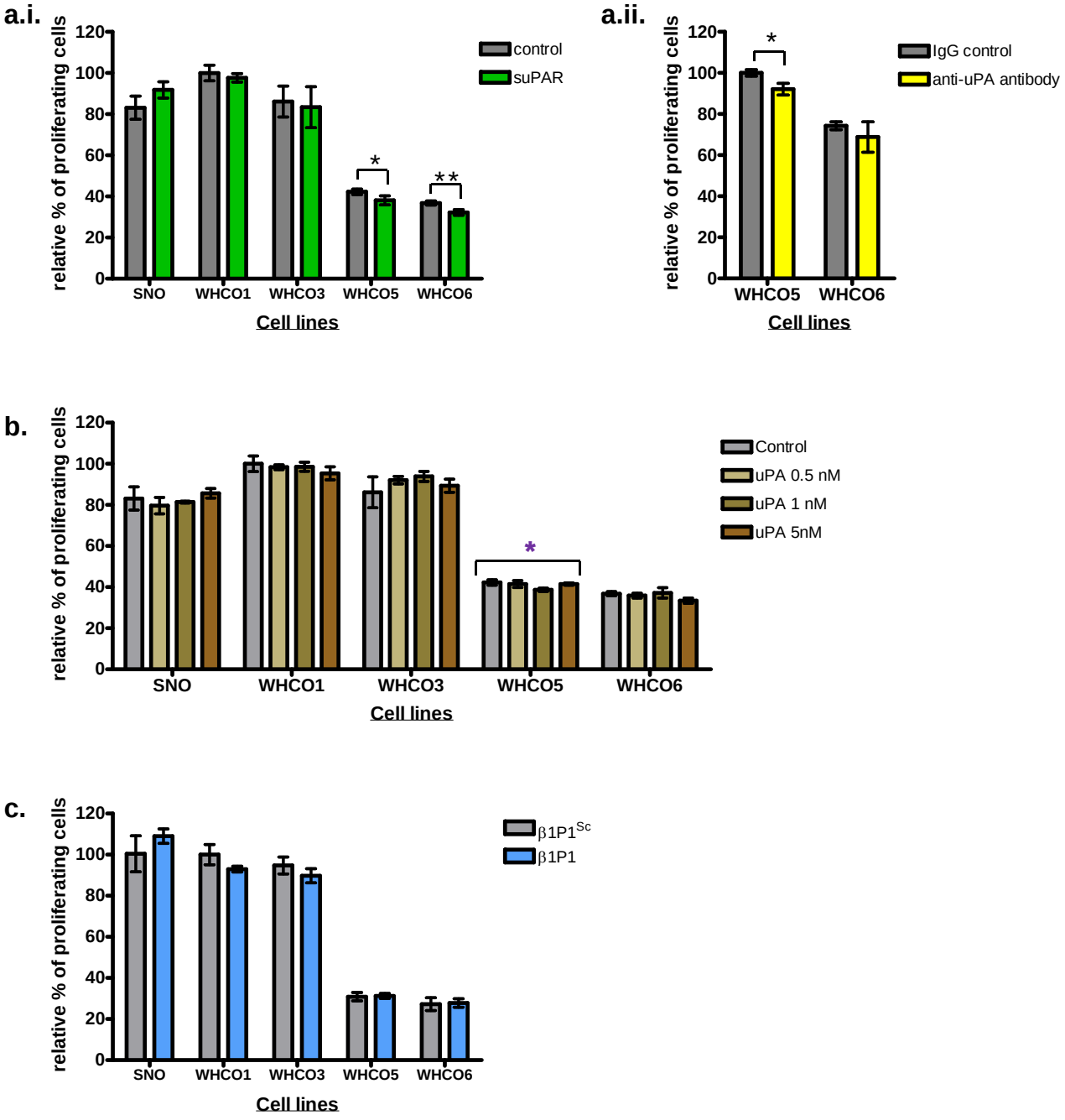

Figure 5.3: Investigation of the role of uPAR on proliferation of the HOSCC cells in the presence of vitronectin substrate. **(a.i)** The proliferation of the HOSCC cells in the absence (control, grey bar) or presence of suPAR (green bar). The mean number of proliferating WHCO1 cells, which were not exposed to suPAR, was set at 100%. **(a.ii)** The proliferation of the HOSCC cells in the presence of an IgG control (grey bar) or anti-uPA antibody (yellow bar). The mean number of proliferating WHCO1 cells, which were not exposed to uPA, was set at 100%. **(b)** The proliferation of the HOSCC cells in the absence (control, grey bar) or presence of exogenous uPA (at concentrations of 0.5 nM, 1 nM and 5 nM). **(c)** The proliferation of the HOSCC cells that were exposed to β1P1^{Sc} control peptide (grey bar) or β1P1 (blue bar). The mean number of proliferating WHCO1 cells, which were exposed to β1P1^{Sc}, was set at 100%. **Note:** An unpaired Student's t-test was used to compare: 1) the proliferation of the HOSCC cells in the absence versus the presence of suPAR; 2) the proliferation of the HOSCC cells in the presence of anti-uPA antibody versus IgG control and 3) the proliferation of the HOSCC cells exposed to β1P1 blocking peptide versus β1P1^{Sc} control peptide. A one way ANOVA was used to compare the proliferation of the HOSCC cells affected by the different uPA concentrations and untreated control. ***P values are indicated by *; * = P<0.05; ** = P<0.01; *** = P<0.001; Standard error bars = Standard deviation; n= 3***.

5.3.4. The interaction of cellular uPAR with vitronectin and its influence on proliferation of the HOSCC cells on vitronectin substrate

The reduced proliferation of the WHCO5 and WHCO6 cells on vitronectin that occurs in the presence of suPAR (Figure 5.3.a.i) could be due to suPAR disrupting the cellular uPAR interaction with vitronectin. TGFβ binds to vitronectin at a region overlapping and proximal to the uPAR binding site and hampers the interaction between cellular uPAR and vitronectin (Huai *et al*., 2008; Schoppet *et al*., 2002). TGFβ was therefore used as a tool to explore further whether proliferation of the HOSCC cells is affected by their cellular uPAR interaction with vitronectin.

The addition of TGFβ did not lead to a considerable variation in the proliferation of the HOSCC cells in the absence of ECM (Figure 5.4.a). Disrupting the cellular uPAR interaction with vitronectin, using TGFβ, led to minor changes in the proliferation of the SNO, WHCO1 and WHCO3 cells on vitronectin, compared with untreated control (Figure 5.4.b). In contrast, the proliferation of the WHCO5 and WHCO6 cells on vitronectin decreased significantly in the presence of TGFβ versus untreated control ($P<0.05$) (Figure 5.4.b). Thus the relationship between cellular uPAR and vitronectin contributed to the proliferation of specifically the WHCO5 and WHCO6 cells on vitronectin.

5.3.5. The influence of the uPAR/ vitronectin interaction on proliferation of the HOSCC cells provided with collagen type I and vitronectin

To provide insight into the proliferative role of the uPAR/vitronectin interaction *in vivo*, a combination of collagen type I and vitronectin was used in this part of the investigation. This is on the assumption that this ECM combination is a better approximation of the ECM *in vivo*. The WHCO5 and WHCO6 cells were used for this analysis since their cellular uPAR interaction with the vitronectin substrate contribute to their proliferation.

Soluble uPAR (suPAR) and TGFβ were used to obstruct the uPAR binding site on vitronectin. Upon the addition of suPAR, there was little variation in the proliferation of the WHCO5 and WHCO6 cells on a combination of collagen type I and vitronectin substrate, compared with untreated control (Figure 5.5.a). Similarly in the presence of TGFβ, the proliferation of WHCO5 and WHCO6 cells on collagen type I and vitronectin substrate did not change significantly compared with untreated control (Figure 5.5.b). Therefore, the

interaction of cellular uPAR with vitronectin and its contribution to the proliferation of the WHCO5 and WHCO6 cells is not significant in the presence of collagen type I together with vitronectin. Further, this means that the presence of collagen type I compensates for the proliferative influence induced by the cellular uPAR interaction with vitronectin.

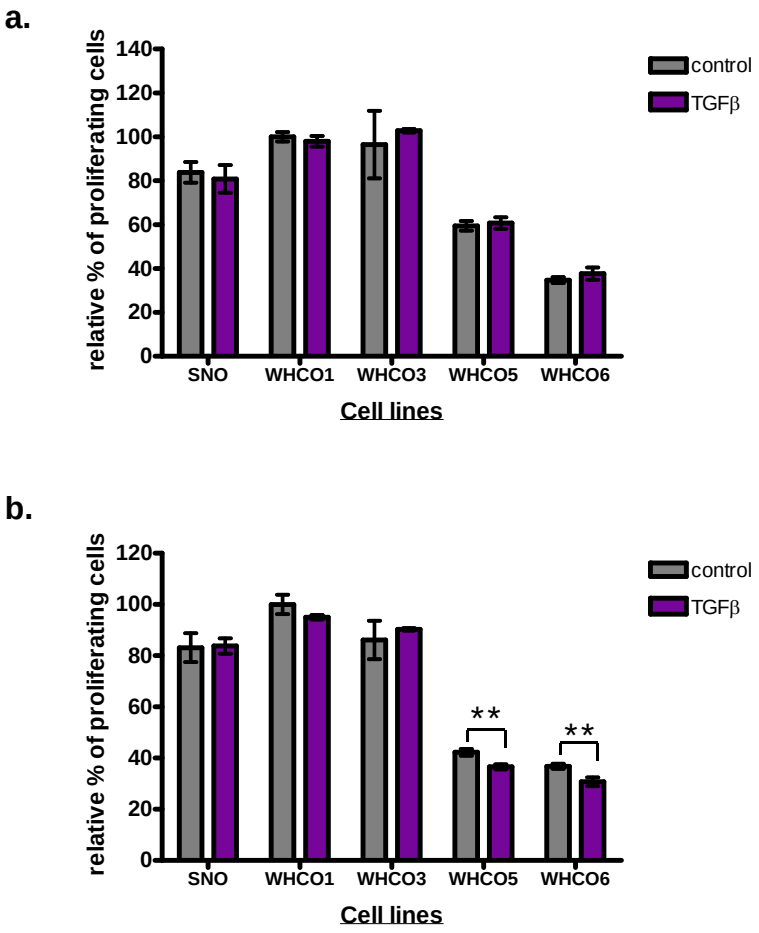

Figure 5.4: Investigation of the role of cellular uPAR/vitronectin interaction on proliferation of the HOSCC cell, using TGFβ. (a) The proliferation of the HOSCC cells in the absence of ECM and upon exposure to TGFβ (purple bar). Untreated HOSCC cells served as control (grey bar). **(b)** The proliferation of the HOSCC cells on vitronectin in the presence of TGFβ (purple bar), while untreated HOSCC cell lines served as control (grey bar). **Note:** The mean number of proliferating WHCO1 cells, which were not exposed to TGFβ, was set at 100%. An unpaired Student's t-test was used to compare the proliferation of HOSCC cells exposed to TGFβ treated versus untreated control HOSCC cells. ***P values are indicated by *; * = P<0.05; ** = P<0.01; *** = P<0.001; Standard error bars = Standard deviation; n= 3***.

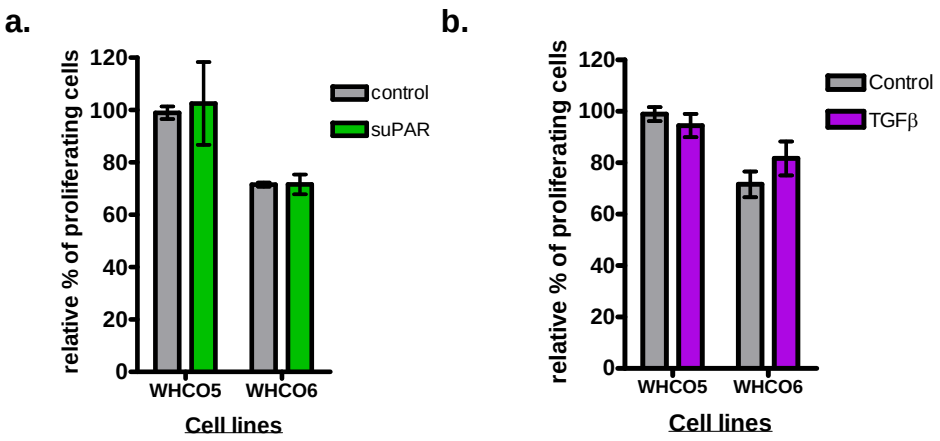

Figure 5.5: The proliferation of the WHCO5 and WHCO6 cells in the presence of collagen type I and vitronectin combination substrate. The proliferation of the HOSCC cells upon exposure to **(a)** suPAR (green bar) or **(b)** TGFβ (purple bar) on collagen type I and vitronectin substrate. Untreated HOSCC served as control (grey bar). **Note:** The mean number of proliferating WHCO5 cells, which were not treated was set at 100%. An unpaired Student's t-test was used to compare the proliferation of HOSCC cells exposed to suPAR or TGFβ treated versus untreated control HOSCC cells.

5.4 Discussion

The current investigation established for that uPAR contributes to the proliferation of the HOSCC cells. Furthermore, the uPAR impact on proliferation of the HOSCC cell lines is influenced by the ECM and/or the interaction of uPAR with its ligands.

This is the first demonstration that uPAR has a proliferative role in HOSCC as evident by the reaction of all the HOSCC cell lines. These results in conjunction with others studies demonstrate that uPAR plays a proliferative role in different carcinomas, such as oral, breast, and prostate (Jo *et al*., 2003; Piccolella *et al*., 2008; Liang *et al*, 2008). The involvement of uPAR on proliferation of the HOSCC cells is affected by the absence or presence of collagen type I or vitronectin. Furthermore, the uPAR role in proliferation of the HOSCC cells is mediated via the uPAR interaction with uPA, β1-integrin and/or vitronectin.

The endogenous uPA/uPAR complex plays a part in the proliferation of the SNO, WHCO3 and WHCO5 cells on collagen type I and the proliferation of the WHCO5 cells on vitronectin. Previous studies established that the endogenous uPA/uPAR complex was involved in the proliferation of breast cancer cells (MDA-MB-231) and prostate carcinoma cells (Jo *et al*., 2003; Piccolella *et al*., 2008). These experiments were performed in the absence of an ECM component. The current investigation shows that the endogenous uPA/uPAR complex contributes to the proliferation of the SNO, WHCO3 and WHCO5 cells, exclusively in the presence of ECM. This demonstrates that there is a relationship between uPAR activation by endogenous uPA and the ECM in terms of proliferation of HOSCC cells.

Increasing the concentration of uPA available to uPAR with different concentrations of exogenous HMW uPA, did not increase the proliferation of the HOSCC cells. This was seen in all the HOSCC cells in the absence of ECM or presence of collagen type I or vitronectin substrate. It is interesting to note that in the presence of exogenous uPA, the proliferation of the WHCO3 and WHCO5 cells does not increase. However, the endogenous uPA/uPAR complex contributes to the proliferation of the WHCO3 and WHCO5 cells on the ECM substrates tested.

The concentration of uPA secreted by these cells is therefore at the threshold level that complexes with uPAR to play a role in proliferation. This means that the increased amount of uPA available to uPAR is regulated possibly by mechanisms such as uPAR cleavage, expression and secretion of plasminogen activator inhibitor 1 (PAI) (Czekay *et al*., 2001; Mazzieri *et al*., 2006). Cleavage of uPAR occurs at the linker region between domains 1 and

2 and alters the ability of uPAR to interact with uPA (Mazzieri *et al*., 2006; Blasi and Sidenius, 2010). The PAI-1 protein together with uPA/uPAR and the LRP-1 receptor form a complex that leads to uPAR internalization thereby reducing the number of uPA/uPAR complexes (Czekay *et al*., 2003).

The uPAR interaction with β1-integrin contributes to the proliferation of the WHCO3 and WHCO6 cells in the absence of ECM and WHCO1 cells on vitronectin. The results of this investigation, in conjunction with other studies, demonstrate that the uPAR interaction with β1-integrin plays a part in proliferation of squamous cell carcinomas such as head and neck (Aguirre-Ghiso *et al*., 2002).

In the presence of β1P1 peptide, which disrupts the uPAR/β1-integrin interaction, the decrease in proliferation of the WHCO1 and WHCO3 cells was significant at the $P<0.1$. This indicates that the uPAR interaction with β1-integrin does play a part, although not significant, in the proliferation of these cells. Other factors also affect proliferation of the HOSCC cells such as different expression of growth factors and their receptors, for example TGF α and the EGF receptors (Jones *et al*., 1993). These factors, together with the uPAR/β1-integrin interaction, influence the overall proliferation of HOSCC.

Interestingly, the uPAR interaction with β1-integrin did not contribute to proliferation of the HOSCC cell lines on collagen type I. It is possible that collagen receptors such as the α1β1, α2β1 and α3β1 integrins, rather than the uPAR/β1-integrin interaction, influence the proliferation of HOSCC cells on collagen type I (Pozzi *et al*., 1998; Vitale *et al*., 1997; Conti *et al*., 2008). These collagen receptors are in fact involved in proliferation of mouse embryonic fibroblast, human thyroid cells and colorectal carcinoma cell lines in the presence of collagen type I (Pozzi *et al*., 1998; Vitale *et al*., 1997; Conti *et al*., 2008). Therefore, when the uPAR interaction with β1-integrin is compromised in the HOSCC cells, these collagen receptors may compensate for the lack of the interaction in terms of proliferation.

The interaction between vitronectin and the uPAR of the WHCO5 and WHCO6 cells was necessary for their proliferation on a vitronectin substrate. This was established by disrupting the association of cellular uPAR interaction with vitronectin with suPAR or TGFβ (see section 5.3.4 for detail). Previous studies established that $uPAR^{-/-}$ endothelial cells had reduced proliferation on vitronectin compared with wild type endothelial cells (Balsara *et al*., 2011). The result of this study is outstanding and demonstrates that uPAR and its interaction with vitronectin also has a role in proliferation of carcinomas such as HOSCC.

The endogenous uPA/uPAR complex as well as the cellular uPAR/vitronectin complex contributed to the proliferation of the WHCO5 cells on vitronectin. Interestingly, the uPA protein is known to enhance the uPAR/vitronectin interaction (Stepanova and Tkachuk, 2002; Huai *et al*., 2008). It is likely that a complex of uPA/uPAR/vitronectin occurs in the WHCO5 cells, which is involved in proliferation of these cells on vitronectin.

The interaction of uPAR with vitronectin played a part in the proliferation of the WHCO5 and WHCO6 cells on vitronectin but not on a combination of collagen type I and vitronectin substrate. This indicates that the uPAR/vitronectin interaction and its contribution to the proliferation of these cells is outweighed by the presence of collagen type I. In the event that the interaction of uPAR and vitronectin is disturbed, the presence of collagen type I compensates for the lack of this interaction in terms of proliferation.

General comment with regard to HOSCC: This study established that in all the HOSCC cell lines, uPAR contributed to cell proliferation in the absence or the presence of collagen type I or vitronectin. The HOSCC cell lines used in this study are derived from moderately differentiated tumours from patients with metastatic disease. Therefore, during the progression of the cells to their transformed state, it is very possible that uPAR and its relationship with the ECM, contributed to their proliferation.

In conclusion:

The uPAR system, previously only considered to have a role in the ECM degradation pathway, has an impact on the proliferation of the HOSCC cell lines. This proliferation is influenced by the unique relationship of uPAR with its ligands (uPA and β1-integrin) and the ECM (collagen type I and vitronectin).

Chapter 6: The influence of growth factors, extracellular matrix and uPAR on the proliferation of the HOSCC cells

6.1 Introduction

The specific interplay between growth factors, their receptors and the ECM is an essential aspect in the regulation of cell-ECM induced proliferation of epithelial cells (Hollier *et al*., 2005; Chiarugi, 2008). Epidermal growth factor (EGF) is a growth factor vital in epithelial tissue development (Schneider and Wolf, 2009). However, EGF also plays a significant role in carcinoma development and metastasis (Andl *et al*., 2003; Zhang *et al*., 2010).

Interaction of EGF with its receptor EGFR or ERBB1/HER1, causes the EGFR to form homodimers or heterodimers with other members of the EGFR family (ERBB2/HER2/NEU, ERBB3/HER3 and ERBB4/HER4) (Schneider and Wolf, 2009; Mitsudomi and Yatabe, 2010). This leads to tyrosine kinase activity of the receptors and autophosphorylation of specific tyrosine residues in their cytoplasmic domain (Schneider and Wolf, 2009; Mitsudomi and Yatabe, 2010). The result is the downstream signalling and activation of the v-Src, MAPK, and signal transducer and activator of transcription (STAT) signalling pathways, which affect events such as cellular proliferation (Schneider and Wolf, 2009; Mitsudomi and Yatabe, 2010).

With respect to HOSCC, EGF is an important mitogen as several studies have demonstrated the overexpression of EGFR in HOSCC, including the HOSCC cell lines used in the current study (Veale and Thornely., 1989; Jones *et al*., 1993; Zhang *et al*., 2010). Furthermore, the overexpression of the EGFR receptor and the EGF/EGFR pathway is associated with poor prognosis and survival rate of patients with HOSCC (Mukaida *et al*., 1991; Zhang *et al*., 2010).

Several studies have demonstrated that EGF also influences the proliferation of cells on different ECM surfaces such as the ones used in this investigation, collagen type I and vitronectin (Kawahara *et al*., 2002; Hollier *et al*., 2005). For example, in the presence of EGF proliferation of A431 squamous cell carcinoma cell line on a collagen type I surface was reduced (Kawahara *et al*., 2002). Additionally, EGF (10 ng/ml) stimulates proliferation of HaCAT squamous cell carcinoma cell line in the presence of plasma vitronectin (Hollier *et al*., 2005).

Importantly to this study, there is a specific relationship between EGF, EGFR and uPAR in terms of cellular proliferation (Jo *et al*., 2007). EGF induced proliferation of murine keratinocytes, murine embryonic fibroblasts (MEF) as well as breast cancer cells (MDA-MB-231 and MDA-MB-468) *in vitro* required uPAR expression (Jo *et al*., 2007; D'Alessio *et al*., 2008).

Given that: 1) the EGF/EGFR pathway is linked with HOSCC progression (Andl *et al*., 2003; Zhang *et al*., 2010); 2) EGF affect on the proliferation of certain carcinomas is influenced by the ECM (Hollier *et al*., 2005); 3) uPAR contributes to cell-ECM based proliferation of HOSCC (chapter 5); and 4) EGF induced proliferation involves uPAR in different cell types (Jo *et al*., 2007); this brings us to the aims in this component of the study: to determine whether the known effect of EGF on squamous cell carcinoma is influenced by components such as ECM and in conjunction with uPAR. This would provide an understanding of whether uPAR and its relationship with the ECM are involved in EGF stimulation of proliferation in carcinomas.

6.2 Materials and methods

6.2.1 Cell Lines and tissue culture

The HOSCC cell lines previously described in section 2.2.1 were used. Cells were maintained as described in section 2.2.1.

6.2.2 Coating of tissue culture dishes with collagen type I or vitronectin

The 96-well plates were coated with collagen type I and vitronectin according to the procedure described in section 4.2.2 and 5.2.2.

6.2.3. Antibodies

-Anti-uPAR (399R) antibody (section 2.2.6)
-IgG control antibody (section 5.2.3)

6.2.4 Cell Proliferation assay

Day 1: The HOSCC cells were harvested and seeded onto the 96-well plate coated with or without the ECM components (collagen type I, vitronectin, collagen type I/vitronectin mix). This was done according to the "Day 1" procedure described in section 5.2.4.

Day 2: The cells were rinsed with 100 μl of PBS and tissue culture medium (100 μl) was added to the cells. The cells were incubated in incubated at 37^{o}C in 5% CO_2 atmosphere in a humidified incubator for 4 hours. The cells were rinsed with tissue culture medium and 100 μl of DMEM was added to the cells. The cells growing in the absence of ECM (non-coated wells) or presence of ECM (collagen type I, vitronectin, collagen type I/vitronectin mix), were exposed to the following different treatments:

EGF: The cells were supplemented with or without EGF (10 ng/ml) for 24 hours. This was the concentration used by Driver (2007) to activate EGFR in the HOSCC cell lines.

EGF treatment in the presence of anti-uPAR (399R) or control IgG antibodies: The cells were supplemented with or without EGF in the presence of 0.005 mg/ml anti-uPAR (399R) antibody. This was the concentration of antibody that inhibits the uPAR interaction with uPA (American diagnostica 399R product sheet). In a control experiment, the cells were supplemented with or without EGF in the presence of 0.005 mg/ml control IgG antibody.

EGF treatment in the presence of β1P1 or β1P1^{Sc} peptides: The cells were supplemented with or without EGF in the presence of 0.02 mM β1P1 peptide. In the control experiment, the cells were supplemented with or without EGF in the presence of control 0.02 mM β1P1^{Sc}.

All the different experimental treatments were made to a final volume of 100 μl/well with DMEM/Hams F12. The plate was incubated at 37^{o}C for 24 hours.

Day 3: The number of viable cells was counted by MTT method. This was done according to the "Day 3" procedure described in section 5.2.4. The proliferation assays were performed in triplicates.

6.2.5 Statistical analysis

Unpaired Student's t-test was performed using GraphPad Prism version 4.00 statistical program. Statistical difference at the 5% level was considered a significant difference.

6.3 Results

6.3.1 EGFR activation affects on proliferation of the HOSCC cells in the absence of ECM and the role of uPAR

Activation of EGFR with EGF increased the proliferation of the WHCO1, WHCO3, WHCO5 and WHCO6 cells compared with untreated control ($P<0.05$) (Figure 6.1). However, the proliferation of the SNO cells was significantly reduced upon addition of EGF ($P<0.05$) (Figure 6.1). These results indicate that EGFR activation stimulated the proliferation of the majority of the HOSCC cell lines. The four HOSCC cell lines, with the established increase in proliferation upon EGFR activation, were further used to examine the role of uPAR during EGF induced proliferation.

EGFR activation with EGF significantly increased the proliferation of the WHCO1, WHCO3 and WHCO5 cells even when the endogenous uPA interaction with uPAR was blocked with an anti-uPAR antibody (anti-uPAR 399R antibody) ($P<0.05$) (Figure 6.2.a.i). The WHCO6 cell line served as an intriguing exception since EGFR activation did not affect the proliferation of this cell line when the uPAR interaction with uPA was disrupted with the anti-uPAR antibody (Figure 6.2.a.i). To determine whether this outcome is uniquely due to the presence of this antibody, an IgG control was applied in the proliferation assay. This IgG control compensates for the presence of an IgG and does not target a specific molecule in human cells. EGF caused a significant increase in proliferation of the WHCO6 cells in the presence of an IgG control ($P<0.05$) (Figure 6.2.a.ii). This confirms that the EGFR activation required the endogenous uPA/uPAR complex to stimulate the proliferation of specifically the WHCO6 cells.

EGFR activation significantly increased of proliferation of the four HOSCC cell lines even when the uPAR interaction with β1-integrin was blocked with the β1P1 peptide ($P<0.05$) (Figure 6.2.b). Therefore, the EGFR activation and its stimulation of proliferation of the HOSCC cell lines, is not due to the uPAR/ β1-integrin interaction.

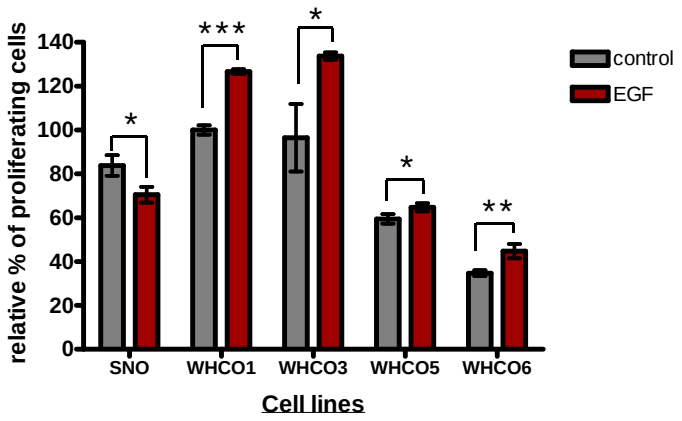

Figure 6.1: The proliferation of the different HOSCC cell lines upon exposure to EGF. The proliferation of the different cell lines in the absence (control, grey bar) or presence of EGF (red bar). The mean number of proliferating WHCO1 cells, which were not exposed to EGF, was set at 100%. **Note:** An unpaired Student's t-test was used to compare the proliferation of HOSCC cells exposed to EGF versus untreated control. ***P values are indicated by *; * = P<0.05; ** = P<0.01; *** = P<0.001; Standard error bars = Standard deviation; n= 3***

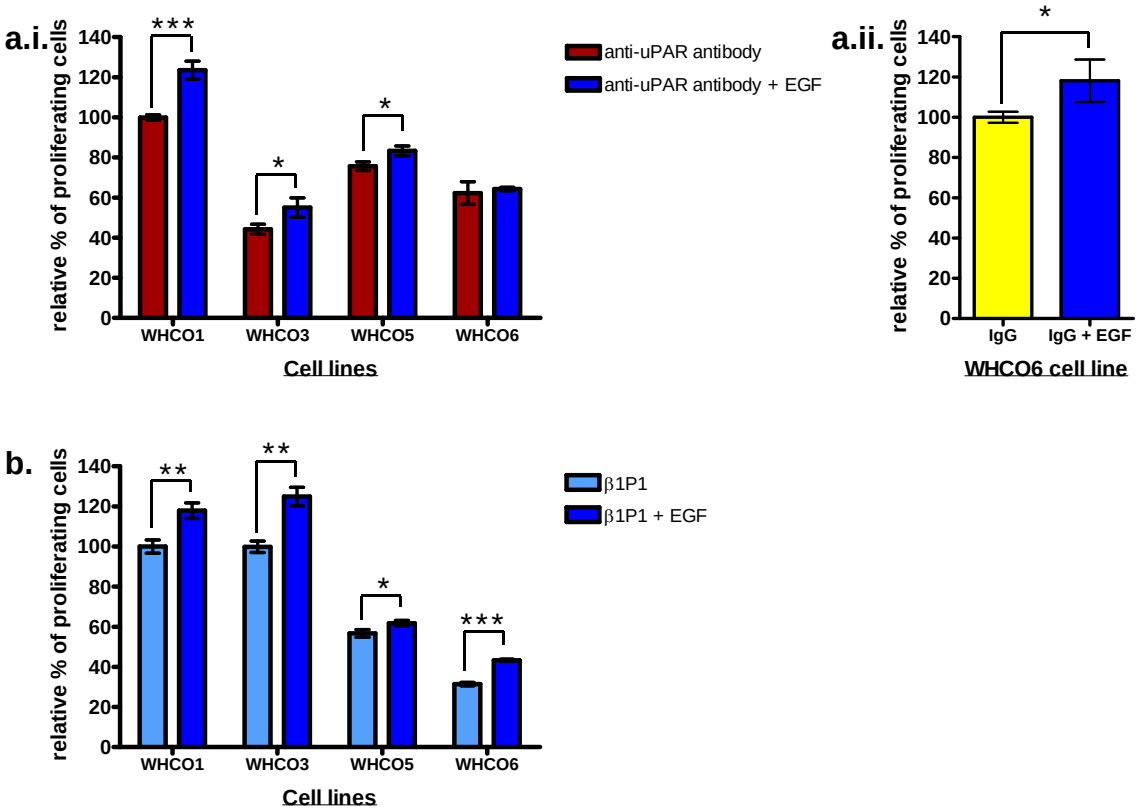

Figure 6.2: Investigation of the role of uPAR in EGF stimulation of proliferation of HOSCC cells. **(a.i)** The proliferation of the HOSCC cells were exposed to EGF in the presence of an anti-uPAR antibody (blue bar). HOSCC cell exposed to only the anti-uPAR antibody served as control (red bar). The mean number of proliferating WHCO1 cells, which were exposed to anti-uPAR antibody, was set at 100%. **(a.ii)** The proliferation of the WHCO6 cells were exposed to EGF in the presence of IgG control (blue bar). WHCO6 cell treated with IgG only served as control (yellow bar). The mean number of proliferating WHCO6 cells, which were exposed to IgG control, was set at 100%. **(b)** The proliferation of the HOSCC cells exposed to EGF in the presence of β1P1 (dark blue bar). HOSCC cell treated with β1P1 only served as control (light blue bar). The mean number of proliferating WHCO1 cells, which were exposed to β1P1, was set at 100%. **Note:** An unpaired Student's t-test was used to compare the proliferation of cells exposed to EGF in conjunction with either anti-uPAR antibody, IgG control or β1P1 (royal blue bar) versus the respective controls. ***P values are indicated by *; * = P<0.05; ** = P<0.01; *** = P<0.001; Standard error bars = Standard deviation; n= 3***

6.3.2. EGFR activation affects on proliferation of the HOSCC cells in the presence of collagen type I and the role of uPAR

EGFR activation by EGF stimulated the proliferation of the WHCO1, WHCO3 and WHCO6 cells on collagen type I ($P<0.05$) (Figure 6.3). The EGFR activation did not influence the proliferation of the WHCO5 cell line, while the proliferation of the SNO cells on collagen type I substrate was significantly reduced ($P<0.05$) (Figure 6.3). Therefore, EGFR activation induced the proliferation of the majority of the HOSCC cell lines on collagen type I substrate.

The consequent step was to determine whether the EGFR activation and its stimulation of proliferation of the three HOSCC cell lines is via uPAR mechanisms. EGFR activation with EGF significantly increased the proliferation of the WHCO1 and WHCO6 cells on collagen type I when the uPAR interaction with uPA was blocked with the anti-uPAR antibody ($P<0.05$) (Figure 6.4). Interestingly, EGFR activation does not induce the proliferation of the WHCO3 cells on collagen type I when the uPA/uPAR interaction was blocked with the anti-uPAR antibody (Figure 6.4.a.i). Nevertheless, in the presence of IgG control, EGF significantly increased the proliferation of the WHCO3 cells on collagen type I substrate ($P<0.05$) (Figure 6.4.1.ii). Therefore the EGFR activation required the concomitant uPAR activation to induce proliferation of specifically the WHCO3 cells on collagen type I.

EGFR activation with EGF significantly induced the proliferation of the WHCO1 and WHCO3 cells on collagen type I substrate when their uPAR interaction with β1-integrin was blocked with β1P1 ($P<0.05$) (Figure 6.4). However, a striking observation was that in the presence of β1P1 blocking peptide the addition of EGF did not stimulate the proliferation of the WHCO6 cells on collagen type I (Figure 6.4.b.i). To establish whether this result is specifically due to the mode of action induced by the β1P1 blocking peptide, a $\beta1P1^{Sc}$ peptide was used as a control peptide in the proliferation assays. The presence of EGF in conjunction with $\beta1P1^{Sc}$ control peptide significantly increased the proliferation of the WHCO6 cells on collagen type I when compared to the presence of $\beta1P1^{Sc}$ control ($P<0.05$) (Figure 6.4.b.ii). Therefore EGFR activation involved the uPAR/β1-integrin interaction to particularly induce the proliferation the WHCO6 cells on collagen type I substrate.

Overall the data presented in this section illustrate that EGFR activation and resultant induction of proliferation of two of the three HOSCC cell lines on collagen type I was via mechanisms that involved uPAR. This includes the activation of uPAR with endogenous uPA or the interaction of uPAR with β1-integrin.

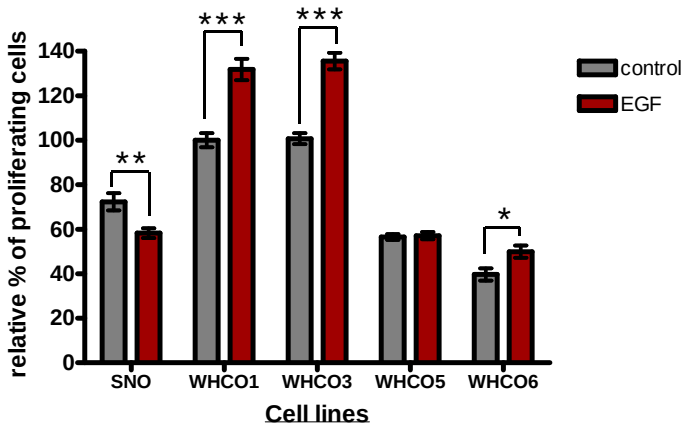

Figure 6.3: The proliferation of the different HOSCC cell lines on collagen type I substrate upon exposure to EGF. The proliferation of the different cell lines in the absence (control, grey bar) or presence of EGF (red bar). The mean number of proliferating WHCO1 cells, which were not exposed to EGF, was set at 100%. **Note:** An unpaired Student's t-test was used to compare the proliferation of HOSCC cells exposed to EGF versus untreated control. ***P values are indicated by *; * = P<0.05; ** = P<0.01; *** = P<0.001; Standard error bars = Standard deviation; n= 3***

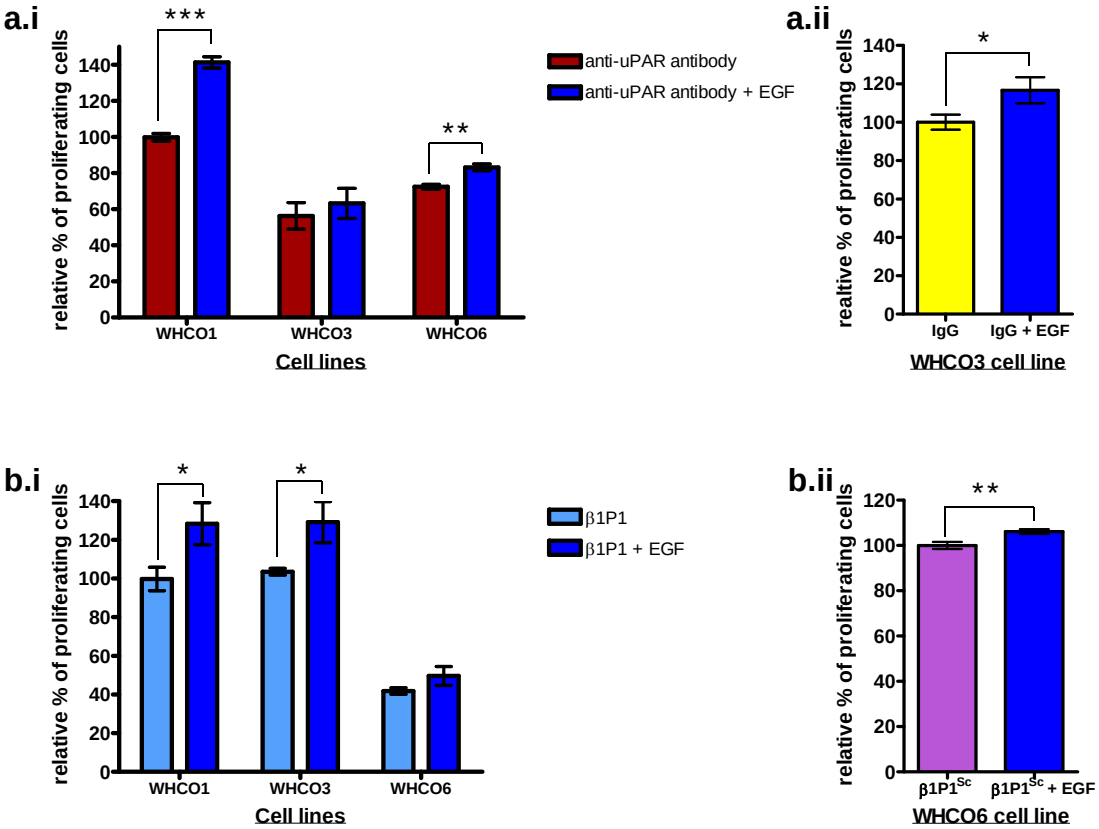

Figure 6.4: Note: Legend for this figure continues on the following page

Figure 6.4: Investigation of the role of uPAR in EGF stimulated proliferation of HOSCC cells on collagen type I substrate. **(a.i)** The proliferation of the HOSCC cells were exposed to EGF in the presence of an anti-uPAR antibody (blue bar). HOSCC cell exposed to only the anti-uPAR antibody served as control (red bar). The mean number of proliferating WHCO1 cells, which were exposed to

anti-uPAR antibody, was set at 100%. **(a.ii)** The proliferation of the WHCO3 cells were exposed to EGF in the presence of IgG control (blue bar). WHCO3 cell treated with IgG only served as control (yellow bar). The mean number of proliferating WHCO3 cells, which were exposed to IgG control, was set at 100%. **(b.i)** The proliferation of the HOSCC cells exposed to EGF in the presence of β1P1 (dark blue bar). HOSCC cell treated with β1P1 only served as control (light blue bar). The mean number of proliferating WHCO1 cells, which were exposed to β1P1, was set at 100%. **(b.ii)** The proliferation of the WHCO6 cells exposed to EGF in the presence of $\beta1P1^{Sc}$ (dark blue bar). HOSCC cell exposed to $\beta1P1^{Sc}$ only served as control (purple bar). The mean number of proliferating WHCO6 cells, which were exposed to $\beta1P1^{Sc}$, was set at 100%. **Note:** An unpaired Student's t-test was used to compare the proliferation of cells exposed to EGF in conjunction with either anti-uPAR antibody, IgG control, β1P1 or $\beta1P1^{Sc}$ (royal blue bar) versus the respective controls. ***P values are indicated by *; * = P<0.05; ** = P<0.01; *** = P<0.001; Standard error bars = Standard deviation; n= 3***.

6.3.3 EGFR activation affects on proliferation of the HOSCC cells in the presence of vitronectin substrate and the role of uPAR

There was little variation in proliferation of the SNO, WHCO1, WHCO3 and WHCO6 cells on vitronectin substrate, in the presence of EGF when compared to untreated control (Figure 6.5). The WHCO5 cell lines served as an exception as the addition of EGF significantly reduced the proliferation of this cell line (Figure 6.5). Therefore the EGFR activation does not increase the proliferation of the HOSCC cell lines grown on vitronectin substrate. Consequently, the role of uPAR in EGFR activation and stimulation of proliferation of the HOSCC cell lines on just vitronectin substrate was not examined.

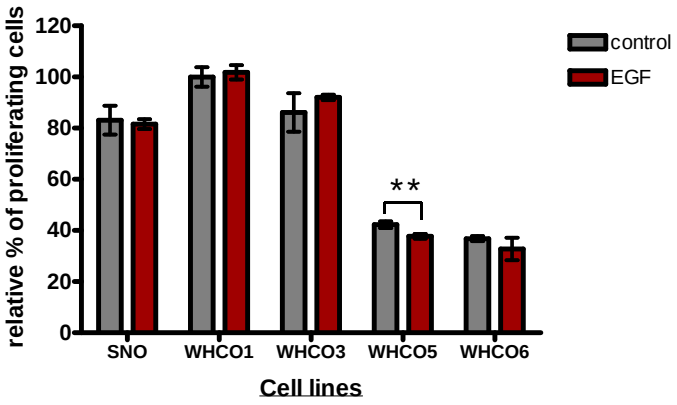

Figure 6.5: The proliferation of the different HOSCC cell lines on vitronectin substrate upon exposure to EGF. The proliferation of the different cell lines in the absence (control, grey bar) or presence of EGF (red bar). The mean number of proliferating WHCO1 cells, which were not exposed to EGF, was set at 100%. **Note:** An unpaired Student's t-test was used to compare the proliferation of HOSCC cells exposed to EGF versus untreated control. ***P values are indicated by *; * = P<0.05; ** = P<0.01; *** = P<0.001; Standard error bars = Standard deviation; n= 3***.

6.3.4 EGFR activation affects on proliferation of the HOSCC cells in the presence of collagen type I and vitronectin combination substrate and the role of uPAR

EGFR activation by its cognate ligand, EGF, with respect to its influence on proliferation of the HOSCC cell lines was examined on a collagen type I and vitronectin combination substrate which was assumed to better represent the ECM *in vivo*.

EGFR activation with EGF significantly reduced the proliferation of the SNO and WHCO3 cell lines when compared with untreated control ($P<0.05$) (Figure 6.6). On the contrary, the proliferation of the WHCO1 and WHCO6 cells on collagen type and vitronectin combination substrate significantly increased upon the addition of EGF ($P<0.05$) (Figure 6.6). EGFR activation did not influence the proliferation of the WHCO5 cell line (Figure 6.6). Therefore, EGFR activation stimulated the proliferation of specifically the WHCO1 and WHCO6 cells on collagen type I and vitronectin substrate. Consequently, these two HOSCC cell lines were used to examine the influence of role of uPAR in the EGF induced proliferation.

EGFR activation by EGF induced proliferation of the WHCO1 cells on collagen type I and vitronectin substrate when the endogenous uPA/uPAR interaction was blocked with the anti-uPAR antibody ($P<0.05$) (Figure 6.7.a.i). In contrast, the exposure of the WHCO6 cells to EGF failed to stimulate proliferation of these cells on collagen type I/vitronectin substrate in the presence of the anti-uPAR antibody (Figure 6.7.a.i). Nonetheless, the addition of EGF stimulated the proliferation of the WHCO6 cells in the presence of IgG control ($P<0.05$) (Figure 6.7.a.ii). Therefore, the EGFR activation required the endogenous uPA/uPAR complex to induced proliferation of specifically the WHCO6 cells on collagen type I/vitronectin combination substrate.

EGFR activation significantly induced the proliferation of the WHCO1 cells when the uPAR/β1-integrin interaction was blocked with the β1P1 peptide ($P<0.05$) (Figure 6.7). On the contrary, EGFR activation did not increase the proliferation of the WHCO6 cells on collagen type I/vitronectin substrate in the presence of β1P1 blocking peptide (Figure 6.7.b.i). However, EGFR activation significantly stimulated the proliferation of the WHCO6 cell line in the presence of $\beta1P1^{Sc}$ control peptide ($P<0.05$) (Figure 6.7.b.ii). This confirms that EGFR activation involved the interaction between uPAR and β1-integrin to stimulate the proliferation of particularly the WHCO6 cells on collagen type I and vitronectin substrate.

The data presented here confirms that EGFR activation and its stimulation of proliferation of WHCO6 cells on collagen type I and vitronectin substrate required the interaction of uPAR with endogenous uPA or β1-integrin.

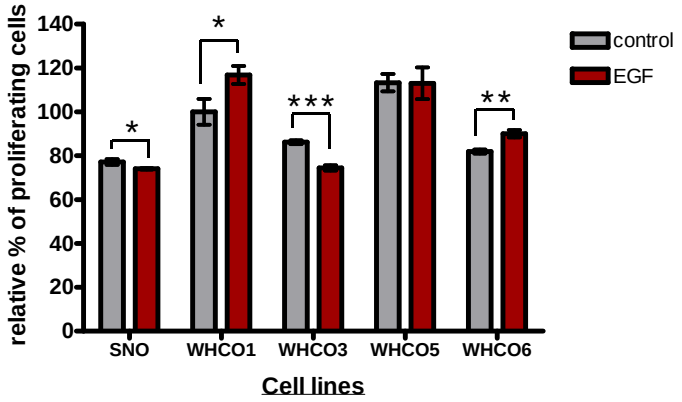

Figure 6.6: The proliferation of the different HOSCC cell lines on collagen type I and vitronectin combination substrate upon exposure to EGF. The proliferation of the different cell lines in the absence (control, grey bar) or presence of EGF (red bar). The mean number of proliferating WHCO1 cells, which were not exposed to EGF, was set at 100%. **Note:** An unpaired Student's t-test was used to compare the proliferation of HOSCC cells exposed to EGF versus untreated control. ***P values are indicated by *; * = P<0.05; ** = P<0.01; *** = P<0.001; Standard error bars = Standard deviation; n= 3.***

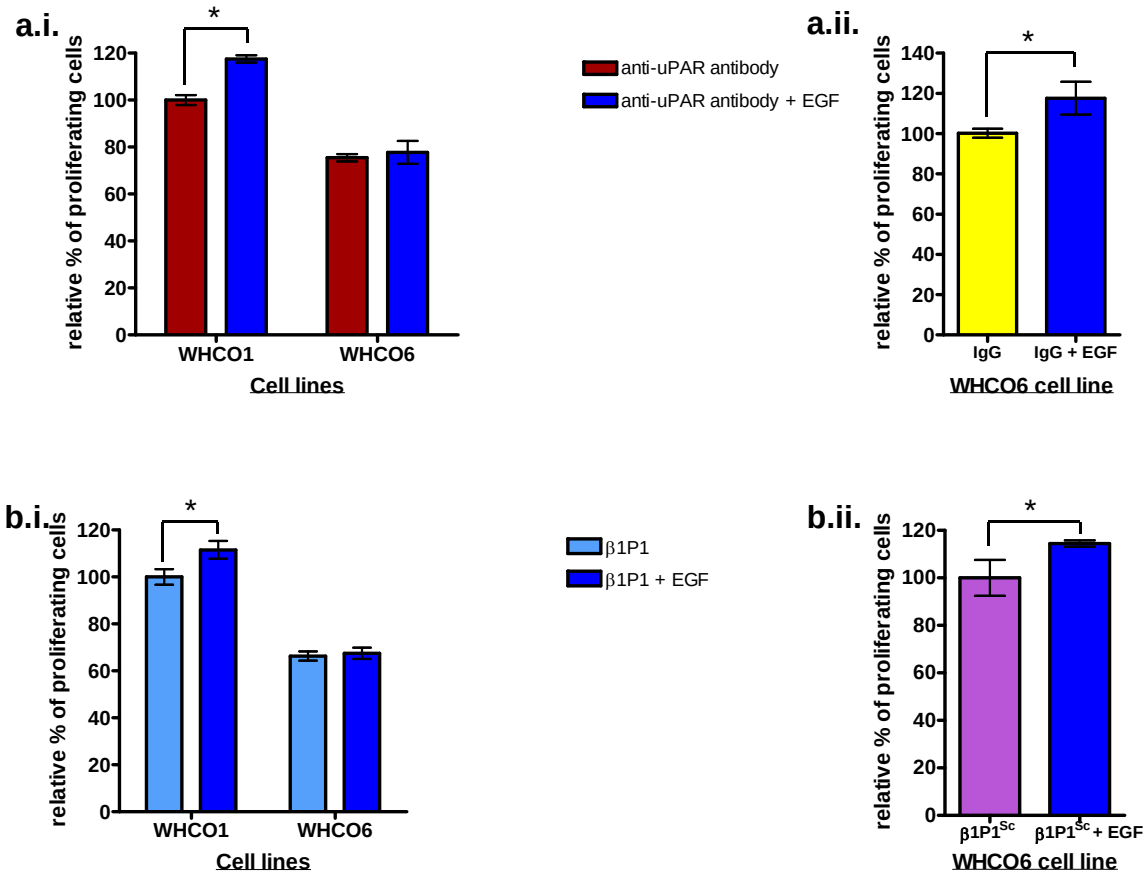

Figure 6.7: Investigation of the role of uPAR in EGF stimulated proliferation of HOSCC cells on collagen type I and vitronectin combination substrate. **(a.i)** The proliferation of the HOSCC cells were exposed to EGF in the presence of an anti-uPAR antibody (blue bar). HOSCC cell exposed to only the anti-uPAR antibody served as control (red bar). The mean number of proliferating WHCO1 cells, which were exposed to anti-uPAR antibody, was set at 100%. **(a.ii)** The proliferation of the WHCO6 cells were exposed to EGF in the presence of IgG control (blue bar). WHCO6 cell treated with IgG only served as control (yellow bar). The mean number of proliferating WHCO6 cells, which were exposed to IgG control, was set at 100%. **(b.i)** The proliferation of the HOSCC cells exposed to EGF in the presence of β1P1 (dark blue bar). HOSCC cell treated with β1P1 only served as control (light blue bar). The mean number of proliferating WHCO1 cells, which were exposed to β1P1, was set at 100%. **(b.ii)** The proliferation of the WHCO6 cells exposed to EGF in the presence of $\beta1P1^{Sc}$ (dark blue bar). HOSCC cell exposed to $\beta1P1^{Sc}$ only served as control (purple bar). The mean number of proliferating WHCO6 cells, which were exposed to $\beta1P1^{Sc}$, was set at 100%. **Note:** An unpaired Student's t-test was used to compare the proliferation of cells exposed to EGF in conjunction with either anti-uPAR antibody, IgG control, β1P1 or $\beta1P1^{Sc}$ (royal blue bar) versus the respective controls. ***P values are indicated by *; * = P<0.05; ** = P<0.01; *** = P<0.001; Standard error bars = Standard deviation; n= 3***.

6.4 Discussion

This study provides unique data regarding the interplay between uPAR, the ECM, and activated EGFR, to regulate proliferation of the HOSCC cell lines.

The EGF activation of EGFR stimulated the proliferation of the majority of the HOSCC cells (with the exception of SNO). This EGF stimulation of proliferation was observed in the absence of ECM or the presence of collagen type I or collagen type I/vitronectin mix. These remarkable observations mean that in all the HOSCC cell lines, the EGF influence on proliferation is governed by the absence or the presence of ECM components. This prompts the question of "how" the ECM influences the EGF induced proliferation of the HOSCC cell lines. One mechanism to consider is the sequestration of the EGF by specific ECM components such as vitronectin (Hollier *et al*., 2005). For example, Hollier *et al*. (2005) demonstrated the complex formation of EGF with vitronectin (in its plasma form), which is due to the direct interaction between EGF and the heparin binding domain of vitronectin (Schoppet *et al*., 2002). The possibility of vitronectin "sequestering" EGF explains the reason that EGF did not induce the proliferation of the HOSCC cell lines on vitronectin.

The ECM may also influence the EGF stimulation of proliferation via its crosstalk between molecules involved in cell-ECM adhesion and EGFR. This investigation shows a clear relationship between the ECM, different uPAR mechanisms and EGF stimulation of proliferation of specific HOSCC cell lines. These uPAR mechanisms involved the activation of uPAR by endogenous uPA or the interaction of uPAR with β1-integrin.

EGF induced proliferation via uPAR or the interaction of uPAR with uPA or β1-integrin in cell types such as breast carcinoma cell lines (MDA-MB-231 and MDA-MB-468), murine embryonic fibroblasts and murine keratinocytes (Jo *et al*., 2007; D'Alessio *et al.*, 2008). However this occurred specifically when the cell lines grew in the absence of ECM (Jo *et al*., 2007; D'Alessio *et al.*, 2008). The current data provides evidence that EGF stimulation of proliferation of the HOSCC cell lines is influenced by the ECM and uPAR. This, however, is specific to the cell lines that uPAR significantly contributes to their adhesion or proliferation in the presence of a particular ECM (chapter 4, chapter 5). For example, in the WHCO3 cell line, the endogenous uPA/uPAR complex contributes to the proliferation of these cells in the presence of collagen type I. The EGF stimulation of proliferation of this WHCO3 cell line required the interaction of endogenous uPA with uPAR in the presence of collagen type I.

In a different scenario, uPAR contributed to the adhesion of the WHCO1 cell line on collagen type I or vitronectin, but this contribution was non-significant. Consequently, the EGF stimulation of proliferation of this cell line on collagen type I or collagen type I/vitronectin combination substrate was considered not to be via uPAR.

The ECM also influences whether the EGF stimulation of proliferation, is via uPAR with uPA or β1-integrin. For example: adhesion of the WHCO6 cell line on collagen type I engages the uPAR/β1-integrin interaction (Chapter 4). The engagement of the uPAR/β1-integrin interaction by collagen type I was necessary for the EGF stimulation of proliferation of the WHCO6 cells. Furthermore, the uPA activation of uPAR was necessary for adhesion of these cells on vitronectin (Chapter 4). Consequently, in the presence of collagen type I/vitronectin mix, EGF induced proliferation of these cells required the interaction of uPAR with β1-integrin and uPA. This means that in the presence of collagen type I in conjunction with vitronectin, EGF induced proliferation of the WHCO6 cells required these ECM components and their specific engagement of uPAR.

Liu *et al*. (2002) and Aguirre-Ghiso *et al*. (2003) demonstrated that in HEp3 head and neck squamous cell carcinoma cell line, in the presence of fibronectin, but independent of EGF, there is complex consisting of uPAR, EGFR and α5β1. A complex consisting of these same components was also detected in the human keratinocyte derived SCC12F2 cell line (SCC12) (Wang *et al*., 2005). It is, therefore, possible that in both the WHCO3 and WHCO6 cell lines, a complex consisting of uPA, uPAR, β1-integrin and EGFR exists, to stimulate proliferation in the presence of EGF. These cell lines have the uPAR interaction with membrane associated β1-integrin (chapter 2), which supports the hypothesis that this complex exists in the WHCO3 and WHCO6 cell lines.

In MCF-7 breast carcinoma cells, the presence of EGF increased the association of uPAR with EGFR, which led to proliferation (Guerrero *et al*., 2004). It is possible that the same scenario occurs in the WHCO3 and WHCO6 cell lines. Since uPAR is GPI anchored and does not have a cytoplasmic tail, its interaction with EGFR (in the presence of uPA) or β1-integrin can influence signalling events such as proliferation. This may explain the reason that EGF induced proliferation of these cell lines is either via the interaction of uPAR with uPA or β1-integrin depending on the specific engagement with the ECM component.

The HOSCC cell lines used in this study overexpress the EGFR and the EGF/EGFR signalling pathways are therefore important in these cell lines (Veale and Thornley, 1989).

The HOSCC cell lines are derived from patients with well advanced tumours and therefore there are sequences of events that may have contributed to the progression of HOSCC (Veale and Thornley, 1989). This study provides detail of the relationship between uPAR, ECM components, EGF and EGFR, which may have played a role during the progression of the HOSCC cells to the transformed state.

In conclusion:

This investigation established that EGFR activation and its influence on proliferation of the HOSCC cell lines depends on the presence of specific ECM substrates such as collagen type I and vitronectin. EGF stimulated proliferation via uPAR mechanisms only in the HOSCC cells wherein uPAR has a significant role in their adhesion and proliferation on that ECM. This study uniquely disentangles the complex set of environmental cues considered central to the development of moderately differentiated HOSCC cells.

Chapter 7: General discussion

Originally, investigations regarding proliferation and invasion, in the context of metastasis, were considered as separate issues with researchers focusing on the specific molecular contribution to either proliferation or invasion (Garbisa *et al*., 1992; Greig *et al*., 1988). Proliferation studies were primarily directed on growth factor signalling pathways such as EGFR activation and downstream MAPK pathway, or molecules involved in cell cycle progression such as the cyclin dependent kinases (Greig *et al*., 1988; Schmidt-Ullrich *et al*., 1997; Jordan *et al*., 1998). On the other hand, matrix metalloproteases and the plasminogen activation pathways were predominantly considered during studies of invasion and ECM degradation (Garbisa *et al*., 1992; Colombi *et al*., 1984).

However, closer examination of reports of an allied nature revealed that key players in invasion such as uPA and uPAR also play a role in proliferation, forging a more directed link between invasion and proliferation (Jo *et al*., 2005; Piccolella *et al*., 2008). It also became apparent that uPAR and uPA, besides playing a role in ECM degradation, also contribute to cell-ECM adhesion and subsequent events such as migration and proliferation (Piccolella *et al*., 2008; Tang *et al*., 2008). With this knowledge, this research set out to disentangle the roles of uPA and uPAR on the structural and molecular basis using HOSCC as the model. The consequential steps in this discussion analyse the specific relationship between the major players in ECM degradation, adhesion based signalling and proliferation. The nature of these relationships is scrutinized in this discussion and how they may feed into the proliferative component of tumour development.

7.1 The relationship between the major players in ECM degradation, adhesion-based signalling and proliferation

The key players involved in ECM degradation, uPAR and uPA, are expressed and secreted by all the HOSCC cell lines. Similarly, a major molecule in cell-ECM adhesion, the β1-integrin, is expressed in all the HOSCC cell lines. It was established that in all the HOSCC cell lines, uPAR is present in a complex with ILK scaffolding protein.

This analysis also established a definite relationship between uPAR, its ligands uPA and β1-integrin and molecules that affect outside-in signalling such as the structural ECM components, collagen type I and vitronectin, or soluble growth factors such as TGFβ and

EGF. This provides the molecular backdrop to the analysis of the integrated nature of the uPAR relationship with cell-ECM adhesion-based signalling and proliferation.

7.2 What is the nature of the uPAR and cell-ECM adhesion relationship?

With respect to elucidating the role of uPAR in cell-ECM adhesion signalling and proliferation, uPAR would require a connection with the cytoskeleton. In all the HOSCC cell lines there was an interaction between uPAR and ILK scaffolding protein, which in turn interacts with several actin adaptor proteins such as vinculin, paxillin, and PARVIN (Figure 7.1) (Ho and Bendeck 2009). In the HOSCC cell lines, the interaction between uPAR and ILK requires caveolin expression (chapter 3). Chun *et al*. (2005) demonstrated that ILK, which has a caveolin binding motif, interacts with caveolin and the two molecules co-localised at the cytosol and focal adhesion sites. Interestingly, ILK with a mutated caveolin binding motif, which does not associate with caveolin, failed to localize at focal adhesions (Chun *et al*., 2005). Therefore caveolin maintains ILK at focal adhesion sites, which strongly suggests that the complex containing uPAR/caveolin/ILK occurs at focal adhesion sites of the HOSCC cell lines. This complex is very likely to provide an association between uPAR and the actin cytoskeleton in the HOSCC cell lines during cell-ECM adhesion (Figure 7.1). The complex containing uPAR/caveolin/ILK may be a feature unique to HOSCC or limited to cells that express caveolin, which would be an interesting question for future studies.

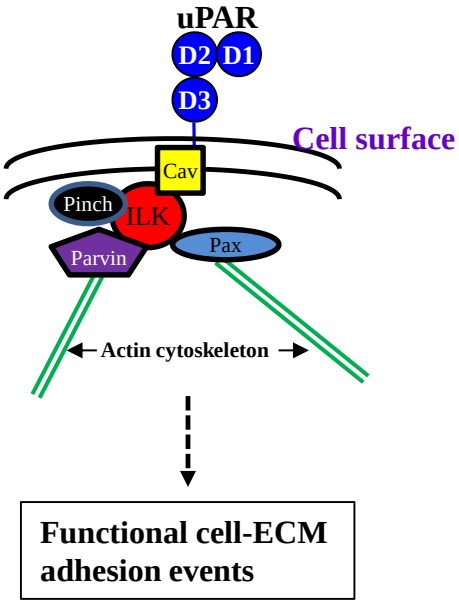

Figure 7.1: The complex containing uPAR, caveolin and ILK provides structural stability during cell-ECM adhesion based events. The unique complex containing uPAR/caveolin and ILK provides uPAR with the essential link to the actin cytoskeleton during cell-adhesion events since ILK interacts with actin associated molecules such as parvin and paxillin (Fielding and Dedhar, 2009). **Note:** Cav = caveolin; Pax = paxillin.

The adhesion of the majority of the HOSCC cell lines is influenced by the relationship of uPAR with uPA and β1-integrin as well as collagen type I or vitronectin (chapter 4). The different scenarios in which uPAR contributes to ECM adhesion of the HOSCC cells are discussed in the following text.

The uPAR/β1-integrin interaction influenced adhesion of two HOSCC cell lines on collagen type I (chapter 4). In these cell lines expression of α2 integrin was lower than that of other HOSCC cell lines (Miller and Veale, 2001). This α2 integrin is necessary to form the α2β1 integrin heterodimer. Both α2β1 heterodimer and the uPAR/β1-integrin interaction contribute to collagen type I adhesion (chapter 4; Humphries *et al*., 2006). Therefore, it is logical that when expression of α2β1 is reduced in HOSCC cells, the uPAR/β1-integrin interaction has a more prominent role in adhesion of these cells. Hence, the ratio of adhesion molecules, such as the integrin heterodimers versus the uPAR/β1-integrin interaction, determines whether the uPAR/β1-integrin association influences adhesion of the HOSCC cells on collagen type I.

In the circumstance that uPAR activation increased adhesion of HOSCC cells on vitronectin, it occurred specifically in HOSCC cells that have a detectable uPAR/β1-integrin interaction. Interestingly, the uPAR/β1-integrin complex in lung carcinoma cells increased adhesion on vitronectin via the uPAR interaction with α3β1 (Tang *et al*., 2008). This suggests that in cells that react this way, uPA forms a complex with uPAR and β1-integrin to stimulate their adhesion on vitronectin.

Alternatively, there are other mechanisms involving uPAR that could affect adhesion of the HOSCC cells on vitronectin. These mechanisms include the direct interaction between uPAR and the somatomedin B domain of vitronectin, which is enhanced by uPA (Madsen *et al*., 2007; Huai *et al*., 2008). In HT1080 fibrosarcoma cells and MCF-7, uPA and uPAR formed a complex with αvβ5 to mediate adhesion-based migration of these cells on vitronectin (Carriero *et al*., 1999). The HOSCC cell lines in this study all express the αV integrin subunit and, therefore, it is very possible that the cell-vitronectin adhesion in the HOSCC cell lines is via αV-uPAR in the presence of uPA (Miller and Veale, 2001).

The uPAR interaction with uPA or β1-integrin played a role in adhesion of the majority (the exception discussed in the paragraph below) of the HOSCC cell lines on either collagen type I or vitronectin, but not both. For example, the uPAR contributed to the adhesion of the WHCO3 cells on vitronectin, but not collagen type I. This can be explained by collagen type I or vitronectin engaging various receptors for adhesion and not only uPAR. Collagen type I

engages the α1β1, α2β1 and α3β1 integrins, while the αvβ3 and αvβ5 integrins recognise vitronectin (Humphries *et al*., 2006; Janes and Watt, 2004). This goes back to the point made earlier that the ratio of these integrins versus uPAR would govern whether uPAR plays a part in adhesion of the HOSCC cells on these ECM components.

Reviewing the scenario that uPAR contributed to adhesion of HOSCC cells on collagen type I and vitronectin, it occurred specifically in the cells line that expressed the most uPAR (WHCO6 cell line; chapter 4). Thus in the HOSCC cells, there appears to be a relationship between the expression of uPAR, its interaction with β1-integrin and its versatile role in adhesion.

There is a situation where uPAR does not influence the adhesion of the HOSCC cells (eg: WHCO5 cells) on the representative ECM components. As a reminder to the reader, the HOSCC cell lines are derived from moderately differentiated tumours of different patients (Veale and Thornley, 1989). The composition of the ECM environment *in vivo* of the HOSCC cell lines may have differed across the lines. It is feasible that in the cell lines, adhesion is influenced by the relationship between uPAR and ECM components to which the cells were originally exposed *in vivo*. With that being said, there is the possibility that uPAR influences adhesion of the WHCO5 cells on other ECM components such as laminin and fibronectin. Interestingly, in these cells there is a relationship between uPAR and vitronectin from the proliferation perspective (chapter 5). It is likely that in these cells adhesion complexes between uPAR and vitronectin develop some time later and therefore may have been overlooked.

The data presented in this study demonstrated how different possible relationships in the context of uPAR mechanism and ECM components influence adhesion of the HOSCC cells. The relevance of the uPAR and cell-ECM adhesion in the context of HOSCC is discussed in section 7.4. Importantly, one of the consequences to cell-adhesion is proliferation.

7.3. How does the uPAR relationship with uPA, β1-integrin and cell-ECM adhesion feed into proliferation?

The contribution of uPAR to proliferation of the HOSCC cell lines is unequivocal. The uPAR role in proliferation is clearly influenced by its interaction with uPA or β1-integrin, the collagen type I and vitronectin ECM components as well as growth factors, TGFβ and EGF.

This allows us to dissect the various perspectives in which uPAR, an invasion related protein, plays a part in proliferation.

The activation of uPAR by endogenous uPA contributed to the proliferation of three of the five HOSCC cell lines on the representative ECM components (Figure 7.2.a). It is likely that in the HOSCC cells, the uPAR activation induced proliferation via the FAK or ERK pathways (Figure 7.2.a). These pathways are commonly activated in response to the endogenous uPA/uPAR complex as was observed in carcinomas such as breast and prostate (Jo *et al*., 2003; Piccolella *et al*., 2008).

One of the circumstances in which uPAR adds to proliferation of the HOSCC cells involves its interaction with β1-integrin (Figure 7.2.a; chapter 5). The uPAR interaction with β1-integrin triggers activation of Src, FAK, Akt or ERK activation pathways (Tang *et al*., 2008; Aguirre-Ghiso *et al*., 2002). It is feasible that the uPAR/β1-integrin contributed to proliferation of these HOSCC cells by activating one or more of these pathways (Figure 7.2.a).

The unique relationship of uPAR, vitronectin and TGFβ influenced the proliferation of two of the HOSCC cell lines (chapter 5). In this event, the presence of TGFβ interferes with the uPAR/vitronectin association, which decreased proliferation of these cells (Figure 7.2.b; chapter 5). TGFβ is an inhibitor of epithelial cell growth during early stage of carcinogenesis (Kang, 2006). This scenario represents an interesting perspective on the way that TGFβ and its relationship with uPAR and vitronectin influence proliferation of epithelial cells.

The activation of EGFR by EGF and its effect on the proliferation of the HOSCC cells is undoubtedly influenced by the ECM (Figure 7.2.b; chapter 6). In the presence of ECM, crosstalk between EGFR activation and uPAR stimulated proliferation of HOSCC cells that their uPAR had a significant relationship with that particular ECM (chapter 6). During these events, it is likely that proliferation occurred due to EGFR Tyr 845 phosphorylation, STAT5b and/or ERK activation as was observed in murine embryonic fibroblasts and mouse keratinocytes (Figure 7.2.b) (Jo *et al*., 2007; D'Alessio *et al*., 2008). Liu *et al*. (2002) demonstrated that in HEp3 head and neck squamous cell carcinoma cell line, in the presence of fibronectin, there is complex consisting of uPAR, EGFR and α5β1. This study, together with ours, suggests that the relationship of EGFR activation with the ECM and uPAR is a feature that occurs in squamous cell carcinomas.

An interesting point to consider concerning the relationship between uPAR and EGFR activation in the WHCO3 and WHCO6 HOSCC cells, is the role of caveolin. Caveolin expression in human foreskin fibroblasts is essential for uPAR mediated activation and phosphorylation of EGFR at Tyr 845 (Monaghan-Benson *et al*., 2008). Since uPAR and caveolin associate in these HOSCC cell lines, it is very possible that the uPAR/caveolin interaction is necessary for the complete EGFR activation of these cells.

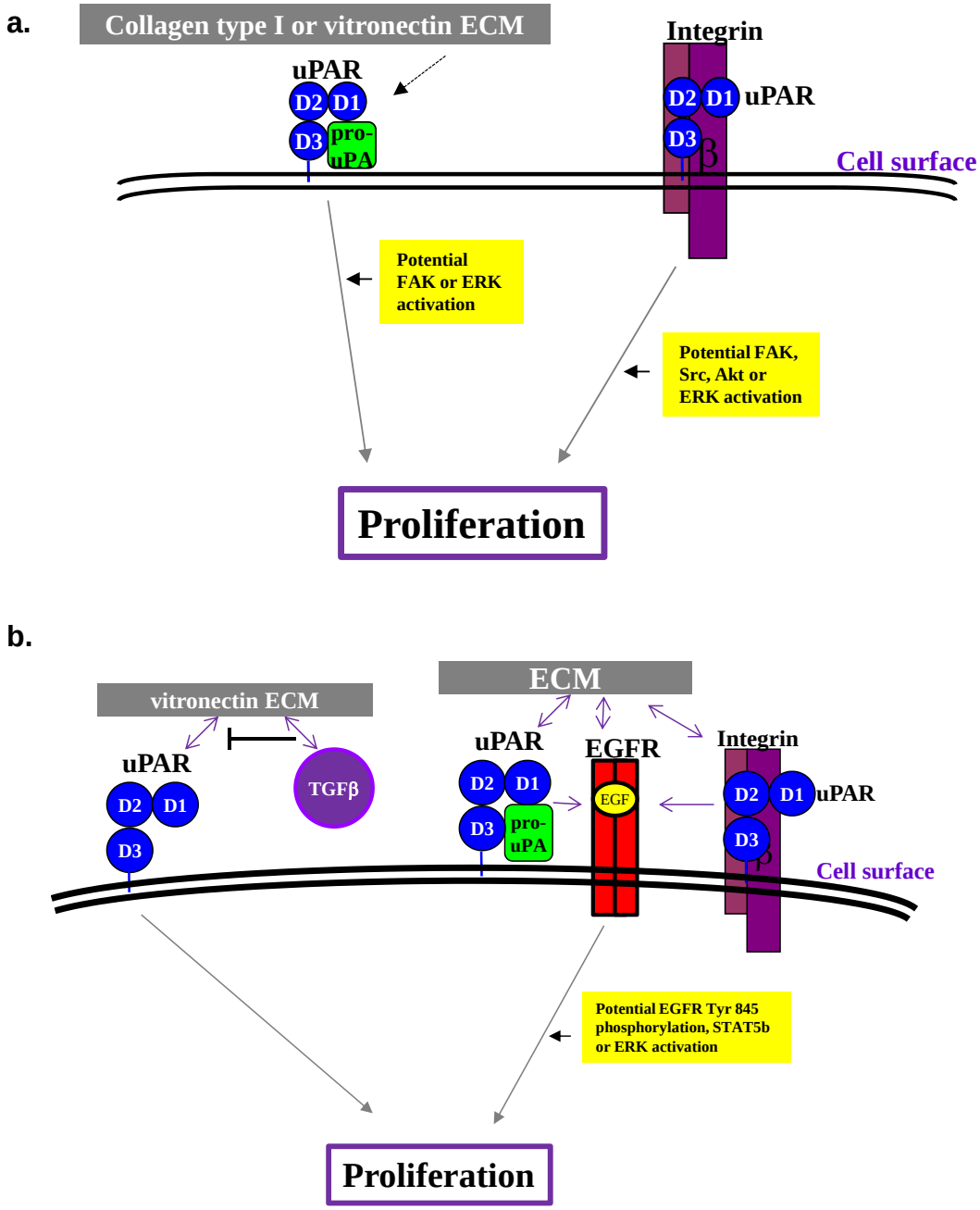

Figure 7.2: Note: Legend for this figure continues on the following page.

Figure 7.2: uPAR influenced cell-ECM adhesion based proliferation in the HOSCC cells (a) Proliferation of the HOSCC cells is influenced by activation of uPAR by uPA or the uPAR/β1-integrin interaction. The uPAR activation led to proliferation of the HOSCC cells on a particular ECM most likely via activation of FAK and/or ERK pathways (Jo *et al*., 2003; Piccolella *et al*., 2008). The

uPAR/β1-integrin interaction, which is known to activate the Src, FAK, Akt and ERK pathways (Aguirre-Ghiso *et al*., 2002; Tang *et al*., 2008), affects proliferation of the HOSCC cells. **(b)** The uPAR relationship with ECM and growth factors (EGF and TGFβ) influences the proliferation of the HOSCC cells. In the presence of TGFβ, which interferes with uPAR/vitronectin interaction (Schoppet *et al*., 2002), proliferation of specific HOSCC cells on vitronectin decreases. The relationship between ECM, uPAR and it ligands (uPA and/or β1-integrin) and activation of EGFR by EGF affected proliferation of the HOSCC cells. During this proliferation, it is feasible that phosphorylation EGFR Tyr 854 and activation of the STAT5b and/or ERK pathways occurs (Jo *et al*., 2007; D'Alessio *et al*., 2008).

There were some cases where uPAR contributed to adhesion but not proliferation of specific HOSCC cells on a particular ECM component (eg: WHCO3 cells adhesion on vitronectin). In this situation, uPAR played a role in the initial engagement between cells and ECM. By the time the cells begin to proliferate, it is possible that integrins or growth factor receptors such as EGFR have a dominant role in proliferation rather than the adhesion complex of uPAR and the ECM.

The uPAR protein is involved in the proliferation of normal cells such as endothelial cells and mouse keratinocytes (D'Alessio *et al*., 2008; Balsara *et al*., 2011). However, our studies in conjunction with others, demonstrate that uPAR contributes to the proliferation of HOSCC, breast carcinoma, prostate carcinoma and oral squamous cell carcinoma (Jo *et al*., 2007; Piccolella *et al*., 2008, Liang *et al*., 2008). This is important considering that uPAR overexpression is often linked with cancer progression and may potentially augment the proliferative effect in cancers (Aguirre-Ghiso *et al*., 2003). Interestingly, in the HOSCC cell lines, there is a relationship between the expression of uPA or uPAR and proliferation. For example: the HOSCC cell line (WHCO5) that secrete the most uPA, was the only cell line in which the uPAR activation significantly contributed to its proliferation on collagen type I and vitronectin. Additionally, uPAR played a significant role in the proliferation of the cell line that has the highest expression of uPAR (WHCO6). The contribution of uPAR to proliferation of these cells occurred in the absence or presence of collagen type I and vitronectin. It is therefore possible that during the progression of HOSCC, the increased expression level of uPA and or uPAR add to the cellular proliferation.

7.4 Does uPAR have a role during the progression of HOSCC?

The HOSCC cell lines used in this study are moderately differentiated and derived from patients with metastatic disease (Veale and Thornley, 1989). Based on our results, it is probable that during the progression of the HOSCC cell lines to their transformed state, uPAR played a role in cell-ECM adhesion based events.

The question then becomes “how does uPAR cell-ECM adhesion based events potentiate the HOSCC condition?” The cell-ECM adhesion event is a requisite for cell migration (Zhu *et al*., 2009). The uPAR contribution to cell ECM dependent migration is not limited to carcinoma and was also observed in “normal” mouse keratinocytes (D’Alessio *et al*., 2008). However, considering that uPAR expression is upregulated in several carcinomas, it may play a significant role in their migration (de Bock and Wang, 2004). In fact the uPAR mediated cell-ECM adhesion events plays a role in migration of carcinoma such as adenoid cystic carcinoma cells and oral squamous cell carcinoma (Abu-Ali *et al*., 2005; Liang *et al*., 2008). Considering that cell migration is important during tumour progression, it is possible that the uPAR mediated cell-ECM adhesion affects migration in HOSCC cells.

Another important consequence of cell-ECM interaction is invasion. Tang *et al*. (2008) demonstrated that in lung carcinoma cells, that the specific interaction of uPAR with β1-integrin interaction in the presence of uPA increased matrigel invasion. The complex containing uPAR/β1-integrin and uPA limits proteolysis at sites of cell-ECM contact. It is likely that during the progression of HOSCC, the uPAR interaction with β1-integrin and uPA and its particular engagement with the ECM influences invasion at cell-ECM adhesion sites.

The cell-ECM communication has an impact on cellular proliferation, which was an important component in this study. Sustained cell proliferation is a crucial event during carcinoma development (Hanahan and Weinberg, 2011). The role of uPAR in proliferation is undisputable since it contributes to the proliferation of all five HOSCC cell lines. Furthermore, this study clearly shows the importance of the environment in uPAR influence of proliferation of HOSCC. This includes the ECM environment as well as a growth factor input. In the *in vivo* situation, the presence of ECM and these paracrine growth factors may influence the proliferation of HOSCC via uPAR related mechanisms during the progression of HOSCC.

7.5 A way forward

The uPAR plays an important role in ECM degradation, which is crucial for tumour invasion, including in HOSCC (Morrissey *et al*., 1999). We established that uPAR has an impact on adhesion and/or proliferation of HOSCC. This is influenced by the presence of ECM, the interaction of uPAR with 2 of its ligands (uPA and β1-integrin) and the presence of growth

factors such as TGFβ and EGF. This study provides evidence that during the path that led to the HOSCC condition, uPAR contributes to cell-ECM adhesion and/or proliferation.

One of the major events contributing to carcinoma development is adhesion based migration. It is clear from this study that uPAR influences adhesion of the HOSCC cell lines on collagen type I and vitronectin and uPAR also contributes to migration of adenoid cystic carcinoma and oral squamous cell carcinoma cells (Abu-Ali *et al*., 2005; Liang *et al*., 2008). A valuable analysis for the future would be to examine the contribution of uPAR in adhesion based migration in the HOSCC cells to further elucidate its role during HOSCC progression. Wound healing migration assays and lamellipodia formation could be used to examine whether uPAR and/or its interaction with its ligands influence migration of the HOSCC cells on the different ECM surfaces.

Shiomi *et al*. (2000) detected the presence of uPAR mRNA and antigen in HOSCC cells (via *in situ* hybridization and immunohistochem), while in normal epithelial cells, uPAR was not detected. Given this fact and with the data presented here, uPAR may have a considerable value as a therapeutic target for HOSCC. In uPAR gene knock-out mice there was a delayed wound healing and abnormal keratinocytes migration and proliferation but it did not cause severe phenotype changes (Blasi and Carmeliet, (2002) cited in: Jo *et al*., 2007; D'Alessio *et al*., 2008). Therefore targeting uPAR is an attractive option as a possible treatment for HOSCC. Indeed, currently there are attempts at developing mechanisms to inhibit uPAR or its interaction with its ligands as a target therapy in cancers (Duriseti *et al*., 2010; Liang *et al*., 2008). This includes siRNA targeting uPAR, and antibodies, which target the interaction between uPAR and uPA or β1-integrin (Duriseti *et al*., 2010; Liang *et al*., 2008). It would be useful to study whether these products reduce development of HOSCC *in vivo* and could be used as potential treatments for HOSCC.

Conclusion: The current study unravels the exclusive mechanisms in which uPAR, originally thought to be involved in ECM degradation pathway, contribute to cell-ECM adhesion and proliferation of HOSCC. This study further emphasizes that crosstalk between cells and their environmental components such as ECM and growth factors play a significant role in critical events, such as adhesion and proliferation, during cancer progression.

Chapter 8: References

Abu-Ali, S., Sugiura, T., Takahashi, M., Shiratsuchi, T., Ikari, T., Seki, K. and Hiraki, A. (2005). Expression of the urokinase receptor regulates focal adhesion assembly and cell migration in adenoid cystic carcinoma cells. *J. Cell Physiol*., **203**:410-9.

Adams, C.L., Nelson, W.J. and Smith, S.J. (1996). Quantitative analysis of cadherin-catenin-actin reorganization during development of cell-cell adhesion. *J. Cell Biol.,* **135***:*1899-1911.

Agelaki, S., Spiliotaki, M., Markomanolaki, H., Kallergi, G., Mavroudis, D., Georgoulias,V. and Stournaras, C. (2009). Caveolin-1 regulates EGFR signaling in MCF-7 breast cancer cells and enhances gefitinib-induced tumor cell inhibition. *Cancer Biol. Ther*., **8**:1470-7.

Aguirre-Ghiso, J.A., Kovalski, K. and Ossowski, L. (1999). Tumor dormancy induced by downregulation of urokinase receptor in human carcinoma involves integrin and MAPK signaling. *J. Cell Biol*., **147**:89-104.

Aguirre-Ghiso, J.A. (2002). Inhibition of FAK signaling activated by urokinase receptor induces dormancy in human carcinoma cells *in vivo*. *Oncogene*, **21**:2513-24.

Aguirre-Ghiso, J.A., Estrada, Y., Liu, D. and Ossowski, L. (2003). ERK(MAPK) activity as a determinant of tumor growth and dormancy; regulation by p38(SAPK). *Cancer Res*., **63**:1684-1695.

Ahmed, N., Oliva, K., Wang, Y., Quinn, M. and Rice, G. (2003). Downregulation of urokinase plasminogen activator receptor expression inhibits Erk signalling with concomitant suppression of invasiveness due to loss of uPAR-β1 integrin complex in colon cancer cells. *Br. J. Cancer,* **89**: 374-84.

Allgayer, H. (2010). Translational research on u-PAR. *Eur. J. Cancer*, **46**:1241-51.

Andl, C.D., Mizushima, T., Nakagawa, H., Oyama, K., Harada, H., Chruma, K., Herlyn, M. and Rustgi, A.K.(2003). Epidermal growth factor receptor mediates increased cell proliferation, migration, and aggregation in esophageal keratinocytes *in vitro* and *in vivo*. *J. Biol. Chem*., **278**:1824-30.

Andreasen, P.A., Egelund, R. and Petersen, H.H. (2000). The plasminogen activation system in tumor growth, invasion, and metastasis. *Cell Mol. Life Sci*., **57**:25-40.

Bacchiocchi, R., Rubini, C., Pierpaoli, E., Borghetti, G., Procacci, P., Nocini, P.F., Santarelli, A., Rocchetti, R., Ciavarella, D., Lo Muzio, L. and Fazioli, F. (2008). Prognostic value analysis of urokinase-type plasminogen activator receptor in oral squamous cell carcinoma: an immunohistochemical study. *BMC. Cancer,* **8**:220

Balsara, R.D., Merryman, R., Virjee, F., Northway, C., Castellino, F.J. and Ploplis, V.A. (2011). A deficiency of uPAR alters endothelial angiogenic function and cell morphology. *Vasc. Cell,* **3**:10

Baramova, E.N., Bajou, K., Remacle, A., L'Hoir, C., Krell, H.W., Weidle, U.H., Noel, A. and Foidart, J.M. (1997). Involvement of PA/plasmin system in the processing of pro-MMP-9 and in the second step of pro-MMP-2 activation. *FEBS Lett*., **405**:157-162.

Behrendt, N., Ronne, E. and Danø, K. (1996). Domain interplay in the urokinase receptor. Requirement for the third domain in high affinity ligand binding and demonstration of ligand contact sites in distinct receptor domains. *J. Biol. Chem*., **271**:22885-94.

Bernstein, A.M., Greenberg, R.S., Taliana, L. and Masur, S.K. (2004). Urokinase anchors uPAR to the actin cytoskeleton. *Invest. Ophthalmol. Vis. Sci*., **45**:2967-77.

Bey, E., Alexander, J., Whitcutt, J.M., Hunt, J.A. and Gear, J.H. (1976). Carcinoma of the esophagus in Africans: establishment of a continuously growing cell line from a tumor specimen. *In Vitro*, **12**:107-14.

Bhattacharya, A., Lakka, S.S., Mohanam, S., Boyd, D. and Rao J.S. (2001). Regulation of the urokinase-type plasminogen activator receptor gene in different grades of human glioma cell lines. *Clin. Cancer Res*., **7**:267-276.

Bird-Lieberman, E.L. and Fitzgerald, R.C. (2009). Early diagnosis of oesophageal cancer. *Br. J. Cancer*, **101**:1-6.

Blasi, F. and Carmeliet, P. (2002). uPAR: a versatile signalling orchestrator. *Nat. Rev. Mol. Cell Biol*., **3**:932-43.

Blasi, F. and Sidenius, N. (2010). The urokinase receptor: focused cell surface proteolysis, cell adhesion and signaling. *FEBS Lett*., **584**:1923-30.

Brakebusch, C., Bouvard, D., Stanchi, F., Sakai, T. and Fassler, R. (2002). Integrins in invasive growth. *J. Clin. Invest.,* **109**:999-1006.

Brakebusch, C. and Fässler, R. (2003). The integrin-actin connection, an eternal love affair. *EMBO J*., **22**:2324-33.

Bramhall, S., Noack, N., Wu, M. and Loewenberg, J.R. (1969). A simple colorimetric method for determination of protein. *Anal. Biochem*., **31**:146-148.

Burgermeister, E., Liscovitch, M., Röcken, C., Schmid, R.M. and Ebert, M.P. (2008). Caveats of caveolin-1 in cancer progression. *Cancer Lett*., **268**:187-201.

Cantero, D., Friess, H., Deflorin, J., Zimmermann, A., Bründler, M.A., Riesle, E., Korc, M. and Büchler, M.W. (1997). Enhanced expression of urokinase plasminogen activator and its receptor in pancreatic carcinoma. *Br. J. Cancer,* **75**:388-95.

Cantrell, D.A. (2001). Phosphoinositide 3-kinase signalling pathways. *J. Cell Sci*., **114**:1439-1445.

Cao, L., Yao, Y., Lee, V., Kiani, C., Spaner, D., Lin, Z., Zhang, Y., Adams, M.E. and Yang, B.B. (2000). Epidermal growth factor induces cell cycle arrest and apoptosis of squamous carcinoma cells through reduction of cell adhesion. *J. Cell Biochem*., **77:**569-83.

Cao, D.J., Guo, Y.L. and Colman, R.W. (2004). Urokinase-type plasminogen activator receptor is involved in mediating the apoptotic effect of cleaved high molecular weight kininogen in human endothelial cells. *Circ. Res*., **94**:1227-1234.

Carriero, M.V., Del Vecchio, S., Capozzoli, M., Franco, P., Fontana, L., Zannetti, A., Botti, G., D'Aiuto, G., Salvatore, M. and Stoppelli, M.P. (1999). Urokinase receptor interacts with α(v)β5 vitronectin receptor, promoting urokinase-dependent cell migration in breast cancer. *Cancer Res.*, **59**:5307-14.

Carter, E.M. and Raggio, C.L. (2009). Genetic and orthopedic aspects of collagen disorders. *Curr. Opin. Pediatr*., **21**:46-54.

Chandrasekar, N., Mohanam, S., Gujrati, M., Olivero, W.C., Dinh, D.H. and Rao, J.S. (2003). Downregulation of uPA inhibits migration and PI3k/Akt signaling in glioblastoma cells. Oncogene, **22**:392-400.

Charalabopoulos, K., Mittari, E., Karakosta, A., Golias, C. and Batistatou, A. (2005). Integrins adhesion molecules and some of their ligands in laryngeal cancer. *Exp. Oncol*., **27**:86-90.

Chaurasia, P., Aguirre-Ghiso, J.A., Liang, O.D., Gardsvoll, H., Ploug, M. and Ossowski, L. (2006). A region in urokinase plasminogen receptor domain III controlling a functional association with α5β1 integrin and tumor growth. *J. Biol. Chem*., **281**:14852-63.

Chaurasia, P., Mezei, M., Zhou, M.M. and Ossowski, L. (2009). Computer aided identification of small molecules disrupting uPAR/α5β1--integrin interaction: a new paradigm for metastasis prevention. *PLoS One*, **4**:e4617

Chiarugi, P. (2008). From anchorage dependent proliferation to survival: lessons from redox signalling. IUBMB Life, **60**:301-7.

Chitaev, N.A. and Troyanovsky, S.M. (1998). Adhesive but not lateral E-cadherin complexes require calcium and catenins for their formation. *J. Cell Biol*., **142**:837-846.

Chun, J., Hyun, S., Kwon, T., Lee, E.J., Hong, S.K. and Kang, S.S. (2005). The subcellular localization control of integrin linked kinase 1 through its protein-protein interaction with caveolin-1. *Cell Signal*, **17**:751-760.

Colombi, M., Barlati, S., Magdelenat, H. and Fiszer-Szafarz, B. (1984). Relationship between multiple forms of plasminogen activator in human breast tumors and plasma and the presence of metastases in lymph nodes. *Cancer Res*., **44**:2971-5.

Conti, J.A., Kendall, T.J., Bateman, A., Armstrong, T.A., Papa-Adams, A., Xu, Q., Packham, G., Primrose, J.N., Benyon, R.C. and Iredale, J.P. (2008). The desmoplastic reaction surrounding hepatic colorectal adenocarcinoma metastases aids tumor growth and survival via αV integrin ligation. *Clin. Cancer Res*., **14**:6405-13.

Cretu, A. and Brooks, P.C. (2007). Impact of the non-cellular tumor microenvironment on metastasis: potential therapeutic and imaging opportunities. *J. Cell Physiol*., **213**:391-402.

Czekay, R.P., Aertgeerts, K., Curriden, S.A. and Loskutoff, D.J. (2003). Plasminogen activator inhibitor-1 detaches cells from extracellular matrices by inactivating integrins. *J. Cell. Biol*., **160**:781-791.

Czekay, R.P., Kuemmel, T.A., Orlando, R.A. and Farquhar, M.G. (2001). Direct binding of occupied urokinase receptor (uPAR) to LDL receptor-related protein is required for endocytosis of uPAR and regulation of cell surface urokinase activity. *Mol. Biol. Cell*, **12**:1467-1479.

Dagnino, L. (2011). Integrin-linked kinase: a Scaffold protein unique among its ilk. *J. Cell Commun. Signal*., **5**:81-3.

D'Alessio, S., Gerasi, L. and Blasi, F. (2008). uPAR-deficient mouse keratinocytes fail to produce EGFR-dependent laminin-5, affecting migration *in vivo* and *in vitro*. *J. Cell Sci*., **121**:3922-32.

Daley, W.P., Peters, S.B. and Larsen, M. (2008). Extracellular matrix dynamics in development and regenerative medicine. *J. Cell Sci*., **121**:255-64.

Dass, K., Ahmad, A., Azmi, A.S., Sarkar, S.H. and Sarkar, F.H. (2008). Evolving role of uPA/uPAR system in human cancers. *Cancer Treat Rev*., **34**:122-36.

de Bock, C.E. and Wang, Y. (2004). Clinical significance of urokinase-type plasminogen activator receptor (uPAR) expression in cancer. *Med. Res. Rev*., **24**:13-39.

DeClerck, Y.A., Mercurio, A.M., Stack, M.S., Chapman, H.A., Zutter, M.M., Muschel, R.J., Raz, A., MaTrisian, L.M., Sloane, B.F., Noel, A., Hendrix, M.J., Coussens, L. and Padarathsingh, M. (2004). Proteases, extracellular matrix, and cancer: a workshop of the path B study section. *Am J Pathol*., **164**:1131-1139.

Delcommenne, M., Tan, C., Gray, V., Rue, L., Woodgett, J. and Dedhar, S. (1998). Phosphoinositide-3-OH kinase-dependent regulation of glycogen synthase kinase 3 and protein kinase B/AKT by the integrin-linked kinase. *Proc. Natl. Acad. Sci. U.S.A.*, **95**:11211-11216.

Deng, G., Curriden, S.A., Hu, G., Czekay, R.P. and Loskutoff, D.J. (2001). Plasminogen activator inhibitor-1 regulates cell adhesion by binding to the somatomedin B domain of vitronectin. *J. Cell. Physiol*., **189**:23-33.

Driver, G.A. (2007). Integrin-linked Kinase (ILK) Expression in Moderately Differentiated Human Oesophageal Squamous Carcinoma Cell Lines – Growth Factor Modulation , Activity and Link to Adhesion. University of the Witwatersrand, PhD thesis, William Cullen library.

Duriseti, S., Goetz, D.H., Hostetter, D.R., LeBeau, A.M., Wei, Y. and Craik, C.S. (2010). Antagonistic anti-urokinase plasminogen activator receptor (uPAR) antibodies significantly inhibit uPAR-mediated cellular signaling and migration. *J. Biol. Chem*., **285**:26878-88.

Ekman, S., Bergqvist, M., Heldin, C.H. and Lennartsson, J. (2007). Activation of growth factor receptors in esophageal cancer--implications for therapy. *Oncologist*, **12**:1165-77.

ffrench-Constant, C. and Colognato, H. (2004). Integrins: versatile integrators of extracellular signals. *Trends Cell Biol.,* **14**:678-686.

Fidler, I.J. (2002). The organ microenvironment and cancer metastasis. *Differentiation,* **70**:498-505.

Fielding, A.B. and Dedhar, S. (2009). The mitotic functions of integrin-linked kinase. *Cancer Metastasis Rev*., **28**:99-111.

Friedl, P. and Brocker, E.B. (2000). The biology of cell locomotion within three-dimensional extracellular matrix. *Cell Mol. Life Sci*., ***57***:41-64.

Gandhari, M., Arens, N., Majety, M., Dorn-beineke, A. and Hildenbrand, R. (2006). "Urokinase-type plasminogen activator induces proliferation in breast cancer cells." *Int. J. Oncol.,* **28**:1463-70.

Garbisa, S., Scagliotti, G., Masiero, L., Di Francesco, C., Caenazzo, C., Onisto, M., Micela, M., Stetler-Stevenson, W.G. and Liotta, L.A. (1992). Correlation of serum metalloproteinase levels with lung cancer metastasis and response to therapy. *Cancer Res*., **52**:4548-9.

Gheyara, A.L., Vallejo-Illarramendi, A., Zang, K., Mei, L., St-Arnaud, R., Dedhar, S. and Reichardt, L.F. (2007). "Deletion of integrin-linked kinase from skeletal muscles of mice resembles muscular dystrophy due to α 7 β 1-integrin deficiency." *Am. J. Pathol.,* **171**:1966-77.

Ghosh, S., Brown, R., Jones, J.C., Ellerbroek, S.M. and Stack, M.S. (2000). Urinary-type plasminogen activator (uPA) expression and uPA receptor localization are regulated by α 3β 1 integrin in oral keratinocytes. *J. Biol. Chem*., **275**: 23869-76.

Gonzalez, A.M., Bhattacharya, R., deHart, G.W. and Jones, J.C. (2010). Transdominant regulation of integrin function: mechanisms of crosstalk. *Cell Signal*., **22**:578-83.

Gooding, J.M., Yap, K.L. and Ikura, M. (2004). The cadherin-catenin complex as a focal point of cell adhesion and signalling: new insights from three-dimensional structures. *Bioessays*, **26**:497-511.

Gore, R.M. (1997). Esophageal cancer. Clinical and pathologic features. *Radiol. Clin. North. Am.,* **35**:243-263.

Grashoff, C., Thievessen, I., Lorenz, K., Ussar, S. and Fassler, R. (2004). Integrin-linked kinase: integrin's mysterious partner. *Curr. Opin. Cell Biol*., **16**:565-571.

Greig, R., Dunnington, D., Murthy, U. and Anzano, M. (1988). Growth factors as novel therapeutic targets in neoplastic disease. *Cancer Surv*., **7**:653-74.

Guerrero, J., Santibanez, J.F., Gonzalez, A. and Martinez, J. (2004). EGF receptor transactivation by urokinase receptor stimulus through a mechanism involving Src and matrix metalloproteinases. *Exp. Cell Res*., **292**:201-208.

Haeckel, C., Krueger, S. and Roessner, A. (1998). Antisense inhibition of urokinase: effect on malignancy in a human osteosarcoma cell line. *Int. J. Cancer*, **77**:153-60.

Haier, J., Nasralla, M. and Nicolson, G.L. (1999). Different adhesion properties of highly and poorly metastatic HT-29 colon carcinoma cells with extracellular matrix components: role of integrin expression and cytoskeletal components. *Br. J. Cancer*, **80**:1867-74.

Hanahan, D. and Weinberg, R.A. (2011). Hallmarks of cancer: the next generation. *Cell*, **144**:646-74.

Hayman, E.G., Pierschbacher, M.D., Ohgren, Y. and Ruoslahti, E. (1983). Serum spreading factor(vitronectin) is present at the cell surface and in tissues. *Proc. Natl. Acad. Sci. U.*, **80**:4003-7.

Higazi, A.A., Upson, R.H., Cohen, R.L., Manuppello, J., Bognacki, J., Henkin, J., McCrae, K.R., Kounnas, M.Z., Strickland, D.K., Preissner, K.T. Lawler, J. and Cines, D.B. (1996). Interaction of single-chain urokinase with its receptor induces the appearance and disappearance of binding epitopes within the resultant complex for other cell surface proteins. *Blood*, **88**:542-551.

Hillig, T., Engelholm, L.H., Ingvarsen, S., Madsen, D.H., Gårdsvoll, H., Larsen, J.K., Ploug, M., Danø, K., Kjøller, L. and Behrendt, N. (2008). A composite role of vitronectin and urokinase in the modulation of cell morphology upon expression of the urokinase receptor. *J. Biol. Chem.*, **283**:15217-23.

Hirohashi, S. and Kanai, Y. (2003). Cell adhesion system and human cancer morphogenesis. *Cancer Sci.*, **94**:575-581.

Ho, B. and Bendeck, M.P. (2009). Integrin linked kinase (ILK) expression and function in vascular smooth muscle cells. *Cell Adh. Migr.*, **3**:174-6.

Hollier, B., Harkin, D.G., Leavesley, D. and Upton, Z. (2005). Responses of keratinocytes to substrate-bound vitronectin: growth factor complexes. *Exp. Cell Res.*, **305**:221-32.

Hong, S.I., Park, I.C., Son, Y.S., Lee, S.H., Kim, B.G., Lee, J.I., Lee, T.W., Kook, Y.H., Min, Y.I. and Hong, W.S. (1996). Expression of urokinase-type plasminogen activator, its receptor, and its inhibitor in gastric adenocarcinoma tissues. *J. Korean Med. Sci.*, **11**:33-37.

Huai, Q., Zhou, A., Lin, L., Mazar, A.P., Parry, G.C., Callahan, J., Shaw, D.E., Furie, B., Furie, B.C. and Huang, M. (2008). Crystal structures of two human vitronectin, urokinase and urokinase receptor complexes. *Nat Struct. Mol. Biol.*, **15**:422-3.

Humphries, J.D., Byron, A. and Humphries, M.J. (2006). Integrin ligands at a glance. *J. Cell Sci.* **119**:3901-3.

Hynes, R.O. (2002). Integrins: bidirectional, allosteric signaling machines. *Cell*, **110**:673-87.

Inoue, H., Nojima, H. and Okayama, H. (1990). High efficiency transformation of *Escherichia coli* with plasmids. *Gene*, **96**:23-8.

Ivaska, J. and Heino, J. (2000). Adhesion receptors and cell invasion: mechanisms of integrin-guided degradation of extracellular matrix. *Cell Mol. Life Sci.*, **57**:16-24.

Janes, S.M. and Watt, F.M. (2004). Switch from αvβ5 to αvβ6 integrin expression protects squamous cell carcinomas from anoikis. *J. Cell Biol.*, **166**:419-31.

Janes, S.M. and Watt, F.M. (2006). New roles for integrins in squamous-cell carcinoma. *Nat. Rev. Cancer*, **6**:175-83.

Jo, M., Thomas, K.S., Wu, L. and Gonias, S.L. (2003). Soluble urokinase-type plasminogen activator receptor inhibits cancer cell growth and invasion by direct urokinase-independent effects on cell signaling. *J. Biol. Chem.*, **278**:46692-8.

Jo, M., Thomas, K.S., Marozkina, N., Amin, T.J., Silva, C.M., Parsons, S.J. and Gonias, S.L. (2005). Dynamic assembly of the urokinase-type plasminogen activator signaling receptor complex determines the mitogenic activity of urokinase-type plasminogen activator. *J. Biol. Chem.*, **280**:17449-57.

Jo, M., Thomas, K.S., Takimoto, S., Gaultier, A., Hsieh, E.H., Lester, R.D. and Gonias, S.L. (2007). Urokinase receptor primes cells to proliferate in response to epidermal growth factor. *Oncogene*, **26**:2585-94.

Jonkman, M.F., Pas, H.H., Nijenhuis, M., Kloosterhuis, G. and Steege, G. (2002). Deletion of a cytoplasmic domain of integrin β4 causes epidermolysis bullosa simplex. *J. Invest. Dermatol.*, **119**:1275-81.

Jones, G.J., Heiss, N.S., Veale, R.B. and Thornley, A.L. (1993). Amplification and expression of the TGF-α, EGF receptor and c-myc genes in four human oesophageal squamous cell carcinoma lines. *Biosci. Rep.*, **13**:303-12.

Jordan, R.C., Bradley, G. and Slingerland, J. (1998). Reduced levels of the cell-cycle inhibitor p27Kip1 in epithelial dysplasia and carcinoma of the oral cavity. *Am. J. Pathol.*, **152**:585-90.

Juretic, N., Santibáñez, J.F., Hurtado, C. and Martínez, J. (2001). ERK 1,2 and p38 pathways are involved in the proliferative stimuli mediated by urokinase in osteoblastic SaOS-2 cell line. *J. Cell Biochem.*, **83**:92-8.

Kaminska, B., Wesolowska, A. and Danilkiewicz, M. (2005). TGF β signalling and its role in tumour pathogenesis. *Acta. Biochim. Pol.*, **52**:329-37.

Kan, T., Shimada, Y., Sato, F., Maeda, M., Kawabe, A., Kaganoi, J., Itami, A., Yamasaki, S. and Imamura, M. (2001). Gene expression profiling in human esophageal cancers using cDNA microarray. *Biochem. Biophys. Res. Commun.*, **286**:792-801.

Kang, Y. (2006). Pro-metastasis function of TGFbeta mediated by the Smad pathway. *J. Cell Biochem.*, **98**:1380-90.

Kanse, S.M., Chavakis, T., Kuo, A., Bdeir, K., Cines, D.B. and Preissner, K.T. (2004). Variability in the expression of urokinase receptor (CD87) mutants on cells: relevance to cell adhesion. *Cell Biochem. Funct.*, **22**:257-64.

Kashyap, M.K., Marimuthu, A., Kishore, C.J., Peri, S., Keerthikumar, S., Prasad, T.S., Mahmood, R., Rao, S., Ranganathan, P., Sanjeeviah, R.C., Vijayakumar, M., Kumar, K.V., Montgomery, E.A., Kumar, R.V. and Pandey, A. (2009). Genomewide mRNA profiling of esophageal squamous cell carcinoma for identification of cancer biomarkers. *Cancer Biol. Ther.,* **8**:36-46.

Katsuhiko, M., Shimada, T. And Uchida, Y. (1997). Morphology of the lamina propria in the human esophagus with special reference to the proprial papillae. *Medical Electron Microscopy,* **30**:15-24.

Kawabe, J., Okumura, S., Lee, M.C., Sadoshima, J. and Ishikawa, Y. (2004). Translocation of caveolin regulates stretch-induced ERK activity in vascular smooth muscle cells. *Am. J. Physiol. Heart Circ. Physiol*., **286**:H1845-52.

Kawahara, E., Nakada, N., Hikichi, T., Kobayashi, J. and Nakanishi, I. (2002). EGF and β1 integrin convergently regulate migration of A431 carcinoma cell through MAP kinase activation. *Exp. Cell Res*., **272**:84-91.

Kjøller, L. and Hall, A. (2001). Rac mediates cytoskeletal rearrangements and increased cell motility induced by urokinase-type plasminogen activator receptor binding to vitronectin. *J. Cell Biol*., **152**:1145-57.

Koch, A.W., Manzur, K.L. and Shan, W. (2004). Structure-based models of cadherin-mediated cell adhesion: the evolution continues. *Cell Mol. Life Sci.,* **61**:1884-95.

Kolácná, L., Bakesová, J., Varga, F., Kostáková, E., Plánka, L., Necas, A., Lukás, D., Amler, E. and Pelouch, V. (2007). Biochemical and biophysical aspects of collagen nanostructure in the extracellular matrix. *Physiol. Res*., **56**:S51-60.

Kollarova, H., Machova, L., Horakova, D., Janoutova, G. and Janout, V. (2007). Epidemiology of esophageal cancer--an overview article. *Biomed. Pap. Med. Fac. Univ. Palacky. Olomouc. Czech. Repub.,***151**:17-20.

Koshy, M., Esiashvilli, N., Landry, J.C., Thomas, C.R.Jr. and Matthews, R.H. (2004). Multiple management modalities in esophageal cancer: epidemiology, presentation and progression, work-up, and surgical approaches. *Oncologist*., **9**:137-46.

Kuwano, H., Nakajima, M., Miyazaki, T. and Kato, H. (2003). Distinctive clinicopathological characteristics in esophageal squamous cell carcinoma. *Ann. Thorac. Cardiovasc. Surg.,* **9**:6-13.

Laemmli, U.K. (1970). Cleavage of structural proteins during the assembly of the head of bacteriophage. T4. *Nature*, **227**:680-685.

Lamar, J. and DiPersio, M. (2011). Chapter 2: Roles of integrins in the development and progression of squamous cell carcinoma. *Signaling pathways in aquamous cancer*, Springer publishers.

Larsen, M., Artym, V.V., Green, J.A. and Yamada, K.M. (2006). The matrix reorganized: extracellular matrix remodeling and integrin signaling. *Curr. Opin. Cell Biol*.,**18**:463-71.

Lash, G.E., Fitzpatrick, T.E. and Graham, C.H. (2001). Effect of hypoxia on cellular adhesion to vitronectin and fibronectin. *Biochem. Biophys. Res. Commun*., **287**:622-9.

Legrand, C., Polette, M., Tournier, J.M., de Bentzmann, S., Huet, E., Monteau, M. and Birembaut, P. (2001). uPA/plasmin system-mediated MMP-9 activation is implicated in bronchial epithelial cell migration. *Exp. Cell Res*., **264**:326-336.

Li, Y., Lawrence, D.A. and Zhang, L. (2003). Sequences within domain II of the urokinase receptor critical for differential ligand recognition. *J. Biol. Chem*., **278**:29925-32.

Li, Y.J., Wei, Z.M., Meng, Y.X. and Ji, X.R. (2005). β-catenin up-regulates the expression of cyclinD1, c-myc and MMP-7 in human pancreatic cancer: relationships with carcinogenesis and metastasis. *World J. Gastroenterol*., **11**:2117-2123.

Liang, X., Yang, X., Tang, Y., Zhou, H., Liu, X., Xiao, L., Gao, J. and Mao, Z. (2008). RNAi-mediated downregulation of urokinase plasminogen activator receptor inhibits proliferation, adhesion, migration and invasion in oral cancer cells. *Oral Oncol*., **44**:1172-80.

Liu, D., Aguirre-Ghiso, J., Estrada, Y. and Ossowski, L. (2002). EGFR is a transducer of the urokinase receptor initiated signal that is required for *in vivo* growth of a human carcinoma. *Cancer Cell*, **1**:445-57.

Liu, G.C., Zhang, J., Liu, S.G., Gao, R., Long, Z.F., Tao, K. and Ma, Y.F. Detachment of esophageal carcinoma cells from extracellular matrix causes relocalization of death receptor 5 and apoptosis. (2009). *World J. Gastroenterol*., **15**:836-44.

Lopez, J.I., Mouw, J.K. and Weaver, V.M. (2008). Biomechanical regulation of cell orientation and fate. *Oncogene*, **27**:6981-93.

Lu, S.H. (2000). Alterations of oncogenes and tumor suppressor genes in esophageal cancer in China. *Mutat Res*., **462**:343-53.

Madsen, C.D. and Sidenius, N. (2008). The interaction between urokinase receptor and vitronectin in cell adhesion and signalling. *Eur. J. Cell Biol*., **87**:617-29.

Madsen, C.D., Ferraris, G.M., Andolfo, A., Cunningham, O and Sidenius, N. (2007). uPAR-induced cell adhesion and migration: vitronectin provides the key. *J. Cell Biol*., **177**:927-39.

Mandard, A.M., Hainaut, P. and Hollstein, M. (2000). Genetic steps in the development of squamous cell carcinoma of the esophagus. *Mutat. Res.,* **462**:335-342.

Margadant, C. and Sonnenberg, A. (2010). Integrin-TGF-β crosstalk in fibrosis, cancer and wound healing. *EMBO Rep*., **11**:97-105.

Matsumoto, K., Shimada, T. and Uchida, Y. (1997). "Morphology of the lamina propria in the human esophagus with special reference to the proprial papillae." *Medical Electron Microscopy*, **30**:15-24.

Maupas-Schwalm, F., Bedel, A., Augé, N., Grazide, M.H., Mucher, E., Thiers, J.C., Salvayre, R. and Nègre-Salvayre, A. (2009). Integrin α(v)β(3), metalloproteinases, and sphingomyelinase-2 mediate urokinase mitogenic effect. *Cell Signal*., **21**:1925-34.

Mazzieri, R., D'Alessio, S., Kenmoe, R.K., Ossowski, L. and Blasi, F. (2006). An uncleavable uPAR mutant allows dissection of signaling pathways in uPA-dependent cell migration. *Mol. Biol. Cell.,* **17**:367-78.

McDonald, P.C., Fielding, A.B. and Dedhar, S. (2008). Integrin-linked kinase--essential roles in physiology and cancer biology. *J. Cell Sci*., **121**:3121-32.

McGlashan, N.D. (1988). Oesophageal cancer in the black people of South Africa. *S. Afr. J. Sci.,* **84**:92-99.

McGlashan, N.D., Harington, J.S. and Chelkowska, E. (2003). Changes in the geographical and temporal patterns of cancer incidence among black gold miners working in South Africa, 1964-1996. *Br. J. Cancer*, **88**:1361-9.

Melhado, R.E., Alderson, D. and Tucker, O. (2010). The changing face of esophageal cancer. *Cancers*, **2**: 1379-1404.

Memarzadeh, S., Kozak, K.R., Chang, L., Natarajan, S., Shintaku, P., Reddy, S.T. and Farias-Eisner, R. (2002). Urokinase plasminogen activator receptor: Prognostic biomarker for endometrial cancer. *Proc. Natl. Acad. Sci. U.S.A.,* **99**:10647-10652.

Miller, S.E. (2001). Expression of αV, α2 and β1 integrins by human oesophageal squamous cell carcinomas. University of the Witwatersrand, MSc dissertation, William Cullen library.

Miller, S.E. and Veale, R.B. (2001). Environmental modulation of α(v), α(2) and β(1) integrin subunit expression in human oesophageal squamous cell carcinomas. *Cell Biol. Int*., **25**:61-69.

Mitsudomi, T. and Yatabe, Y. (2010). Epidermal growth factor receptor in relation to tumor development: EGFR gene and cancer. *FEBS J.,* **277**:301-8.

Monaghan-Benson, E., Mastick, C.C.and McKeown-Longo, P.J. (2008). A dual role for caveolin-1 in the regulation of fibronectin matrix assembly by uPAR. *J. Cell Sci*., **121**:3693-703.

Monick, M.M., Carter, A.B., Robeff, P.K., Flaherty, D.M., Peterson, M.W. and Hunninghake, G.W. (2001). Lipopolysaccharide activates Akt in human alveolar macrophages resulting in nuclear accumulation and transcriptional activity of β-catenin. *J. Immunol.,* **166**:4713-4720.

Montuori, N., Carriero, M.V., Salzano, S., Rossi, G. and Ragno, P. (2002). The cleavage of the urokinase receptor regulates its multiple functions. *J. Biol. Chem*., **277**:46932-9.

Mori, R., Ishiguro, H., Kuwabara, Y., Kimura, M., Mitsui, A., Tomoda, K., Mori, Y., Ogawa, R., Katada, T., Harata, K. and Fujii, Y. (2008). Targeting β1 integrin restores sensitivity to docetaxel of esophageal squamous cell carcinoma. *Oncol. Rep*., **20**:1345-51.

Morrissey, D., O'Connell, J., Lynch, D., O'Sullivan, G.C., SHanahan, F. and Collins, J.K. (1999). Invasion by esophageal cancer cells: functional contribution of the urokinase plasminogen activation system, and inhibition by antisense oligonucleotides to urokinase or urokinase receptor. *Clin. Exp. Metastasis*, **17**:77-85.

Mukaida, H., Toi, M., Hirai, T., Yamashita, Y. and Toge, T. (1991). Clinical significance of the expression of epidermal growth factor and its receptor in esophageal cancer. *Cancer*, **68**:142-8.

Mukhopadhyay, N.K., Gordon, G.J., Chen, C.J., Bueno, R., Sugarbaker, D.J. and Jaklitsch, M.T. (2005). Activation of focal adhesion kinase in human lung cancer cells involves multiple and potentially parallel signaling events. *J. Cell Mol. Med.*, **9**:387-397.

Nair, K.S., Naidoo, R. and Chetty, R. (2005). Expression of cell adhesion molecules in oesophageal carcinoma and its prognostic value. *J. Clin. Pathol.*, **58**:343-351.

Nassar, T., Yarovoi, S., Fanne, R.A., Waked, O., Allen, T.C., Idell, S., Cines, D.B. and Higazi, A.A. (2011). Urokinase plasminogen activator regulates pulmonary arterial contractility and vascular permeability in mice. *Am. J. Respir. Cell Mol. Biol.*, **45**: 1015-21.

Nelson, W.J. (2003). Epithelial cell polarity from the outside looking in. *News Physiol. Sci.*, **18**:143-146.

Nho, R.S., Xia, H., Kahm, J., Kleidon, J., Diebold, D. and Henke, C.A. (2005). Role of integrin-linked kinase in regulating phosphorylation of Akt and fibroblast survival in type I collagen matrices through a β1 integrin viability signaling pathway. *J. Biol. Chem.*, **280**:26630-9.

Nozaki, S., Endo, Y., Kawashiri, S., Nakagawa, K., Yamamoto, E., Yonemura, Y. and Sasaki, T. (1998). Immunohistochemical localization of a urokinase-type plasminogen activator system in squamous cell carcinoma of the oral cavity: association with mode of invasion and lymph node metastasis. *Oral Oncol.*, **34**:58-62.

Obama, H. and Ozawa, M. (1997). Identification of the domain of α-catenin involved in its association with β-catenin and plakoglobin (γ-catenin). *J. Biol. Chem.*, **272**:11017-20.

Oloumi, A., McPhee, T. and Dedhar, S. (2004). Regulation of E-cadherin expression and β-catenin/Tcf transcriptional activity by the integrin-linked kinase. *Biochim. Biophys. Acta.*, **1691**:1-15.

Orgel, J.P., Irving, T.C., Miller, A. and Wess, T.J. (2006). Microfibrillar structure of type I collagen *in situ*. *Proc. Natl. Acad. Sci. U S A.*, **103**:9001-5.

Ortiz, C.M., Ito, T., Hashimoto, Y., Nagayama, S., Iwai, A., Tsunoda, S., Sato, F., Martorell, M., Garcia, J.A., Perez, A. and Shimada,Y. (2010). Effects of small interfering RNAs targeting fascin on human esophageal squamous cell carcinoma cell lines. *Diagn. Pathol.*, **5**:41.

Ossowski, L. and Aguirre-Ghiso, J.A. (2000). Urokinase receptor and integrin partnership: coordination of signaling for cell adhesion, migration and growth. *Curr. Opin. Cell Biol.*, **12**:613-620.

Pacella-Norman, R., Urban, M.I., Sitas, F., Carrara, H., Sur, R., Hale, M., Ruff, P., Patel, M., Newton, R., Bull, D. and Beral, V. (2002). Risk factors for oesophageal, lung, oral and laryngeal cancers in black South Africans.
Br. J. Cancer, **86**:1751-6.

Parsons, J.T. (2003). Focal adhesion kinase: the first ten years. *J. Cell Sci*., **116**:1409-1416.

Petreaca, M. and Martins-Green, M. (2007). Chapter 7: The Dynamics of Cell – ECM Interactions. *Principles of Tissue Engineering*, 3rd Edition, Elsevier Science Publishers.

Peyrollier, K., Hajduch, E., Gray, A., Litherland, G.J., Prescott, A.R., Leslie, N.R. and Hundal, H.S. (2000). A role for the actin cytoskeleton in the hormonal and growth-factor-mediated activation of protein kinase B. *Biochem. J*., **352**:617-622.

Piccolella, M., Festuccia, C., Millimaggi, D., Locatelli, A., Bologna, M., Motta, M. and Dondi, D. (2008). suPAR, a soluble form of urokinase plasminogen activator receptor, inhibits human prostate cancer cell growth and invasion. *Int. J. Oncol*., **32**:185-91.

Plesner, T., Behrendt, N. and Ploug, M. (1997). Structure, function and expression on blood and bone marrow cells of the urokinase-type plasminogen activator receptor, uPAR. *Stem Cells*., **15**:398-408.

Ploug, M., Rahbek-Nielsen, H., Nielsen, P.F., Roepstorff, P. and Danø, K. (1998). Glycosylation profile of a recombinant urokinase-type plasminogen activator receptor expressed in Chinese hamster ovary cells. *J. Biol. Chem*., **273**:13933-43.

Ploug, M., Ostergaard, S., Gardsvoll, H., Kovalski, K., Holst-Hansen, C., Holm, A., Ossowski, L. and Danø, K. (2001). Peptide-derived antagonists of the urokinase receptor. affinity maturation by combinatorial chemistry, identification of functional epitopes, and inhibitory effect on cancer cell intravasation. *Biochemistry*, **40**:12157-68.

Pluskota, E., Soloviev, D.A. and Plow, E.F. (2003). Convergence of the adhesive and fibrinolytic systems: recognition of urokinase by integrin α Mβ 2 as well as by the urokinase receptor regulates cell adhesion and migration. *Blood*., **101**:1582-1590.

Pozzi, A., Wary, K.K., Giancotti, F.G. and Gardner, H.A. (1998). Integrin α1β1 mediates a unique collagen-dependent proliferation pathway *in vivo*. *J. Cell Biol*., **142**:587-94.

Qin, J., Vinogradova, O. and Plow, E.F. (2004). Integrin bidirectional signaling: a molecular view. *PLoS Biol*., **2**:e169.

Ragno, P., Montuori, N., Covelli, B., Hoyer-Hansen, G. and Rossi, G. (1998). Differential expression of a truncated form of the urokinase-type plasminogen-activator receptor in normal and tumor thyroid cells. *Cancer Res*., **58**:1315-9.

Rameh, L.E. and Cantley, L.C. (1999). The role of phosphoinositide 3-kinase lipid products in cell function. *J. Biol. Chem*., **274**:8347-8350.

Reinmuth, N., Liu, W., Ahmad, S.A., Fan, F., Stoeltzing, O., Parikh, A.A., Bucana, C.D., Gallick, G.E., Nickols, M.A., Westlin, W.F. and Ellis, L.M. (2003). Avβ3 integrin antagonist S247 decreases colon cancer metastasis and angiogenesis and improves survival in mice. *Cancer Res*., **63**:2079-87.

Ricard-Blum, S. and Ruggiero, F. (2005). The collagen superfamily: from the extracellular matrix to the cell membrane. *Pathol. Biol (Paris*)., **53**:430-42.

Rofstad, E.K., Mathiesen, B. and Galappathi, K. (2004). Increased metastatic dissemination in human melanoma xenografts after subcurative radiation treatment: radiation-induced increase in fraction of hypoxic cells and hypoxia-induced up-regulation of urokinase-type plasminogen activator receptor. *Cancer Res*., **64**:13-18.

Roldan, A.L., Cubellis, M.V., Masucci, M.T., Behrendt, N., Lund, L.R., Danø, K., Appella, E. and Blasi, F. (1990). Cloning and expression of the receptor for human urokinase plasminogen activator, a central molecule in cell surface, plasmin dependent proteolysis. *EMBO J*., **9**:467-74.

Sambrook, J., Fritsch, E.F. and Maniatis, T. (1989). In: *Molecular Cloning, A Laboratory Manual.* Second Edition. (New York: Cold Spring Harbour Laboratory Press): pp 1.25-1.28

Santala, A., Saarinen, J., Kovanen, P. and Kuusela, P. (2000). Corrigendum to: activation of interstitial collagenase, MMP-1, by staphylococcus aureus cells having surface-bound plasmin: a novel role of plasminogen receptors of bacteria. *FEBS Lett*., **469**:213

Sato, S., Kopitz, C., Grismayer, B., Beaufort, N., Reuning, U., Schmitt, M., Luther, T., Kotzsch, M., Krüger, A. and Magdolen, V. (2011). Overexpression of the urokinase receptor mRNA splice variant uPAR-del4/5 affects tumor-associated processes of breast cancer cells *in vitro* and *in vivo*. *Breast Cancer Res. Treat*., **127**:649-57.

Schmidt-Ullrich, R.K., Mikkelsen, R.B., Dent, P., Todd, D.G., Valerie, K., Kavanagh, B.D., Contessa, J.N., Rorrer, W.K. and Chen, P.B. (1997). Radiation-induced proliferation of the human A431 squamous carcinoma cells is dependent on EGFR tyrosine phosphorylation. *Oncogene*, **15**:1191-7.

Schneider, M.R. and Wolf, E. (2009). The epidermal growth factor receptor ligands at a glance. *J. Cell Physiol*., **218**:460-6.

Schoppet, M., Chavakis, T., Al-Fakhri, N., Kanse, S.M. and Preissner, K.T. (2002). Molecular interactions and functional interference between vitronectin and transforming growth factor-β. *Lab Invest*., **82**:37-46.

Schvartz, I., Seger, D. and Shaltiel, S. (1999). Vitronectin. *Int. J. Biochem. Cell Biol*., **31**:539-44.

Shao, C., Chen, S., Chen, L., Cobos, E., Wang, J.S., Haab, B.B. and Gao, W. (2009). Antibody microarray analysis of serum glycans in esophageal squamous cell carcinoma cases and controls. *Proteomics Clin. Appl*., **3**:923-31.

She, S., Xu, B., He, M., Lan, X. and Wang, Q. (2010). Nm23-H1 suppresses hepatocarcinoma cell adhesion and migration on fibronectin by modulating glycosylation of integrin beta1. *J. Exp. Clin. Cancer Res*., **29**:93.

Shimada, Y. and Sato, F. (2007). Molecular factors related to metastasis of esophageal squamous cell carcinoma. *Esophagus*, **4**:7-18.

Shiomi, H., Eguchi, Y., Tani, T., Kodama, M. and Hattori, T. (2000). Cellular distribution and clinical value of urokinase-type plasminogen activator, its receptor, and plasminogen activator inhibitor-2 in esophageal squamous cell carcinoma. *Am. J. Pathol*., **156**:567-575.

Sidenius, N., Andolfo, A., Fesce, R. and Blasi, F. (2002). Urokinase regulates vitronectin binding by controlling urokinase receptor oligomerization. *J. Biol. Chem*., **277**:27982-90.

Simon, D.I., Rao, N.K., Xu, H., Wei, Y., Majdic, O., Ronne, E., Kobzik, L. and Chapman, H.A. (1996). Mac-1 (CD11b/CD18) and the urokinase receptor (CD87) form a functional unit on monocytic cells. *Blood*, **88**:3185-94.

Smeds, J., Berggren, P., Ma, X., Xu, Z., Hemminki, K. and Kumar, R. (2002). Genetic status of cell cycle regulators in squamous cell carcinoma of the oesophagus: the CDKN2A (p16(INK4a) and p14(ARF)) and p53 genes are major targets for inactivation. *Carcinogenesis*, **23**:645-55.

Srichai, M. B. and Zent, R. (2010). Chapter 2: Integrin Structure and Function. *Cell-Extracellular matrix interactions in cancer.* , Springer Publishers.

Stepanova, V.V. and Tkachuk, V.A. (2002). Urokinase as a multidomain protein and polyfunctional cell regulator. *Biochemistry (Moscow)*, **67**:109-18.

Stewart, C.E. and Sayers, I. (2009). Characterisation of urokinase plasminogen activator receptor variants in human airway and peripheral cells. *BMC Mol. Biol*., **10**:75

Stoner, G.D. and Gupta, A. (2001). Etiology and chemoprevention of esophageal squamous cell carcinoma. *Carcinogenesis*, **22**:1737-1746.

Stoner, G.D., Wang, L.S. and Chen, T. (2007). Chemoprevention of esophageal squamous cell carcinoma. *Toxicol. Appl. Pharmacol*., **224**:337-49.

Streuli, C.H. and Akhtar, N. (2009). Signal co-operation between integrins and other receptor systems. *Biochem. J*., **418**:491-506.

Tang, C.H., Hill, M.L., Brumwell, A.N., Chapman, H.A. and Wei, Y. (2008). Signaling through urokinase and urokinase receptor in lung cancer cells requires interactions with β1 integrins. *J. Cell Sci*., **121**:3747-56.

Tarui, T., Andronicos, N., Czekay, R.P., Mazar, A.P., Bdeir, K., Parry, G.C., Kuo, A., Loskutoff, D.J., Cines, D.B. and Takada Y. (2003). Critical role of integrin α 5 β 1 in urokinase (uPA)/urokinase receptor (uPAR, CD87) signaling. *J. Biol. Chem*., **278**:29863-29872.

Thunø, M., Macho, B. and Eugen-Olsen, J. (2009). suPAR: the molecular crystal ball. *Dis. Markers*, **27**:157-72.

Timmer, A., Oosterhuis, J.W., Schraffordt Koops, H., Sleijfer, D.T., Szabo, B.G. and Timens, W. (1994). The tumor microenvironment: possible role of integrins and the extracellular matrix in tumor biological behavior of intratubular germ cell neoplasia and testicular seminomas. *Am. J. Pathol*., **144**:1035-44.

Towbin, H., Staehelin, T. and Gordon, J. (1979). Electrophoretic transfer of proteins from polyacrylamide gels to nitrocellulose sheets: procedure and some applications. *Proc. Natl. Acad. Sci. U S A.*, **76**:4350-4.

Tran, N.L., Adams, D.G., Vaillancourt, R.R. and Heimark, R.L. (2002). Signal transduction from N-cadherin increases Bcl-2. Regulation of the phosphatidylinositol 3-kinase/Akt pathway by homophilic adhesion and actin cytoskeletal organization. *J. Biol. Chem.*, **277**:32905-32914.

Troussard, A.A., Mawji, N.M., Ong, C., Mui, A., St –Arnaud, R. and Dedhar, S. (2003). Conditional knock-out of integrin-linked kinase demonstrates an essential role in protein kinase B/Akt activation. *J. Biol. Chem.*, **278**:22374-8.

Ulisse, S., Baldini, E., Sorrenti, S. and D'Armiento, M. (2009). The urokinase plasminogen activator system: a target for anti-cancer therapy. *Curr. Cancer Drug Targets*, **9**:32-71.

van der Pluijm, G., Sijmons, B., Vloedgraven, H., van der Bent, C., Drijfhout, J.W., Verheijen, J., Quax, P., Karperien, M., Papapoulos, S. and Löwik, C. (2001). Urokinase-receptor/integrin complexes are functionally involved in adhesion and progression of human breast cancer *in vivo*. *Am. J. Pathol.*, **159**:971-82.

Veale, R.B. and Thornley, A.L. (1989). Increased single class low-affinity EGF receptors expressed by human oesophageal squamous carcinoma cell lines. *S. Afr. J. Sci.*, **85**:375-379.

Veale, R.B., Thornley, A.L. and Scott, E. (1990). Plasminogen activator secretion by human oesophageal scc cells and its regulation by TGFß. *S. Afr. Med. J.*, **78**:369

Vitale, M., Illario, M., Di Matola, T., Casamassima, A., Fenzi, G. and Rossi, G. (1997). Integrin binding to immobilized collagen and fibronectin stimulates the proliferation of human thyroid cells in culture. *Endocrinology*, **138**:1642-8.

Wang, X.Q., Sun, P. and Paller, A.S. (2005). Gangliosides inhibit urokinase-type plasminogen activator (uPA)-dependent squamous carcinoma cell migration by preventing uPA receptor/αβ integrin/epidermal growth factor receptor interactions. *J. Invest. Dermatol.*, **124**:839-48.

Wang, J., Guo, F., Wei, H., Dong, J. and Wu, J. (2006). Expression of urokinase-type plasminogen activator receptor is correlated with metastases of lingual squamous cell carcinoma. *Br. J. Oral Maxillofac. Surg.*, **44**:515-9.

Wary, K.K., Mariotti, A., Zurzolo, C. and Giancotti, F.G. (1998). A requirement for caveolin-1 and associated kinase Fyn in integrin signaling and anchorage-dependent cell growth. *Cell.*, **94**:625-34.

Wei, Y., Yang, X., Liu, Q., Wilkins, J.A. and Chapman, H.A. (1999). A role for caveolin and the urokinase receptor in integrin-mediated adhesion and signaling. *J. Cell Biol.*, **144**:1285-94.

Wei, Y., Eble, J.A., Wang, Z., Kreidberg, J.A. and Chapman, H.A. (2001). Urokinase receptors promote β1 integrin function through interactions with integrin α3β1. *Mol. Biol. Cell*, **12**:2975-86.

Wei, Y., Czekay, R.P., Robillard, L., Kugler, M.C., Zhang, F., Kim, K.K., Xiong, J.P., Humphries, M.J. and Chapman, H.A. (2005) Regulation of α5β1 integrin conformation and function by urokinase receptor binding. *J. Cell Biol.*, **168**:501-11.

Wessel, D. and Flügge, U.I. (1984). A method for the quantitative recovery of protein in dilute solution in the presence of detergents and lipids. *Anal. Biochem.*, **138**:141-3.

Westhoff, M.A., Serrels, B., Fincham, V.J., Frame, M.C. and Carragher, N.O. (2004). SRC-mediated phosphorylation of focal adhesion kinase couples actin and adhesion dynamics to survival signaling. *Mol. Cell Biol.*, **24**:8113-33.

Wickström, S.A., Lange, A., Montanez, E. and Fässler, R. (2010). The ILK/PINCH/parvin complex: the kinase is dead, long live the pseudokinase! *EMBO J.*, **29**:281-91.

Wilhelm, O., Weidle, U., Höhl, S., Rettenberger, P., Schmitt, M. and Graeff, H. (1994). Recombinant soluble urokinase receptor as a scavenger for urokinase-type plasminogen activator (uPA). Inhibition of proliferation and invasion of human ovarian cancer cells. *FEBS Lett.*, **337**:131-4.

Wodarz, A. (2002). Establishing cell polarity in development. *Nat. Cell Biol.*, **4**:39-44.

Xie, J.J., Xu, L.Y., Xie, Y.M., Zhang, H.H., Cai, W.J., Zhou, F., Shen, Z.Y. and Li, E.M. (2009). Roles of ezrin in the growth and invasiveness of esophageal squamous carcinoma cells. *Int. J. Cancer*, **124**:2549-58.

Yebra, M., Goretzki, L., Pfeifer, M. and Mueller, B.M. (1999). Urokinase-type plasminogen activator binding to its receptor stimulates tumor cell migration by enhancing integrin-mediated signal transduction. *Exp. Cell Res.*, **250**:231-40.

Yuan, C. and Huang, M. (2007). Does the urokinase receptor exist in a latent form? *Cell Mol. Life Sci.*, **64**:1033-7.

Zhang, G., Zhang, Q., Zhang, Q., Yin, L., Li, S., Cheng, K., Zhang, Y., Xu, H. and Wu, W. (2010). Expression of nucleostemin, epidermal growth factor and epidermal growth factor receptor in human esophageal squamous cell carcinoma tissues. *J. Cancer Res. Clin. Oncol.*, **136**:587-94.

Zhao, J. and Guan, J.L. (2009). Signal transduction by focal adhesion kinase in cancer. *Cancer Metastasis Rev.*, **28**:35-49.

Zhu, S., Gladson, C.L., White, K.E., Ding, Q., Stewart, J. Jr., Jin, T.H., Chapman, H.A. Jr. and Olman, M.A. (2009). Urokinase receptor mediates lung fibroblast attachment and migration toward provisional matrix proteins through interaction with multiple integrins. *Am. J. Physiol. Lung Cell Mol. Physiol.*, **297**:L97-108.

Ziober, A.F., Falls, E.M. and Ziober, B.L. (2006). The extracellular matrix in oral squamous cell carcinoma: friend or foe? *Head Neck*, **28**:740-9.

Zolkiewska, A. (2005). Ecto-ADP-ribose transferases: cell-surface response to local tissue injury. *Physiology (Bethesda)*, **20**:374-81.

Chapter 9: Appendix A

9.1 List of Reagents

3-[4,5-dimethylthiazol-2-yl]-2,5-diphenyl tetrazolium bromide (MTT, Sigma)

β1P1 and β1P1^{Sc} peptides (Sylvean Biotech)

Bovine serum albumin (BDA Laboratory reagents)

dNTP mix (Abgene)

Dulbecco's Modified Eagles Medium (DMEM)/Hams F12 (Highveld Biologicals)

EDTA (BDA Laboratory reagents)

Epidermal growth factor (Sigma)

Exactacruz^{TM} F kit (Santa Cruz Biotechnology, Inc)

Fetal calf serum (FCS) (Highveld Biologicals)

GeneRuler 100 bp DNA ladder (Fermentas)

High Molecular Weight urokinase plasminogen activator (Merck)

Moloney Murine Leukemia Virus Reverse Transcriptase (Promega)

Moloney Murine Leukemia Virus Reverse Transcriptase buffer (Promega)

PageRuler^{TM} prestained protein ladder (Fermentas)

PCR Master mix (Roche)

PMSF (Merck)

Protein G-beads (Sigma)

Random hexamer primers (Roche)

Soluble uPAR 807-UK (R&D systems)

SuperSignal West Pico Chemiluminescent substrate kit (Pierce)

Taq polymerase (Roche)

Transforming growth factor β1 (Sigma)

Trasylol (Bayer)

TRIzol (Gibco BRL)

Trypsin (Gibco BRL)

Vectashield Hardset ^{TM} mounting medium (Vector Laboratories)

Vitronectin V9881 (Sigma)

Appendix B

9.2.1 Trypsin/EDTA solution

9.2.1.a Trypsin solution

0.01% Trypsin

Make up to final volume with PBS

9.2.1.b EDTA solution

0.004% EDTA

Make up to final volume with PBS

MIX:

50% Trypsin solution

50% EDTA solution

Store at 4°C

9.2.2 DMEM/Hams 12 (3:1) medium

9.2.2.a DMEM solution

1.37% DMEM

0.37% Sodium bicarbonate

2% Penicillin/Streptomycin solution (Penicillin: 500 U/ml; Streptomycin: 0.5%)

Make up to final volume with dH_2O

9.2.2.b Hams F12 medium solution

1.07% Hams F12 medium

0.118% Sodium bicarbonate

2% Penicillin/Streptomycin solution (Penicillin: 500 U/ml; Streptomycin: 0.5%)

Make up to final volume with dH_2O

MIX:

3 volumes DMEM medium solution

1 volume Hams F12 medium solution

Filter sterilize

Store at 4°C

9.2.3 Phosphate buffer saline (1x)

136.9 mM	Sodium chloride
2.68 mM	Potassium chloride
10.1 mM	Disodium hydrogen phosphate dodecahydrate
1.76 mM	Potassium dihydrogen phosphate

Adjust pH between 8.2 to 7.3

Make up to final volume with dH_2O

Sterilise for 20 min at 151 lbq

Store at 4^oC

9.2.4 Phenol

100 g	Phenol
20 ml	2 M Tris-HCl, pH 7.4
26 ml	dH_2O

Incubate at 37^oC carefully until all phenol is dissolved

Remove aqueous upper phase

ADD:

20 ml	2 M Tris-HCl, pH 7.4
5 ml	M-cresol
200 µl	β-mercaptoethanol
100 mg	8-Hydroxyquinoline

Store aqueous and phenol phase together in hood at room temperature.

Use yellow phenol for extraction and store at 4^oC

9.2.5 Agarose gel (1 %)

1% agarose

Make up to final volume with 1X TAE (5% of 20X TAE (section 8.2.6);

Make to final volume with dH_2O)

-Boil until agarose dissolves

-Wait for solution to cool

-Add 0.05% Ethidium bromide

-Pour

-Allow 30 min for gel to set

9.2.6 Tris-Acetate-EDTA (TAE) 20X

1 M	Tris-HCl, pH 8.2
0.5 M	Sodium acetate
25.5 mM	EDTA

Make up final volume in dH_2O

Sterilise for 20 min at 151 lbq

9.2.7 Loading buffer

50%	2X TAE (10% of 20X TAE; Make to final volume with dH_2O)
50%	glycerol
0.001%	Bromophenol blue

Store at -20^{o}C

9.2.8 PBS/PMSF/Trasylol solution

0.5%	PMSF stock solution (20 mM in Methanol)
1%	Trasylol

Make up to final volume with PBS

9.2.9 RIPA buffer

50 mM	Tris-HCl, pH 7.5
150 mM	Sodium Chloride
0.5%	Deoxycholate
0.5%	Triton X-100
0.05%	SDS
1 mM	PMSF and Trasylol

Make up to final volume with dH_2O

Store at 4^{o}C

9.2.10 Laemmli single lysis buffer

61.9 mM	Tris-HCl, pH 6.8
2%	SDS
10%	glycerol
5%	β-mercaptoethanol

Make up to final volume with dH_2O

Store at 4^oC

9.2.11 Coomassie Blue solution (0.25%)

0.25%	Coomassie brilliant blue powder
50%	Methanol
10%	Glacial acetic acid

Make up to final volume with dH_2O

9.2.12 Destaining solution

12%	Glacial acetic acid
10%	Methanol

Make up to final volume with dH_2O

9.2.13 Elution solution

66%	Methanol
33%	dH_2O
1%	Ammonia

9.2.14 Example of standard curve (protein estimation)

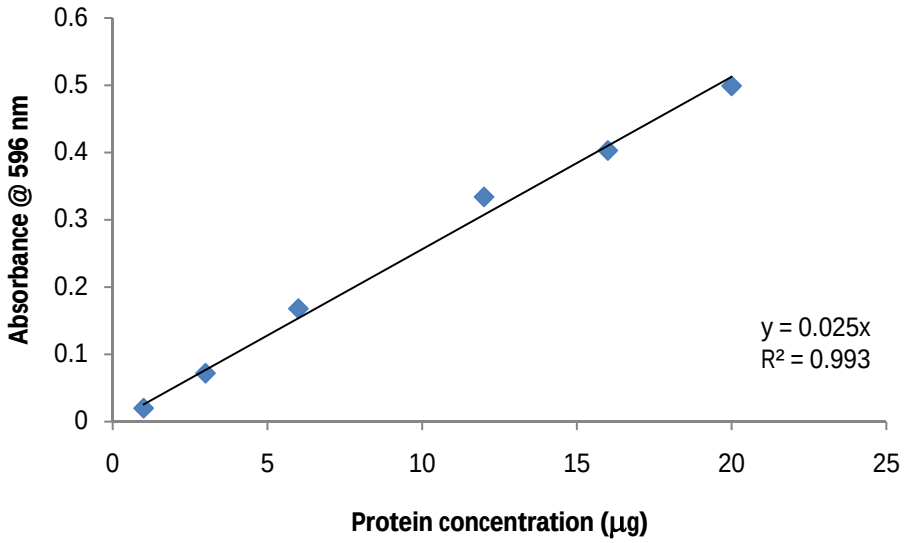

Figure A.1: Example of a protein estimation standard curve. The specific BSA standards, at varying concentrations, in µg (x-axis) and their respective absorbance value at 596 nm (y-axis) were used to create the curve. The equation of the curve was used to calculate the unknown protein concentration in a given sample. R^2 = linear regression.

9.2.15 Laemmli double lysis buffer

123.8 mM	Tris-HCl, pH 6.8
4%	SDS
20%	glycerol
10%	β-mercaptoethanol

Make up to final volume with dH_2O

Store at 4^oC

9.2.16 Immunoprecipitation buffer

20 mM	Tris-HCl, pH 8.0
0.5%	NP-40
0.9%	NaCl

Make up to final volume with dH_2O

9.2.17 Separating gel

10%	Acrylamide
0.1%	NN'-methylenebisacrylamide
375 mM	Tris-HCl, pH 8.8
0.2%	SDS

Make up to final volume with dH_2O
Just before use add: 1mM Ammonium persulphate
0.25% N,N,N'N'-tetramethylenediamine (TEMED)

9.2.18 Stacking gel

10%	Acrylamide
0.1%	NN'-methylenebisacrylamide
125 mM	Tris-HCl, pH 6.8
0.2%	SDS

Make up to final volume with dH_2O
Just before use add: 1mM Ammonium persulphate
0.25% TEMED

9.2.19 Electrophoresis buffer

3.74 mM	SDS
25 mM	Tris-HCl, pH 8.3
192.5 mM	Glycine

Make up to final volume with dH_2O

9.2.20 Destain solution

10%	Acetic acid
10%	Methanol

Make up to final volume with dH_2O

9.2.21 Towbin electrophoresis transfer buffer (Towbin *et al*., 1979)

25 mM	Tris-HCl, pH 8.3
1.41%	Glycine
20%	Methanol

Make up to final volume with dH_2O

Store at 4^oC

9.2.22 Tris Buffer Saline

50 mM	Tris-HCl, pH 7.8
150 mM	Sodium Chloride

Make up to final volume with dH_2O

9.2.23 Developer solution

6.4 M	Metol
0.6 M	Sodium sulphite (anhydrous)
80 mM	Hydroquinine
0.45 mM	Sodium carbonate (anhydrous)
34 mM	Potassium bromide

Make up to final volume with dH_2O

Store in the dark

9.2.24 Fixer solution

0.8 M	Sodium thiosulphate
0.2 M	Sodium metabisulphite

Make up to final volume with dH_2O

Store in the dark

9.2.25 BLOTTO

50 mM	Tris-HCl, pH 7.8
150 mM	Sodium Chloride
2 mM	Calcium chloride dihydrate
5%	non-fat milk powder
0.05%	Triton-X 100

Make up to final volume with dH_2O

Store at 4^oC

9.2.26 Paraformaldehyde (4%)

9.2.26.a Solution A

0.14 M	Sodium dihydrogen orthophosphate (anhydrous)

Make up to final volume with dH_2O

9.2.26.b Solution B

0.63 M	Sodium hydroxide

Make up to final volume with dH_2O

DISSOLVE: 4% paraformaldehyde in

83%	Solution A
17%	Solution B

Make up to final

Heat to approximately 80^oC

Stir until solution is clear

Allow solution to cool

Adjust pH between 8.2 to 7.3

Filter and store solution at 4^oC

Appendix C

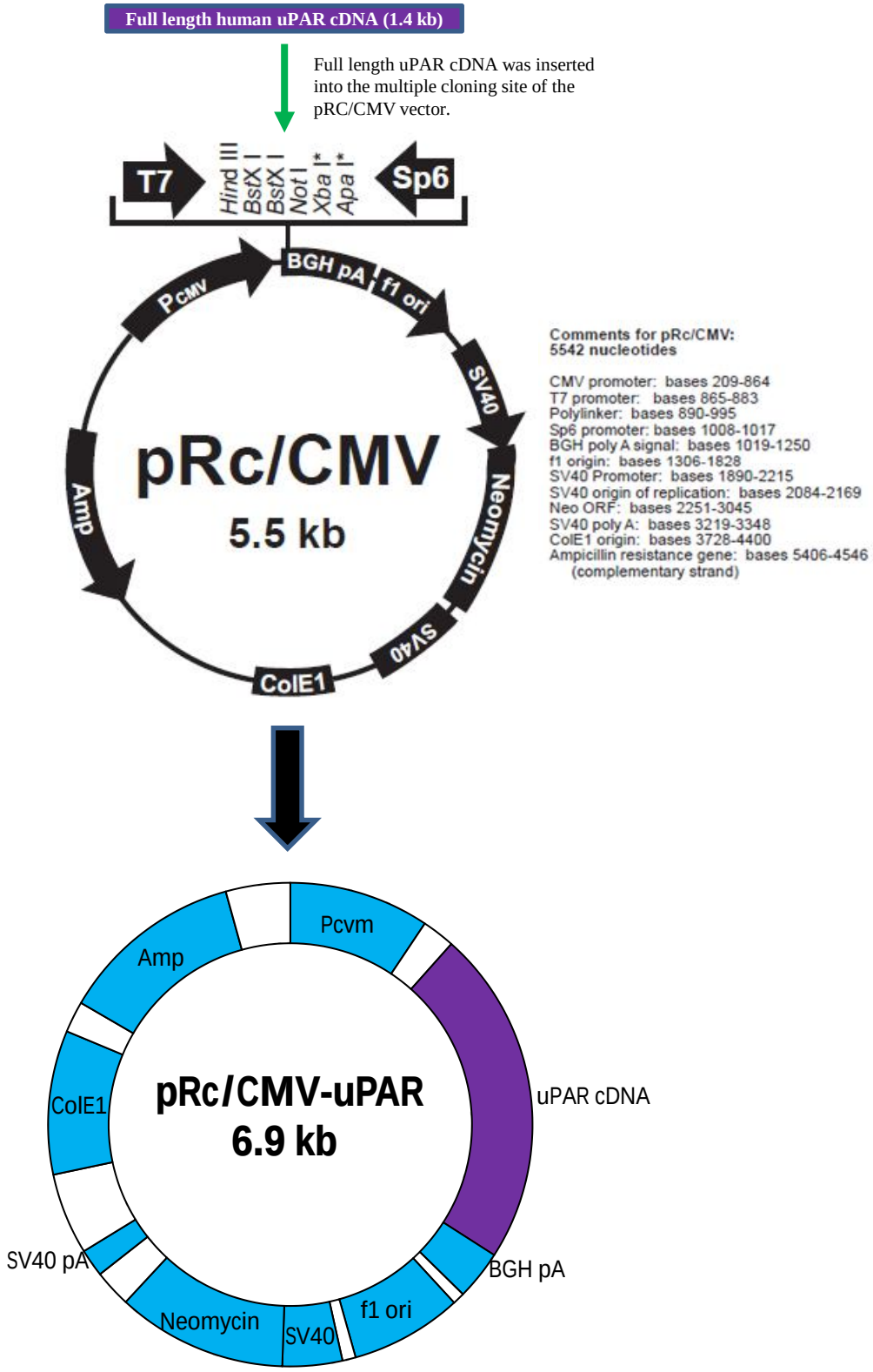

Figure C.1: The pRc/CMV-uPAR vector. A full length human cDNA (1.4 kb; Roldan *et al*., 1990) was ligated into the multiple cloning site of the pRc/CMV vector (Invitrogen) to produce the pRc/CMV-uPAR vector (Kjøller and Hall, 2001; Hillig *et al*., 2008). **Note:** The structure and information of the pRc/CMV vector is a direct citation obtained from Invitrogen™ Life technologies.

9.3.1 The uPAR sequencing results from the HOSCC cell lines

Note:

Sample preparation and primers required for sequencing the pRc/CMV-uPAR vector: XL-1 blue *Escherichia coli* (*E.coli*) were transformed with the pRc/CMV-uPAR vector (Kjøller and Hall, 2001) via heat shock transformation according to the protocol proposed by Inoue *et al*. (1990). The pRc/CMV-uPAR plasmid was extracted from selected colonies of XL-1 blue *E.coli* cells grown on a Luria agar plate containing 5% amplicillin via a crude alkaline-extraction procedure (Sambrook *et al*., 1989). Colonies of XL-1 blue *E.coli* cells, which contained a plasmid the size of the pRc/CMV-uPAR vector (6.9 kb), were used by Inqaba Biotech to perform forward sequencing using the T7 universal primer.

Sample preparation and primers required for sequencing uPAR transcript from the HOSCC cell lines: The RT-PCR amplification products from the different HOSCC cell lines (section 2.2.5) were sequenced using the uPAR forward and reverse primers (section 2.2.4).

The Sanger sequencing method was performed by Inqaba Biotech using the ABI 3130XL sequencer.

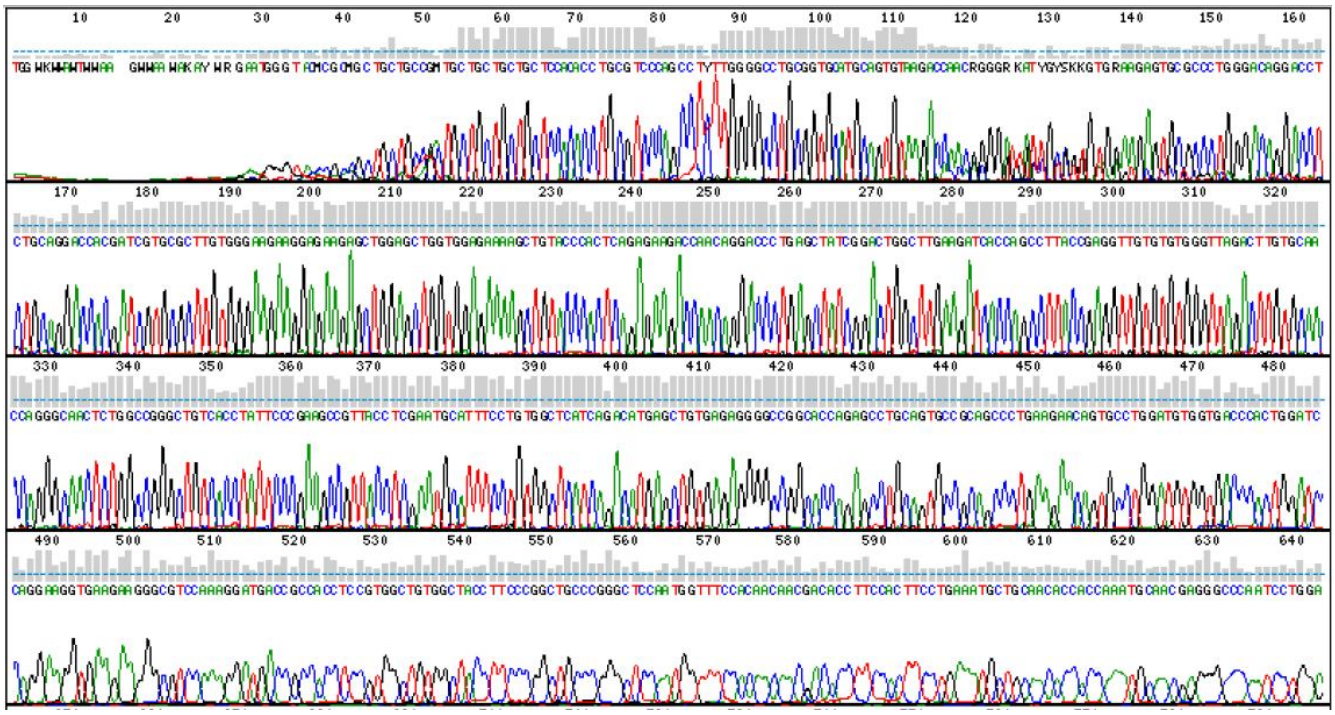

Figure C.2: Chromatogram of the uPAR sequence from the pRc/CMV-uPAR plasmid (using T7 primer).

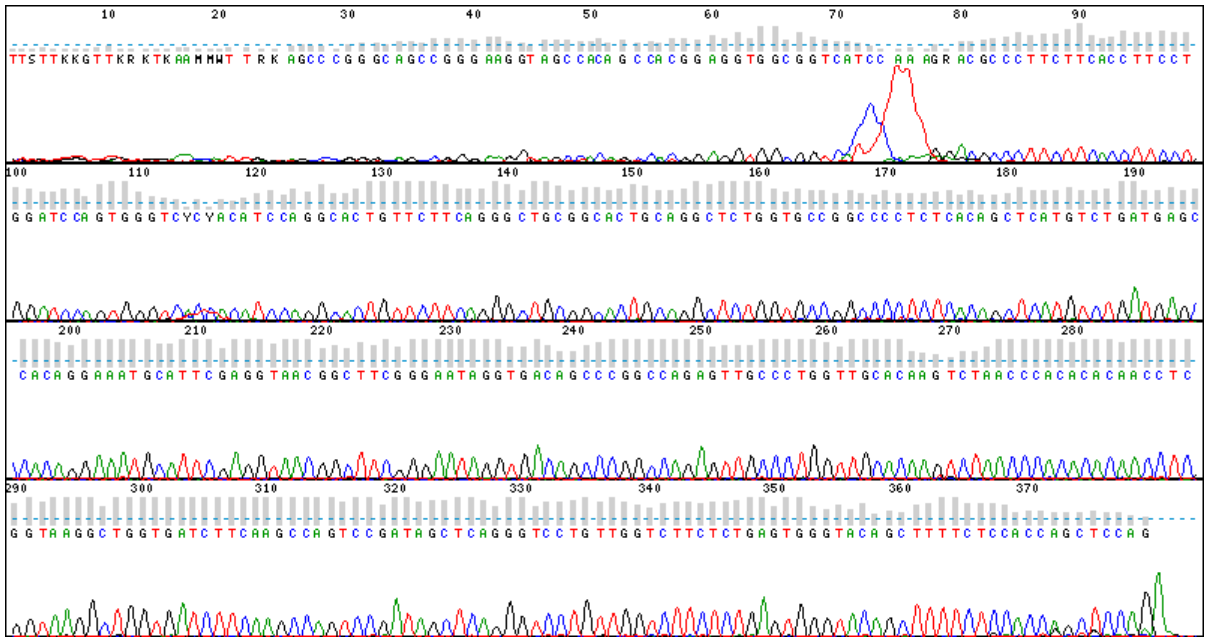

Figure C.3: Chromatogram of the uPAR sequence from the SNO cell line (using the reverse primer).

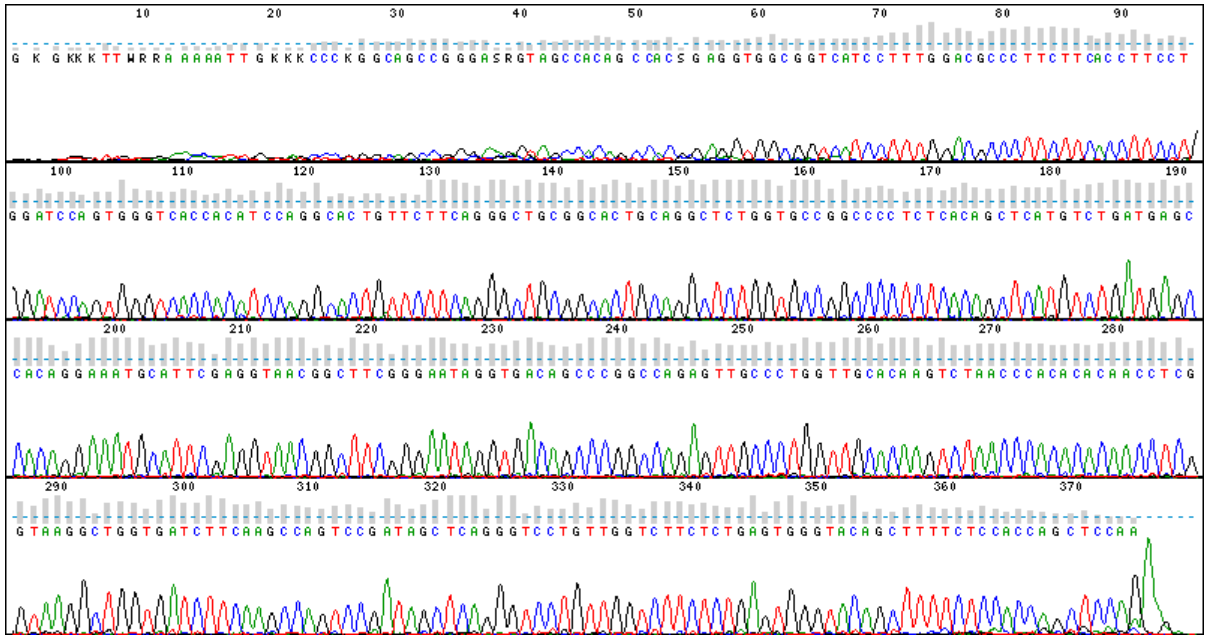

Figure C.4: Chromatogram of the uPAR sequence from the WHCO1 cell line (using the reverse primer).

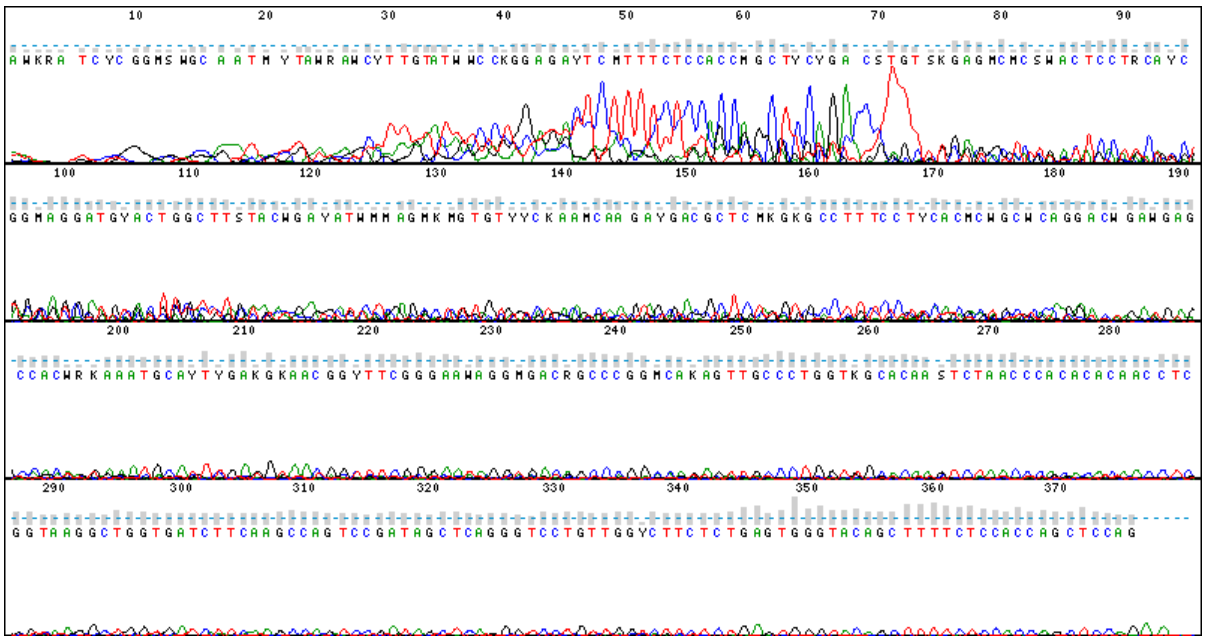

Figure C.5: Chromatogram of the uPAR sequence from the WHCO3 cell line (using the reverse primer).

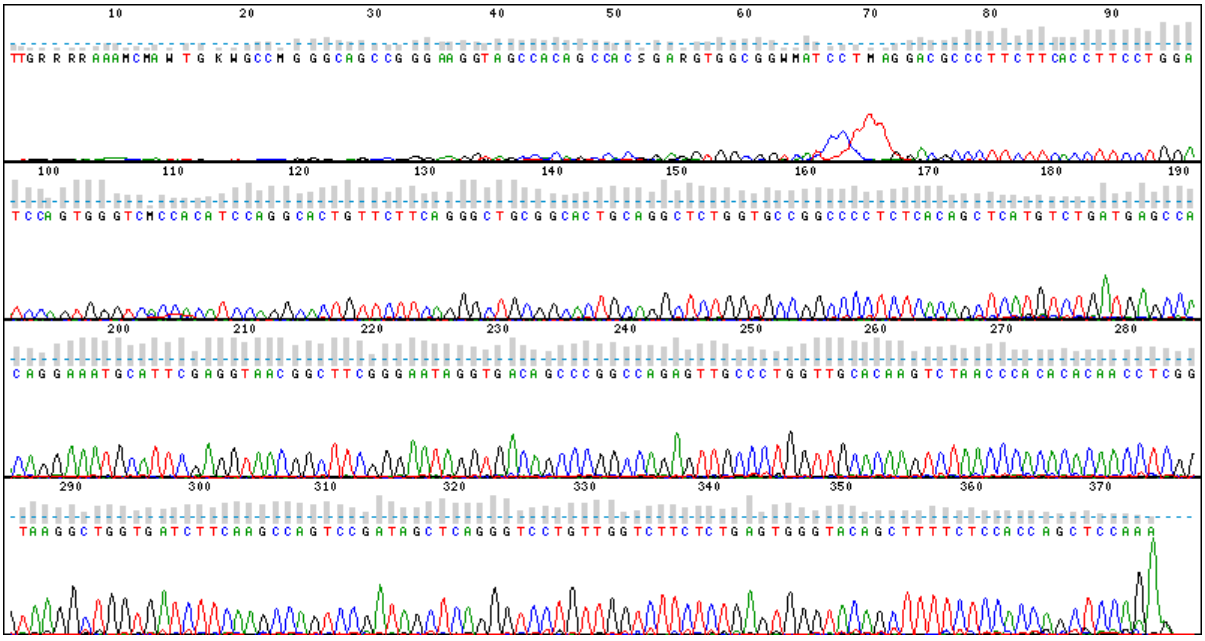

Figure C.6: Chromatogram of the uPAR sequence from the WHCO5 cell line (using the reverse primer).

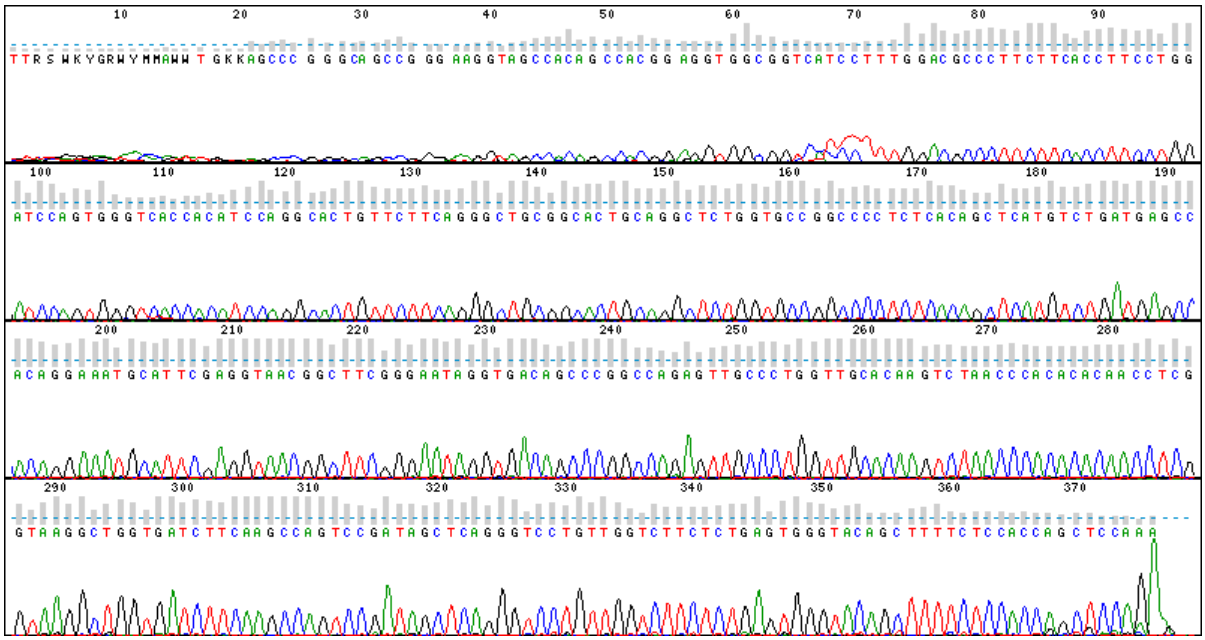

Figure C.7: Chromatogram of the uPAR sequence from the WHCO6 cell line (using the reverse primer).

9.3.2 Adhesion assays statistical data on collagen type I

Table 1.1. One way ANOVA of the numbers of adherent HOSCC cells on collagen type I

P value	P<0.0001		
P value summary	***		
Are means signif. different? (P < 0.05)	Yes		
Number of groups	5		
F	39.12		
R squared	0.9399		
ANOVA Table	**SS**	**df**	**MS**
Treatment (between columns)	56260	4	14070
Residual (within columns)	3595	10	359.5
Total	59860	14	

Table 1.2. P-values calculated by Tukey's multiple comparison post-ANOVA test (comparison between adhesion of the HOSCC cell lines on collagen type I)

Cell lines	SNO Collagen	WHCO1 Collagen	WHCO3 Collagen	WHCO5 Collagen	WHCO6 Collagen
SNO Collagen		P < 0.001	P > 0.05	P < 0.001	P > 0.05
WHCO1 Collagen	P < 0.001		P < 0.001	P > 0.05	P < 0.001
WHCO3 Collagen	P > 0.05	P < 0.001		P < 0.001	P > 0.05
WHCO5 Collagen	P < 0.001	P > 0.05	P < 0.001		P < 0.001
WHCO6 Collagen	P > 0.05	P < 0.001	P > 0.05	P < 0.001	

P < 0.05 indicates significant difference.

Table 1.3.a. The mean and standard deviation of the number of adherent HOSCC cells on collagen type I versus BSA

Cell lines	SNO		WHCO1		WHCO3		WHCO5		WHCO6	
	BSA	Collagen	BSA	Collagen	BSA	Collagen	BSA	Collagen	BSA	Collagen
Mean	24.63	107.1	100	221.1	29.54	82.32	77.95	200.6	33.25	75.69
Std. Deviation	2.167	11.33	13.04	9.52	3.666	1.672	12.96	39.35	7.89	5.247

The mean number of adherent WHCO1 cells on BSA was normalised to 100%

Table 1.3.b. P-values calculated by an unpaired Student's t-test (comparison between the number of adherent HOSCC cells on collagen type I versus BSA)

Cell lines	SNO	WHCO1	WHCO3	WHCO5	WHCO6
P value	0.0002	0.0002	< 0.0001	0.0069	0.0015

P < 0.05 indicates significant difference.

Table 1.4. One way ANOVA of the numbers of adherent HOSCC cells on collagen type I, in the absence or presence of 0.5 nM and 1 nM uPA

Cell lines	SNO			WHCO1			WHCO3			WHCO5			WHCO6		
P value	0.0477			0.1921			0.7548			0.0894			0.0894		
P value summary	*			ns			ns			ns			ns		
Are means signif. different? (P < 0.05)	Yes			No			No			No			No		
Number of groups	3			3			3			3			3		
F	5.271			2.199			0.295			3.709			3.709		
R squared	0.6373			0.423			0.08952			0.5528			0.5528		
ANOVA Table	SS	df	MS	SS	df	MS	SS	df	MS	SS	df	MS	SS	df	MS
Treatment (between columns)	974.8	2	487.4	500.8	2	250.4	24.25	2	12.13	1259	2	629.6	1259	2	629.6
Residual (within columns)	554.7	6	92.46	683.2	6	113.9	246.7	6	41.11	1018	6	169.7	1018	6	169.7
Total	1530	8		1184	8		270.9	8		2278	8		2278	8	

P < 0.05 indicates significant difference.

Table 1.5. P-values calculated by Dunnett's multiple comparison post-ANOVA test (comparison between adhesion of the SNO cells on collagen type I, in the absence or presence of 0.5 nM and 1 nM uPA)

Dunnett's Multiple Comparison Test	P value
SNO control vs. 0.5 nM uPA	P > 0.05
SNO control vs. 1 nM uPA	P > 0.05

Table 1.6.a. The mean and standard deviation of the number of adherent HOSCC cells on collagen type I versus BSA, in the presence of 0.5 nM uPA

Cell lines	SNO		WHCO1		WHCO3		WHCO5		WHCO6	
	BSA	collagen	BSA	collagen	BSA	collagen	BSA	collagen	BSA	collagen
Mean	24.63	127	95.35	208.1	26.61	82.32	80.1	185.9	33.25	72.97
Std. Deviation	3.739	5.666	7.717	11.67	7.782	6.027	17.34	6.618	8.749	9.653

The adhesion of the WHCO1 cells on BSA, without uPA treatment, was set as a reference point.

Table 1.6.b. P-values calculated by an unpaired Student's t-test (comparison between the number of adherent HOSCC cells on collagen type I versus BSA, in the presence of 0.5 nM uPA)

Cell lines	SNO	WHCO1	WHCO3	WHCO5	WHCO6
P value	< 0.0001	0.0002	0.0006	0.0006	0.0062

P < 0.05 indicates significant difference.

Table 1.7.a. The mean and standard deviation of the number of adherent HOSCC cells on collagen type I versus BSA, in the presence of 1 nM uPA

Cell lines	SNO		WHCO1		WHCO3		WHCO5		WHCO6	
	BSA	collagen	BSA	collagen	BSA	collagen	BSA	collagen	BSA	collagen
Mean	24.55	103.3	115.3	203.5	36.43	78.84	104	180.1	26.44	70.02
Std. Deviation	5.162	10.81	7.036	10.71	8.774	9.177	6.378	21.93	5.447	1.861

The adhesion of the WHCO1 cells on BSA, without uPA treatment, was set as a reference point.

Table 1.7.b. **P-values calculated by an unpaired Student's t-test (comparison between the number of adherent HOSCC cells on collagen type I versus BSA, in the presence of 1 nM uPA)**

Cell lines	SNO	WHCO1	WHCO3	WHCO5	WHCO6
P value	0.0003	0.0003	0.0044	0.0045	0.0002

P < 0.05 indicates significant difference.

Table 1.8.a. **The mean and standard deviation of the number of adherent HOSCC cells on collagen type I in the presence of $\beta1P1^{Sc}$ versus β1P1 peptides**

Cell lines	SNO		WHCO1		WHCO3		WHCO5		WHCO6	
	$\beta1P1^{Sc}$	β1P1	$\beta1P1^{Sc}$	β1P1	$\beta1P1^{Sc}$	β1P1	$\beta1P1^{Sc}$	β1P1	$\beta1P1^{Sc}$	β1P1
Mean	121.2	107.9	132	119.4	64.49	55.02	179.7	174.2	74.7	53.5
Std. Deviation	9.772	11.46	4.183	7.205	2.061	9.714	11.05	4.951	4.118	12.51

The adhesion of the WHCO1 cells on BSA, treated with $\beta1P1^{Sc}$, was set as a reference point

Table 1.8.b. **P-values calculated by an unpaired Student's t-test (comparison between the number of adherent HOSCC cells on collagen type I in the presence of $\beta1P1^{Sc}$ versus β1P1 peptides)**

Cell lines	SNO	WHCO1	WHCO3	WHCO5	WHCO6
P value	0.1996	0.0578	0.1738	0.4763	0.0494

P < 0.05 indicates significant difference.

Table 1.9.a. **The mean and standard deviation of the number of adherent HOSCC cells on collagen type I versus BSA, in the presence of $\beta1P1^{Sc}$ peptide**

Cell lines	SNO		WHCO1		WHCO3		WHCO5		WHCO6	
	BSA	collagen	BSA	collagen	BSA	collagen	BSA	collagen	BSA	collagen
Mean	56.07	121.2	100.2	132	44.96	64.49	97.59	179.7	41.86	74.7
Std. Deviation	18.83	9.772	11.72	4.183	7.782	2.061	20.37	11.05	14.6	4.118

The mean number of adherent WHCO1 cells on BSA, treated with $\beta1P1^{Sc}$, was normalized to 100%

Table 1.9.b. **P-values calculated by an unpaired Student's t-test (comparison between the number of adherent HOSCC cells on collagen type I versus BSA, in the presence of $\beta1P1^{Sc}$ peptide)**

Cell lines	SNO	WHCO1	WHCO3	WHCO5	WHCO6
P value	0.006	0.0114	0.0137	0.0036	0.02

P < 0.05 indicates significant difference.

Table 1.10.a. **The mean and standard deviation of the number of adherent HOSCC cells on collagen type I versus BSA, in the presence of β1P1 peptide.**

Cell lines	SNO		WHCO1		WHCO3		WHCO5		WHCO6	
	BSA	collagen	BSA	collagen	BSA	collagen	BSA	collagen	BSA	collagen
Mean	29.03	107.9	81.48	119.4	27.05	55.02	89.75	174.2	39.53	53.5
Std. Deviation	11.4	11.46	7.597	7.205	9.278	9.714	13.48	4.951	13.21	12.51

The adhesion of the WHCO1 cells on BSA, treated with $\beta1P1^{Sc}$, was set as a reference point.

Table 1.10.b. P-values calculated by an unpaired Student's t-test (comparison between the number of adherent HOSCC cells on collagen type I versus BSA, in the presence of β1P1 peptide)

Cell lines	SNO	WHCO1	WHCO3	WHCO5	WHCO6
P value	0.0011	0.0033	0.0226	0.0005	0.2546

P < 0.05 indicates significant difference.

9.3.3 Adhesion assays statistical data on vitronectin

Table 2.1. One way ANOVA of the numbers of adherent HOSCC cells on vitronectin

P value	P<0.0001		
P value summary	***		
Are means signif. different? (P < 0.05)	Yes		
Number of groups	5		
F	84.77		
R squared	0.9714		
ANOVA Table	SS	df	MS
Treatment (between columns)	44810	4	11200
Residual (within columns)	1321	10	132.1
Total	46130	14	

Table 2.2. P-values calculated by Tukey's multiple comparison post-ANOVA test (comparison between adhesion of the HOSCC cells on vitronectin)

Cell lines	SNO Vitronectin	WHCO1 Vitronectin	WHCO3 Vitronectin	WHCO5 Vitronectin	WHCO6 Vitronectin
SNO Vitronectin		P < 0.001	P > 0.05	P < 0.001	P > 0.05
WHCO1 Vitronectin	P < 0.001		P < 0.001	P < 0.01	P < 0.001
WHCO3 Vitronectin	P > 0.05	P < 0.001		P < 0.001	P > 0.05
WHCO5 Vitronectin	P < 0.001	P < 0.01	P < 0.001		P < 0.001
WHCO6 Vitronectin	P > 0.05	P < 0.001	P > 0.05	P < 0.001	

P < 0.05 indicates significant difference.

Table 2.3.a. The mean and standard deviation of the number of adherent HOSCC cells on vitronectin versus BSA

Cell lines	SNO		WHCO1		WHCO3		WHCO5		WHCO6	
	BSA	Vitronectin	BSA	Vitronectin	BSA	Vitronectin	BSA	Vitronectin	BSA	Vitronectin
Mean	24.63	24.32	100	115	29.54	44.89	77.95	170	33.25	44.33
Std. Deviation	2.167	0.6603	13.04	2.053	3.666	4.827	12.96	24.66	7.89	4.955

The mean number of adherent WHCO1 cells on BSA was normalized to 100%

Table 2.3.b. P-values calculated by an unpaired Student's t-test (comparison between the number of adherent HOSCC cells on vitronectin versus BSA

Cell lines	SNO	WHCO1	WHCO3	WHCO5	WHCO6
P value	0.8213	0.1212	0.0118	0.0046	0.1084

P < 0.05 indicates significant difference.

Table 2.4. One way ANOVA of the numbers of adherent HOSCC cells on vitronectin, in the absence or presence of 0.5 nM and 1 nM uPA

Cell lines	SNO			WHCO1			WHCO3			WHCO5			WHCO6		
P value	0.6377			0.8316			0.0229			0.9202			0.2026		
P value summary	ns			ns			*			ns			ns		
Are means signif. different? (P < 0.05)	No			No			Yes			No			No		
Number of groups	3			3			3			3			3		
F	0.4855			0.1901			7.56			0.08437			2.108		
R squared	0.1393			0.0596			0.7159			0.02735			0.4127		
ANOVA Table	SS	df	MS	SS	df	MS	SS	df	MS	SS	df	MS	SS	df	MS
Treatment (between columns)	11.93	2	5.967	160.9	2	80.45	279.6	2	139.8	45.28	2	22.64	155.9	2	77.97
Residual (within columns)	73.75	6	12.29	2539	6	423.1	111	6	18.49	1610	6	268.3	221.9	6	36.99
Total	85.69	8		2700	8		390.6	8		1655	8		377.9	8	

Table 2.5. P-values calculated by Dunnett's multiple comparison post-ANOVA test (comparison between adhesion of the WHCO3 cells on vitronectin, in the absence or presence of 0.5 nM and 1 nM uPA)

Dunnett's Multiple Comparison Test	P value
WHCO3 control vs. 0.5 nM uPA	P > 0.05
WHCO3 control vs. 1 nM uPA	P < 0.05

P < 0.05 indicates significant difference.

Table 2.6.a. The mean and standard deviation of the number of adherent HOSCC cells on vitronectin versus BSA, in the presence of 0.5 nM uPA

Cell lines	SNO		WHCO1		WHCO3		WHCO5		WHCO6	
	BSA	Vitronectin	BSA	Vitronectin	BSA	Vitronectin	BSA	Vitronectin	BSA	Vitronectin
Mean	24.63	24.95	95.35	119.4	26.61	47.22	80.1	166.2	33.25	53.16
Std. Deviation	3.739	5.164	7.717	34.78	7.782	4.072	17.34	3.424	8.749	1.36

The adhesion of the WHCO1 cells on BSA, without uPA treatment, was set as a reference point

Table 2.6.b P-values calculated by an unpaired Student's t-test (comparison between the number of adherent HOSCC cells on vitronectin versus BSA, in the presence of 0.5 nM uPA)

Cell lines	SNO	WHCO1	WHCO3	WHCO5	WHCO6
P value	0.9366	0.3065	0.0153	0.0011	0.0176

P < 0.05 indicates significant difference.

Table 2.7.a. **The mean and standard deviation of the number of adherent HOSCC cells on vitronectin versus BSA, in the presence of 1 nM uPA**

Cell lines	SNO		WHCO1		WHCO3		WHCO5		WHCO6	
	BSA	Vitronectin	BSA	Vitronectin	BSA	Vitronectin	BSA	Vitronectin	BSA	Vitronectin
Mean	24.55	22.25	115.3	125.3	36.43	57.71	104	171.5	26.44	53.16
Std. Deviation	5.162	3.126	7.036	7.448	8.774	3.95	6.378	13.6	5.447	9.196

The adhesion of the WHCO1 cells on BSA, without uPA treatment, was set as a reference point

Table 2.7.b. **P-values calculated by an unpaired Student's t-test (comparison between the number of adherent HOSCC cells on vitronectin versus BSA, in the presence of 1 nM uPA).**

Cell lines	SNO	WHCO1	WHCO3	WHCO5	WHCO6
P value	0.5456	0.1676	0.0186	0.0015	0.0124

P < 0.05 indicates significant difference.

Table 2.8.a. **The mean and standard deviation of the number of adherent HOSCC cells on vitronectin in the presence of $\beta1P1^{Sc}$ versus β1P1 peptides**

Cell lines	SNO		WHCO1		WHCO3		WHCO5		WHCO6	
	$\beta1P1^{Sc}$	β1P1	$\beta1P1^{Sc}$	β1P1	$\beta1P1^{Sc}$	β1P1	$\beta1P1^{Sc}$	β1P1	$\beta1P1^{Sc}$	β1P1
Mean	29.02	26.83	84.56	56.51	37.73	29.56	163	155.6	53.52	31.72
Std. Deviation	2.071	4.231	26.43	11.61	8.174	7.502	2.174	16.98	12.08	6.716

The adhesion of the WHCO1 cells on BSA, treated with $\beta1P1^{Sc}$, was set as a reference point

Table 2.8.b. **P-values calculated by an unpaired Student's t-test (comparison between the number of adherent HOSCC cells on vitronectin in the presence of $\beta1P1^{Sc}$ versus β1P1 peptides)**

Cell lines	SNO	WHCO1	WHCO3	WHCO5	WHCO6
P value	0.4651	0.1676	0.2711	0.491	0.0523

P < 0.05 indicates significant difference.

Table 2.9.a. **The mean and standard deviation of the number of adherent HOSCC cells on vitronectin versus BSA, in the presence of $\beta1P1^{Sc}$ peptide**

Cell lines	SNO		WHCO1		WHCO3		WHCO5		WHCO6	
	BSA	Vitronectin	BSA	Vitronectin	BSA	Vitronectin	BSA	Vitronectin	BSA	Vitronectin
Mean	56.07	29.02	100.2	84.56	44.96	37.73	97.59	163	41.86	53.52
Std. Deviation	18.83	2.071	11.72	26.43	7.782	8.174	20.37	2.174	14.6	12.08

The adhesion of the WHCO1 cells on BSA, treated with $\beta1P1^{Sc}$, was set as a reference point

Table 2.9.b. **P-values calculated by an unpaired Student's t-test (comparison between the number of adherent HOSCC cells on vitronectin versus BSA, in the presence of $\beta1P1^{Sc}$ peptide)**

Cell lines	SNO	WHCO1	WHCO3	WHCO5	WHCO6
P value	0.0686	0.4027	0.3294	0.0052	0.3466

P < 0.05 indicates significant difference.

Table 2.10.a. The mean and standard deviation of the number of adherent HOSCC cells on vitronectin versus BSA, in the presence of β1P1 peptide

Cell lines	SNO		WHCO1		WHCO3		WHCO5		WHCO6	
	BSA	Vitronectin	BSA	Vitronectin	BSA	Vitronectin	BSA	Vitronectin	BSA	Vitronectin
Mean	29.03	26.83	81.48	56.51	27.05	29.56	89.75	155.6	39.53	31.72
Std. Deviation	11.4	4.231	7.597	11.61	9.278	7.502	13.48	16.98	13.21	6.716

The adhesion of the WHCO1 cells on BSA, treated with β1P1^{Sc}, was set as a reference point

Table 2.10.b P-values calculated by an unpaired Student's t-test (comparison between the number of adherent HOSCC cells on vitronectin versus BSA, in the presence of β1P1 peptide)

Cell lines	SNO	WHCO1	WHCO3	WHCO5	WHCO6
P value	0.7695	0.0356	0.7336	0.0063	0.4124

P < 0.05 indicates significant difference.

9.3.4. Proliferation assays statistical data (in the absence of ECM)

Table 3.1.a The mean and standard deviation of the number of viable HOSCC cells in the absence and presence of suPAR

Cell lines	SNO		WHCO1		WHCO3		WHCO5		WHCO6	
	control	suPAR	control	suPAR	control	suPAR	control	suPAR	control	suPAR
Mean	83.8	81.89	100	100.4	96.44	88.07	59.45	58.97	34.71	37.1
Std. Deviation	4.695	10.27	2.128	0.7038	15.39	2.646	2.196	1.161	1.359	1.508

The mean number of viable WHCO1 cells, untreated, was normalized to 100 %

Table 3.1.b P-values calculated by an unpaired Student's t-test (comparison between the number of viable HOSCC cells in the absence or presence of suPAR)

Cell lines	SNO	WHCO1	WHCO3	WHCO5	WHCO6
P value	0.7842	0.8001	0.4053	0.7551	0.1111

P < 0.05 indicates significant difference.

Table 3.2. One way ANOVA of the numbers of viable HOSCC cells in the absence or presence of 0.5 nM, 1 nM and 5 nM uPA

Cell lines	SNO			WHCO1			WHCO3			WHCO5			WHCO6		
P value	0.113			0.8607			0.5977			0.6495			0.0861		
P value summary	ns			ns			ns			ns			ns		
Are means signif. different? (P < 0.05)	No			No			No			No			No		
Number of groups	4			4			4			4			4		
F	2.741			0.2478			0.6629			0.5714			3.154		
R squared	0.5069			0.08503			0.1991			0.1765			0.5419		
ANOVA Table	SS	df	MS	SS	df	MS	SS	df	MS	SS	df	MS	SS	df	MS
Treatment (between columns)	238.1	3	79.36	3.901	3	1.3	120.4	3	40.14	9.405	3	3.135	16.71	3	5.571
Residual (within columns)	231.6	8	28.95	41.97	8	5.246	484.5	8	60.56	43.89	8	5.487	14.13	8	1.766
Total	469.7	11		45.87	11		604.9	11		53.3	11		30.84	11	

Table 3.3.a The mean and standard deviation of the number of viable HOSCC cells in the presence of β1P1^{Sc} versus β1P1 peptides

Cell lines	SNO		WHCO1		WHCO3		WHCO5		WHCO6	
	β1P1^{Sc}	β1P1	β1P1^{Sc}	β1P1	β1P1^{Sc}	β1P1	β1P1^{Sc}	β1P1	β1P1^{Sc}	β1P1
Mean	83.88	78.97	100	94.76	100.9	94.64	57.91	53.71	33.77	29.78
Std. Deviation	3.724	5.32	7.343	1.845	4.289	1.176	2.495	3.58	1.332	1.646

The mean number of viable WHCO1 cells, treated with β1P1^{Sc}, was normalized to 100 %

Table 3.3.b P-values calculated by an unpaired Student's t-test (comparison between the number of viable HOSCC cells in the presence of β1P1^{Sc} versus β1P1 peptides)

Cell lines	SNO	WHCO1	WHCO3	WHCO5	WHCO6
P value	0.2611	0.2963	0.0727	0.1703	0.031

P < 0.05 indicates significant difference.

Table 3.4.a. The mean and standard deviation of the number of viable HOSCC cells in the absence or presence of TGFβ

Cell lines	SNO		WHCO1		WHCO3		WHCO5		WHCO6	
	control	TGFβ	control	TGFβ	control	TGFβ	control	TGFβ	control	TGFβ
Mean	83.8	80.8	100	97.96	96.44	102.8	59.45	60.74	34.71	37.63
Std. Deviation	4.695	6.28	2.128	2.396	15.39	0.7917	2.196	2.622	1.359	2.788

The mean number of viable WHCO1 cells, untreated, was normalized to 100 %

Table 3.4.b. P-values calculated by an unpaired Student's t-test (comparison between the number of viable HOSCC cells in the absence or presence TGFβ)

Cell lines	SNO	WHCO1	WHCO3	WHCO5	WHCO6
P value	0.5437	0.3274	0.5134	0.5492	0.1782

P < 0.05 indicates significant difference.

9.3.5. Proliferation assays statistical data (in the presence of collagen type I)

Table 4.1.a The mean and standard deviation of the number of viable HOSCC cells on collagen type I in the absence or presence of suPAR

Cell lines	SNO		WHCO1		WHCO3		WHCO5		WHCO6	
	control	suPAR	control	suPAR	control	suPAR	control	suPAR	control	suPAR
Mean	72.3	65.21	100	100.2	100.7	92.21	56.52	51.4	39.67	38.13
Std. Deviation	3.862	3.189	3.166	8.175	2.508	3.683	1.283	2.889	2.763	0.5776

The mean number of viable WHCO1 cells, untreated, was normalized to 100 %

Table 4.1.b P-values calculated by an unpaired Student's t-test (comparison between the number of viable HOSCC cells on collagen type I in the absence or presence suPAR)

Cell lines	SNO	WHCO1	WHCO3	WHCO5	WHCO6
P value	0.0703	0.9629	0.0301	0.0485	0.399

P < 0.05 indicates significant difference.

Table 4.2. One way ANOVA of the numbers of viable HOSCC cells on collagen type I, in the absence or presence of 0.5 nM, 1 nM and 5 nM uPA

Cell lines	SNO			WHCO1			WHCO3			WHCO5			WHCO6		
P value	0.0934			0.1585			0.2814			0.1928			0.5797		
P value summary	ns			ns			ns			ns			ns		
Are means signif. different? (P < 0.05)	No			No			No			No			No		
Number of groups	4			4			4			4			4		
F	3.028			2.261			1.523			1.999			0.6966		
R squared	0.5317			0.4588			0.3636			0.4285			0.2071		
ANOVA Table	SS	df	MS	SS	df	MS	SS	df	MS	SS	df	MS	SS	df	MS
Treatment (between columns)	123.7	3	41.23	34.36	3	11.45	15.75	3	5.251	33.19	3	11.06	10.11	3	3.37
Residual (within columns)	108.9	8	13.62	40.53	8	5.066	27.57	8	3.447	44.28	8	5.535	38.7	8	4.837
Total	232.6	11		74.89	11		43.33	11		77.47	11		48.81	11	

Table 4.3.a. The mean and standard deviation of the number of viable HOSCC cells on collagen type I, in the presence of β1P1^{Sc} versus β1P1 peptides

Cell lines	SNO		WHCO1		WHCO3		WHCO5		WHCO6	
	β1P1^{Sc}	β1P1	β1P1^{Sc}	β1P1	β1P1^{Sc}	β1P1	β1P1^{Sc}	β1P1	β1P1^{Sc}	β1P1
Mean	68.45	71.83	100	99.58	105	103.4	54.7	54	38.24	41.69
Std. Deviation	7.008	5.095	6.976	4.45	2.708	3.431	2.142	1.69	2.394	2.634

The mean number of viable WHCO1 cells, treated with β1P1^{Sc}, was normalized to 100 %

Table 4.3.b. P-values calculated by an unpaired Student's t-test (comparison between the number of viable HOSCC cells on collagen type I in the presence of β1P1^{Sc} versus β1P1 peptides)

Cell lines	SNO	WHCO1	WHCO3	WHCO5	WHCO6
P value	0.5358	0.9338	0.5453	0.6805	0.1686

P < 0.05 indicates significant difference.

9.3.6. Proliferation assays statistical data (in the presence of vitronectin)

Table 5.1.a. The mean and standard deviation of the number of viable HOSCC cells on vitronectin in the absence or presence of suPAR

Cell lines	SNO		WHCO1		WHCO3		WHCO5		WHCO6	
	control	suPAR	control	suPAR	control	suPAR	control	suPAR	control	suPAR
Mean	83.09	91.78	99.99	97.63	99.99	97.63	42.26	38.11	36.8	32.21
Std. Deviation	5.641	3.944	3.792	2.106	3.792	2.106	1.31	2.199	0.9851	1.381

The mean number of viable WHCO1 cells, untreated, was normalized to 100 %

Table 5.1.b. P-values calculated by an unpaired Student's t-test (comparison between the number of viable HOSCC cells on vitronectin in the absence or presence of suPAR)

Cell lines	SNO	WHCO1	WHCO3	WHCO5	WHCO6
P value	0.0941	0.3993	0.719	0.0482	0.0094

P < 0.05 indicates significant difference.

Table 5.2.a. The mean and standard deviation of the number of viable HOSCC cells on vitronectin in the presence of IgG control or anti-uPA antibody

Cell lines	WHCO5		WHCO6	
	IgG control	anti-uPA antibody	IgG control	anti-uPA antibody
Mean	100	92.1	74.27	68.8
Std. Deviation	1.549	2.832	1.899	7.362

The mean number of viable WHCO5 cells, treated with IgG control, was normalized to 100 %

Table 5.2.b. P-values calculated by an unpaired Student's t-test (comparison between the number of viable HOSCC cells in the presence of IgG control or anti-uPA antibody)

Cell lines	WHCO5	WHCO6
P value	0.0133	0.2811

P < 0.05 indicates significant difference.

Table 5.3. One way ANOVA of the numbers of viable HOSCC cells on vitronectin in the absence or presence of 0.5 nM, 1 nM and 5 nM uPA

Cell lines	SNO			WHCO1			WHCO3			WHCO5			WHCO6		
P value	0.295			0.2841			0.2313			0.0257			0.0771		
P value summary	ns			ns			ns			*			ns		
Are means signif. different? (P < 0.05)	No			No			No			Yes			No		
Number of groups	4			4			4			4			4		
F	1.467			1.512			1.765			5.36			3.331		
R squared	0.3548			0.3618			0.3983			0.6678			0.5554		
ANOVA Table	SS	df	MS	SS	df	MS	SS	df	MS	SS	df	MS	SS	df	MS
Treatment (between columns)	58.79	3	19.6	34.28	3	11.43	101.1	3	33.72	21.91	3	7.304	25.94	3	8.647
Residual (within columns)	106.9	8	13.36	60.45	8	7.557	152.8	8	19.1	10.9	8	1.363	20.77	8	2.596
Total	165.7	11		94.73	11		254	11		32.81	11		46.71	11	

Table 5.4. **P-values calculated by Dunnett's multiple comparison post-ANOVA test (comparison between the number of viable HOSCC cells of the WHCO5 cells on vitronectin, in the absence or presence of 0.5 nM and 1 nM uPA)**

Dunnett's Multiple Comparison Test	P value
control vs. 0.5 nM uPA	P > 0.05
control vs. 1 nM uPA	P < 0.05
control vs. 5 nM uPA	P > 0.05

P < 0.05 indicates significant difference.

Table 5.5.a. **The mean and standard deviation of the number of viable HOSCC cells on vitronectin in the presence of β1P1^{Sc} versus β1P1 peptides**

Cell lines	SNO		WHCO1		WHCO3		WHCO5		WHCO6	
	β1P1^{Sc}	β1P1	β1P1^{Sc}	β1P1	β1P1^{Sc}	β1P1	β1P1^{Sc}	β1P1	β1P1^{Sc}	β1P1
Mean	100.4	109	100	92.95	94.74	89.75	30.86	31.21	27.23	27.79
Std. Deviation	8.757	3.492	4.95	1.403	4.127	3.434	2.03	1.196	3.124	2.104

The mean number of viable WHCO1 cells, treated with β1P1^{Sc}, was normalized to 100 %

Table 5.5.b. **P-values calculated by an unpaired Student's t-test (comparison between the number of viable HOSCC cells on vitronectin in the presence of β1P1^{Sc} versus β1P1 peptides)**

Cell lines	SNO	WHCO1	WHCO3	WHCO5	WHCO6
P value	0.1877	0.0765	0.1833	0.8077	0.8103

P < 0.05 indicates significant difference.

Table 5.6.a. **The mean and standard deviation of the number of viable HOSCC cells on vitronectin in the absence or presence of TGFβ**

Cell lines	SNO		WHCO1		WHCO3		WHCO5		WHCO6	
	control	TGFβ	control	TGFβ	control	TGFβ	control	TGFβ	control	TGFβ
Mean	83.09	83.76	99.99	95.01	86.14	90.28	42.26	36.57	36.8	30.73
Std. Deviation	5.641	2.972	3.792	0.8595	7.523	0.4665	1.31	1.01	0.9851	1.691

The mean number of viable WHCO1 cells, untreated, was normalized to 100 %

Table 5.6.b. **P-values calculated by an unpaired Student's t-test (comparison between the number of viable HOSCC cells on vitronectin in the absence or presence of TGFβ)**

Cell lines	SNO	WHCO1	WHCO3	WHCO5	WHCO6
P value	0.864	0.0908	0.3954	0.004	0.0058

P < 0.05 indicates significant difference.

9.3.7. Proliferation assays statistical data (in the presence of collagen type I and vitronectin)

Table 6.1.a. **The mean and standard deviation of the number of viable HOSCC cells, on collagen type I and vitronectin, in the absence or presence of suPAR**

Cell lines	WHCO5		WHCO6	
	control	suPAR	control	suPAR
Mean	98.94	102.5	71.5	71.58
Std. Deviation	2.402	15.81	0.7999	3.779

The mean number of viable WHCO5 cells, untreated, was normalized to 100 %

Table 6.1.b. **P-values calculated by an unpaired Student's t-test (comparison between the number of viable HOSCC cells, on collagen type I and vitronectin, in the absence or presence of suPAR)**

Cell lines	WHCO5	WHCO6
P value	0.7202	0.9748

Table 6.2.a. **The mean and standard deviation of the number of viable HOSCC cells, on collagen type I and vitronectin, in the absence or presence of TGFβ**

Cell lines	WHCO5		WHCO6	
	control	TGFβ	control	TGFβ
Mean	98.94	94.5	71.5	81.55
Std. Deviation	2.723	4.51	4.973	6.591

The mean number of viable WHCO5 cells, untreated, was normalized to 100 %

Table 6.2.b. **P-values calculated by an unpaired Student's t-test (comparison between the number of viable HOSCC cells, on collagen type I and vitronectin, in the absence or presence of TGFβ)**

Cell lines	WHCO5	WHCO6
P value	0.2187	0.1028

9.3.8. Proliferation assays statistical data of EGF treatments (in the absence of ECM)

Table 7.1.a. **The mean and standard deviation of the number of viable HOSCC cells in the absence or presence of EGF**

Cell line	SNO		WHCO1		WHCO3		WHCO5		WHCO6	
	control	EGF	control	EGF	control	EGF	control	EGF	control	EGF
Mean	83.8	70.49	100	126.6	96.44	133.7	59.45	64.72	34.71	44.77
Std. Deviation	4.695	3.606	2.128	1.146	15.39	1.686	2.196	1.903	1.359	3.294

The mean number of viable WHCO1 cells, untreated, was normalized to 100 %

Table 7.1.b. **P-values calculated by an unpaired Student's t-test (comparison between the number of viable HOSCC cells, in the absence or presence of EGF.**

Cell line	SNO	WHCO1	WHCO3	WHCO5	WHCO6
P value	0.0176	P < 0.0001	0.014	0.0348	0.0081

P < 0.05 indicates significant difference.

Table 7.2.a. **The mean and standard deviation of the number of viable HOSCC cells treated with or without EGF, in the presence of anti-uPAR antibody**

Cell line	WHCO1		WHCO3		WHCO5		WHCO6	
	anti-uPAR Ab	anti-uPAR Ab + EGF	anti-uPAR Ab	anti-uPAR Ab + EGF	anti-uPAR Ab	anti-uPAR Ab + EGF	anti-uPAR Ab	anti-uPAR Ab + EGF
Mean	99.89	123.5	44.2	55.02	75.62	83.33	62.25	64.26
Std. Deviation	1.353	4.491	2.559	4.859	2.138	2.425	5.626	0.8349

The mean number of viable WHCO1 cells, treated with anti-uPAR antibody, was normalized to 100 %

Table 7.2.b. **P-values calculated by an unpaired Student's t-test (comparison between the number of viable HOSCC cells treated with or without EGF, in the presence of anti-uPAR antibody)**

Cell line	WHCO1	WHCO3	WHCO5	WHCO6
P value	0.0009	0.0269	0.0145	0.575

P < 0.05 indicates significant difference.

Table 7.2.c. **The mean and standard deviation of the number of viable WHCO6 cells treated with or without EGF, in the presence of IgG control**

Cell line	WHCO6	
	IgG control	IgG control + EGF
Mean	99.99	118.1
Std. Deviation	2.758	10.53

The mean number of viable WHCO6 cells, treated with IgG control, was normalized to 100 %

Table 7.2.d. **P-values calculated by an unpaired Student's t-test (comparison between the number of viable WHCO6 cells treated with or without EGF, in the presence of IgG control)**

Cell line	WHCO6
P value	0.0446

P < 0.05 indicates significant difference.

Table 7.3.a. **The mean and standard deviation of the number of viable HOSCC cells treated with or without EGF, in the presence of β1P1**

Cell lines	WHCO1		WHCO3		WHCO5		WHCO6	
	β1P1	β1P1 + EGF	β1P1	β1P1 + EGF	β1P1	β1P1 + EGF	β1P1	β1P1 + EGF
Mean	99.98	117.9	99.86	124.9	56.67	61.71	31.43	43.25
Std. Deviation	3.34	3.854	2.832	4.632	1.907	1.416	0.8298	0.5563

The mean number of viable WHCO1 cells, treated with β1P1, was normalized to 100 %

Table 7.3.b. **P-values calculated by an unpaired Student's t-test (comparison between the number of viable WHCO6 cells treated with or without EGF, in the presence of β1P1)**

Cell lines	WHCO1	WHCO3	WHCO5	WHCO6
P value	0.0037	0.0013	0.0213	P < 0.0001

P < 0.05 indicates significant difference.

9.3.9. Proliferation assays statistical data of EGF treatments (in the presence of collagen type I)

Table 8.1.a. **The mean and standard deviation of the number of viable HOSCC cells, on collagen type I in the absence or presence of EGF**

Cell lines	SNO		WHCO1		WHCO3		WHCO5		WHCO6	
	control	EGF	control	EGF	control	EGF	control	EGF	control	EGF
Mean	72.3	58.26	100	131.8	100.7	135.6	56.52	57.09	39.67	49.92
Std. Deviation	3.862	2.192	3.166	4.775	2.508	3.726	1.283	1.649	2.763	2.763

The mean number of viable WHCO1 cells, untreated, was normalized to 100 %

Table 8.1.b. **P-values calculated by an unpaired Student's t-test (comparison between the number of viable HOSCC cells on collagen type I in the absence or presence of EGF)**

Cell lines	SNO	WHCO1	WHCO3	WHCO5	WHCO6
P value	0.0054	0.0007	0.0002	0.6617	0.0105

P < 0.05 indicates significant difference.

Table 8.2.a. **The mean and standard deviation of the number of viable HOSCC cells, on collagen type I, treated with or without EGF, in the presence of anti-uPAR antibody**

Cell lines	WHCO1		WHCO3		WHCO6	
	anti-uPAR Ab	anti-uPAR Ab + EGF	anti-uPAR Ab	anti-uPAR Ab + EGF	anti-uPAR Ab	anti-uPAR Ab + EGF
Mean	99.8	141.3	56.26	63.2	72.48	83.19
Std. Deviation	2.1	3.133	7.359	8.326	1.296	1.871

The mean number of viable WHCO1 cells, treated with anti-uPAR antibody, was normalized to 100 %

Table 8.2.b. **P-values calculated by an unpaired Student's t-test (comparison between the number of viable HOSCC cells on collagen type I treated with or without EGF, in the presence of anti-uPAR antibody**

Cell lines	WHCO1	WHCO3	WHCO6
P value	P < 0.0001	0.34	0.0012

P < 0.05 indicates significant difference.

Table 8.2.c. **The mean and standard deviation of the number of viable HOSCC cells on collagen type I, treated with or without EGF, in the presence of IgG control**

Cell lines	WHCO3	
	Control IgG	Control IgG + EGF
Mean	100.0	116.6
Std. Deviation	3.944	6.820

The mean number of viable WHCO3 cells, treated with IgG control, was normalized to 100 %

Table 8.2.d. **P-values calculated by an unpaired Student's t-test (comparison between the number of viable WHCO3 cells on collagen type I treated with or without EGF, in the presence of IgG control**

Cell lines	WHCO3
P value	0.0216

P < 0.05 indicates significant difference.

Table 8.3.a. **The mean and standard deviation of the number of viable HOSCC cells, on collagen type I, treated with or without EGF, in the presence of β1P1**

Cell lines	WHCO1		WHCO3		WHCO6	
	β1P1	β1P1 + EGF	β1P1	β1P1 + EGF	β1P1	β1P1 + EGF
Mean	99.73	128.3	103.5	129.1	41.75	49.59
Std. Deviation	6.093	10.86	1.71	10.64	1.684	4.903

The mean number of viable WHCO1 cells, treated with β1P1, was normalized to 100 %

Table 8.3.b. **P-values calculated by an unpaired Student's t-test (comparison between the number of viable HOSCC cells on collagen type I treated with or without EGF, in the presence of β1P1)**

Cell lines	WHCO1	WHCO3	WHCO6
P value	0.0165	0.0147	0.0588

P < 0.05 indicates significant difference.

Table 8.3.c. **The mean and standard deviation of the number of viable WHCO6 cells on collagen type I treated with or without EGF, in the presence of $\beta 1P1^{Sc}$**

Cell lines	WHCO6	
	$\beta 1P1^{Sc}$	$\beta 1P1^{Sc}$ + EGF
Mean	100	106.1
Std. Deviation	1.576	1.042

The mean number of viable WHCO6 cells, treated with $\beta 1P1^{Sc}$, was normalized to 100 %

Table 8.3.d. **P-values calculated by an unpaired Student's t-test (comparison between the number of viable WHCO6 cells on collagen type I treated with or without EGF, in the presence of $\beta 1P1^{Sc}$)**

Cell lines	WHCO6
P value	0.0049

P < 0.05 indicates significant difference.

9.3.10. Proliferation assays statistical data of EGF treatments (in the presence of vitronectin)

Table 9.1.a. **The mean and standard deviation of the number of viable HOSCC cells on vitronectin in the absence or presence of EGF.**

Cell lines	SNO		WHCO1		WHCO3		WHCO5		WHCO6	
	control	EGF	control	EGF	control	EGF	control	EGF	control	EGF
Mean	83.09	81.54	99.99	101.8	86.14	92.01	42.26	37.69	36.8	32.74
Std. Deviation	5.641	1.914	3.792	2.836	7.523	1.058	1.31	0.9508	0.9851	4.417

The mean number of viable WHCO1 cells, untreated, was normalized to 100 %

Table 9.1.b. **The mean and standard deviation of the number of viable HOSCC cells on vitronectin in the absence or presence of EGF.**

Cell lines	SNO	WHCO1	WHCO3	WHCO5	WHCO6
P value	0.6753	0.5447	0.2518	0.0081	0.1954

P < 0.05 indicates significant difference.

9.3.11. Proliferation assays statistical data after EGF treatments (in the presence of collagen type I and vitronectin)

Table 10.1.a. **The mean and standard deviation of the number of viable HOSCC cells, on collagen type I and vitronectin, in the absence or presence of EGF**

Cell lines	SNO		WHCO1		WHCO3		WHCO5		WHCO6	
	control	EGF	control	EGF	control	EGF	control	EGF	control	EGF
Mean	77.15	74.03	100	116.8	86.15	74.4	113.3	113	81.9	90.04
Std. Deviation	1.283	0.3537	5.848	4.077	0.9112	1.222	3.988	7.247	0.9121	1.69

The mean number of viable WHCO1 cells, untreated, was normalized to 100 %

Table 10.1.b. **P-values calculated by an unpaired Student's t-test (comparison between the number of viable HOSCC cells, on collagen type I and vitronectin, in the absence and presence of EGF)**

Cell lines	SNO	WHCO1	WHCO3	WHCO5	WHCO6
P value	0.0154	0.0151	0.0002	0.9475	0.0018

P < 0.05 indicates significant difference.

Table 10.2.a. **The mean and standard deviation of the number of viable HOSCC cells, on collagen type I and vitronectin, treated with or without EGF, in the presence of anti-uPAR antibody**

Cell lines	WHCO1		WHCO6	
	anti-uPAR Ab	anti-uPAR Ab + EGF	anti-uPAR Ab	anti-uPAR Ab + EGF
Mean	100	117.5	75.46	77.73
Std. Deviation	2.099	1.574	1.54	4.89

The mean number of viable WHCO1 cells, treated with anti-uPAR antibody, was normalized to 100 %

Table 10.2.b. **P-values calculated by an unpaired Student's t-test (comparison between the number of viable HOSCC cells, on collagen type I and vitronectin, treated with or without EGF, in the presence of anti-uPAR antibody)**

Cell lines	WHCO1	WHCO6
P value	0.0003	0.4861

P < 0.05 indicates significant difference.

Table 10.2.c. **The mean and standard deviation of the number of viable WHCO6 cells, on collagen type I and vitronectin, treated with or without EGF, in the presence of IgG control**

Cell lines	WHCO6	
	IgG control	IgG control + EGF
Mean	100.2	117.6
Std. Deviation	2.245	8.184

The mean number of viable WHCO6 cells, treated with IgG control, was normalized to 100 %

Table 10.2.d. **P-values calculated by an unpaired Student's t-test (comparison between the number of viable WHCO6 cells, on collagen type I and vitronectin, treated with or without EGF, in the presence of IgG control)**

Cell lines	WHCO6
P value	0.0238

P < 0.05 indicates significant difference.

Table 10.3.a. **The mean and standard deviation of the number of viable HOSCC cells, on collagen type I and vitronectin, treated with or without EGF, in the presence of β1P1**

Cell lines	WHCO1		WHCO6	
	β1P1	β1P1 + EGF	β1P1	β1P1 + EGF
Mean	100	111.5	66.3	67.49
Std. Deviation	3.288	3.806	1.976	2.394

The mean number of viable WHCO1 cells, treated with β1P1, was normalized to 100 %

Table 10.3.b. **P-values calculated by an unpaired Student's t-test (comparison between the number of viable HOSCC cells, on collagen type I and vitronectin, treated with or without EGF, in the presence of β1P1)**

Cell lines	WHCO1	WHCO6
P value	0.0166	0.5438

P < 0.05 indicates significant difference.

Table 10.3.c. **The mean and standard deviation of the number of viable WHCO6 cells, on collagen type I and vitronectin, treated with or without EGF, in the presence of $\beta 1P1^{Sc}$**

Cell lines	WHCO6	
	$\beta 1P1^{Sc}$	$\beta 1P1^{Sc}$ + EGF
Mean	100	114.5
Std. Deviation	7.553	1.367

The mean number of viable WHCO6 cells, treated with $\beta 1P1^{Sc}$, was normalized to 100 %

Table 10.3.d. **P-values calculated by an unpaired Student's t-test (comparison between the number of viable WHCO6 cells, on collagen type I and vitronectin, treated with or without EGF, in the presence of β1P1^{Sc})**

Cell lines	WHCO6
P value	0.0311

P < 0.05 indicates significant difference.